(760) 872-1168
FAX: (760) 873-5695

EMAIL: inyowaterdept@telis.org
WEB: www.inyowater.org

163 May Street
Bishop, CA 93514

COUNTY OF INYO
WATER DEPARTMENT

October 15, 2004

Timothy J. Durbin
Timothy J. Durbin, Inc.
5330 Primrose Dr.
Suite 228
Fair Oaks, CA 95628

Dear Mr. Durbin:

This letter is in response to your inquiry regarding evapotranspiration measurements conducted in the Owens Valley. Enclosed is the final report for a study conducted by the Inyo County Water Department under California Department of Water Resources Local Groundwater Management Assistance Grant #4600001827. The study involved updates to a regional groundwater model, field measurements of evapotranspiration, and development of a vadose zone water balance.

If you have any questions, please feel free to contact me at (760) 872-1168.

Sincerely,

Bob Harrington, Hydrologist
Inyo County Water Department

DEVELOPMENT OF HYDROLOGIC AND VADOSE MODELS TO IMPROVE GROUNDWATER MANAGEMENT IN THE OWENS VALLEY

A Final Report Prepared by The County of Inyo Water Department For the State of California, Department of Water Resources, Grant Agreement No. 460001827 under the Local Groundwater Management Assistance Act

Robert Harrington and Aaron Steinwand

with contributions by Dani Or, Univ. of Connecticut; Wesley Danskin, U.S. Geological Survey; Jan Hendrickx, New Mexico Technical Institute; and Jim Stroh, The Evergreen State College.

November 10, 2003

Executive Summary

The County of Inyo and the City of Los Angeles and its Department of Water and Power have adopted a Long Term Groundwater Management Plan to manage groundwater and surface water in the Owens Valley to avoid adverse changes to phreatophytic vegetation while continuing to supply water to Los Angeles. Experience gained through monitoring and research during the last decade revealed the ineffectiveness of existing monitoring and management procedures. The purpose of this research project was to improve prediction tools used to evaluate the potential effects of proposed groundwater pumping. Specifically, this project focused on revision and testing of existing groundwater and vadose zone models and collection of field measurements to study the conceptualization of the models.

A post-audit for the period 1989-2002 was completed for a regional groundwater model of the Owens Valley originally prepared by Danskin (1998). In addition, the model was revised to separate the water balance components into custom MODFLOW packages to facilitate evaluation of each component. The model now simulates the period 1963-2002. It successfully simulated the drawdown due to the high pumping of 1987 through 1990 and the subsequent period of low pumping to allow water table recovery. The post-audit confirmed the earlier conclusions that the primary influence in most areas of the valley is pumping. Transient simulations supported conclusions based on steady state simulations that the time frame for response of the groundwater system was five to ten years. This suggests that there may be a lag of as much as a decade for the groundwater system to fully respond to changes in natural

hydrologic inputs such as runoff or evapotranspiration or management of pumping and recharge. Future work to enhance the use of the model should focus on refinement of historical data inputs, testing of additional future scenarios, and further revision of the model itself

In work associated with the model revision, we experimented with two methods to construct estimates of spatial evapotranspiration (ET), a major component of the groundwater budget of the basin. A series of ET maps for the post audit period was developed based on field and remote sensing vegetation measurements and empirically derived transpiration coefficients (Kc). Future work will incorporate the ET maps into the groundwater model to examine the effect of different ET estimates on model performance. SEBAL (Surface Energy Balance Algorithm for Land) is an alternative method developed recently that estimates ET directly from satellite measurements. Results of initial tests of the method conducted as part of this project were promising and generated interest in the scientists developing the technique to use the Owens Valley as a test site for their research.

A field investigation was conducted to measure ET using micrometeorological methods to compare with vegetation based Kc methods like those used to prepare the ET maps for the groundwater model. Along with the ET and vegetation measurements, soil water and water table measurements were collected to account for sources and locations of plant uptake. These results were used to evaluate and examine the parameterization of a vadose zone water balance model for phreatophytes that can account for direct groundwater uptake. Turbulent fluxes of heat and water measured by the eddy covariance ET system did not account for approximately one-third of the available energy similar as has been observed in other studies. Based on a side-by-side comparison with Bowen ratio instruments that rely on different theory to measure ET, we

developed recommendations to correct the ET measurements to account for all the available energy. After correction for energy imbalance, the measured seasonal ET generally agreed with estimates derived from Kc models and LAI measurements when the site conditions met assumptions of the Kc models. The sensitivity of the Kc estimates to correctly sampling the peak leaf area, however, suggests the practice of obtaining a single vegetation measurement is potentially error prone.

The portion of ET derived from the water table was estimated from the water balance as the difference between measured ET, soil water depletion, precipitation, and evaporation. Direct uptake accounted for 70 to 80% of ET for high cover sites with water table depths of 1 to 3 m. The field results suggest that a general relationship may exist that relates the partitioning of plant uptake (ET) to depth to water table. Additional field results are necessary as well as simulations using the existing partitioning function to determine which approach more accurately models changes in soil water. The vadose zone model was revised during this project to take advantage of experimental data collected since it was developed. The stochastic model of reference ET was updated by incorporating an additional 10 years of data obtained from the California Irrigation Management Information System station in the Owens Valley, and the model code was revised to allow input of site specific estimates of Kc as well as empirical Kc and vegetation measurements. This added flexibility allows use of the best available ET estimates. Future model revisions will be to incorporate and test model performance with the functions developed from the results of the field investigation of the soil water balance partitioning.

TABLE OF CONTENTS

LIST OF FIGURES

LIST OF TABLES

I. Introduction

The Owens Valley is a long, narrow valley on the eastern slope of the Sierra Nevada in Inyo County, California. It is a closed basin drained by the Owens River which terminates at saline Owens Lake. Although the climate of the valley floor is arid (mean precipitation of 10 to 15 cm), snowmelt runoff from the Sierra Nevada creates a shallow water table that supports approximately 70,000 acres of native phreatophytic shrubs and grasses and riparian areas. Since the early 1900's, the water resources of the Owens Valley have been managed by the Los Angeles Department of Water and Power (LADWP) as the primary water supply for the city. Nearly the entire floor of the valley is owned by Los Angeles and most is leased for grazing and irrigated agriculture. The Owens River and small creeks emanating from the Sierra Nevada are diverted into the Los Angeles Aqueduct below Tinemaha Reservoir and delivered to Los Angeles. In addition to surface water sources, Los Angeles has constructed approximately 95 groundwater wells to supply local water uses and for export.

In 1991, the County of Inyo and the City of Los Angeles and its Department of Water and Power adopted a Long Term Groundwater Management Plan (Plan) to settle two decades of litigation over the effects of Los Angeles' export of groundwater from the Owens Valley. The Plan requires management of groundwater and surface water in the Owens Valley to avoid adverse changes to phreatophytic vegetation while continuing to supply water to Los Angeles. The technical information required for implementation of the Plan is based upon vadose zone water and vegetation monitored at permanent monitoring sites located in wellfield areas throughout the Owens Valley. Each monitoring site is linked to nearby pumping wells.

Predicted transpiration values derived from vegetation measurements are compared to the plant-available water stored in the vadose zone. If available water at a site is insufficient to meet the projected vegetation water demand, pumping from the wells linked to the site is halted to allow water table recovery to replenish the water stored in the vadose zone. Pumping can only resume when the vadose zone water is restored to levels sufficient to meet plant requirements when the wells were turned off. This monitoring and management program was implemented to minimize excessive lowering of the water table below plant root zones that would result in extended periods of water stress and decline in vegetation cover.

In addition to permanent monitoring sites, vegetation response to pumping is monitored at other locations throughout the Valley. Selected areas encompassing approximately 8000 acres inside and outside wellfields are annually resampled to compare with the Plan's baseline vegetation conditions based on conditions mapped in 1984-1987. Further, depth to groundwater is regularly monitored by the County and LADWP at approximately 800 piezometers. These data are used to prepare depth to groundwater maps in areas of groundwater-dependant vegetation. The vegetation and groundwater results are integrated into a geographic information system to track whether the vegetation protection goals of the Agreement are being met and are used to develop and review the annual pumping programs proposed by LADWP.

Monitoring and management provisions of the Plan were initiated during 1989. In 1987 and 1988, high amounts of groundwater pumping (more than 200,000 acre feet/year) lowered the water table below the plant root zone under many areas of the valley. Under the Plan, groundwater pumping was greatly reduced in the fall of 1989, but vegetation had already declined below the Plan's baseline conditions in many areas. From 1989 to the present, the

LADWP and the County have agreed to promote water table recovery by reducing annual groundwater pumping below the amount allowed under the original provisions of the Plan. Since 1990, in some areas of the valley groundwater levels and cover of perennial vegetation have recovered to pre-drought levels, but some areas of wellfields have not fully recovered.

Water table and vegetation decline observed during the 1980s and research conducted during the last decade have demonstrated the need to evaluate the effectiveness of existing monitoring and management procedures and to improve prediction tools to evaluate the potential effects of proposed groundwater pumping (Steinwand, 2000a and b; Steinwand and Harrington, 2003). Since its inception, the Plan explicitly recognized the need for ongoing scientific investigations to better achieve its goals.

The purpose of this project was to improve existing groundwater and vadose zone groundwater models that can be used to evaluate the impact of groundwater pumping on groundwater levels and water availability for native vegetation. Field data collected as part of this project and available information collected since the original development of the models will be applied in conjunction with model revisions to accomplish this task.

II. Task 1: Groundwater model

This task consisted of two subtasks, groundwater model development and field investigation of evapotranspiration using micrometeorological methods.

Model Development

Introduction

Research examining the relationship between groundwater pumping and environmental

change was conducted in the 1980's by Inyo County and LADWP with assistance from the U.S. Geological Survey and others. From that effort, the USGS produced a basin-wide MODFLOW application which spanned the period 1963-1988 (Danskin, 1998). This model will be the starting point for further development of numerical groundwater modeling tools in this project.

Numerical models are well suited to exploring hypothetical scenarios because they are based on approximate representations of the physical principles of groundwater flow, and they can generate a spatially complete hydrologic prediction to provide a regional picture of hydrologic response to imposed conditions. Numerical models are time consuming and expensive to calibrate requiring much information to characterize the system, and the uncertainty in model predictions is hard to quantify. The extensive data on the hydrologic, geologic, and vegetation in the Owens Valley, however, make numerical models a particularly attractive method to apply to improve groundwater management (Danskin, 1998; Hollett et al., 1991).

The purpose of this task was to develop numerical groundwater models for critical areas of the Owens Valley that can be used to evaluate the impact of groundwater pumping, climatic variations, surface water management, and other hydrologic changes on groundwater levels. Components of this task contained in the original proposal included a post-audit of the Danskin (1998) model, application of the MODFLOW zonebudget package to develop finer grid models, and development of alternative methods to determine ET, which is the upper boundary condition of the model domain. Under this grant, the model was updated through 2002 and has the capability of simulating future scenarios through 2020, an arrangement which serves to both test the performance of the model in simulating the period 1989-2002, and provide Inyo County and LADWP a tool with which to evaluate future scenarios.

Materials and Methods

Post-audit

Danskin (1998) calibrated his model for steady state conditions using data from 1963 and for transient conditions using data from 1963-1984. Subsequently, Inyo and Los Angeles have collected an extensive database of groundwater levels, pumping, and environmental conditions to test the original calibrated model. A post-audit was completed to evaluate the performance of the model and to develop model input and output for the period subsequent to the calibration/validation period. The post audit included a simulation of observed conditions and an evaluation of the management alternatives presented in Danskin (1998).

The methodology used for the post-audit was to mimic as much as possible the data sets and approach used during the original development of the model. Inyo County and LADWP developed the data sets for the post-audit period (1989-2002) based on descriptions in WSP2370-H and discussions with Wes Danskin, the developer of the original model and consultant retained for the present work. For the purpose of post-auditing, no changes were made to the hydrostratigraphic framework or numerical discretization of the model. The model continued to use annual stress periods, and it models water-years 1963 through 2002. Future scenarios with differing management alternatives were simulated for transient conditions through water year 2020. Transient-mode simulations appeared to be more illustrative of the groundwater system than the steady-state model scenarios used in WSP2370-H. Additionally, the groundwater model code was modified with additional packages so that each specified flux (e.g. discharge from pumped wells, underflow, recharge from tributary streams, etc.) was simulated as a discrete item. The preprocessor modifications allowed for a more direct accounting of the MODFLOW water

budget, but did not affect simulated results. The modeling was done on a UNIX computer system using MODFLOW-88. Much of the actual preparation of the data sets was done using Excel and Emacs, with some manual entry.

The same pre-processing and post-processing programs were used for the original calibration and the post-audit with minor changes for size of arrays and length of simulation. The philosophy from the calibration period of using percent annual runoff as an index of recharge from tributary streams, ungaged runoff, and canals was retained. There remains a lingering question whether the percentages reflect the same historical base period, but this discrepancy would only alter the percent annual runoff by a percent or two. All categories of fluxes were maintained as before except for pumped and flowing wells. The data requirements and preprocessor modifications required for each water budget component are discussed below.

Stream recharge. Additional data required for the stream recharge component were the percent of normal runoff for the post-audit period, which were obtained from LADWP's Totals and Means records.

Agriculture recharge. Additional data required for the agricultural recharge component were the percent of normal runoff for the post-audit period, which were obtained from LADWP's Totals and Means records.

Evapotranspiration. The evapotranspiration component was treated as constant in the original model, therefore no changes were necessary to apply this concept to the post-audit period.

Canal recharge. Additional data required for the canal recharge component were the percent of normal recharge for the post-audit period and the years for which the Geiger and

Collins canals were operated, which were determined from LADWP's Totals and Means records.

Groundwater recharge. Additional data required for the groundwater recharge component were uses and losses for the Laws, Bishop, Big Pine, and Lone Pine areas, and overhead and spillgate releases for the Blackrock-Thibaut, and Lone Pine areas, which were obtained from LADWP's Totals and Means records. Some data for 1989-1992 were estimated because the records in Totals and Means only extended back to 1993. Typically this was done by taking the average of the 1993-2000 record.

Groundwater pumping. The post-audit included a philosophy of separating pumped and flowing well discharge, which was done for water years 1971 through 2002. The pre-processing program for pumpage was modified in minor ways to separate pumped and flowing well discharge. A few pumped wells put into service after the original calibration period (water year 1988) were added to the post-audit. Additional data required for the groundwater pumping component was obtained from LADWP pumping records. Locations and screened intervals for wells constructed since the completion of the original model were obtained from site visits and well construction diagrams. The groundwater pumping preprocessor was modified to accommodate the additional time spanned by the post-audit period.

Underflow. The underflow component was constant in the original model, so no changes were necessary.

Ungaged recharge. Additional data required for the ungaged recharge component were the percent of normal runoff for the post-audit period, which were obtained from LADWP's Totals and Means records. The ungaged recharge preprocessor was modified to accommodate the additional time spanned by the post-audit period.

To ensure that the post-audit was the same model that was used during calibration, fluxes from the post-audit simulation were compared with those published in Table 11 in WSP2370-H. Differences were always less than 0.5% (often less than 0.1%) and were attributable to round-off error.

The post-audit evaluation of model performance was based on visual comparison of simulated and measured hydrographs and a review of the model water budget, which were the same criteria used during the original development of the model. The post-processing program that generated hydrographs, published as Plate 3 in WSP2370-H, was used with more recently measured groundwater levels. No new wells were evaluated as part of the post-audit, mostly to achieve the dual goal of expediency and symmetry with the original calibration. Groundwater fluxes were evaluated on a valley-wide basis to insure that the fluxes were reasonable. No other critique of fluxes was done, including any comparison with measured spring flow or estimated evapotranspiration.

No direct comparison between the post-audit results and the specific scenarios described in WSP2370-H was done, choosing instead to focus first on incorporating historical data through water-year 2002 and general projections through 2020. A post-audit comparison of prior scenarios would be possible and might be illustrative considering the differences that occurred after 1988. The main difference between the earlier scenarios and the actual data was a decrease in pumpage, which resulted in less decline in groundwater levels than was suggested might occur.

Zonebudget

The purpose of this effort was to subdivide the regional flow model into wellfield-sized

individual models. The water balance for each smaller model would be derived from the regional model using the Zonebudget MODFLOW package. This work was slated to be performed after completion of the post-audit. Unfortunately, time to complete the post-audit spanned the time-frame of the project, and this task was not completed or funded by this grant.

Evapotranspiration (ET) maps

The MODFLOW groundwater model of Danskin (1998) applied a constant maximum ET rate at each cell to determine the upper boundary condition of the model domain. Spatial models of ET based on vegetation conditions and remote sensing techniques were developed for the Owens Valley to be linked to the MODFLOW application using a GIS. A time series of ET for the post-audit period was developed from existing remotely sensed thematic maps of vegetation cover (Elmore et al., 2000) and transpiration coefficients (Steinwand, 1999b; Steinwand et al., 2001). Additionally, satellite data were analyzed using an analytic model (SEBAL) to prepare an instantaneous estimate of spatial ET for the valley to test the applicability of this remote sensing method for use in the groundwater model.

Vegetation-based ET map. This method to estimate ET combined measures of vegetation cover with estimates of the transpiration (T) rate per unit of vegetation. It assumes that the primary contributor to ET is transpiration. This assumption was tested during the development of the vadose zone model (see Section III below)

The spatially distributed data consisted of a vegetation community map which included measurements of the species composition and cover for most polygons (Figure 1). The dominant vegetation of Los Angeles-owned land in the Owens Valley was inventoried and mapped by

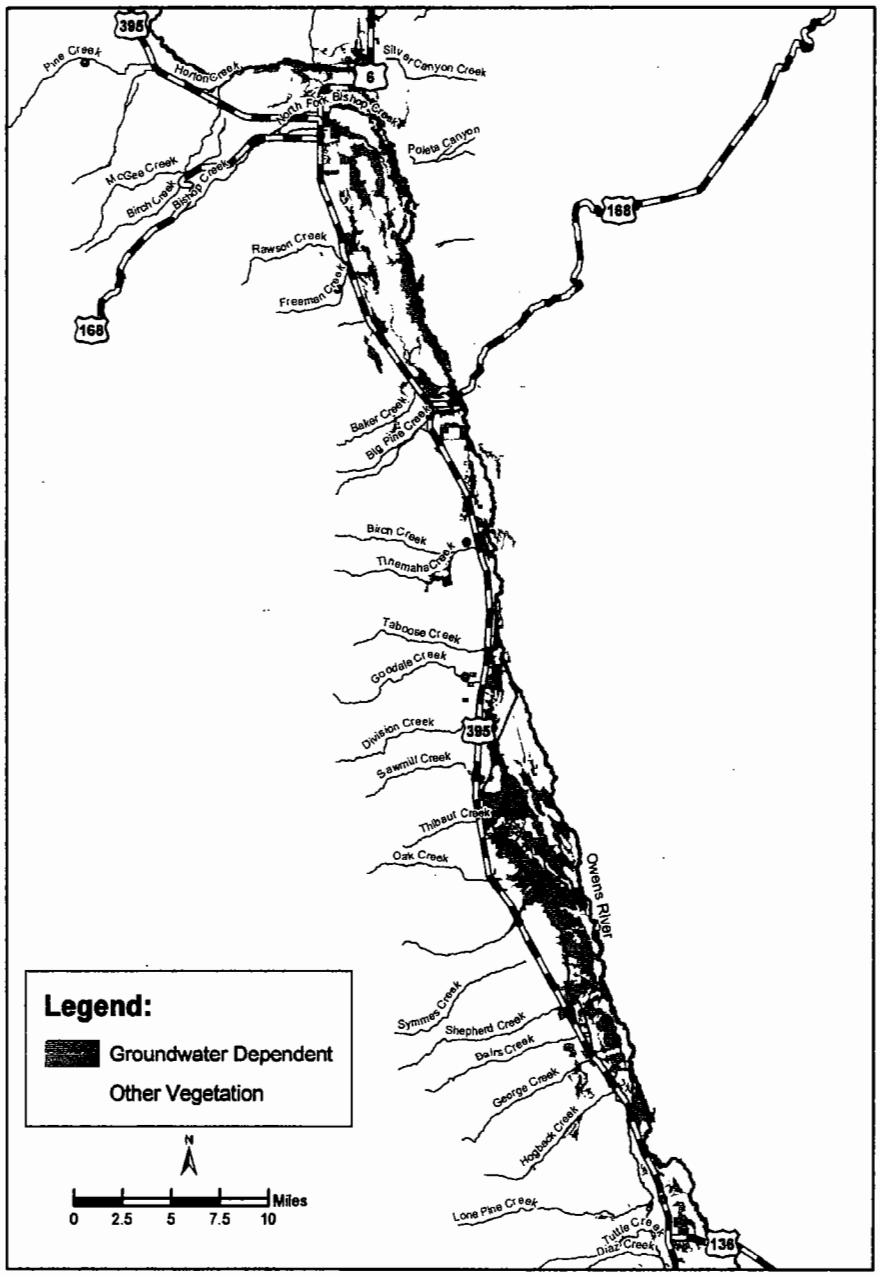

Figure 1. Area of Los Angeles owned lands mapped during vegetation inventory in 1984-87 and general vegetation classification into phreatophytic and nonphyreatophytic types.

Table 1. Vegetation plant communities and miscellaneous land classes mapped in the Owens Valley during 1984-87.

Code Number	Community
14000	Barren Lands
34100	Mojave Creosote Bush Scrub
34210	Mojave Mixed Woody Scrub
34300	Blackbrush Scrub
35100	Great Basin Mixed Scrub
35210	Big Sagebrush Scrub
36110	Desert Saltbush Scrub
36120	Desert Sink Scrub
36130	Desert Greasewood Scrub
36140	Shadscale Scrub
46000	Alkali Playa
35400	Rabbitbrush Scrub
36150	Nevada Saltbush Scrub
45310	Alkali Meadow
45320	Alkali Seep
45340	Rabbitbrush Meadow
45350	Nevada Saltbush Meadow
52320	Transmontane Alkali Marsh
61610	Great Basin Riparian Forest
61700	Mojave Riparian Forest
63600	Great Basin Riparian Scrub
63810	Tamarisk Scrub
11000	Irrigate Agriculture
13100	Permanent Lakes/Reservoirs
13200	Intermittent Ponds
45330	Rush/Sedge Meadow
45500	Non-native Meadow
76100	Black Locust Woodland

LADWP between 1984 and 1987. Vegetation map polygons were delineated into visually contiguous assemblages of plants with relatively similar cover and composition. Historic and current land-use maps also were consulted to delineate non-native or miscellaneous land cover classes (e.g. agriculture and urban lands). Color aerial photographs (scale 1:12,000) taken in

July 1981 were used as the basemap. Ultimately, the polygons were transferred to USGS 7.5' quadrangle maps. Black-and-white air photo prints from 1944 (1:24,000) and 1968 (1:12,000) were also used to verify abandoned agriculture. Field sampling was conducted on most parcels to adjust the parcel boundaries if necessary and to quantify vegetation cover and composition using the line-point method (Kuchler, 1967). Vegetation cover was defined as the crown cover of all live plants in relation to the ground surface. Species composition is synonymous with relative cover and was expressed as a percent of the total live cover. A minimum of five transects were run on each sampled parcel, but if the vegetation cover was particularly heterogeneous, up to twelve transects were run. Vegetation cover and percent composition of up to twelve dominant species were entered into a computer database. Polygons were classified according to (Cheatham and Haller, 1975), as revised to plant community descriptions (Holland, 1986). This system was further refined for the Owens Valley by adding six additional plant communities, non-native vegetation, and miscellaneous lands categories (Table 1). The classification system used is primarily floristic; hence, parcels with similar species composition were grouped together.

The annual T rate (T_{poly}) for each vegetation polygon was computed by

$$T_{poly} = C_p \sum_{s=1}^{q} T_s f_s \qquad (1)$$

where f_s is the fraction (by cover) of species s and C_p is the average vegetation cover for the polygon. T_s is the annual transpiration for a species normalized to 100% cover assuming sufficient soil water/water table conditions. T_s was either determined from the literature or from transpiration coefficients developed previously for the five most prevalent species using,

Table 2. Values and source of annual Ta assigned to species. The values have been normalized to 100% cover to facilitate calculations.

Species	Abbreviation	T_s	Source
		(cm/yr)	
Artemisia tridentata	ARTRT	35.5	Steinwand (1998); Branson et al. (1976)
Atriplex confertifolia	ATCO	59.1	Steinwand (1998); Branson et al. (1976)
Atriplex lentiformis ssp. *torreyi*	ATTO	102.9	Steinwand et al. (2001) and this report
Krascheninnikovia lanata	CELA	31.7	Steinwand (1998); Branson et al. (1976)
Chrysothamnus nauseosus	CHNA2	224.9	Steinwand et al. (2001) and this report
Chrysothamnus viscidiflorus	CHVI8	177.5	Miller (1988)
Distichlis spicata	DISP2	90.3	Steinwand (1999b) and this report
Grayia spinosa	GRSP	33.3	Steinwand (1998); Branson et al. (1976)
Juncus balticus	JUBA	75.5	Miller et al. (1982)
	LAKES	170.2	Lee (1912)
Populus fremontii	POFR3	191.0	Blaney (1954) and references therein
	PONDS	170.2	Lee (1912)
Rosa woodsii	ROWO	48.9	Robinson (1970)
Salix gooddingii	SAGOV	115.6	Robinson (1970)
Salsola tragus	SAKAT	52.0	Schillinger and Young (2000)
Salix sp.	SALIX	115.6	Robinson (1970)
Sarcobatus vermiculatus	SAVE4	192.5	Steinwand et al. (2001) and this report
Sporobolus airoides	SPAI	92.0	Steinwand (1999b) and this report
Tamarix ramosissima	TARA	92.0	Gay and Fritschen (1979); Ball et al. (1994)
Tetradymia axillaris	TEAX	56.0	Steinwand (1998); Branson et al. (1976)
Typha latifolia	TYLA	112.0	Blaney (1954) and references therein
Typha sp.	TYPHA	112.0	Blaney (1954) and references therein

$$T_s = \sum_{j=1}^{n} \sum_{i=1}^{m} Kc_{ij}\, ETr_j \qquad (2)$$

where ETr_j is the reference evapotranspiration for day j, and Kc_{ij} is the transpiration coefficient for species i on day j normalized to 100% cover (Table 2). Normalization to 100% cover in Equations 1 and 2 was simply for convenience in performing calculations utilizing the fraction of live cover. Transpiration coefficients are a dimensionless ratio of actual ET (in this case T) to a

reference or potential ET typically determined over an irrigated grass or alfalfa reference crop (Allen et al., 1998). Coefficients for the five most common phreatophytic species were developed from an extensive database of stomatal conductance, *ETr*, and LAI measurements collected by LADWP, USGS, and Inyo County in the Owens Valley (Steinwand, 1999a and b; Steinwand et al., 2001). ETr_j was derived from the California Irrigation Management Information System at Bishop, California by averaging the reference ET for several years. Cover of species without T_s values were assigned the weighted average T_s of the known species. The contribution of this subjective procedure affects the level of confidence in the T_{poly} estimate, and therefore, it was quantified separately for each polygon. For polygons where greater than 20% of the T_{poly} was due to species for which T_s was not available, the mean T_{poly} of polygons belonging to the same Holland class with less than 20% of T_{poly} attributable to unquantified species was assigned.

Several sources were used to assemble T_s values for common Owens Valley species. Ideally, T_s of all species would be known from measurements taken locally, but few species have been evaluated by local studies. Values of T_s from published studies on several species were used to increase the number of species with assigned T_s. The primary limitations to extracting values from other studies were the variable methods to measure plant cover and T. Sometimes only ET was measured, in which case only measurements where E could be reasonably assumed to be minimal were used. The alternative of relying solely on Kc models derived in the Owens Valley would reduce the number of parcel datasets amenable to derive T_{poly}. Also, T_s for some species reasonably can be assumed to be smaller than the dominant phreatophytic species, and without assigned T_s derived from the literature, these would be ignored or as in this project

assigned the weighted average T_s of phreatophytes.

To develop the ET time series for the years following the initial vegetation mapping, plant cover was estimated from satellite imagery using spectral mixture modeling, where the spectra for each pixel is modeled as a linear combination of bare soil, shadow, and vegetation end members (Elmore et al., 2000). LandSat Thematic Mapper images in late summer or early fall (preferably September) were obtained from 1984 to 2001. Late summer scenes were chosen to minimize the influence of varying phenology and leaf cover of spring annuals on estimates of vegetation abundance. The data sets were coregistered, spectrally calibrated to temporally invariant features, and georeferenced. The LandSat data were processed using the SMA model to estimate percent live plant cover for each pixel (28.5m X 28.5m). The estimates are considered accurate to $\pm$4.0% live cover. All mixture modeling was performed by Brown University as part of a previous study, and the results in GIS format were provided to Inyo County. Full details of the SMA model are given in Elmore et al. (2000).

Assuming temporal variation in T is largely due to changes in cover that reflect changes in water availability (Nichols, 2000), T_{poly} for polygons calculated from the initial vegetation map were adjusted each year based on average remotely-sensed cover (Figure 2). Manning et al. (1999) compared the SMA time series estimates of vegetation cover for the period 1991-1997 with cover measurements determined using field methods similar to those in the original vegetation mapping. SMA cover agreed with field sampling approximately for one third of the 98 polygons examined, but the two methods gave the same measures of cover or were systematically offset (i.e. parallel time series) for 69 of the polygons. Because temporal trends of remotely-sensed cover were more reliable than the magnitude, disagreement between field-

Figure 2. Example of vegetation cover in the Owens Valley in 1984 measured with SMA analysis of LandSat data. The boundaries of the vegetation map correspond with the groundwater model domain.

mapped and remotely-sensed vegetation cover was resolved by normalizing the results by the ratio of mapped cover with remotely-sensed cover of the years when the polygons were mapped. T_{poly} for each polygon for each year was then averaged over each MODFLOW cell to obtain the maximum transpiration rate for each cell.

Remote sensing ET map. The Surface Energy Balance Algorithm for Land (SEBAL) is a physically-based algorithm to estimate ET by solving the surface energy balance on an instantaneous time scale for every pixel of a satellite image (Bastiaanssen et al.1998a,b, 2002; Bastiaanssen 2000). The method is based on the computation of surface albedo, surface temperature, and vegetation index from multispectral satellite data. For this project, one LandSat Thematic Mapper image for September 12, 2002 was provided by Brown University for analysis conducted by Jan Hendrickx of New Mexico Technical Institute. The SEBAL results were compared with the results of the field measurements of ET using the eddy covariance stations. Although developed recently, the SEBAL algorithm has been applied for water balance estimations (e.g. Pelgrum and Bastiaanssen 1996), irrigation performance assessment studies (e.g. Roerink et al. 1997), and in weather prediction studies (e.g. Van de Hurk et al. 1997). The technique is not commonplace, and this analysis was not contemplated in the original proposal. Therefore, the theoretical development of method is described below. SEBAL evaluates the components of the energy balance and determines the ET rate as the residual,

$$R_n - G - H = \lambda E \tag{3}$$

where R_n is the net incoming radiation flux density (W m^{-2}), G is the ground heat flux density (Wm^{-2}), H is the sensible heat flux density (W m^{-2}), and λE is the latent heat flux density (W m^{-2})

or ET rate. The parameter λ is the latent heat of vaporization of water (J kg^{-1}) and E is the vapor flux density (kg m^{-2} s^{-1}).

The primary challenge to implement this approach was to partition the available energy ($R_n - G$) into λE and H. R_n was estimated from the surface albedo spatial variability (calculated from Thematic Mapper bands 1-5 and 7), surface temperature (from Thematic Mapper band 6), and solar radiation calculated from standard astronomical formulae (Iqbal, 1983). The ground heat flux G is determined through semi-empirical relationships with R_n, surface albedo, surface temperature, and Normalized Difference Vegetation Index (NDVI) calculated from Thematic Mapper bands 3 and 4 (Bastiaanssen 2000; Bastiaanssen et al. 1998a, b, 2002). The most complicated factor to solve for is H,

$$H = \rho_a c_p \frac{T_{aero} - T_a}{r_{ah}} \tag{4}$$

where ρ_a is the density of air (kg m^{-3}), c_p is the specific heat of air (J kg^{-1} K^{-1}), r_{ah} is the aerodynamic resistance to heat transfer (s m^{-1}), T_{aero} is the surface aerodynamic temperature, and T_a is the air temperature either measured at a standard screen height or the potential temperature in the mixed layer (Brutsaert et al., 1993). The aerodynamic resistance to heat transfer is affected by wind speed, atmospheric stability, and surface roughness (Brutsaert, 1982). The simplicity of Equation 4 is quite deceptive since T_{aero} cannot be measured by remote sensing. Remote sensing techniques measure the radiometric surface temperature T_{rad} which is not the same as the aerodynamic temperature. The two temperatures usually differ by 1 to 5 °C. Unfortunately, an uncertainty of 1 °C in $T_{aero} - T_a$ can result in a 50 W m^{-2} uncertainty in H

(Campbell and Norman, 1998) which could be approximately equivalent to 1 mm per day of ET. Although many investigators have tried to solve this problem by adjusting r_{ah} or using an additional resistance term, no generally applicable method has been developed yet (Kustas and Norman, 1996).

SEBAL overcomes the problem of inferring the aerodynamic temperature from the radiometric temperature and the need for near-surface air temperature measurements by directly estimating the temperature difference between T_1 and T_2 taken at two arbitrary levels z_1 and z_2 without explicitly deriving the absolute temperature. The temperature difference for a dry surface without evaporation is obtained from the inversion of the sensible heat transfer equation with latent heat flux λE=0 so that H=R_n-G (Bastiaanssen et al., 1998a, 2002),

$$T_1 - T_2 = \Delta T_a = \frac{H\, r_{ah}}{\rho_a\, c_p} \tag{5}$$

For a wet surface all available energy R_n-G is used for evaporation (λE) so that H=0 and ΔT_a=0. Field observations have indicated that land surfaces with a high ΔT_a are associated with high radiometric temperatures and those with a low ΔT_a with low radiometric temperatures (e.g. moist irrigated fields have a much lower ΔT_a than dry rangelands). The two unknowns in Equation 5, ΔT_a and the aerodynamic resistance to heat transfer r_{ah}, are affected by wind speed, atmospheric stability, and surface roughness (Brutsaert, 1982). For heterogeneous landscapes a wind speed near the ground surface is required for each pixel. Wind speed is not affected by local surface heterogeneities at a height of 200 m above ground level and is obtained by an upward extrapolation of a wind speed measurement at 2 or 10 m to 200 m using a logarithmic wind

profile. The wind speed at each pixel is obtained by a downward extrapolation using the surface roughness, which is determined for each pixel using an empirical relationship between surface momentum roughness z_{0m}, Normalized Difference Vegetation Index (NDVI), and the surface albedo α,

$$z_{om} = \exp[(a \times NDVI / \alpha) + b] \tag{6}$$

where a and b are correlation regression coefficients derived from a plot of $\ln(z_{om})$ versus NDVI/α for two or more sample pixels representing specific vegetation types. The end result of all these calculations is the determination of a r_{ah} and ΔT_a for each pixel. Field measurements by several authors (Bastiaanssen et al., 1998b; Wang et al., 1998; Frank and Beven, 1997; and Farah, 2001) have shown that the relationship between T_{rad} and ΔT_a is linear,

$$\Delta T_a = c_1 T_{rad} - c_2 \tag{7}$$

where c_1 and c_2 are the linear regression coefficients valid for one particular moment (the time and date the image is taken) and landscape. By using the minimum and maximum values of ΔT_a as calculated for the coldest and warmest pixel(s), the extremes of H are used to find the regression coefficient c_1 and c_2 to prevent outliers of H-fluxes. The internal auto-calibration process of SEBAL (Equation 7) eliminates the need for actual measurements of T_{rad} and/or ΔT as well as for atmospheric corrections. Thus, the surface temperature T_{rad} is used as a distribution parameter to partition of the sensible and latent heat fluxes. ΔT_a varies above the land surface as it is indexed to T_{rad}, but it does not require actual measurements on the ground or atmospheric corrections. This new approach has only recently been validated (Bastiaanssen et al., 1998a,b; Bastiaanssen, 2000). SEBAL results are most sensitive for the selection of the cold and warm

pixel which determine the outcome of the auto-calibration process. SEBAL is rather insensitive for errors in parameters as NDVI and atmospheric disturbances (Hendrickx et al., 2002).

ET depth function

In the original groundwater model, ET was varied temporally according to a linear function relating maximum ET to depth to groundwater. In the model, maximum ET (the valley-wide average ET) occurred when DTW was at the surface, and it decreased linearly to zero at a depth of 4.5 m. A potentially more robust relationship was developed by deriving an empirical relationship using multiple linear regression and an extensive dataset of depth to water, precipitation, and vegetation cover (to estimate ET) collected during routine monitoring by Inyo County and LADWP. As part of the Plan, Inyo County and Los Angeles established 33 permanent vegetation monitoring transects between 1987 and 1989; 22 are located in wellfield areas, 8 are control sites. Most sites are adjacent to an LADWP monitoring well. Depth to water was measured each month, and vegetation cover and composition were measured using point frame methods (Goodall, 1952; Groeneveld, 1997) each year in late June or early July. Precipitation on the valley floor was measured at seven locations by LADWP.

The multiple linear regression models were based on an annual time step to predict midsummer vegetation cover as a function of vegetation cover the preceding year, DTW at the beginning of the growing season (generally the shallowest water table), and valley-wide average precipitation the preceding winter. In the Owens Valley, winter precipitation predominates; usually summer rain is sparse. The annual time step of the regression models was selected to conform with the groundwater model time step.

Results and Discussion

Post-audit

Five scenarios were tested with the updated model. The scenarios were designed to test the new data-sets and to demonstrate the sensitivity of the model to runoff, groundwater pumpage, and recharge. They were not designed to illustrate a specific management plan. The simulation period was a combination of the historical period (1963-1988), the post-audit period (1989-2002), and future conditions (2003-2020). For each scenario and time period, descriptions of three flux components, percent runoff, pumpage, and groundwater recharge are summarized in Table 3.

Scenario 1. Average runoff, zero pumping. The primary goal of this scenario was to view the effect of average runoff without pumping. Can the model reasonably simulate this condition or will it become numerically unstable? This scenario in some respects represents the unmanaged system, though it includes some groundwater recharge resulting from water management activities. One of the purposes of Scenario 1 is to demonstrate that the model can simulate a high, stable water table, unaffected by pumping after 1988. Another purpose was to critique the separation of pumpage into discharge from pumped well and discharge from flowing wells.

The results of this simulation met these goals reasonably well, and also demonstrate the significant effect pumping has on the system. The results also confirm that the response time of the basin in on the order of 5 to 10 years – the time necessary for a significant change in recharge or discharge to equilibrate throughout the system. A comparison of the pumpage data from the original data sets and the newly acquired data set for 1972-88 shows that there are differences. It

Table 3. Post-audit scenarios.

Scenario 1. Average runoff, zero pumping.			
Period	% Runoff	Pumpage	Groundwater recharge
1963-1988	original model	original model	original model
1989-2002	100% of long-term average	0%	same as WSP 2370-H projection (mean of 1985, 1986, 1988)
2003-2020	100% of long-term average	0%	same as WSP 2370-H projection (mean of 1985, 1986, 1988)
Scenario 2. Historical runoff, zero pumping.			
Period	% Runoff	Pumpage	Groundwater recharge
1963-1988	original model	same as scenario 1	original model
1989-2002	additional data	"	additional data
2003-2020	100% of long-term average	"	same as WSP 2370-H projection (mean of 1985, 1986, 1988)
Scenario 3. Historical runoff and pumping.			
Period	% Runoff	Pumpage	Groundwater recharge
1963-1988	same as scenario 2	original model	same as scenario 2
1989-2002	"	additional data	"
2003-2020	"	100% of long-term average	"
Scenario 4. Average future runoff and pumping.			
Period	% Runoff	Pumpage	Groundwater recharge
1963-1988	same as scenario 2	original model	same as scenario 2
1989-2002	"	additional data	"
2003-2020	"	2001 water-year (76,318 AF)	"
Scenario 5. Transient future runoff and pumping.			
Period	% Runoff	Pumpage	Groundwater recharge
1963-1988	same as scenario 2	original model	original model
1989-2002	"	additional data	additional data
2003-2020	"	water-years 1992-2002 followed by 1992-1997	water-years 1992-2002 followed by 1992-1997

was not obvious why some values for selected wells were different by as much as 100%. The

total annual pumpage was very similar in most cases, but the two data sets were not as comparable as expected.

Scenario 2. Historical runoff, zero pumpage. The goal of this scenario is simply to extend Scenario 1 with runoff data for the new period. Any bias in developing the runoff and recharge data would likely become evident, as would any long-term trend in the data. Results indicate that there does not seem to be any bias in the new recharge data. The trend of the simulated groundwater levels is reasonable and does not appear to be affected by any difference in philosophy between the initial period (1963-88) and the later period (1989-2002).

Scenario 3. Historical runoff and pumping. The purpose of this scenario is to add new pumpage and flowing well data to Scenario 2. Similar to Scenario 2, the goal was to identify any unintended bias in developing, processing, or incorporating the data into the model.

Results indicate that no bias is visually discernible. The new data for pumping wells seems to work well. For water-years 1989-02, the model performed remarkably like the original calibration period 1963-88. Measured groundwater levels and simulated heads in areas that matched well during the initial period continued to match well during the later period; areas where heads were offset in some fashion continued to be offset. Essentially no hydrographs converged or diverged. If they had, it likely would indicate a problem with the model.

Scenario 4. Average future runoff and pumping. The goal of this scenario is to extend the post-audit simulation into the future using reasonably average conditions. The runoff is fixed at 100% of the long-term mean, and pumpage is fixed at a typical value for the years just prior to 2003. This scenario is in essence a future steady-state, but the transient simulation demonstrates the time needed to reach this steady-state. This approach is better and more illustrative than

simply running a steady-state solution as was done for the four alternatives in the earlier modeling effort.

In general, there is a slight upward trend in groundwater levels. This result suggests that the pumpage of about 75,000 acre-feet per year is in balance with the amount of recharge. This is the same result that was found during the testing of water management alternatives described in the earlier modeling effort.

Scenario 5. Transient future runoff and pumping. The purpose of this scenario is to demonstrate a dynamic version of Scenario 4 by incorporating climatic variability. This scenario addresses the question, What response is likely to occur from a typical pattern of varying runoff and pumpage? A recent historical period (1993-2002) was identified that had similar statistics to much longer periods, for example 1935-2002. The cumulative percent runoff was used to select the precise period so that there would not be mass balance discrepancies in moving the simulation from historical conditions in 2002 to hypothetical conditions in 2003 and beyond. This means that there should not be an artificial gain or loss of water from the basin as a result of moving into the future period. To achieve this goal, the cumulative percent runoff curve was manipulated by hand, offsetting it in time, and then rematching one curve on top of the other. This process resulted in 1992 matching 2002.

The 10-year period of runoff also needs to have a range of wet and dry years that are comparable to historical conditions. In essence, the period is a sine curve with a short decline, a long rise, and short decline in runoff, ending about where it started in terms of cumulative runoff for the period. Statistical comparison shows that 1993-2002 substantiates that 1993-2002 is a reasonable period to use as it represents a period of zero net change in storage, and contains

reasonably representative wet and dry periods.

Results of Scenario 5 indicate that there is a range of response of the groundwater system over this period. Compared to the historical period, the response is less because the wet and dry periods do not last as long as during the 1960's (drought) or 1980's (wet period). Therefore, Scenario 5 should be viewed as modest fluctuations, less than would result from simulating the historical period 1963-2002. Simulating this period as a scenario is a worthy effort, but beyond the scope of this first task of the post audit.

ET maps

Vegetation based ET maps. Transpiration was calculated for 1677 of the 2126 polygons delineated on the vegetation map; 449 polygons had no vegetation or had no plant species with assigned T_s. Most of the 449 polygons were irrigated lands, urban lands, barren lands, or playa. The distribution of T for the 1677 parcels is shown in Figure 3. Average T was 24.4 cm/year, but the distribution was highly skewed, and the median was probably a better measure of central tendency (19.2 cm/year). Most parcels dominated by phreatophytes had transpiration estimates greater than average precipitation. Some parcels with degraded vegetation were predicted to transpire less than average precipitation. LandSat data, SMA model results, and the vegetation base map produced a map like Figure 4 for each year during 1984-2001. Figure 5 shows an example how the ET rate changes through time for a single MODFLOW cell. Also shown in Figure 5 are depth to water and precipitation, both of which exhibit the expected correlation with ET. Our method contrasts with other recent efforts to develop regional ET rates for Great Basin vegetation. The satellite imagery was used here only to assess the fractional cover of vegetation, whereas other workers (Laczniak, et al., 1999; Nichols, 2000) have used imagery to classify

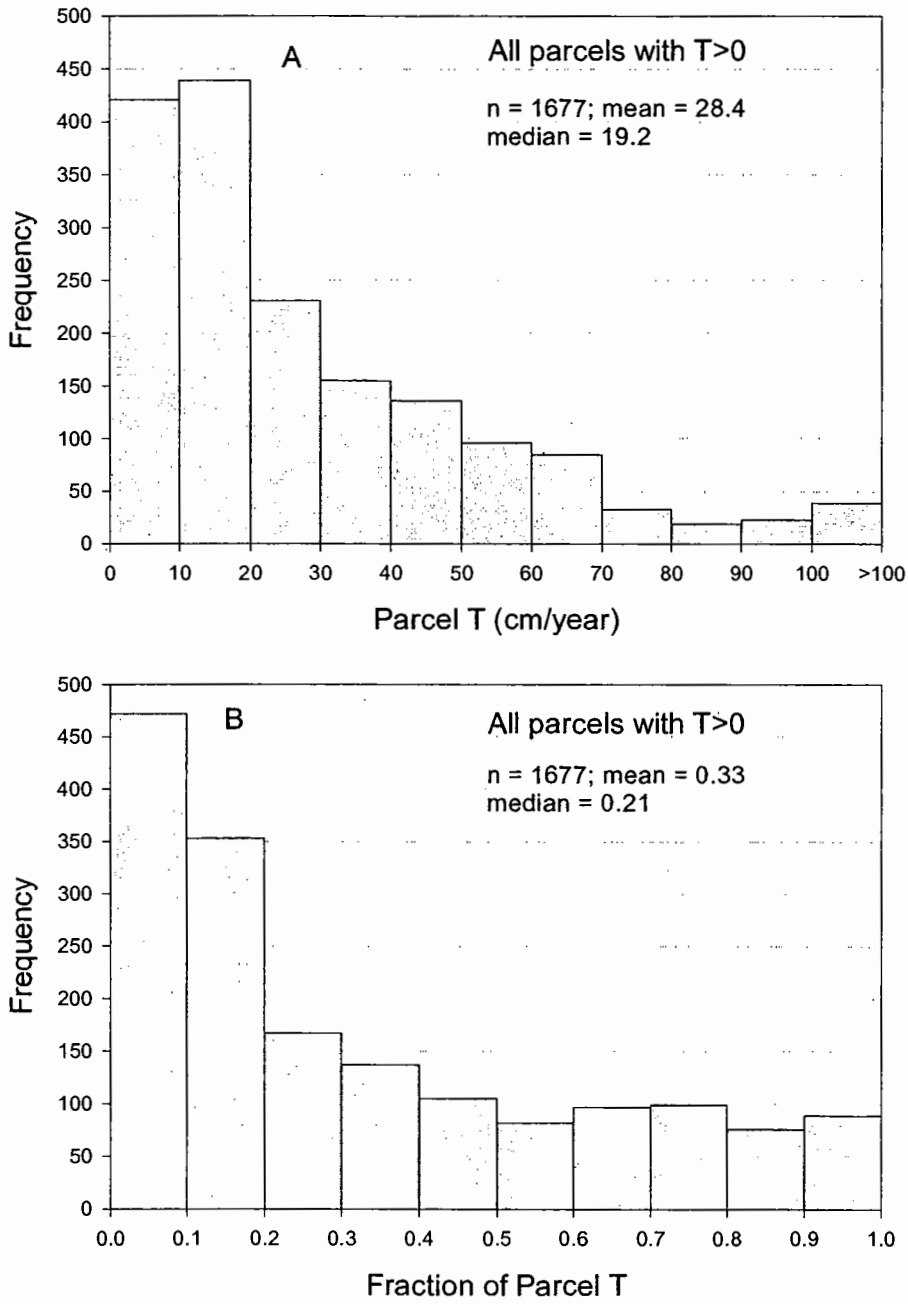

Figure 3. (A) Histogram of T for all parcels with T_{poly} estimates. (B) Histogram of the fraction of T_{poly} contributed by species without assigned T_s values.

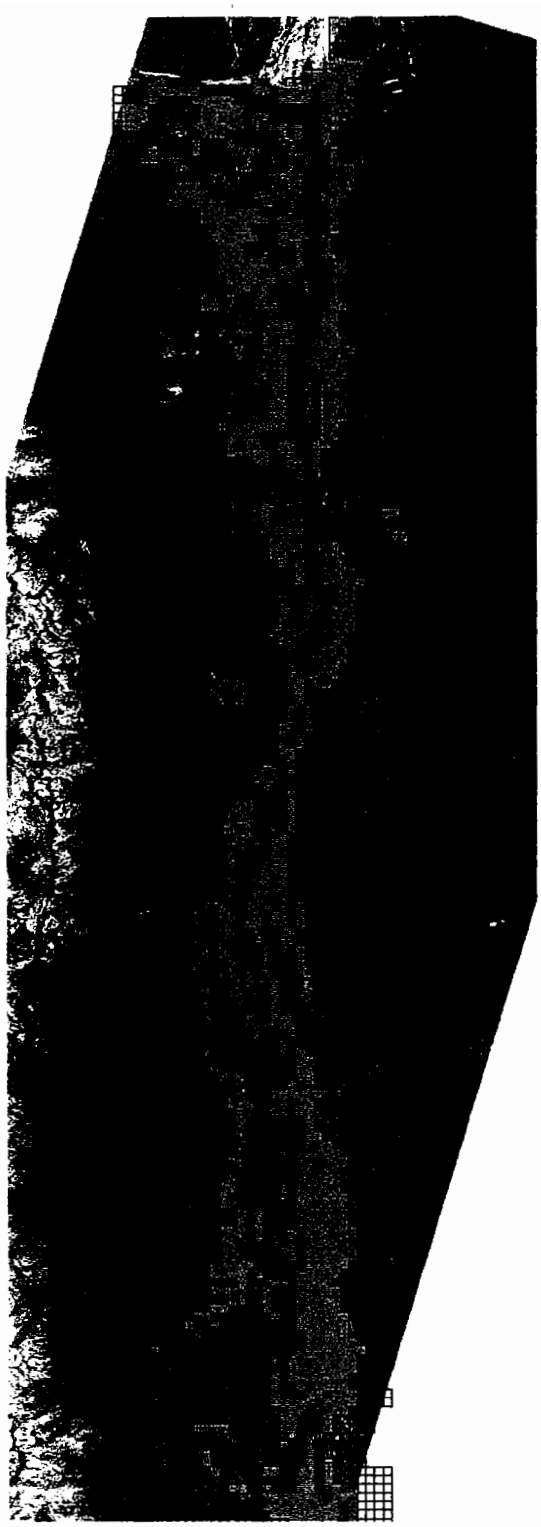

Figure 4. Example of estimated ET for the Owens Valley in 1984 using SMA, transpiration coefficients, and LADWP vegetation inventory.

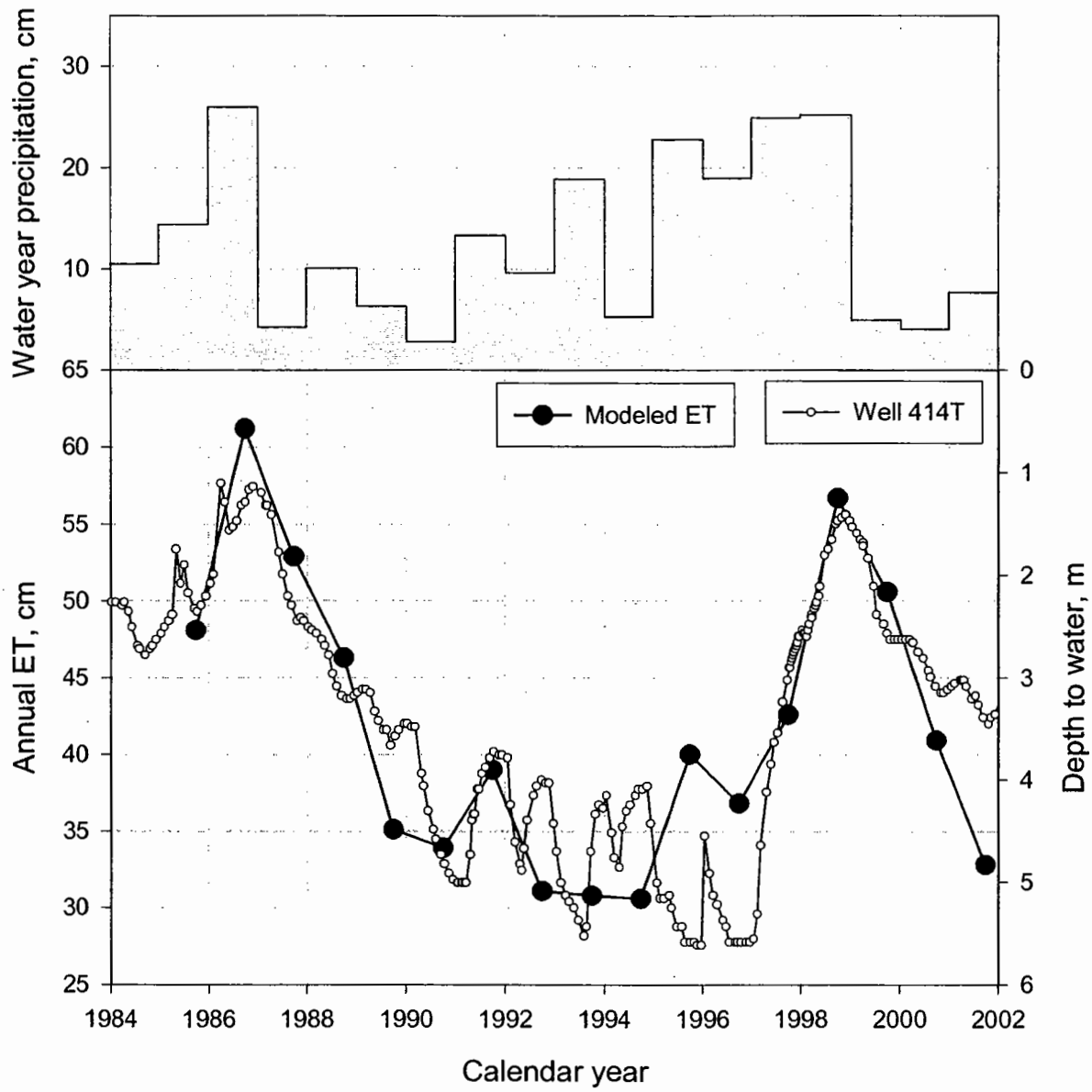

Figure 5. Example of the time series of ET, depth to groundwater, and precipitation for one site instrumented with an eddy covariance tower.

vegetation cover type. Such methods are efficient where there are no preexisting vegetation maps, but if such maps can be constructed or are available from preexisting work, this method allows such information to be used. The parameters required by the MODFLOW ET package are maximum ET rate, ET surface elevation, and ET extinction depth. T_{poly} represents well-watered vegetation at the cover estimated from the imagery, which is analogous the maximum rate required by MODFLOW. However, drought stress or pumping reduces vegetation cover, and the remotely-sensed cover for the early 1990's represents drought stressed vegetation, not well watered vegetation. Alternatively, the computed ET could be considered the actual ET rate. While this could be implemented in MODFLOW, it removes the feedback between ET rates and water table fluctuations. It is presently unclear whether ET as computed above best serves as the maximum ET rate or the actual ET rate. Figure 5 suggests that it may be more correct to treat the computed ET as the maximum rate consistent with the assumptions in the transpiration coefficients of well watered conditions This would allow for reduced actual ET when the water table is deeper than the plant rooting zone, but resolution of this question will require experimentation with the groundwater model that was beyond the scope of this component of the project.

This method presumes that relatively detailed information about vegetation community composition is efficacious for computing regional ET. It may be the case that a coarser scheme of vegetation classification (e.g., groundwater dependent meadow or groundwater dependent scrub) would provide a simpler or more robust method of computing ET.

Remote sensing ET map. The ET map for the SEBAL analysis is presented in Figure 6. Most of the phreatophytic vegetation on the valley floor transpired less than 3mm day^{-1}. Areas

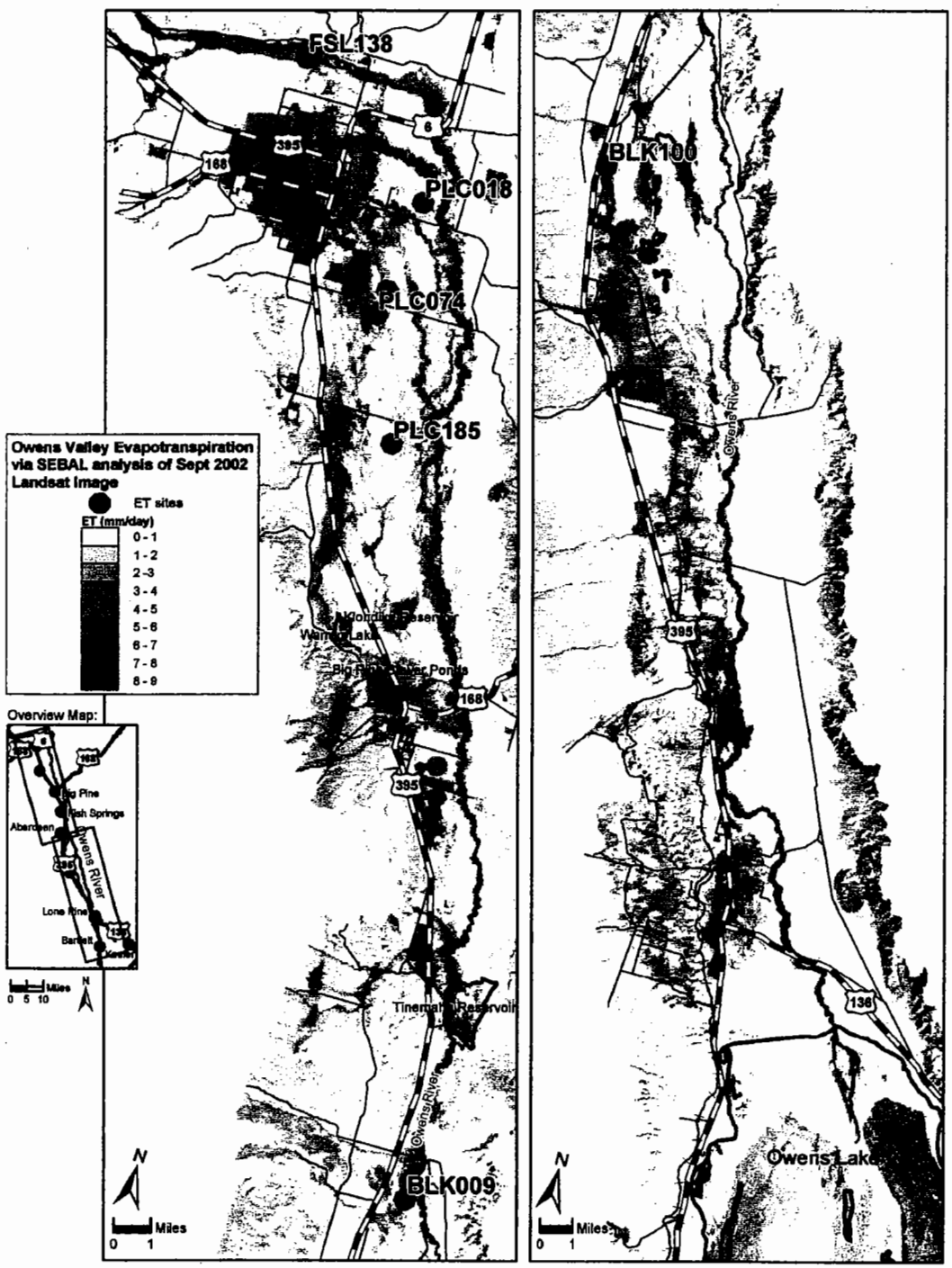

Figure 6. Map of daily ET for September 12, 2002 derived using SEBAL.

Table 4. ET calculated by SEBAL remote sensing algorithm and measured. EC ET is eddy covariance ET corrected for energy imbalance for September 12, 2002.

Site	SEBAL ET (mm/day)			EC ET (mm/day)
	EC site pixel	mean of 9 pixels	mean of 25 pixels	
FSL138	3.0	3.0	3.1	3.0†
PLC018	0.5	0.6	0.6	0.2
PLC074	2.3	2.6	2.7	0.6
PLC185	0.4	0.3	0.3	0.5
BLK100	2.0	2.0	2.0	1.8

†: estimated value as described in the text.

of expected higher ET such as the riparian areas adjacent to the Owens River and creeks emanating from the Sierra Nevada and irrigated lands were clearly distinguished by the SEBAL algorithm. SEBAL produced relatively high ET estimates along the White/Inyo Mountain front (east side) and on rock outcrops on alluvial fans on the west side of the valley. Vegetation in these locations probably was senescent this late in the summer suggesting that additional research is need to examine the application of SEBAL for areas of high relief and/or shade. Four of the five EC stations were operating on the date the LandSat data were collected, September 12, 2002. The EC station at FSL138 ceased functioning on September 5, 2002 preventing a direct comparison of the methods. ET at the EC station was estimated for September 12 based on CIMIS ETr and the average site-scale Kc for the 5 days preceding station malfunction (0.61 ± 0.04).

Table 4 compares ET measurements on the ground with eddy covariance towers with ET estimates from SEBAL. The agreement between ET ground measurements and ET SEBAL estimates was very good for both high and low transpiration sites except for PLC074. The large

difference between the ET ground measurement and ET SEBAL was probably due to the spatial resolution of the thermal band of LandSat 7. The thermal band has a pixel size of 60×60 m, and even after careful georeferencing of a LandSat image, the true location of any given pixel may be within two or three pixels of the location on the image. For site PLC074 a shift of two pixels (120 m) to the west would include an irrigated area not sensed by the tower measurements, while a similar shift to the east would encounter depression with slightly higher cover of grasses. Both these areas probably had a higher ET than the footprint sensed by tower and, thus, the SEBAL ET overestimated the true ET. The data in Table 4 support this argument since the ET values are increasing when averaged over a larger area around the tower (from 1 to 9 to 25 pixels); the larger the area of averaging, the more irrigated or riparian land was included increasing the SEBAL derived ET estimate.

Especially encouraging were the SEBAL ET estimates of sites FSL138, BLK100, and PLC185 that were very close to the ET ground measurements. This result together with results in the riparian areas of the Middle Rio Grande Valley by Dr. Hendrickx's group indicate that SEBAL may be a reliable method for determination of ET in areas with phreatophytic and riparian vegetation. For future testing of SEBAL in the Owens Valley, it is recommended to locate the eddy covariance towers in locations that cover a sufficiently large homogeneous area to eliminate the problems with georeferencing of the thermal band.

ET depth function

Several multiple linear regression models were developed to explore the relationship between vegetation cover, depth to water table and precipitation. Total plant cover was used as the independent variable as a surrogate quantity related to ET (Nichols, 2000). Transpiration

Table 5. Correlation (r) matrix for winter precipitation (October 1 to April 1) measured at seven stations maintained by LADWP in the Owens Valley for 1986-2001.

	Bishop	Tinemaha	Intake	Independence	Alabama gates	Lone Pine	Big Pine
Bishop	1						
Tinemaha	0.93	1					
Intake	0.92	0.92	1				
Independence	0.90	0.95	0.86	1			
Alabama gates	0.93	0.86	0.92	0.84	1		
Lone Pine	0.90	0.84	0.89	0.81	0.98	1	
Big Pine	0.94	0.95	0.90	0.96	0.85	0.82	1

estimates determined using methods described above were not used as the independent variable for this initial analysis because those values are linearly related to plant cover (Steinwand et al., 2001) and because the accuracy of those estimates is under investigation as part of this study.

Development of appropriate dependent variables required exploration of various transformations of the raw data. Plant cover at each site would be expected to respond uniquely to changes in the driving variables because of differing vegetation, soil, and antecedent groundwater conditions. Simply relating depth to water and precipitation with plant cover for sites with a widely varying range of characteristics was not successful. Site specific response could be addressed by preparing models for each location, but the relatively small data sets and lack of replicated measurements makes this a questionable practice. Also, it would be much simpler to incorporate a generalized relationship into the groundwater model. Several strategies were implemented to address the problem of site specificity. Plant cover the previous year was added as a dependent variable and the DTW was standardized to produce a variable with zero

mean and standard deviation equal to 1 (Snedecor and Cochran, 1988). Cover and depth to water data were site specific, but precipitation stations were not located at all sites. The appropriate scale to average the precipitation variable was examined by preparing a correlation matrix of precipitation at the seven locations. Winter precipitation was correlated for all pairs of gauges (Table 5) suggesting little advantage to using data from an individual gauge in favor of a spatially aggregated average for the valley.

Several multiple linear regression models were attempted using various combinations of transformed dependent variables. This work is considered preliminary, but the results were promising. For sites located in wellfields, the tentative relationship developed is given below,

$$Cov = 0.66 * Cov_{prev} + 0.83 * Ppt - 1.38 * DTW_{stand} - 2.48 \quad (8)$$

where Cov is total vegetation cover (%), Cov_{prev} is total vegetation cover the previous year, Ppt is average valley winter precipitation, and DTW_{stand} is standardized DTW. Model coefficients were rational, e.g. increasing DTW corresponds with lower predicted cover. The model accounted for 62% of the variance ($r^2 = 0.62$), and all regression coefficients were significant ($p<0.05$). A similar model was developed for control areas, but as expected, the pumping variable was not significant. Work on this modeling effort continues, including using estimated T as the independent variable and revision of the DTW variable to include threshold values.

Conclusions

In general, the post-audit confirmed the conclusions stated in WSP2370-H that the primary influence in most areas of the valley is pumping. The effect of recharge is most evident on the alluvial fans and in regions such as Laws with less confined aquifers. The scenarios

demonstrated that pumpage tends to have a localized short-term effect, whereas recharge has a more diffuse, long-term effect. The post-audit results successfully simulated the drawdown due to the high pumping of 1987 through 1990 and the subsequent period of recovery. The time frame for response of the groundwater system which was identified in WSP2370-H to be on the order of five to ten years is supported by the transient simulations. This means that there may be a lag of as much as a decade for the system to fully respond to changes in either the natural hydrologic inputs such as runoff or evapotranspiration or human management of pumping and recharge.

Alternative 1 in WSP2370-H examined continued operations at 1988 pumping levels, or about 141,000 acre-feet of pumping, which was substantially more pumping than the 60,000 to 90,000 acre-feet that occurred during the post-audit period. It was noted in WSP2370-H that one of the greatest uncertainties in the results stated in WSP2370-H was how groundwater management would evolve in the future. Alternative 3, which examined increases or decreases in pumping, predicted that groundwater extraction (including 8,000 to 10,000 acre-feet of artesian flow) would have to be approximately 75,000 acre-feet to maintain 1984 groundwater levels. Actual water levels during the post-audit period bear out this conclusion of WSP2370-H.

These observations suggest that the model can continue to be useful in critiquing proposed changes in water management and bracketing the likely long-term effects that will result. Identifying these hydrologic effects by actual monitoring may be difficult or impossible because of the commingling effect of other stresses and the widespread presence of hydrologic buffers as described in WSP2370-H.

This effort has resulted in several significant achievements. The model now simulates

conditions in the basin from 1963 to 2002 in the same manner as it had for the original calibration period (1963-1988). Performance of the model over this extended period was shown to be similar to the original calibration period. The five scenarios examined in this effort generally corroborated the results of Danskin (1998). Water balance components were separated into separate custom MODFLOW packages, including separation of pumped and flowing wells. Future work to enhance the use of the model falls into three categories: refinement of historical data, testing of additional future scenarios, and revision of the model itself.

Refinement of historical data. During development of the simulation period 1989-2002, data for some years had to be estimated from adjacent years, in particular for groundwater recharge. The cumulative effect of these estimates is not believed to significantly alter model performance, at least at the valley-wide scale. It seems likely, however, that credibility of the model would be enhanced by taking additional effort to find specific annual values and to resolve differences between data used in WSP2370-H and that used in the post audit. Other historical input data that may be refined are the flow/recharge regression relationships that determine stream channel recharge, and spatially varying evapotranspiration parameters.

Testing of additional future scenarios. Prior to making any changes in the model code, it may be efficient to test additional future scenarios of interest to Inyo County, LADWP, or others. The scenarios evaluated as part of the post-audit were developed with the goal of testing model sensitivity and the conceptualization of the general hydrologic system, rather than with the goal of evaluating any specific management plan.

Revision of the model. Significant enhancements to the MODFLOW computer code have been made since the original valley-wide model was developed. These improvements include a

more accurate way to simulate faults, streams, and reservoirs, and efficient methods for extracting local sub-models from regional models. Application of these capabilities will likely allow for an improved ability to critique management alternatives and inspect the effect of management changes.

Two methods to construct estimates of spatial ET were developed by this project. A series of ET maps for the post audit period was developed by combining field vegetation measurements, remote sensing measurements of plant cover, empirically derived transpiration coefficients, and transpiration estimates from the scientific literature. These maps can be readily converted into the MODFLOW application to test the sensitivity of the groundwater model to different ET estimates. Future work will be to repeat the transient model simulations for the post-audit period using the new spatial ET estimates and compare those results with the simulations prepared during this study. While not contemplated in the original proposal, the interest generated by the field ET measurements collected by this study and the ongoing cooperative study with LADWP prompted testing of the remote sensing algorithm SEBAL to estimate ET in the Owens Valley. Based on the promising initial results presented in this report, Dr. Hendrickx, New Mexico Technical Institute is seeking additional funding to further test this method in Owens Valley. His group also is processing additional LandSat scenes from 2002 to prepare additional comparisons with the EC groundtruth measurements from this study. Further research will refine the SEBAL method and test whether SEBAL results can be combined with reference ET measurements to develop Kc models to estimate seasonal or annual ET rates.

Field ET investigation

Introduction

There are several methods of measuring ET using micrometeorological measurements (Brutsaert, 1982; Shuttleworth, 1993). All micrometeorological methods measure variables near the land surface (i.e., a few meters above the plant canopy) to determine fluxes of energy, momentum, or trace gases. Micrometeorological methods have been used in previous cooperative studies to measure water vapor fluxes from phreatophytic vegetation (Duell, 1990; Gay, 1992; Duell, 1992; Stannard, 1992), but these measurements were not made concurrently with the necessary vegetation cover measurements to undertake the comparison between micrometeorological results and estimates based on vegetation cover measurements and transpiration coefficients.

The micrometeorological method used in this project was the eddy covariance (EC) method. The eddy covariance method has gained predominance among micrometeorological methods recently because of its minimal theoretical assumptions and improved instrumentation (Shuttleworth, 1993). An advantage of the eddy covariance method is that it is the most direct measurement of sensible and latent heat fluxes that is possible with micrometeorological methods. Inyo County and LADWP have jointly conducted a study to collect eddy covariance ET measurements to compare with transpiration coefficient models in Steinwand et al. (2001) and in the Plan. Because of the similar study design, data from the LADWP funded equipment are included in this report.

The purpose of this task was to measure ET using micrometeorological methods to provide an independent measurement for comparison with estimates from existing transpiration

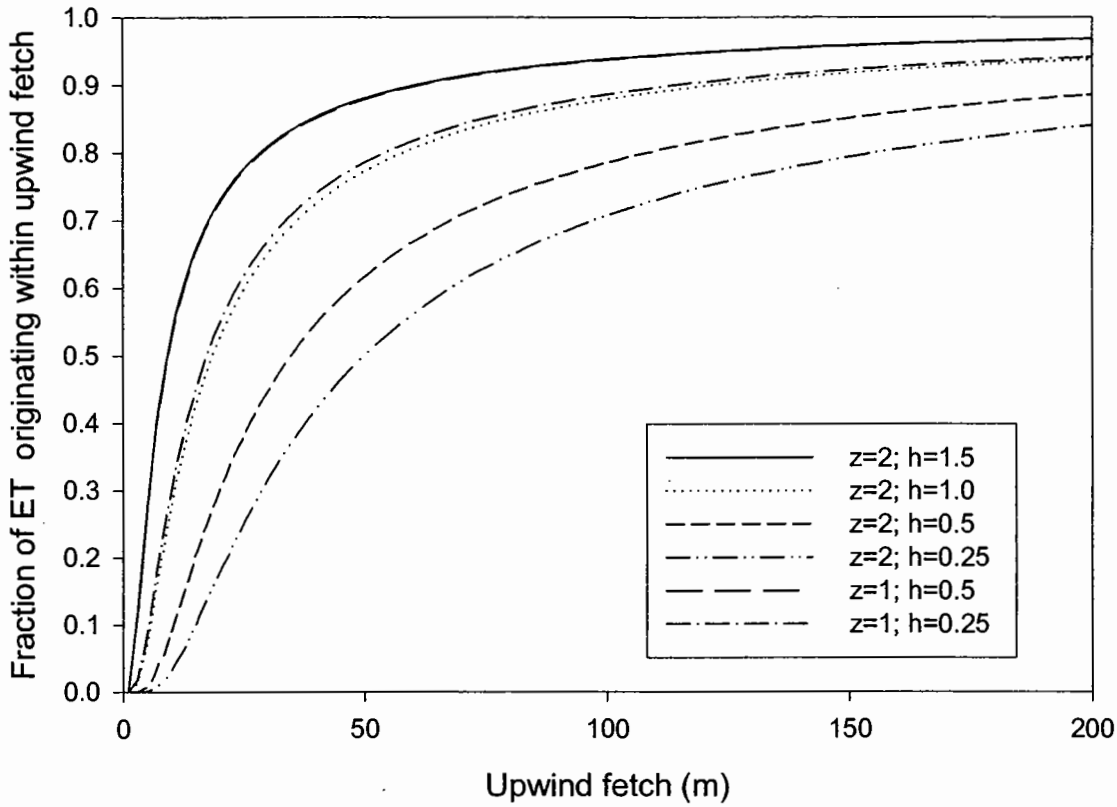

Figure 7. Approximate contributing area upwind of an eddy-covariance stations in unstable conditions according to Gash (1986). Reasonable values were assumed for roughness height, stability, wind speed, and zero-plane displacement; z is instrument height and h is canopy height.

coefficients.

Materials and Methods

Site selection

Sites were selected based on species composition, depth to the water table, and fetch. EC stations were placed in both mixed and monocultural sites ranging from alkali meadow to scrub sites. Except for PLC018 and PLC045, the intent was to select sites with DTW sufficient to

Table 6. Eddy covariance site characteristics. Range of depth to water during the growing season is given. Precipitation values are annual totals beginning October 1 the previous year. Except for PLC45, April to October rain was less than 15mm.

Year	Site	Vegetation type	Dominant Species†	Depth to water	Precipitation
				(m)	(mm)
2000	BLK 100	alkali meadow	SPAI, DISP	2.0-2.5	35.6
2001	BLK 100	alkali meadow	SPAI, DISP	2.2-3.0	71.1
	BLK 9	rabbitbrush meadow	CHNA, SPAI	2.6-3.2	71.1
	PLC 45	Nev.saltbush scrub	ATTO	3.8-4.1(est.)	105.9
2002	BLK 100	alkali meadow	SPAI, DISP	2.3-3.2	32.5
	FSL 138	alkali meadow	DISP, LETR, SPAI	1.2-2.1	21.8
	PLC 18	rabbitbrush scrub	CHNA	>5.0	34.5
	PLC 74	Nev. saltbush meadow	SAVE, ATTO, DISP	2.1-2.4	31.5
	PLC 185	desert sink scrub	SAVE	>4.0	31.5

†grasses: SPAI, *Sporobolus airoides;* DISP, *Distichlis spicata;* LETR, *Leymus triticoides.* shrubs*:* CHNA, *Chysothamnus nauseosus;* ATTO *Atriplex lentiformis* ssp. *torreyi;* SAVE, *Sarcobatus vermiculatus.*

subirrigate the vegetation, but deep enough to minimize surface evaporation. This provision was to allow valid comparisons of measured ET (i.e. minimize E) with the vegetation-based transpiration estimates. Methods in Gash (1986) were used to estimate the size of the potential area contributing to the EC measurements to guide selection of sites (Figure 7). Sites with obvious boundaries between dissimilar vegetation and hydrologic conditions within approximately 150 m of the site were avoided. All the sites were undisturbed by water spreading or irrigation.

Locations of the EC sites is shown on Figures 8 to 14, and environmental characteristics of the sites are summarized in Table 6. Each EC tower was fenced to prevent range cattle from

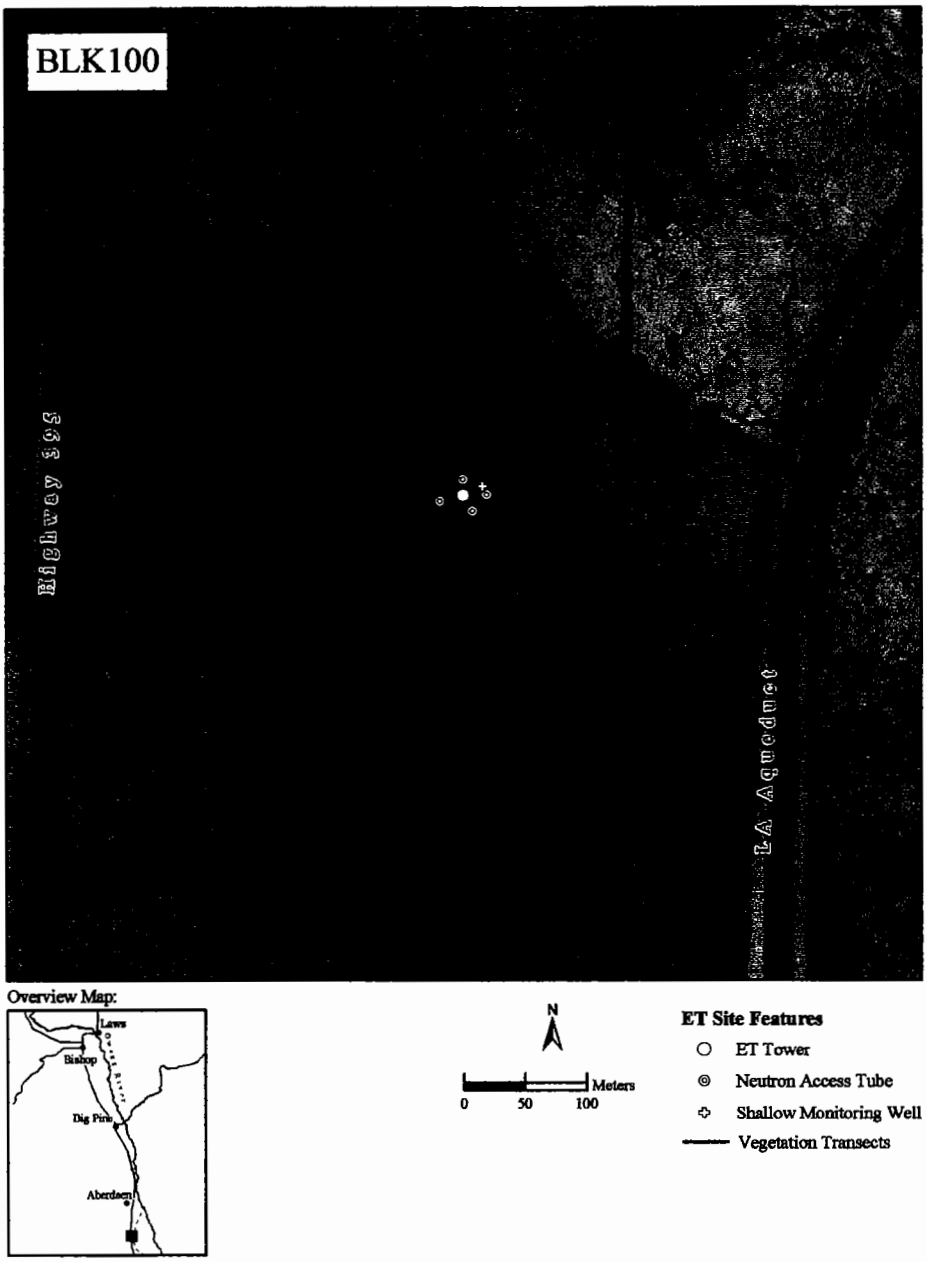

Figure 8. Aerial photograph and measurement locations for ET, soil water, and LAI BLK100.

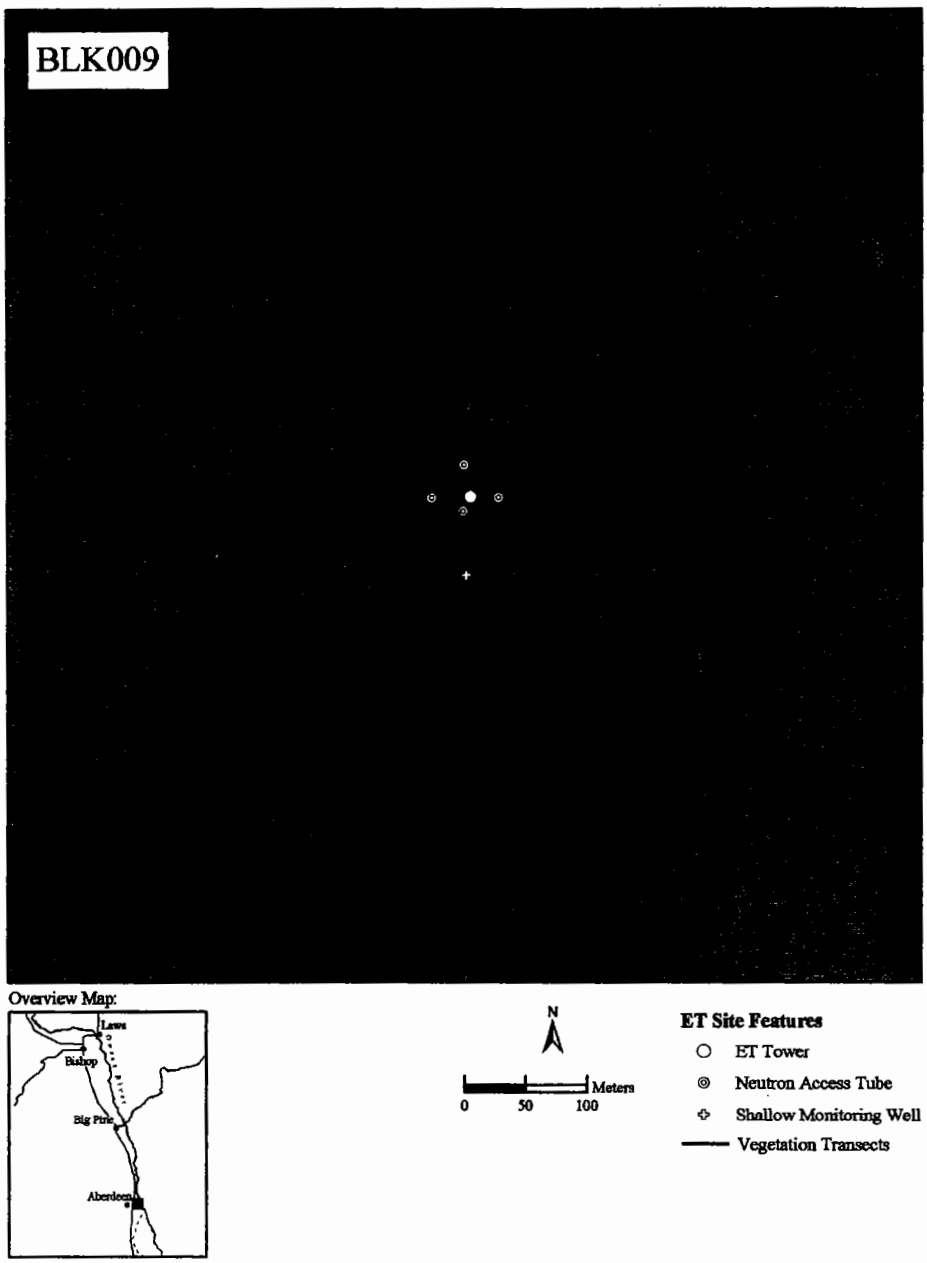

Figure 9. Aerial photograph and EC, soil water and LAI measurement locations at ET site BLK9.

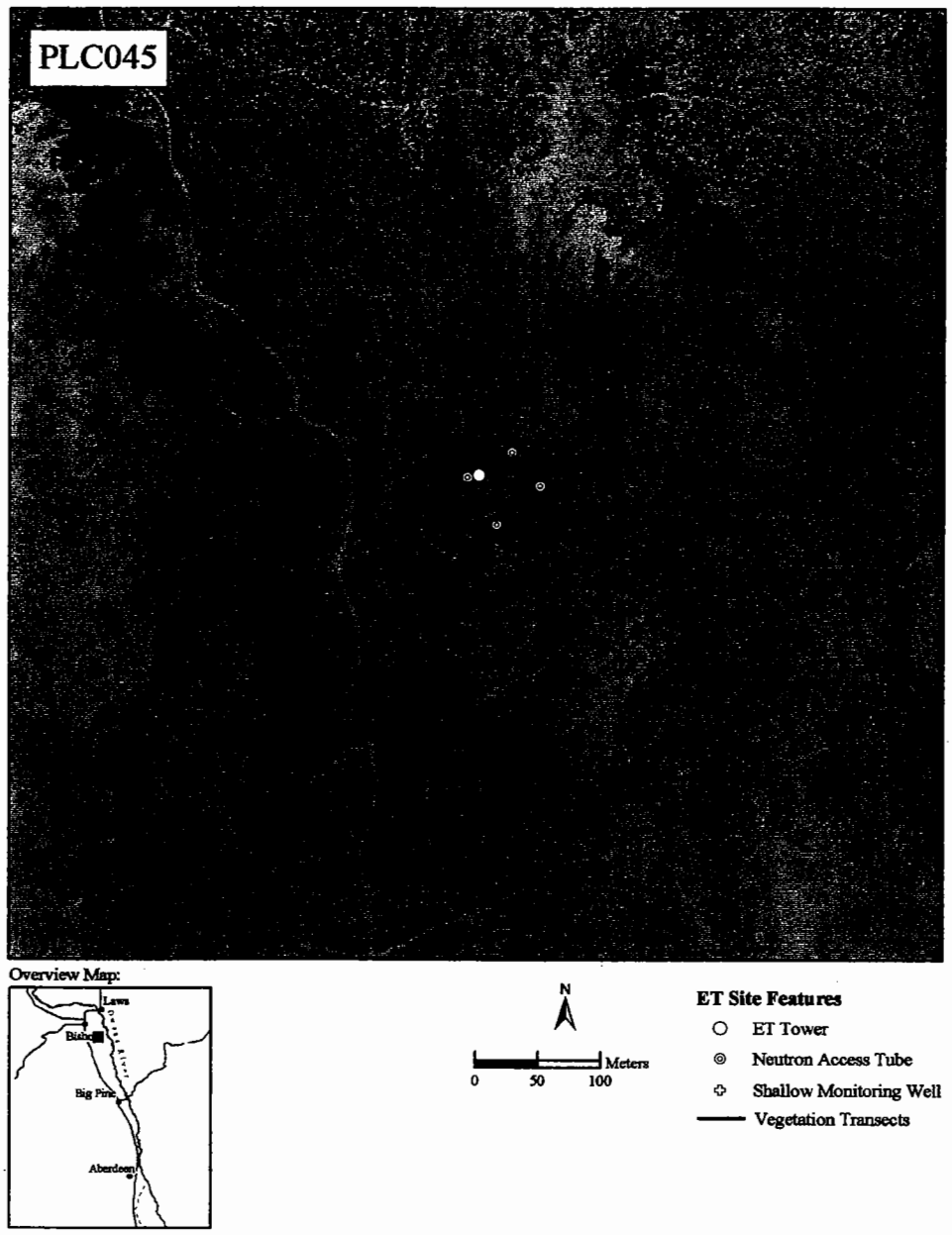

Figure 10. Aerial photograph and EC, soil water and LAI measurement locations at ET site PLC045.

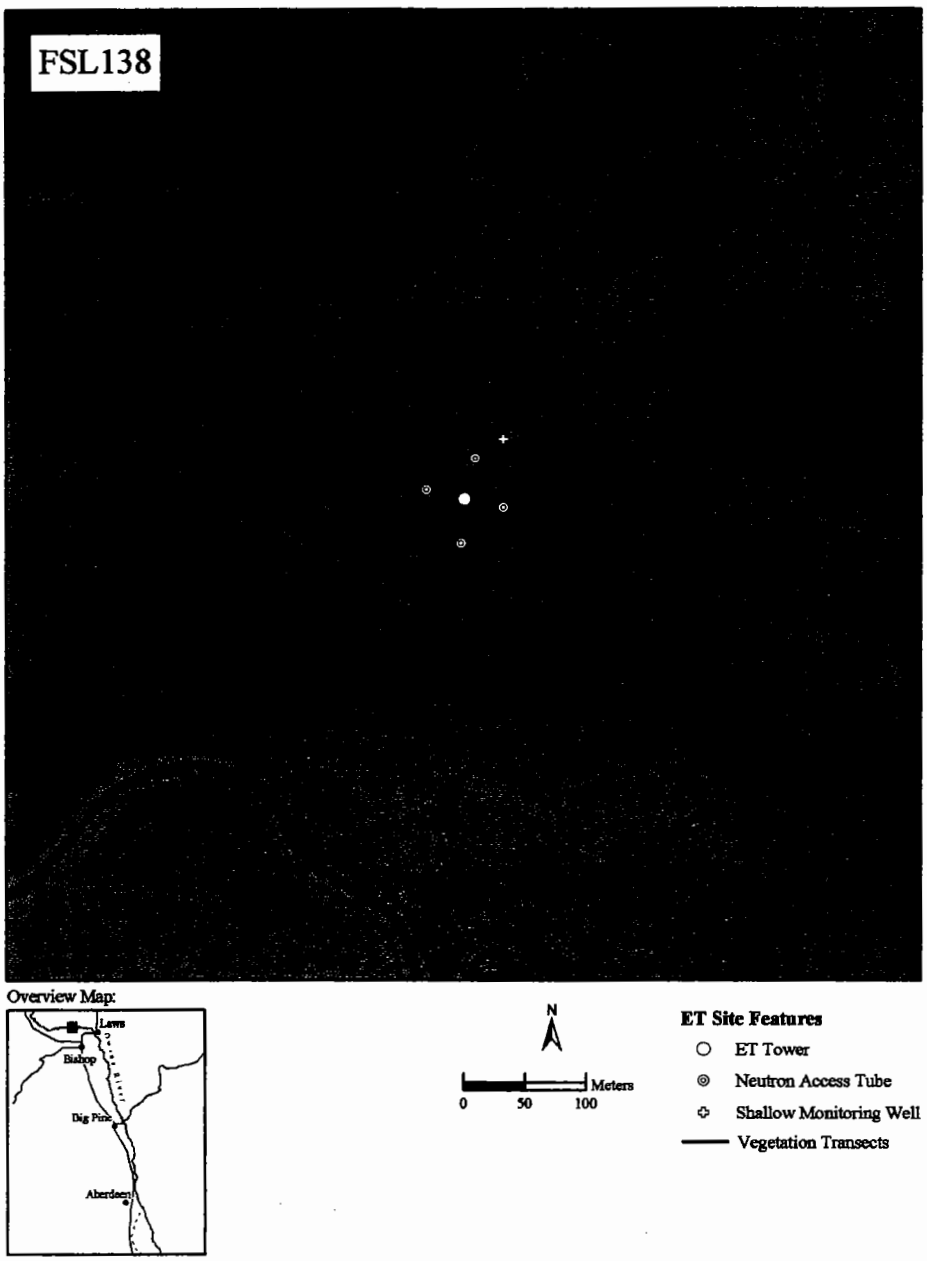

Figure 11. Aerial photograph and EC, soil water and LAI measurement locations at ET site FSL138.

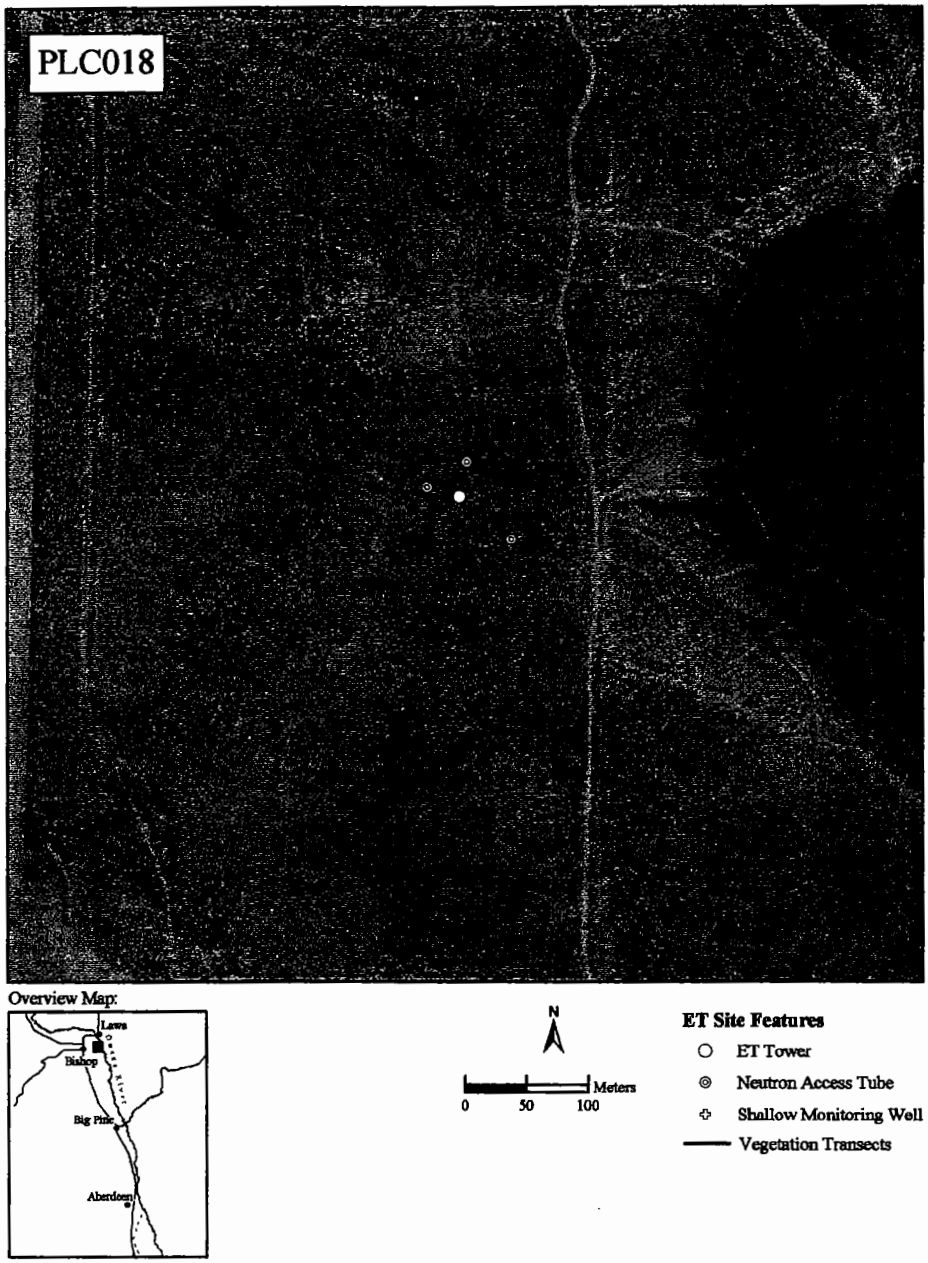

Figure 12. Aerial photograph and EC, soil water and LAI measurement locations at ET site PLC018.

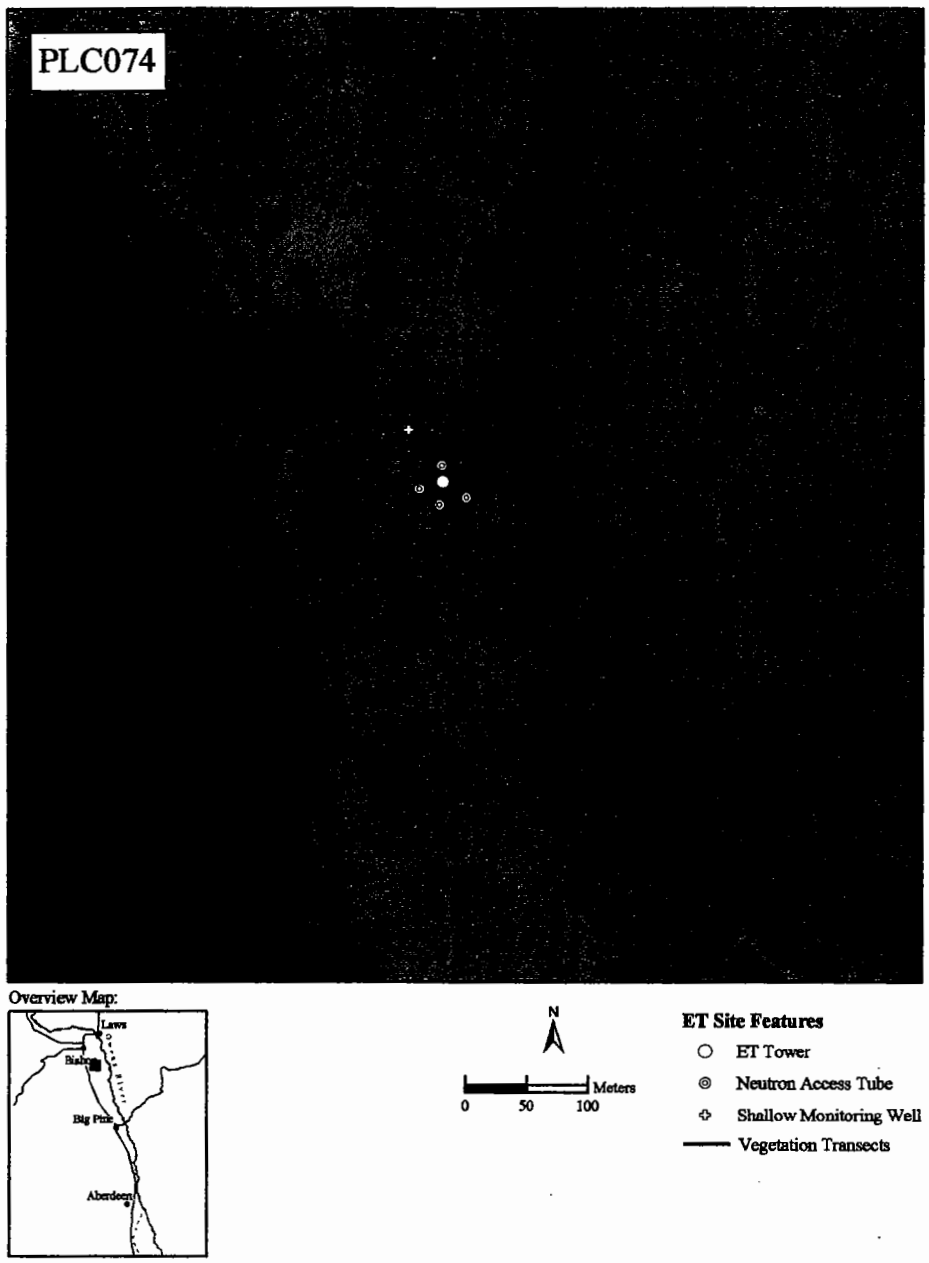

Figure 13. Aerial photograph and EC, soil water and LAI measurement locations at ET site PLC074.

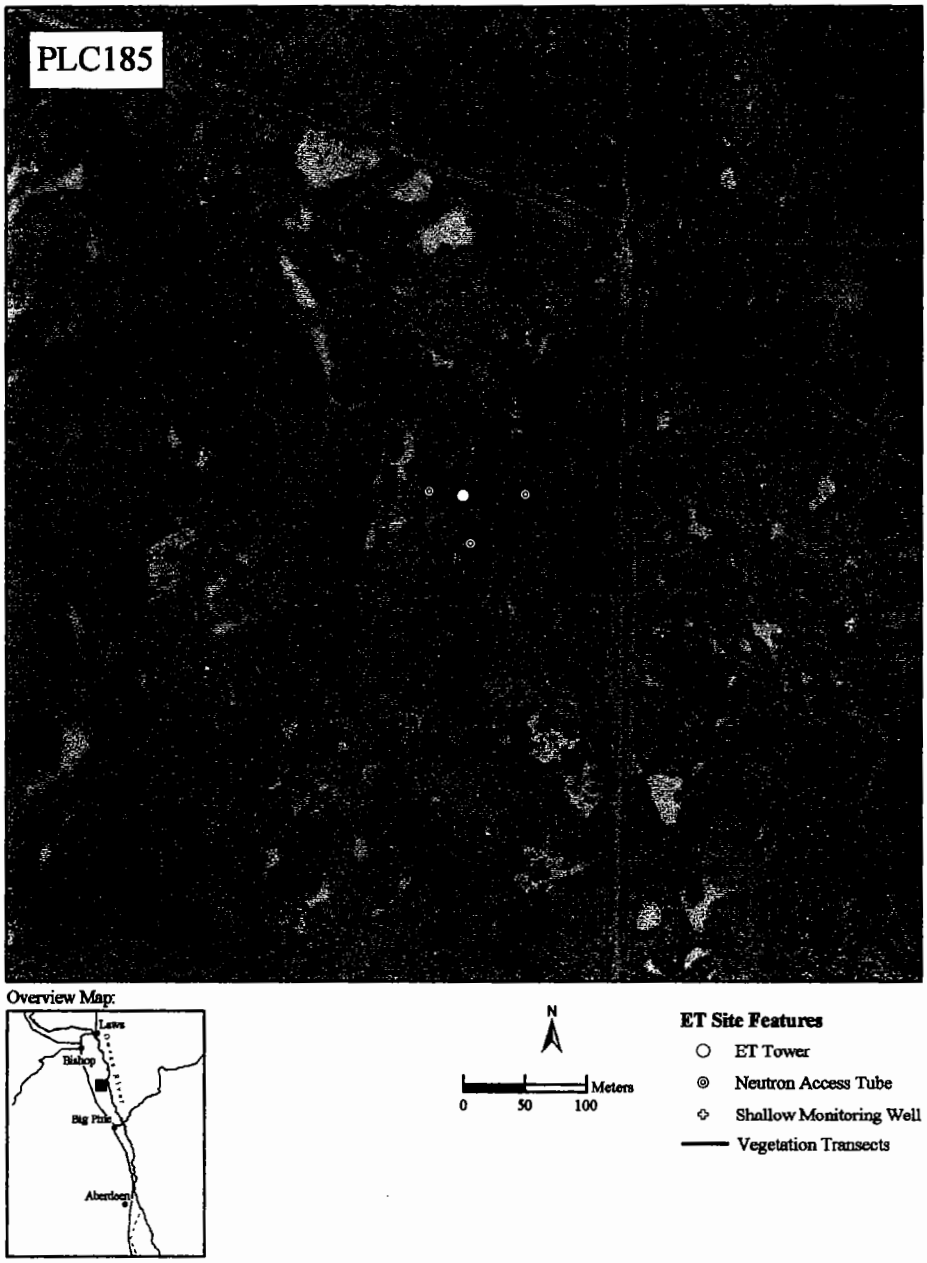

Figure 14. Aerial photograph and EC, soil water and LAI measurement locations at ET site PLC185.

Table 7. Dates of EC station operation.

Year	Site	Date established	Date removed
2000	BLK 100	April 21	January 8, 2001
2001	BLK 100	March 7	November 27
	BLK 9	April 11	November 27
	PLC 45	April 10	November 27
2002	BLK 100	March 12	October 2
	FSL 138	May 3	September 11
	PLC 18	May 2	October 8
	PLC 74	May 25	October 7
	PLC 185	May 24	October 7

damaging the instruments. The fenced exclosure at BLK00 was expanded in 2001 to include the vegetation because of observed grazing impacts adjacent to the tower exclosure late in the growing season and over winter. Table 7 shows the dates ET measurements began and ended each year. In all years, EC measurements encompass the majority of the growing season, approximately March 25 to October 15.

Eddy covariance instrumentation and theory

The EC method of measuring turbulent fluxes uses fast response sensors to measure rapid changes in vertical wind speed and scalar quantities (e.g. water vapor density or air temperature) to compute the flux of the scalar by means of the covariance between the vertical wind and the scalar (Arya, 2001). The latent heat flux is,

$$\lambda E = ET = \lambda \overline{w' \rho_v'} \tag{9}$$

and the sensible heat flux is,

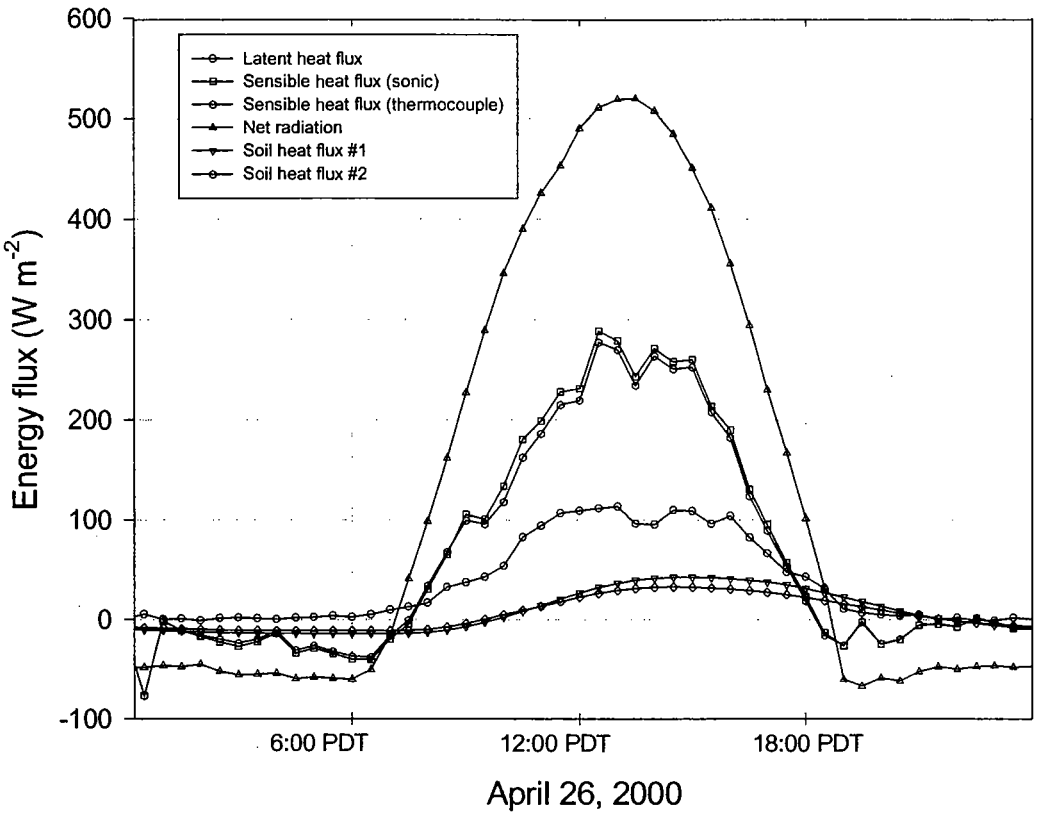

Figure 15. Energy balance components measured at BLK100.

$$H = \rho C_p \overline{w'T'} \tag{10}$$

where w is the vertical wind speed (m s^{-1}), ρ_v is the water vapor density (kg m^{-3}) , ρ is the mean air density (kg m^{-3}), C_p is the specific heat of air (J kg^{-1} K^{-1}), T is the air temperature (primes indicating deviations from the time-averaged mean). The vertical wind speed was measured with a Campbell CSAT sonic anemometer (Campbell Scientific Inc., 1998a), the water vapor density

was measured with a Campbell KH20 krypton hygrometer (Campbell Scientific Inc., 1989), and air temperature was measured using a fine-wire thermocouple, all of which were mounted 2.5 m above the land surface. Sensible heat flux was calculated using both the temperature as calculated from the sonic anemometer and as measured by the fine wire thermocouple, and the two methods had close agreement at BLK100 (Figure 15). The fine wire thermocouples were replaced repeatedly due to breakage which resulted in an intermittent record; therefore, the sonic temperature was used in calculating the seasonal sensible heat flux. The data were acquired and the covariance computed at 10 Hz, and fluxes were averaged over 30 minute intervals. The EC system has the advantage that the computed covariance theoretically provides a direct measure of the scalar flux at the point of measurement. Difficulties in the EC method arise in the demands made on the instrumentation to acquire data at the necessarily rapid sampling rate, and the fact that the measurements in practice are non-collocated volume averages rather than collocated at a point as assumed by Equations 9 and 10.

The EC measurements were corrected for absorption of the krypton hygrometer ultraviolet beam by oxygen (Campbell Scientific Inc., 1998b), and for the effect of fluctuating air density (Webb et al., 1980). These corrections were implemented as,

$$\lambda E = \lambda\left(\overline{w'\rho_v'} + \frac{\rho_v H}{\rho C_p T} + \frac{F k_0 H}{k_w T}\right) \tag{11}$$

where F is a factor to account for the fraction of oxygen in air (gm K J^{-1}), k_o is the oxygen absorption coefficient (0.0045 m^3 gm^{-1} cm^{-1}), and k_w is the water vapor absorption coefficient (0.154 m^3 gm^{-1} cm^{-1}). The first term in the parentheses is the uncorrected EC vapor flux, the second term corrects for fluctuations in air density, and the third term corrects for the effect of

oxygen on the krypton hygrometer.

Though not necessary to make the EC estimate of turbulent fluxes, the EC system was also equipped with a REBS Q-7.1 net radiometer (Campbell Scientific Inc., 1996a), soil heat flux plates (Campbell Scientific Inc., 1999), soil temperature sensors, and a frequency domain reflectometer (Campbell Scientific Inc., 1996b) for measuring soil wetness. These additional instruments allow the energy balance to be computed. Two soil heat flux plates were installed at a depth of 8 cm a few feet apart, and soil temperature thermocouples were installed at depths of 2 and 6 cm between the flux plates. The soil heat flux at the soil surface was computed by correcting the heat flux at the flux plate for thermal storage in the soil above the flux plates,

$$G = G_z + \Delta z \frac{\Delta T}{\Delta t}\left(C_w \theta_v \rho_w + \rho_b C_s\right) \tag{12}$$

where G_z is the average of the two flux plates (W m^{-2}), Δz is the depth of the flux plates, ΔT is the average change in temperature of the two soil temperature thermocouples (C^o), Δt is the time interval over which the flux is averaged (s), C_w is the specific heat capacity of water (4.18 J g^{-1} K^{-1}), θ_v is the volumetric soil water content (0.066 cm^3 water per cm^3 of soil), ρ_w is the density of water (1.00 gm cm^{-3}), ρ_b is the measured soil bulk density (1.11 gm cm^{-3}), and C_s is the specific heat capacity of dry soil material (0.87 J gm^{-1} K^{-1}). Soil bulk density and water content were determined by oven drying of soil samples, and the specific heat capacity of dry soil material was taken from Campbell and Norman, Table 8.2 (1998).

The sign convention adopted throughout this report is as follows: net radiation is positive when directed toward the land surface, sensible and latent heat fluxes are positive when directed away from the land surface, and soil heat flux is positive when directed into the soil.

Quality control

Several quality control measures were implemented to ensure accurate data were collected. The towers were instrumented to measure all components of the energy balance (EB) to allow an independent check of the ET measured by the EC methods using,

$$EB = Rn - G - H - \lambda E \tag{13}$$

EB should equal zero if canopy heat storage, photosynthetic absorption of solar radiation, and advective energy transport processes are negligible. EC measurements collected during this study and others (Bidlake, 2001; Bidlake 2002; Berger et al., 2001; Sumner, 1996; Duell, 1990) have found that EB does not achieve closure, with the sum of the turbulent fluxes ($H + \lambda E$) measured by the EC instruments generally being less than the available energy ($R_n - G$). Results of the analysis of Equation 13 are described more fully in a separate section below.

Post processing of the EC data included inspection of the record for anomalies in all data streams, inspection of the turbulent flux data for sonic anemometer spikes or signal losses. If more than 5% of the 10 Hz signal from the eddy covariance sensors was lost over a thirty-minute sampling interval, that interval was discarded. Routine maintenance and data downloads were done at roughly weekly intervals when the instruments were deployed. Typically, during each of these site visits, the data were downloaded, the windows on the hygrometer were cleaned, the net radiometer domes were cleaned, the sonic anemometer and net radiometer were checked for level, the solar panel was cleaned, and sensor output was examined to make sure all sensors were recording correctly. Upon the completion of measurements each season, the EC instruments

Table 8. Statistics of ET tower comparison at BLK100, alkali meadow site in 2000.

	Tower 1	Tower 2	Tower 3
mean LE flux (W m^{-2})	32.87	34.26	33.89
standard deviation	47.03	48.61	48.36
% of mean of all towers (33.67 W m^{-2})	97.6%	101.7%	100.6%

were removed from the field for return to the factory for recalibration.

During the period July to October, 2000, 62 days of data were collected where three EC systems collected concurrent ET, air temperature, and humidity measurements at BLK100. For this comparison, the instrument towers were placed about 4 meters apart, arrayed roughly perpendicular to the mean wind direction. The most significant data gaps are in the net radiation record, which lost data during the interval from day of year (DOY) 119 to 130 due to a problem with the datalogger program, from DOY 177 to 180 due to a break in the instrument cable, and from DOY 284 though 294 due to a broken radiometer dome. All three systems were powered down and instruments removed from the field during the period DOY 242-245 due to inclement weather. Short intervals of data were lost when the transducer heads of the sonic anemometer were wet due to rain. Simultaneous operation of the collocated systems showed that latent heat fluxes measured by the three systems agreed closely with one another. Table 8 compares the statistics of the latent heat fluxes measured by each system, and Figure 16, shows the 30-minute latent heat fluxes over the period September 1 through 4.

Bowen ratio instruments and theory

Energy fluxes measured by the EC system were compared to fluxes measured with a collocated Bowen ratio (BR) system to examine the EB closure problem and to develop

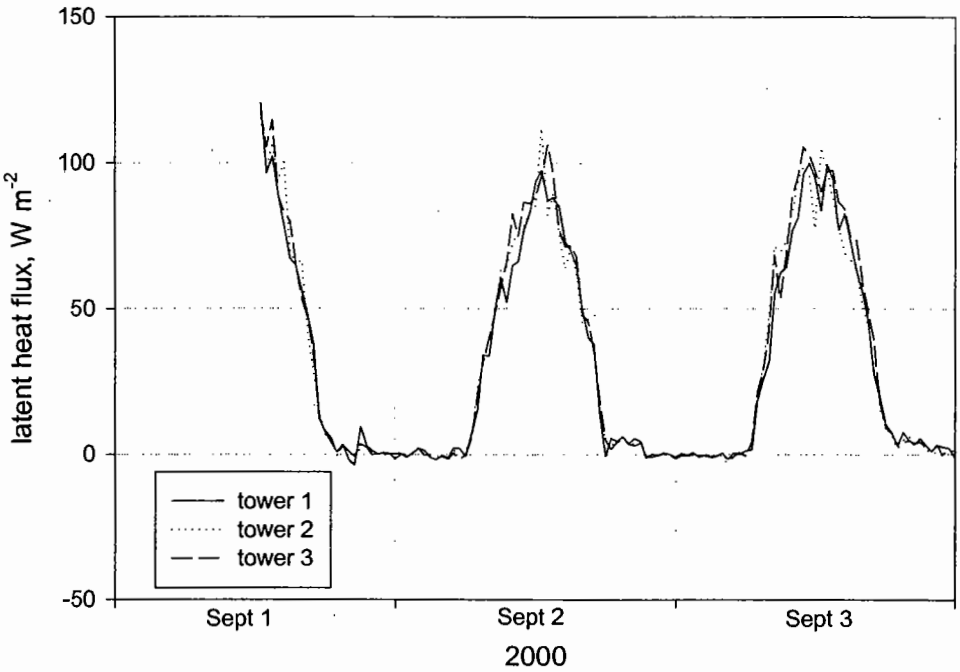

Figure 16. Latent heat flux from three collocated systems at BLK100.

recommendations for processing the EC data to estimate ET. A BR system was installed and operated by Dr. Jim Stroh, Evergreen State College, from August 23 to September 3, 2002 at BLK100. The instrument towers were located 5 m apart in an east-west alignment so wakes on the lee side of each tower would not interfere with the other tower during the prevailing afternoon southeasterly winds. The net radiometers were mounted 5 m apart and 3 m south of their respective instrument towers.

The BR methods relies on different assumptions and instrumentation than the EC to

estimate fluxes. Agreement between the two methods would strongly corroborate the results, and disagreement between the methods can help determine likely sources of error. The BR method uses measurements of water vapor density and temperature at two heights to compute theaverage gradients near the surface, and then by equating the eddy diffusivity for sensible and latent heat, uses Equation 3 and the measured Bowen ratio ($\beta = H/\lambda E$) to compute the turbulent fluxes. Beyond its use in the BR method, β is significant as a measure of the relative partitioning of available energy between sensible and latent heat. The BR system consists of fine wire thermocouples mounted at 1.0 and 2.0 m above the surface, a chilled mirror hygrometer, an air pump and routing system that alternately directs an air stream from the upper and lower sensor arms to the hygrometer, a net radiometer, soil heat flux plates, and soil temperature sensors. Fluxes were averaged over 20 minute intervals. The BR method has the advantage that the instrumentation is relatively simple compared to the EC method, but has the disadvantage that energy balance is used to compute the fluxes. The energy balance cannot be used as a check on the internal consistency of the computed fluxes, and any errors in measuring available energy affect the computation of the turbulent fluxes. The chilled mirror hygrometer has a limited range of environmental conditions under which it will function properly. In very dry conditions, very warm conditions, or very cool conditions, formation of frost on the mirror surface confounds the dew point measurement. The early fall season was chosen for operation of the BR system at this site because it was expected that conditions would be within the applicable range of the chilled mirror hygrometer. Soil heat flux was computed as described for the EC systems.

Two sources of error that are common to both BR and EC measurements are the

mismatch between the sampling areas ("footprints") of the various sensors used to compute fluxes and energy balances, and the variability of the landscape within the footprint. For example, the sonic anemometer and krypton hygrometer combine to sense water vapor flux integrated over a footprint with a radius on the order of 100 m, whereas the calculation of soil heat flux has a footprint of about a square meter. Similar mismatches of measurement areas or volumes are present in the BR instrumentation. Because the land surface properties that affect the energy balance are spatially heterogeneous, these footprint mismatches limit the precision with which the energy balance at a point can be estimated.

Soil water and groundwater measurements

Three or four access tubes were installed adjacent to the vegetation transects, usually to just above the water table. Only one access tube extended to depths below 1m at PLC045 because augered holes collapsed repeatedly in the dry, sandy soil. Access tubes were constructed of PVC except at PLC018 where aluminum tubes were used. The neutron gauge was calibrated by regressing volumetric water content (θ) of samples collected during access tube installation against neutron gauge count ratio (count/field standard count) recorded at the sampling depths. Determination of θ followed Blake and Hartage (1986) and Allen et al. (1993). Soil cores of a known volume were collected, weighed, and dried at 105 °C for 24 hrs to determine the gravimetric water content (g water/g soil) and bulk density (g soil/cm^3 soil). Volumetric water content is the product of gravimetric water content and bulk density (assuming the density of water is 1 g/cm^3). Soil water was measured biweekly during the growing season and approximately monthly in winter. Soil depths below 20 cm were monitored in 15 cm

increments. Shallow depths (0-8 cm) were monitored using gravimetric sampling. Existing on-site test wells were monitored at FSL138, PLC074, BLK009, and BLK100 (beginning in February, 2001). Nearby test wells were monitored at PLC045, and BLK100 (before February, 2001). Sites PLC018 and PLC185 were not located near test wells.

Vegetation measurements

Four 50 m transects aligned north, south, east, and west of the ET station exclosures were established at each site. Point frame measurements with 50 cm pin spacing were conducted approximately monthly, and first contacts and all contacts with green live, green leaves or stems were recorded by species to determine leaf area index (LAI) (Goodall, 1952). Plant cover was calculated as the fraction of pins that contacted at least one green leaf or stem. Contact frequency (total contacts ÷ total pins) was used to calculate LAI according to,

$$LAI = \frac{N}{K} \tag{14}$$

where N is contact frequency for a species and K is an extinction coefficient determined empirically for common Owens Valley species (Groeneveld, 1997). Extinction coefficients for species not examined by Groeneveld (1997) were assigned a value of 0.5, which was a typical value for the common species.

Comparison of EC and of Kc estimates

Transpiration coefficients are a dimensionless ratio of actual ET (in this case T) to a reference or potential ET typically determined over an irrigated grass or alfalfa reference crop. The general form of transpiration coefficients is,

$$Kc = \frac{actualET}{referenceET} \tag{15}$$

Once the Kc for a plant species (usually a crop) is known, actual ET for another site or time can be derived from measurements of reference ET by rearranging Equation 15. Transpiration coefficients take several forms based on modifications for precipitation, growing season weather, time-varying leaf area/canopy closure, or irrigation (Allen et al., 1998).

Transpiration coefficients from Steinwand (1999b) and Steinwand et al. (2001), measured *LAI*, and measured reference ET were used to calculate transpiration (T_{Kc}) using:

$$T_{Kc} = \sum_{j=1}^{n} \sum_{i=1}^{m} (Kc_{ij}\ ETr_i\ LAI_j) \tag{16}$$

where: ETr_i is reference ET for day i, n is number of species, Kc_{ij} is the transpiration coefficient for species j on day i, LAI_j is the midsummer LAI for species j. The Kc models were developed from a large database of stomatal conductance, reference ET, and leaf area index for the five most common Owens Valley plant species and assume soil water conditions are not limiting (Figures 17 and 18). ETr_i was derived at a weather station in Bishop using a modified Penman equation by the California Irrigation Management Information System. Changes in *LAI* during the growing season were incorporated during the construction of the Kc models by relying on models of daily *LAI* normalized to peak *LAI* =1.0. Hence, Equation 16 only requires a single *LAI* measurement near the peak of the growing season to adjust the Kc to provide site-specific estimates of ET. *LAI* of the dominant species at each site determined on the date nearest the maximum *LAI* in the Kc models was used in Equation 16. Dates of LAI measurements used to compute T_{Kc} are given in Table 9. LAI of minor species for which no Kc models were available

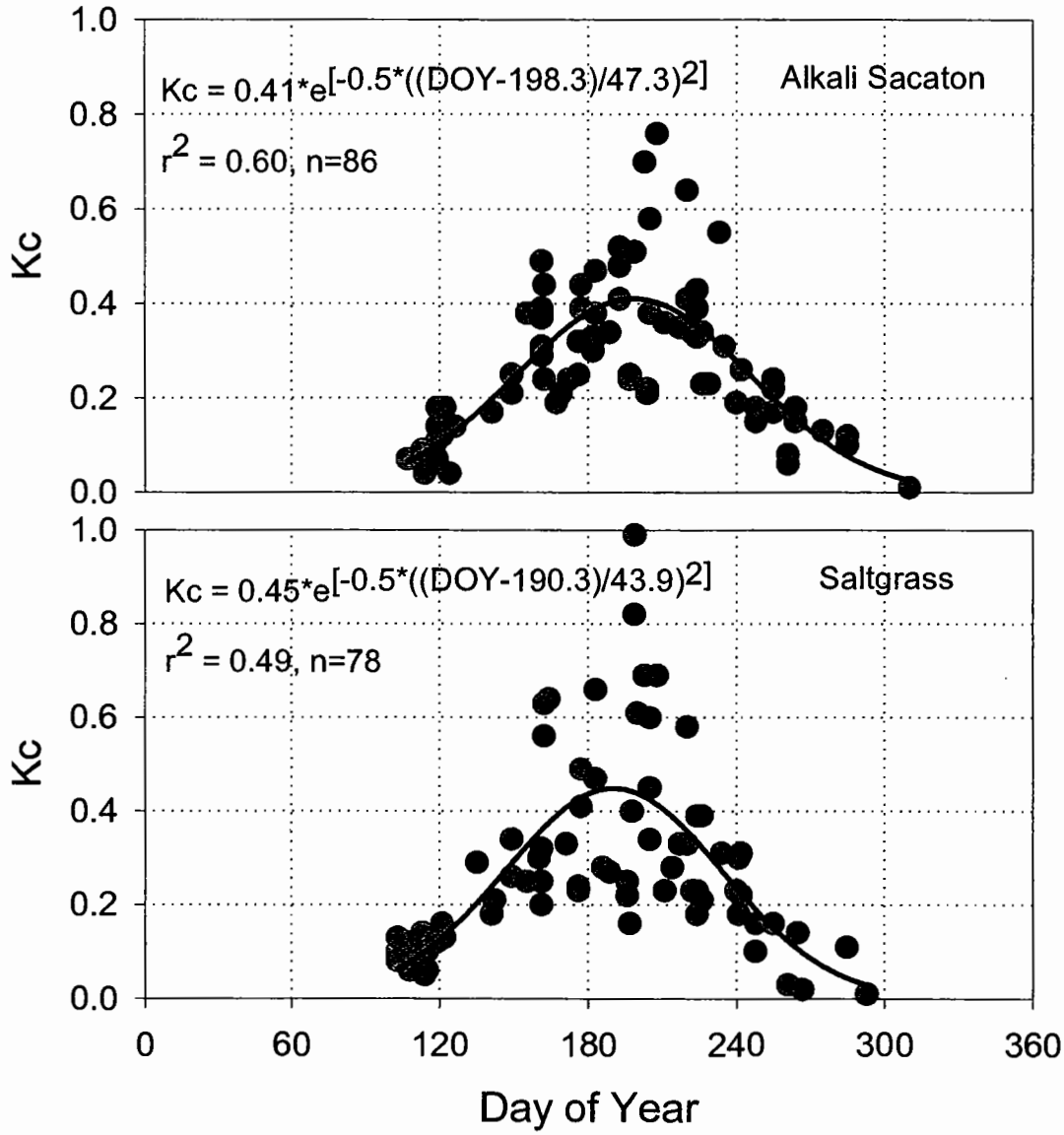

Figure 17. Transpiration coefficients (Kc_{ij}) and fitted models for saltgrass (*Distichlis spicata*) and alkali sacaton (*Sporobolus airoides*).

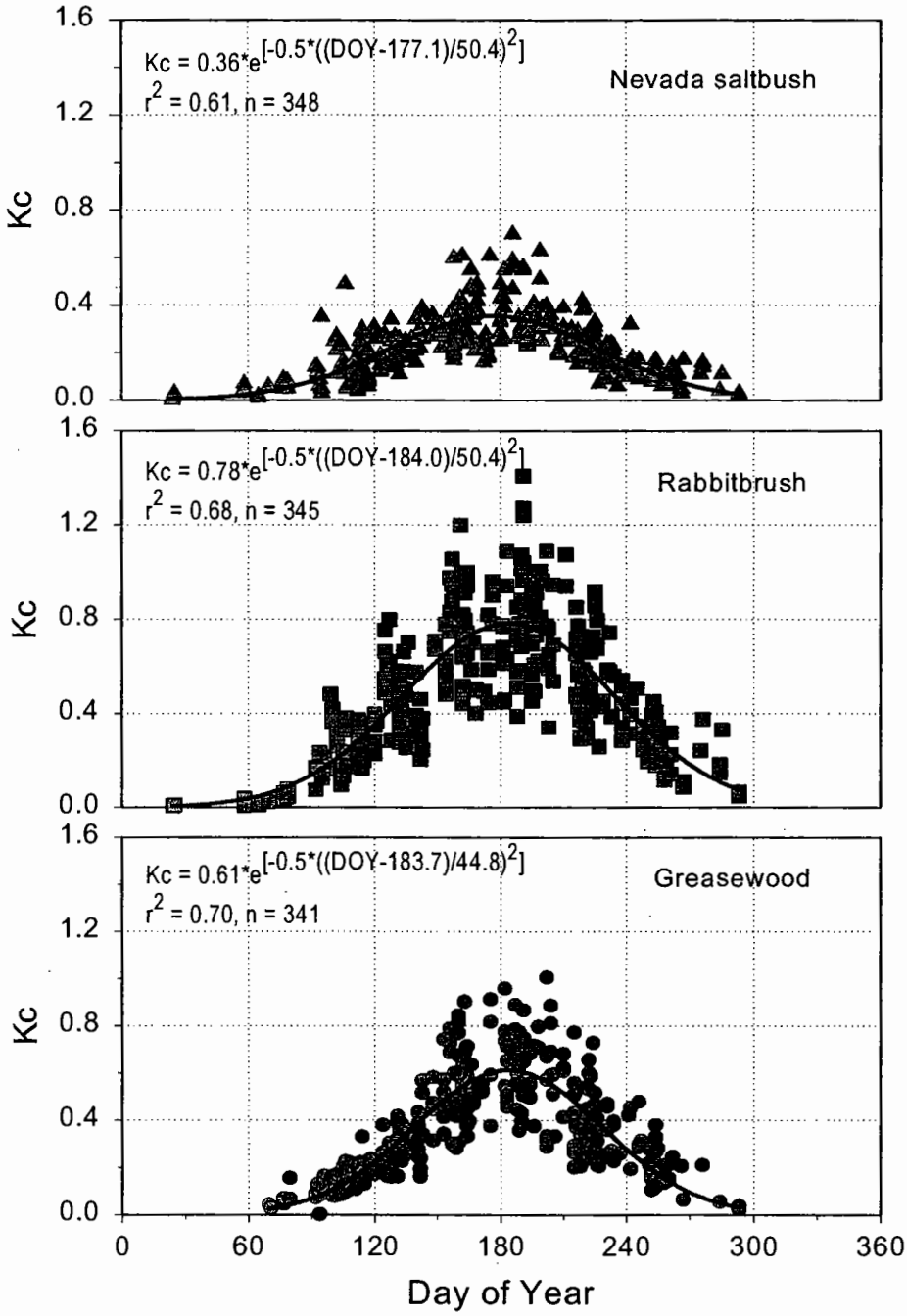

Figure 18. Transpiration coefficients (Kc_{ij}) and fitted models for Nevada saltbush (*Atriplex lentiformis* ssp. *torreyi*), rabbitbrush (*Chrysothamnus nauseosus*) and greasewood (*Sarcobatus vermiculatus*).

Table 9. Day of year for maximum LAI in the Kc models, the LAI sampling DOY used to determine T_{Kc}, and DOY of actual measured maximum LAI for the dominant species at each site.

Year	Site	Dominant species†	Kc LAI model maximum DOY	LAI sampling DOY	Measured LAI maximum DOY
2000	BLK 100	SPAI, DISP2	201, 189	189	188, 250
2001	BLK 100	SPAI, DISP2	201, 189	190	253, 220
	BLK 9	CHNA2, SPAI	184, 201	192	135, 165
	PLC 45	ATTO	163	162	162
2002	BLK 100	SPAI, DISP2	201, 189	191	217,154
	FSL 138	DISP, LETR5,JUBA	189, 201	190	190 (DISP2)
	PLC 18	CHNA2	184	190	154
	PLC 74	SAVE4, ATTO, DISP2	174, 163, 189	156	156,156,186
	PLC 185	SAVE4	174	156	128

†: grasses; SPAI, *Sporobolus airoides;* DISP2, *Distichlis spicata;* LETR5, *Leymus triticoides.* shrubs; JUBA, *Juncus Balticus: C*HNA2, *Chysothamnus nauseosus;* ATTO *Atriplex lentiformis* ssp. *torreyi;* SAVE4, *Sarcobatus vermiculatus.*

was apportioned among the species with Kc values based on their relative proportion of total LAI.

The ET record at all sites contained gaps due to instrument failure or was truncated before the end or after the beginning of the growing season. To prevent the comparison of measured and predicted fluxes from being confounded by the partial record, the EC data were fit to a Fourier model like that used to predict reference ET (ETr, described below). This model was chosen because of its demonstrated ability to model the seasonal changes in evaporative demand in the Owens Valley represented by ETr (Or and Groeneveld, 1994). Fitting the Fourier model also permitted site to site comparisons and year to year comparisons of transpiration between uniform limits for integration. Daily ET_{corr} was modeled using a Fourier series with two

harmonics using procedures described by Salas et al., (1980). ET_{corr} is the daily ET measured by the EC system corrected for the energy imbalance (described below). The first two harmonics series is given by,

$$\overline{ET_{corr}} = < ET_{corr} > + \sum_{j=1}^{2}\left[A(j)\,\mathrm{COS}(\frac{2\pi ij}{365}) + B(j)\,\mathrm{SIN}(\frac{2\pi ij}{365})\right] \qquad (17)$$

where i is the day of year, $<ET_{corr}>$ is mean daily ETr for the entire year, A(1), A(2), B(1), and B(2) are model coefficients. Occasionally the fitted model was poorly constrained and gave negative values during winter when EC data were lacking. When this occurred, daily ET was assumed to be 0.01 mm day^{-1} and the model was revised. This procedure was largely for graphical purposes. The effect on the comparison with Kc models was negligible because only the daily ET or T values during the period with ET_{corr} data or during the growing season were summed.

Results and Discussion

Site characteristics

Depth to water measured at the EC sites is presented in Figures 19 to 23. Typically, the shallowest depth to water occurred in the spring (March or April) and declined to maximum depth at end of the growing season (October). FSL138 was an exception where maximum depth to water occurred in July and August. Water tables at all sites increased during the winter the vegetation was senescent. Test well 850T was installed at BLK100 in 2001, but based on the comparison with nearby test well 454T, DTW fluctuations were similar in all three years EC measurements were collected. No piezometer was located near PLC018 and PLC185. Soil water content at PLC018 at depth was nearly at limiting water content for sandy soil suggesting

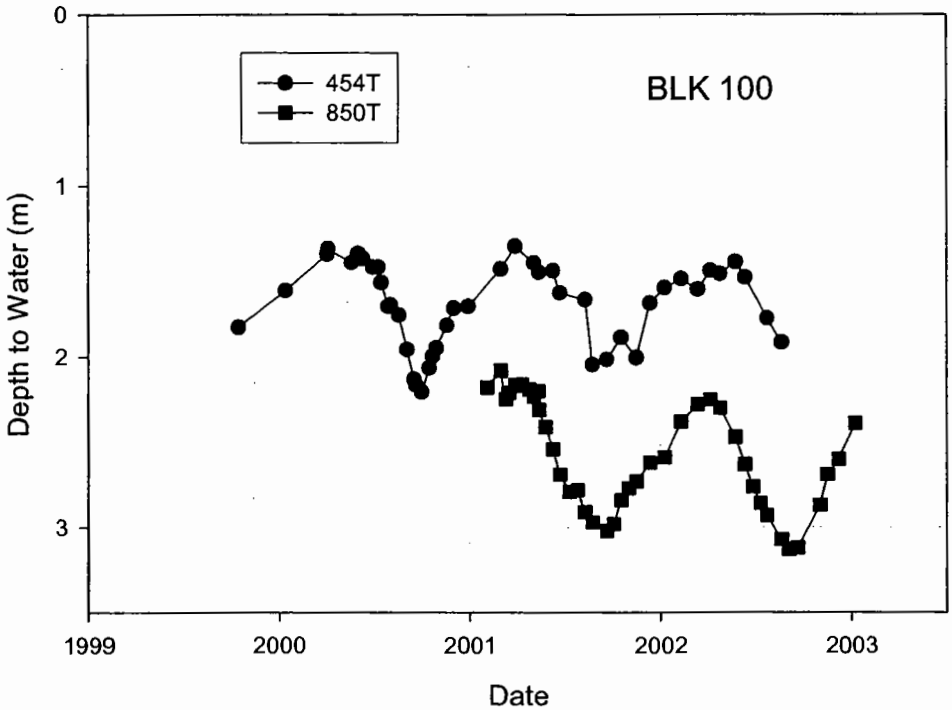

Figure 19. Depth to water in two test well located near BLK100. Test well 850T is adjacent to the EC station; 454T is located south east of the site, adjacent to the LA Aqueduct.

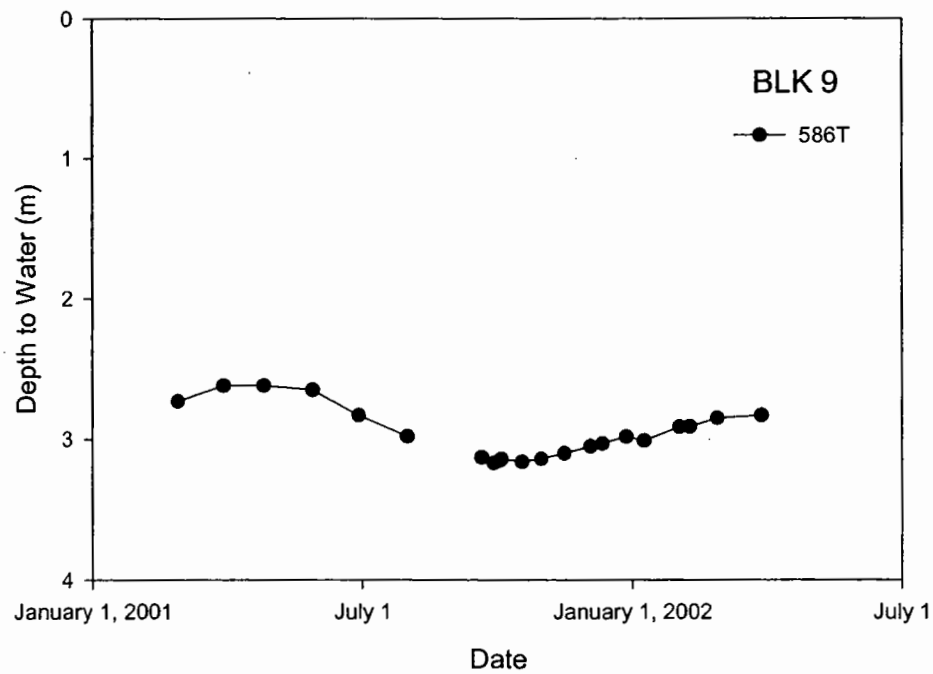

Figure 20. Depth to water in test well 586Tlocated near BLK009.

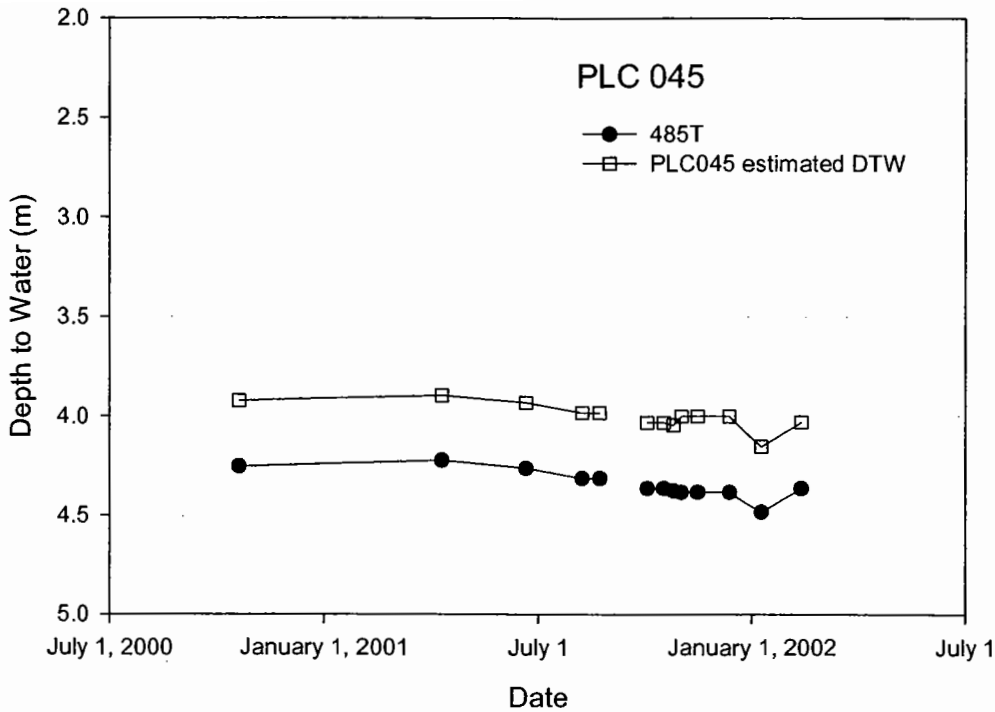

Figure 21. Depth to water in test well 485Tlocated south of PLC045 and estimated DTW at PLC 045.

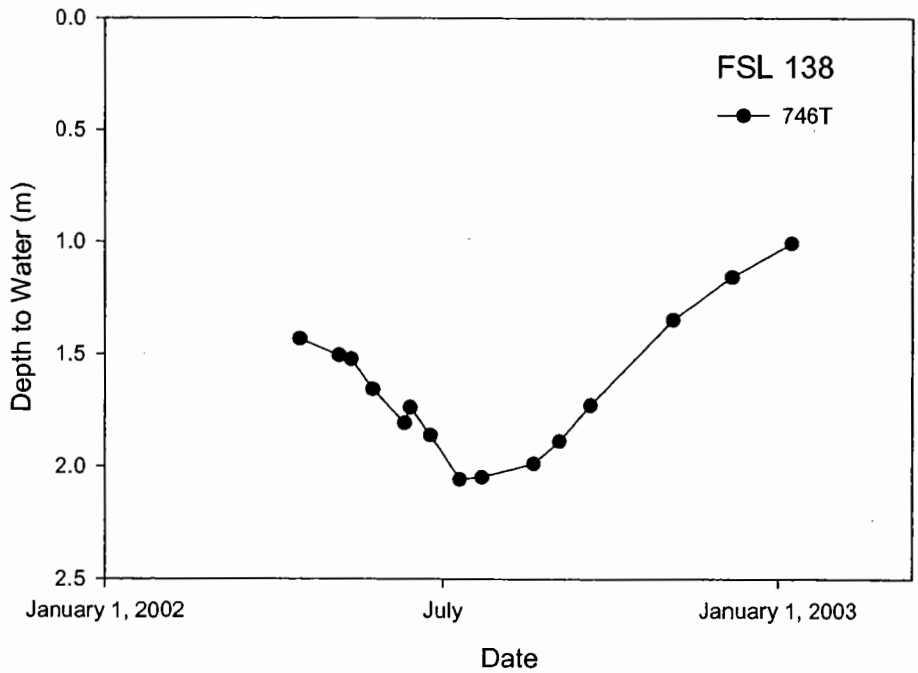

Figure 22. Depth to water in test well 746Tlocated at FSL138.

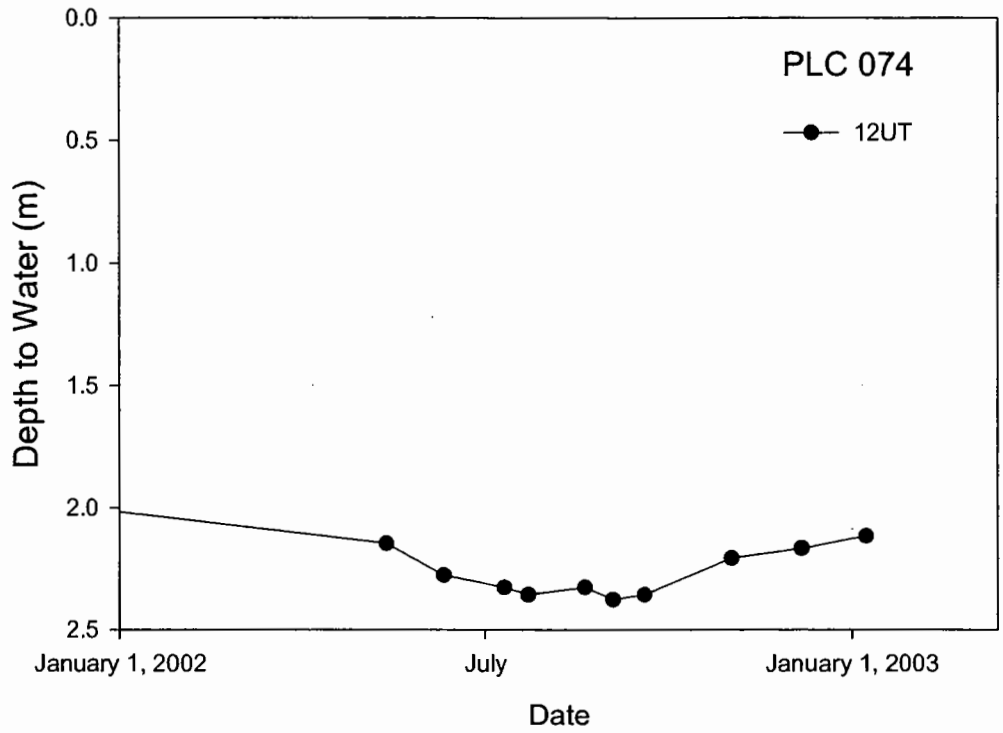

Figure 23. Depth to water in test well test well 12UT located at PLC074.

depth to water was always deeper than 5 m. The water table was encountered at PLC185 during access tube installation in the spring 2002. The water table was approximately 4 m which probably represents the high stand during the growing season. Depth to water at PLC045 was estimated from the initial water table depth (3.9m) observed during access tube installation and fluctuations observed at a test well 485T in similar vegetation 0.5 km from the site. Precipitation preceding the growing seasons each year 2000-2002 consisted of small events, and total precipitation was below normal (about 130 mm) in all years (Table 6). Only two summer storms in July 2001 were of significant size during the project to affect either ET or LAI

measurements, and only at PLC045.

Soil water profiles collected at each access tube, including the shallow gravimetric measurements are presented in Figures 24 through 32. An example of spring, midsummer, and fall conditions are presented for each access tube. Even though estimates of limiting water content are not available, it is evident from the high values that ample soil water was available for plant uptake at sites BLK100 (all years), BLK009, and FSL138. Soil water content at BLK100 fluctuated throughout the profile reflecting the coupling with the water table fluctuations (i.e. capillarity and drainage) and plant uptake. The attempt to discriminate between these two processes is described in the vadose zone model section below. Tube 2 at BLK100 (1002) was located in a small $2m^2$ slickspot nearly devoid of vegetation. At that location, θ in the upper 1.1 m was relatively constant except for precipitation/evaporation suggesting the importance of plant uptake in controlling soil water in the upper part of the soil at vegetated locations. The soil at BLK009 can be divided into three zones. Above 0.9 cm, the soil was affected by infiltrating rain. Soil water content was relatively static at intermediate depths (0.90 to 1.50-2.00 m depending on location). Below the intermediate zone, soil water was coupled to water table fluctuations. At PLC045, soil water increased to 0.50-0.90 m due to winter and summer rains, but below 0.9 m, θ was less than 5% which is approximately the limiting value expected for sandy soils (McCuen et al., 1981). The extreme limit of capillarity above the water table extended to 3.2 m during access tube installation in early spring. Soil water at PLC018 was dry similar to PLC045 except the limit of capillarity was below the deepest monitoring depth of 4.7 m. PLC074 also had very sandy soils (Appendix B), but the water table was relatively

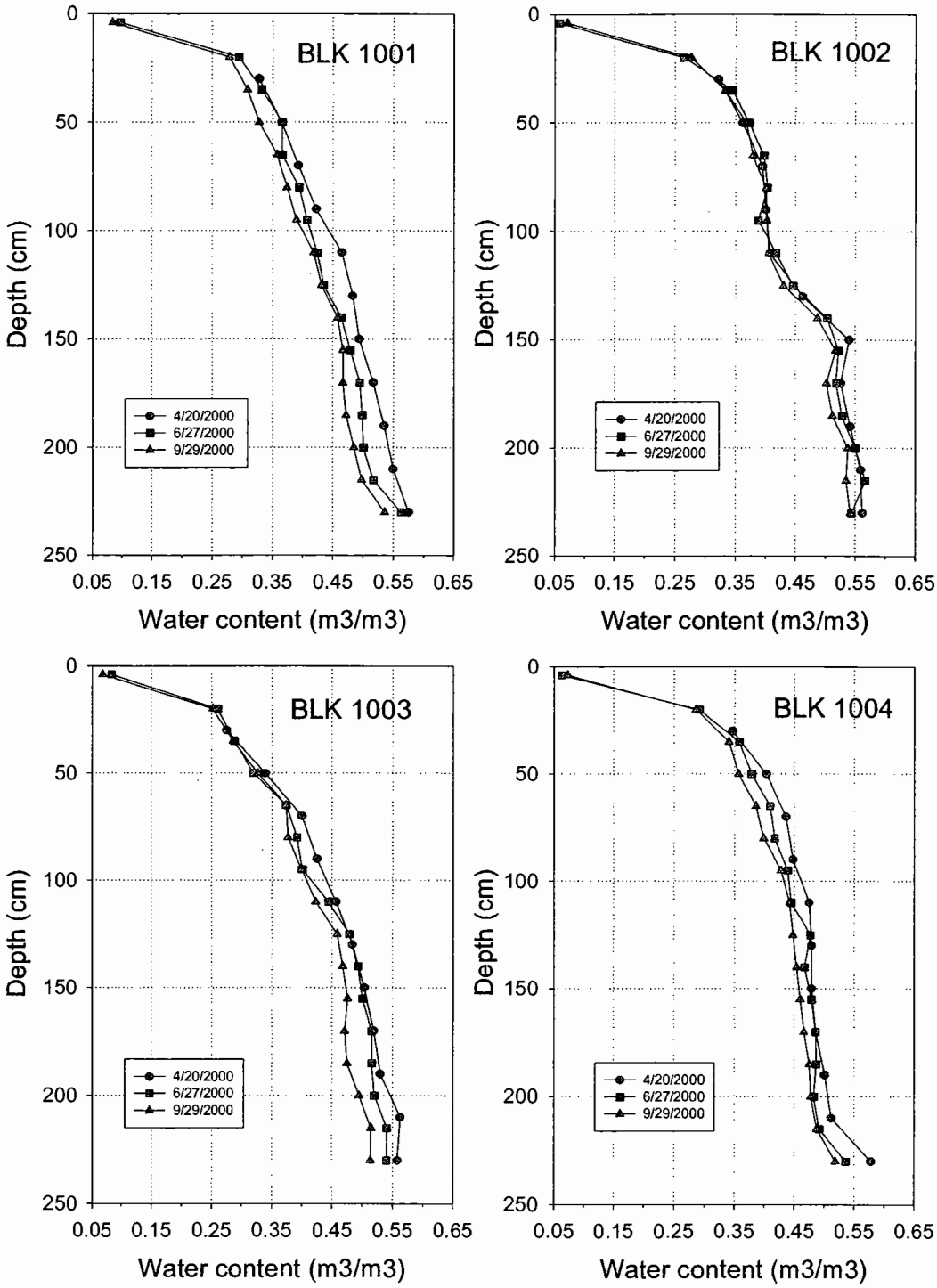

Figure 24. Soil water content θ profiles for spring, summer, and fall conditions in four access tubes at BLK100 in 2000.

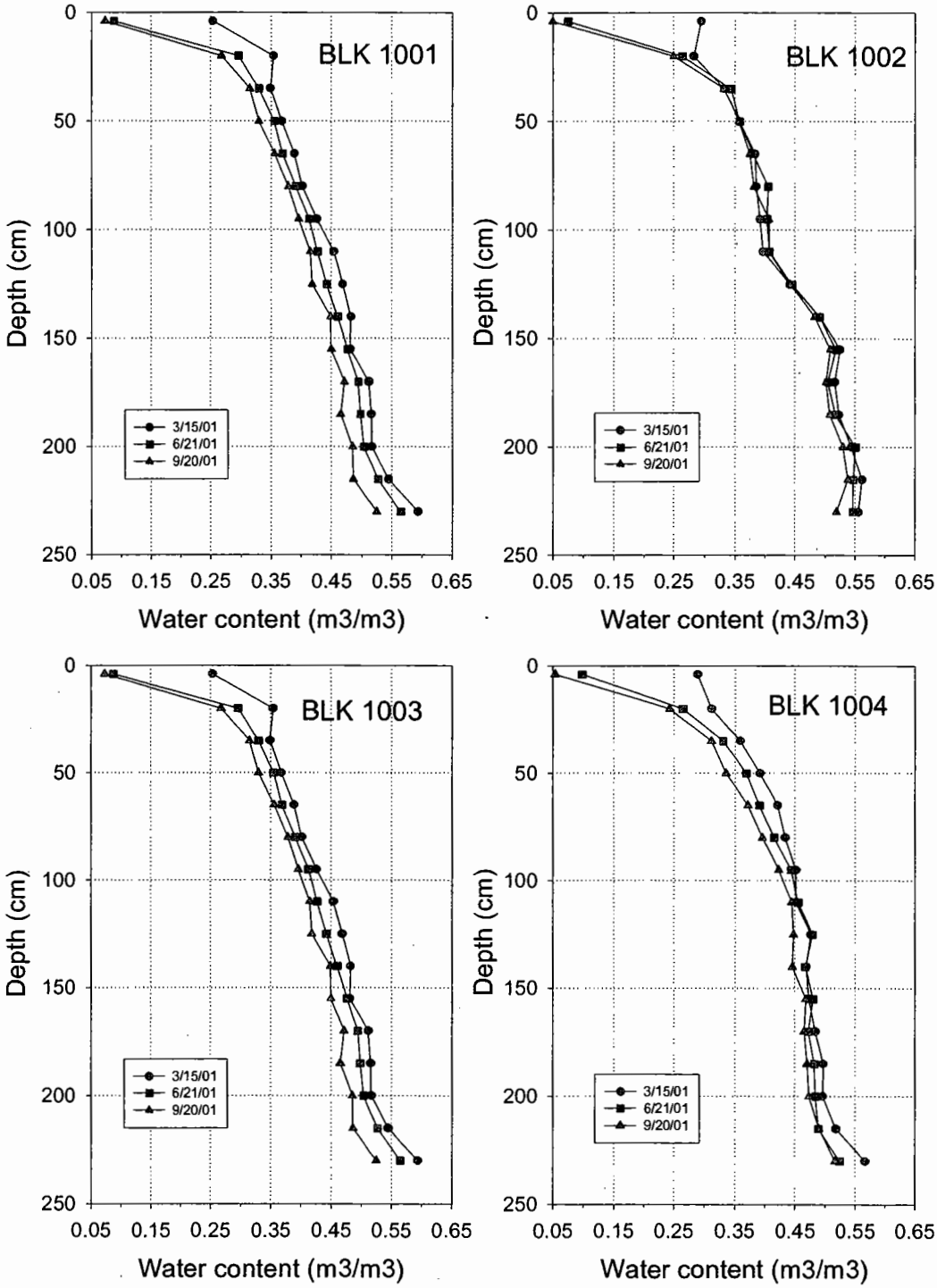

Figure 25. Soil water content θ profiles for spring, summer, and fall conditions in four access tubes at BLK100 in 2001.

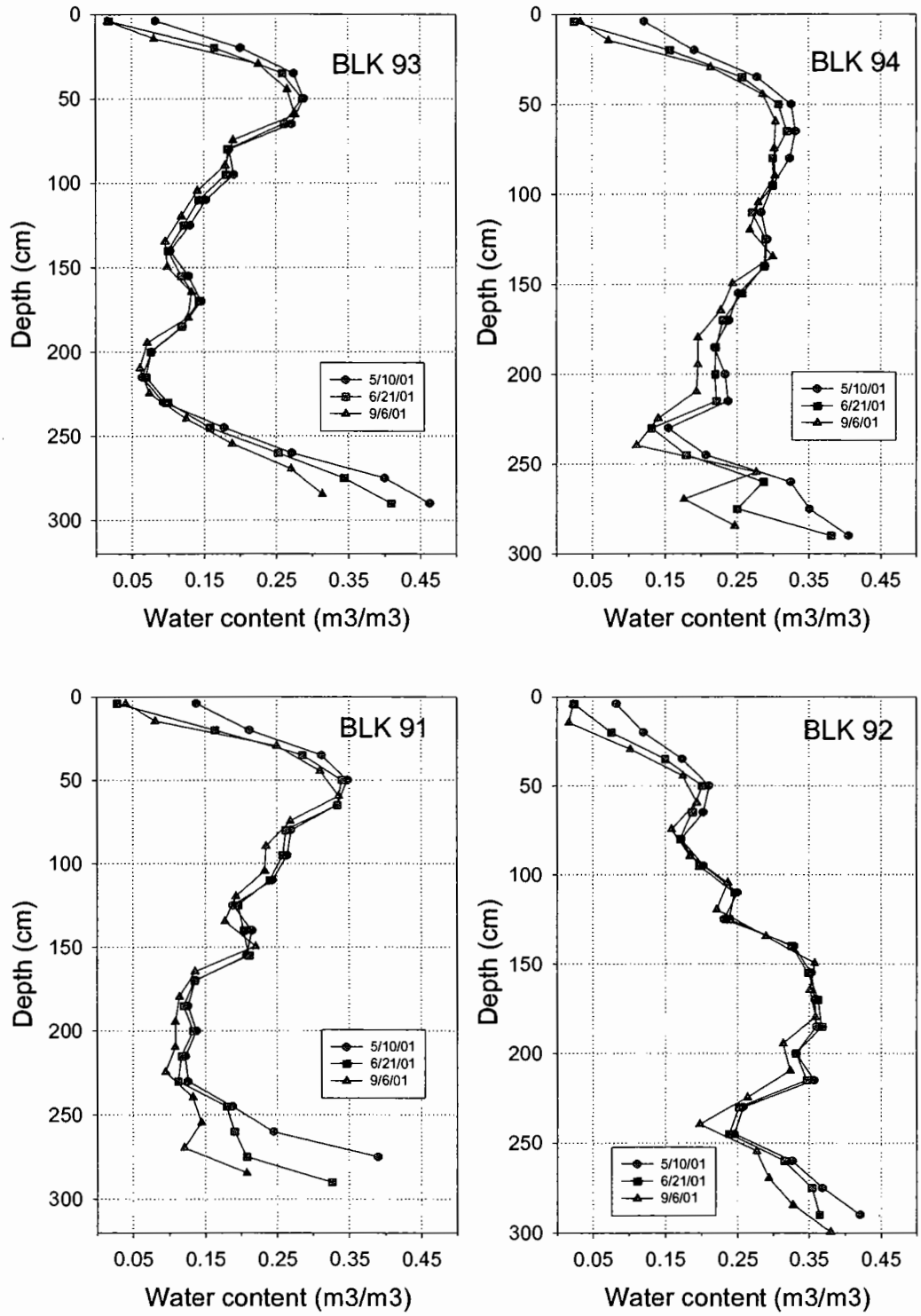

Figure 26. Soil water content θ profiles for spring, summer, and fall conditions in four access tubes at BLK009 in 2001.

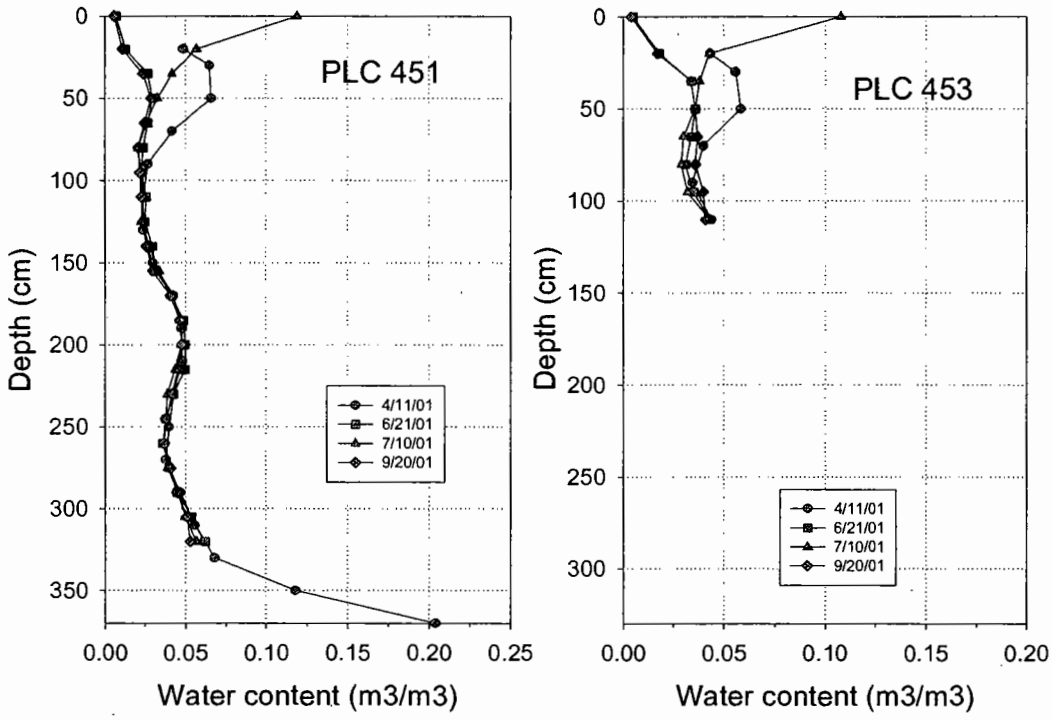

Figure 27. Soil water content θ profiles for spring, summer, and fall conditions in two access tubes at PLC045 in 2001.

shallow (<3 m) and probably accessible to the vegetation. At two locations, the upper 1 m was relatively dry and decoupled from water table changes (Figure 31). At two other locations (tubes 742 and 744), soil water contents in the upper and lower profile were above limiting water contents and was difficult to distinguish whether the upper 1 m was coupled with the water table or whether it reflected uptake of precipitation-derived soil water. All locations were coupled to water table fluctuations at depths below 1 to 1.5 m. Like BLK009, the soil at PLC185 can be divided into three zones based on observed soil water fluctuations. Soil at PLC185 was dry in the upper 1 m except for precipitation inputs. Intermediate depths from 1 m to approximately 2.7

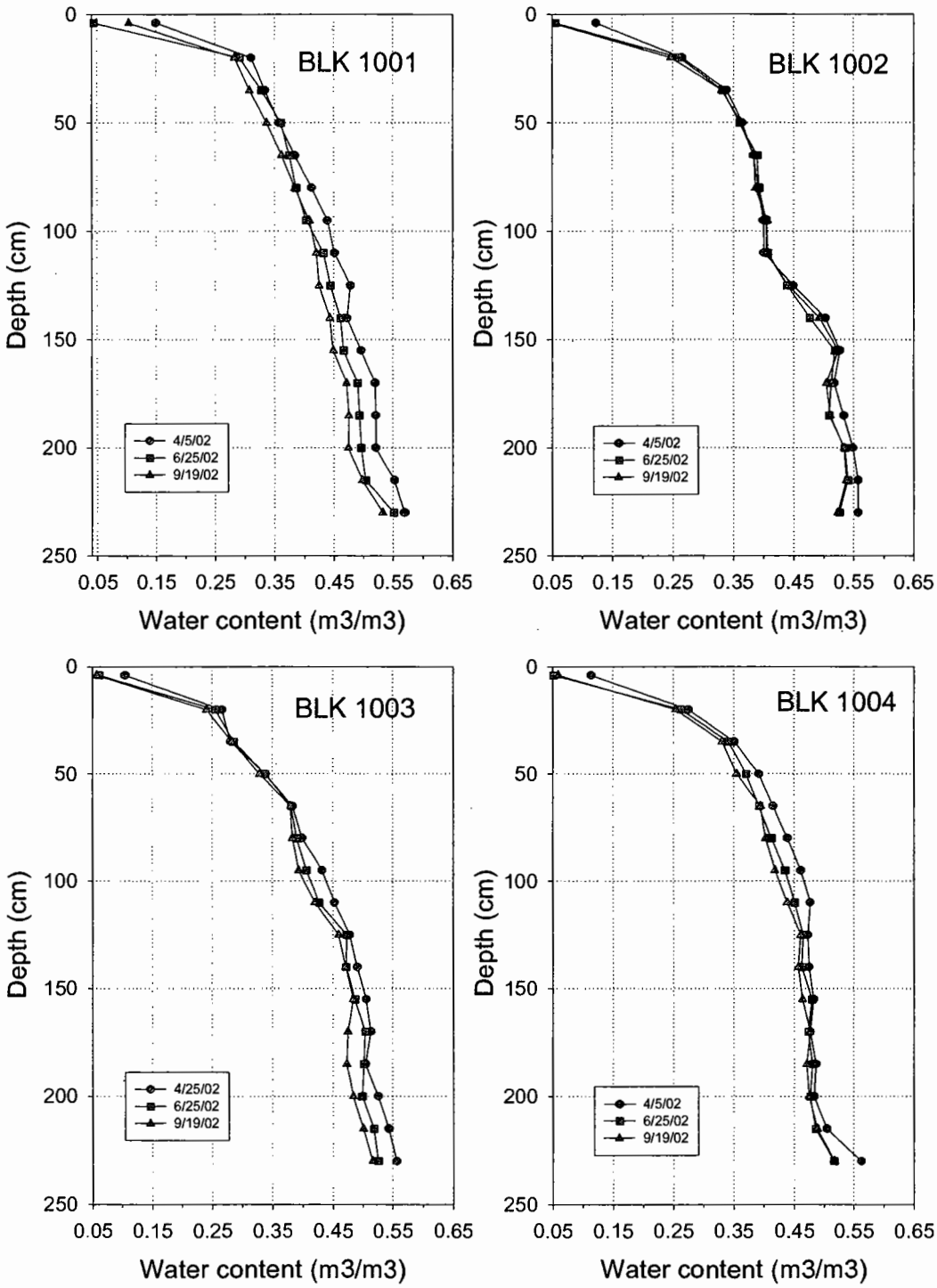

Figure 28. Soil water content θ profiles for spring, summer, and fall conditions in four access tubes at BLK100 in 2002.

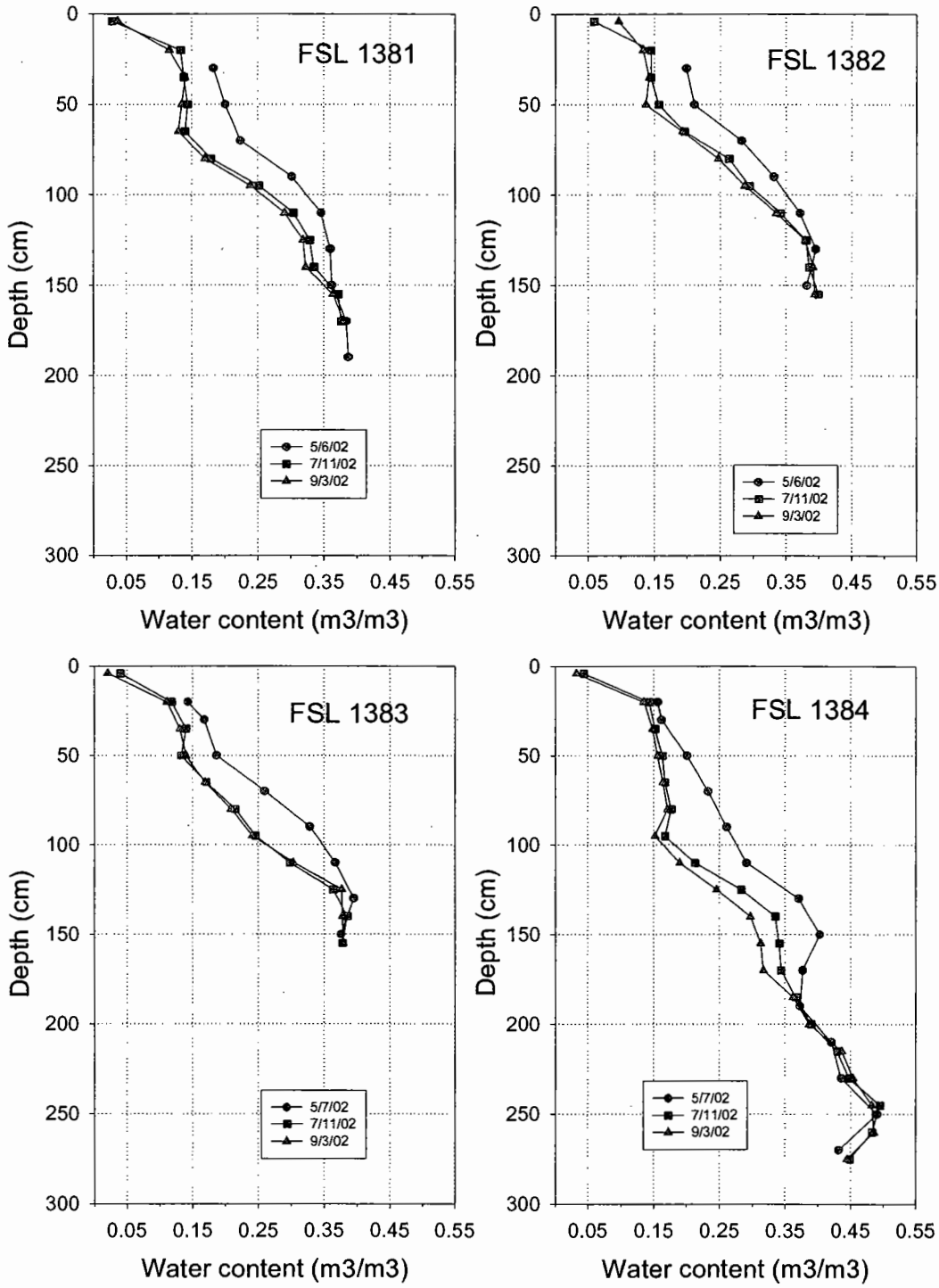

Figure 29. Soil water content θ profiles for spring, summer, and fall conditions in four access tubes at FSL138 in 2002.

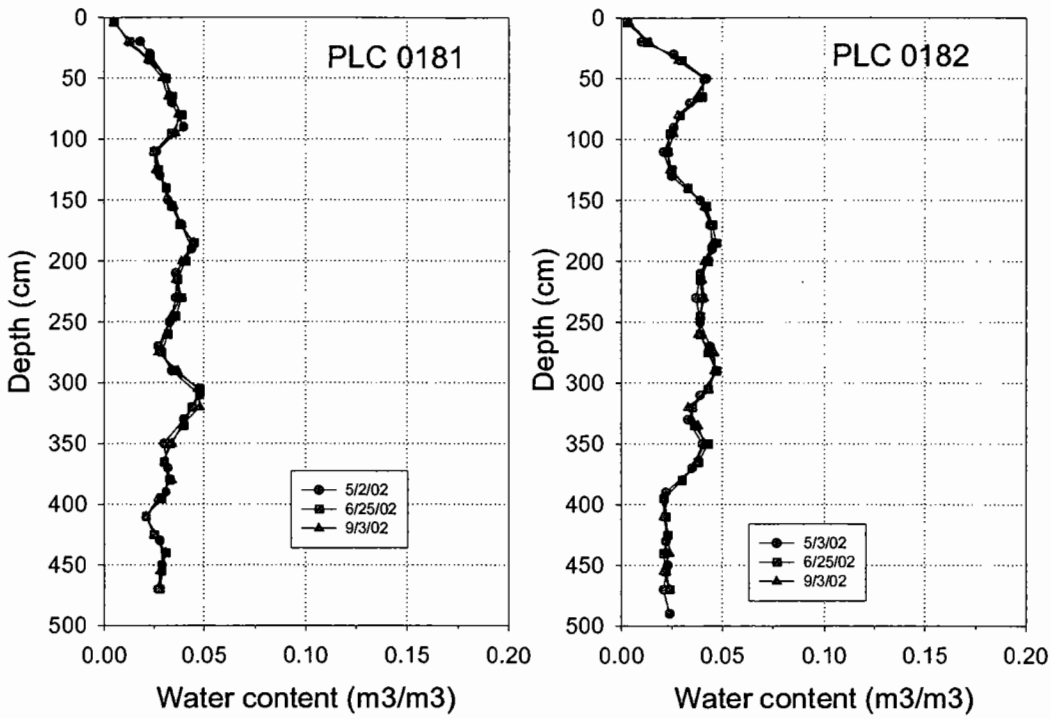

Figure 30. Soil water content θ profiles for spring, summer, and fall conditions in two access tubes at PLC018 in 2002.

to 3.0 m, depending on location had nearly constant water content that varied according to soil texture (higher in finer textured soil). Under the drought conditions of 2002, water in this zone evidently was not available for uptake or uptake at this low cover site was negligible. At lower depths, soil water fluctuations were coupled to water table fluctuations, although the coupling was weak for two of the three locations.

Leaf area index (all species) differed between sites with wet and dry soils (Figure 33). At sites with deeper water tables and/or dry sandy soils (PLC045, PLC018, PLC074, and PLC185), LAI was small and peaked in the first two weeks of June. LAI at shallow water table sites with

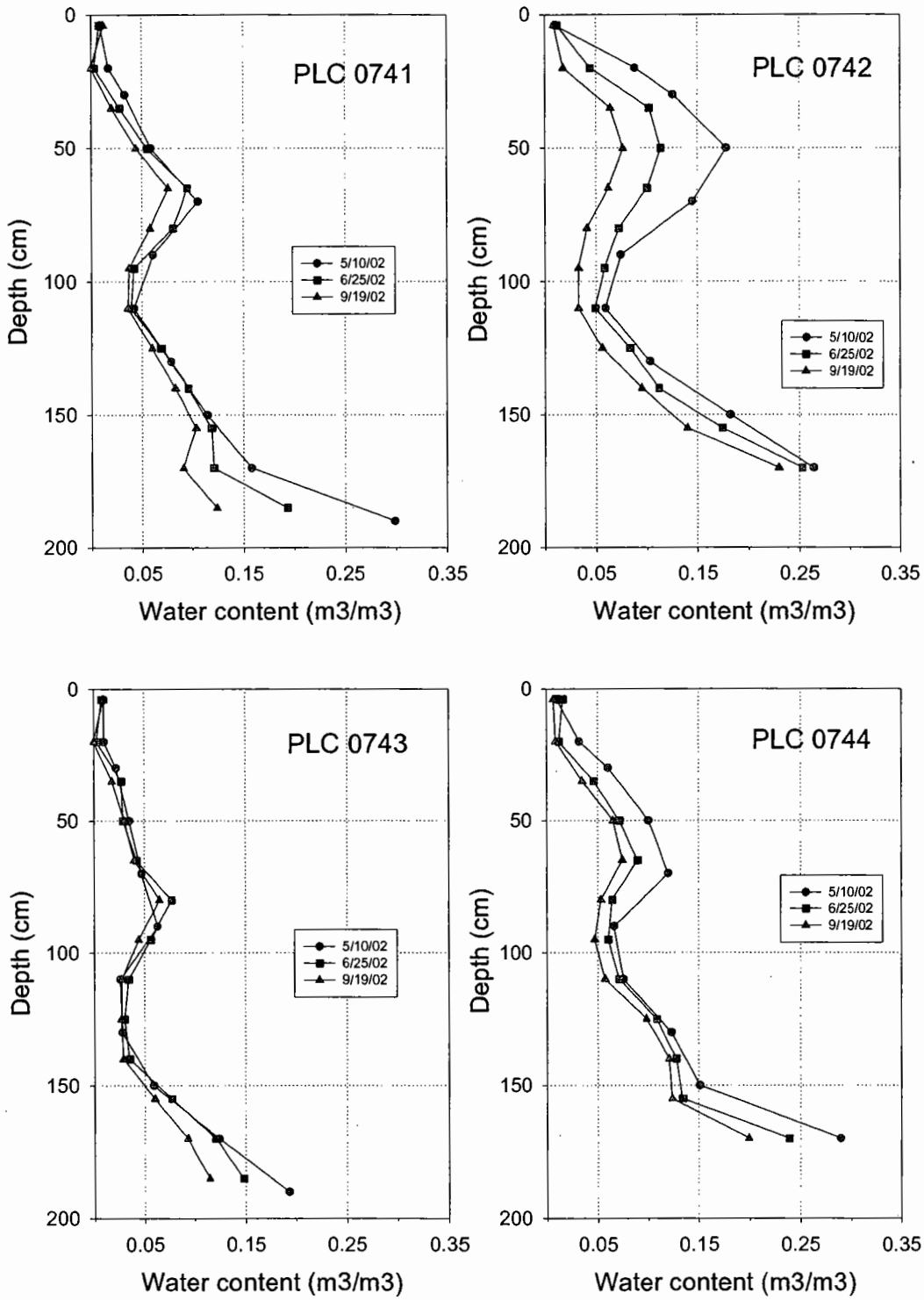

Figure 31. Soil water content θ profiles for spring, summer, and fall conditions in four access tubes at BLK074 in 2002.

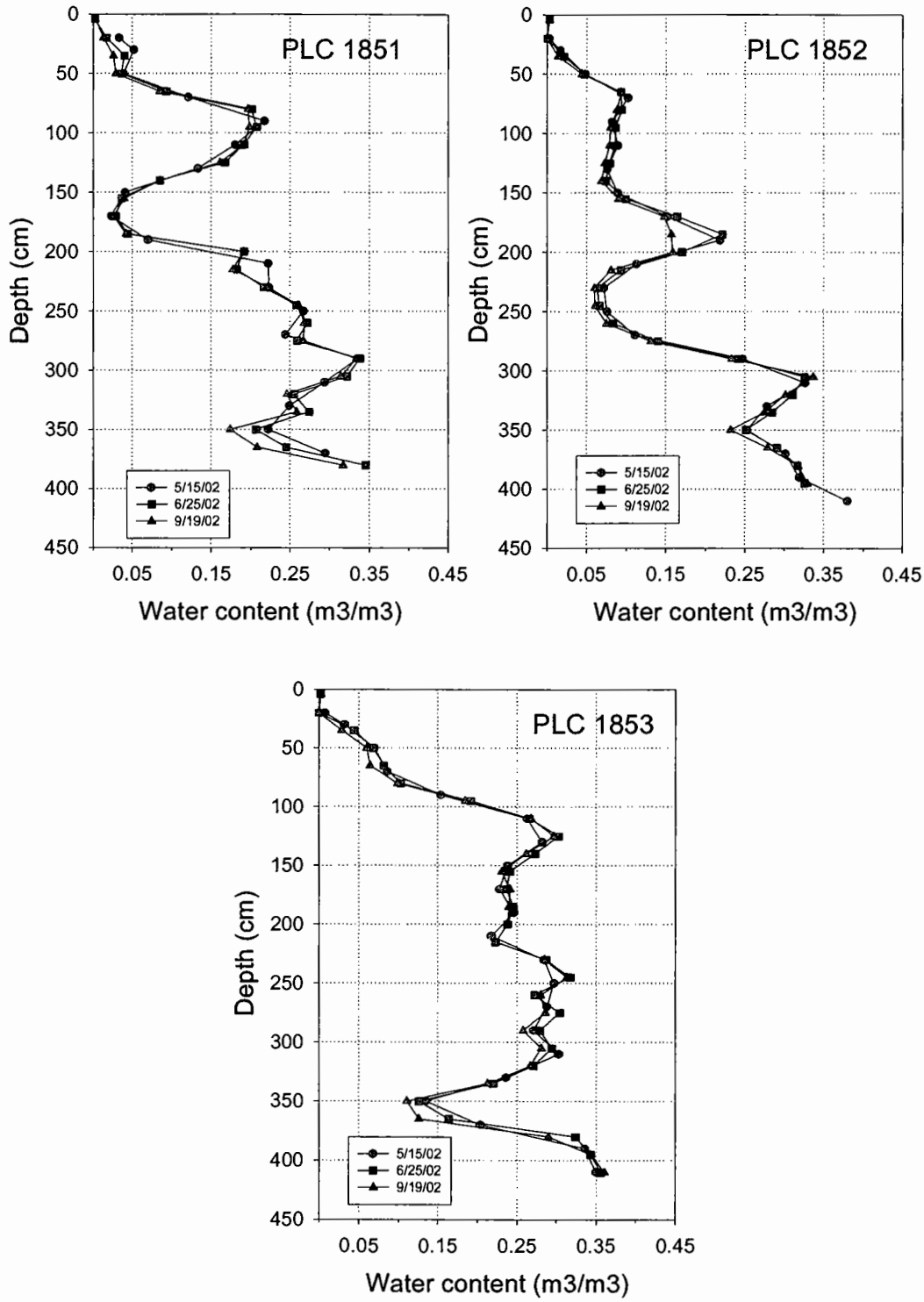

Figure 32. Soil water content θ profiles for spring, summer, and fall conditions in three access tubes at PLC182 in 2002.

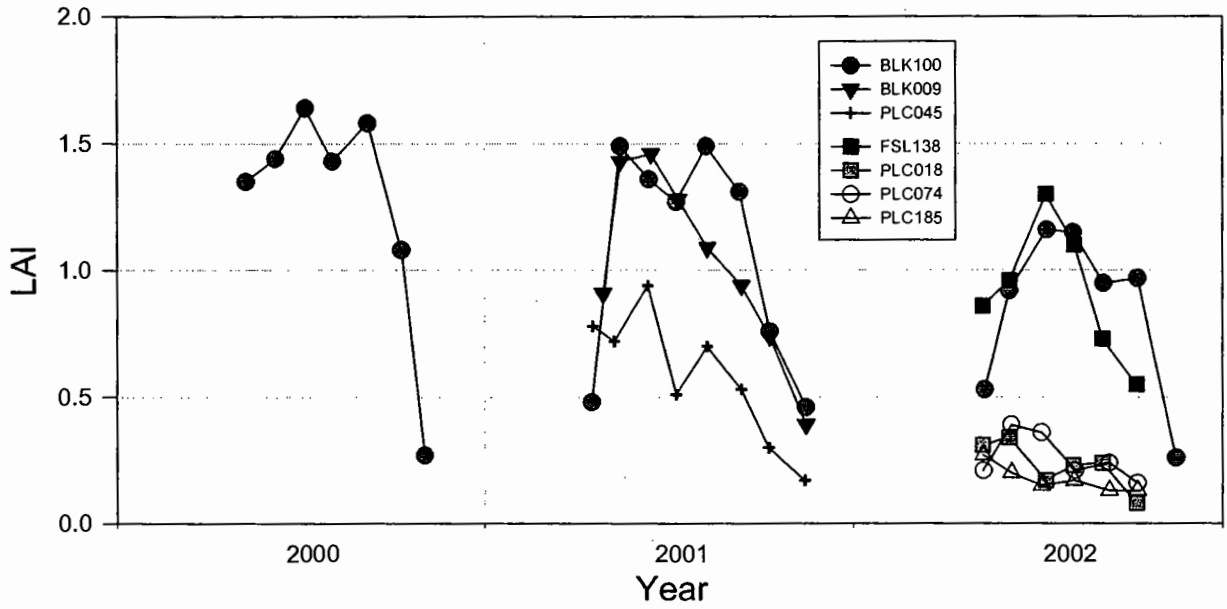

Figure 33. LAI for all sites. Values are the average of four transects.

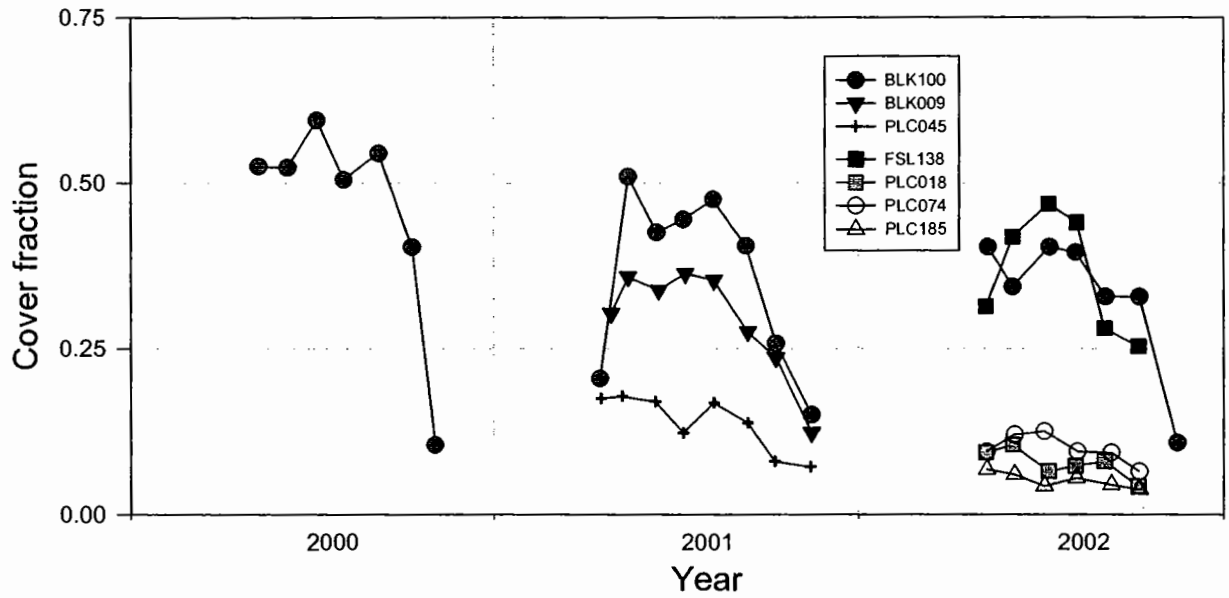

Figure 34. Plant cover of all species (fraction) for all sites. Values are the average of four transects.

relatively wet soils was greater and peaked later in the summer, usually the first week in July. Typically, BLK100 maintained a high leaf area through June, July, and August before declining in September (2000 and 2001) or October (2002). In contrast, FSL138 and BLK009 declined steadily after the peak LAI was attained in June (BLK009) or July (FSL138). Trends in plant cover closely tracked LAI (Figure 34) which was expected given the linear relationship between the quantities (Steinwand, 1999a and b).

EC energy balance components and closure

An example of half-hourly *EB* for the EC system at BLK 100 for several days in 2002 is given in Figure 35. EB ranged from (rarely) near zero to over 100 W m^{-2} with a mean EB closure error over the period of 43.9 W m^{-2}. Mean available energy during this period was 124.0 W m^{-2}, thus the turbulent fluxes did not account for over one-third of the available energy. During DOY 238, the energy balance closure error was greater than 150 W m^{-2}. The closure error tends to be highest during the afternoon, but persisted throughout the day. Comparison of Figures 35 and 36 shows that the EB error tends to be largest during periods of relatively higher wind speeds in the afternoon. The linear correlation coefficient between the horizontal wind speed and the EB error was $r = 0.46$. Except for DOY 238, winds were from the southeast during the afternoon, which should be the most favorable wind direction for the EC instruments, therefore the EB error maxima do not appear to be attributable to disruption of the flow by the sensors and mounting structure. The peak EB closure error occurred on DOY 238, and flow distortion may have contributed to the error that day.

For all sites, the mean *EB* calculated on a daily basis ranged from 56 to 75% (Figures 37 to 40). Highly erratic values of *EB* occurred before and after the growing season

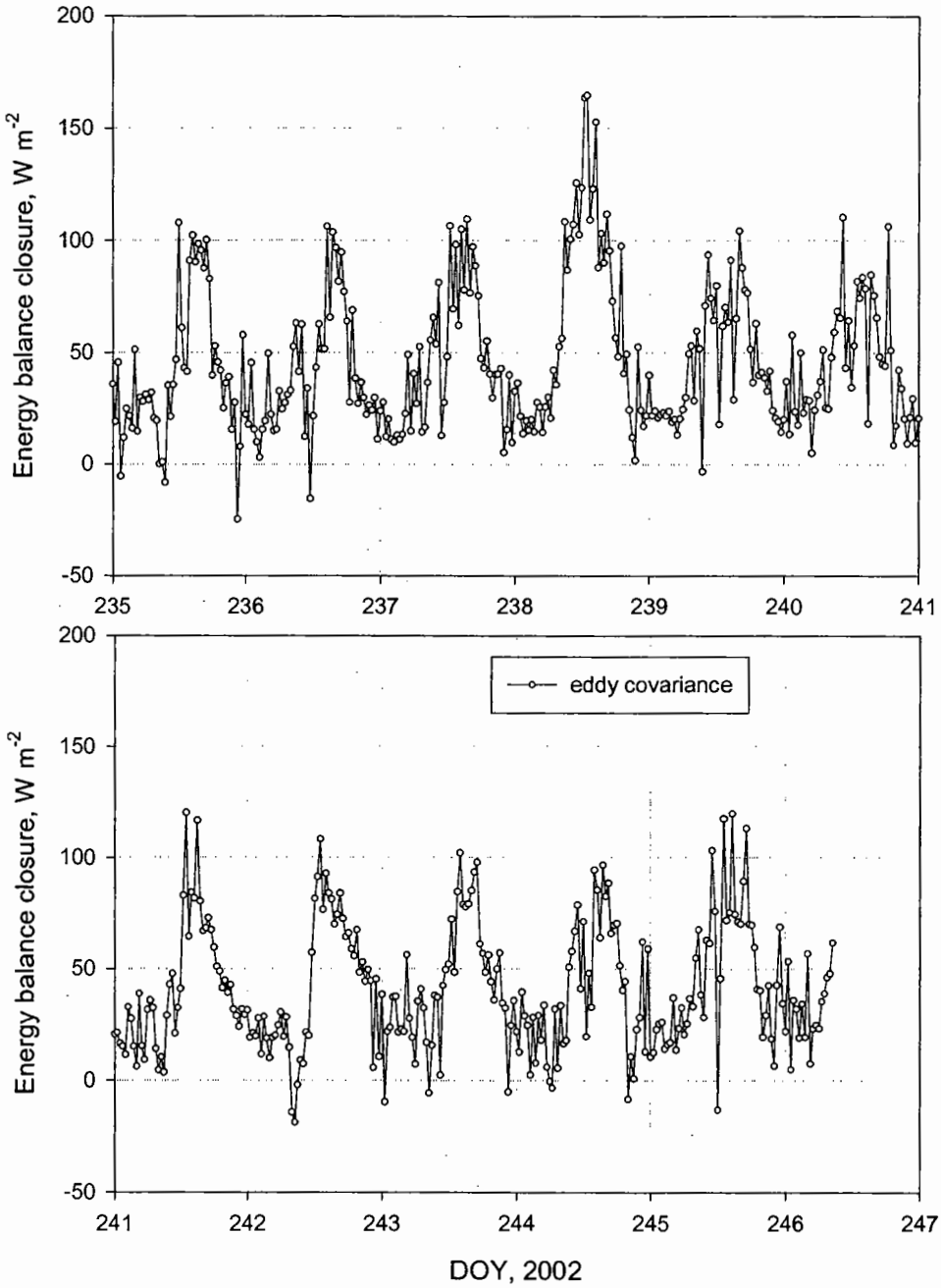

Figure 35. Example of the energy balance closure error for EC system on half hourly basis at BLK 100 during the period of BR system operation.

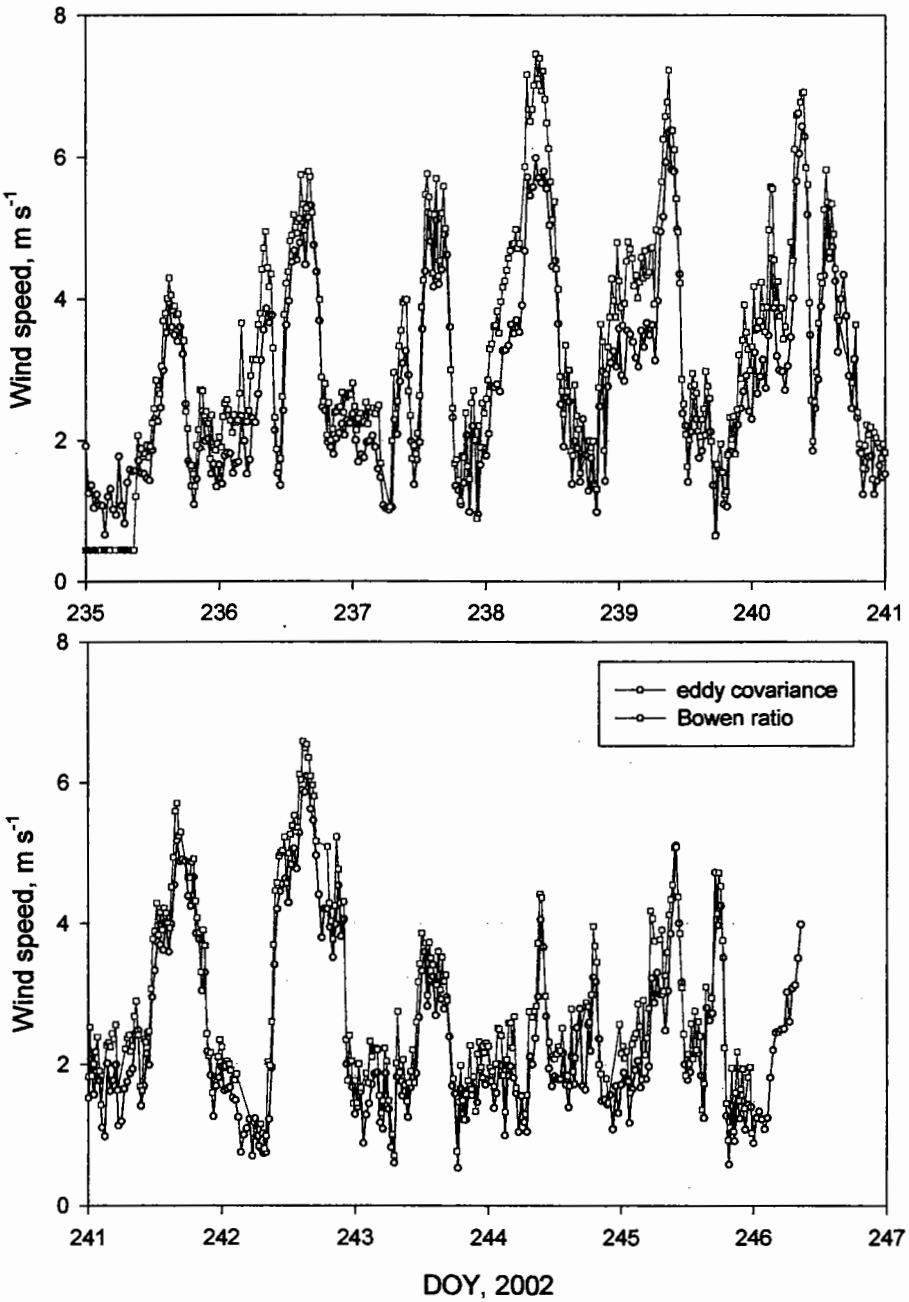

Figure 36. Wind speed at BLK 100 measured with eddy covariance and Bowen Ratio instruments in 2002.

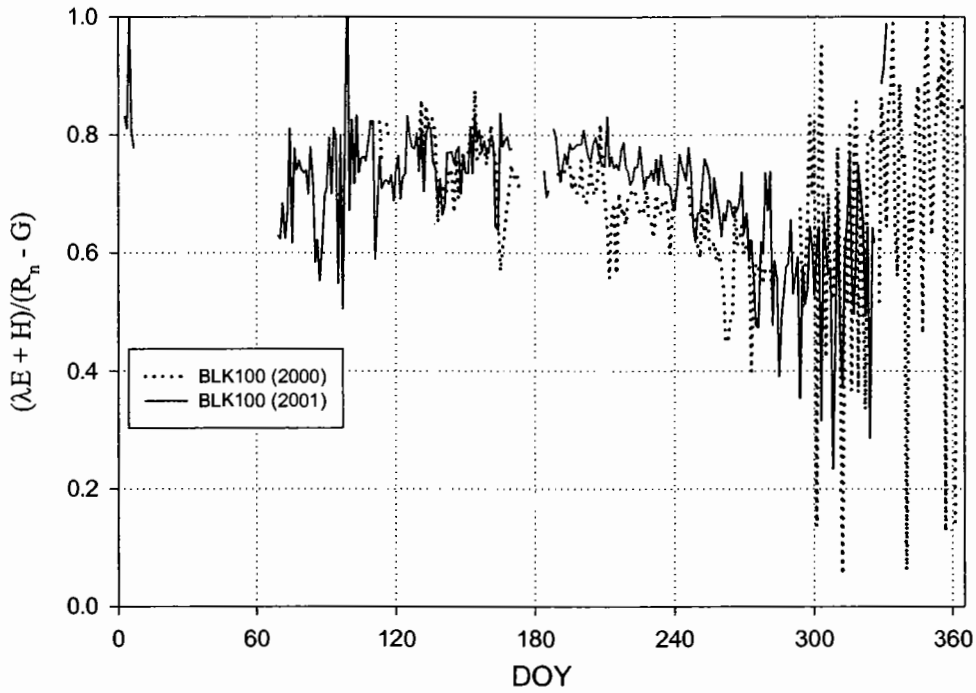

Figure 37. *EB* for BLK100 in 2000 and 2001.

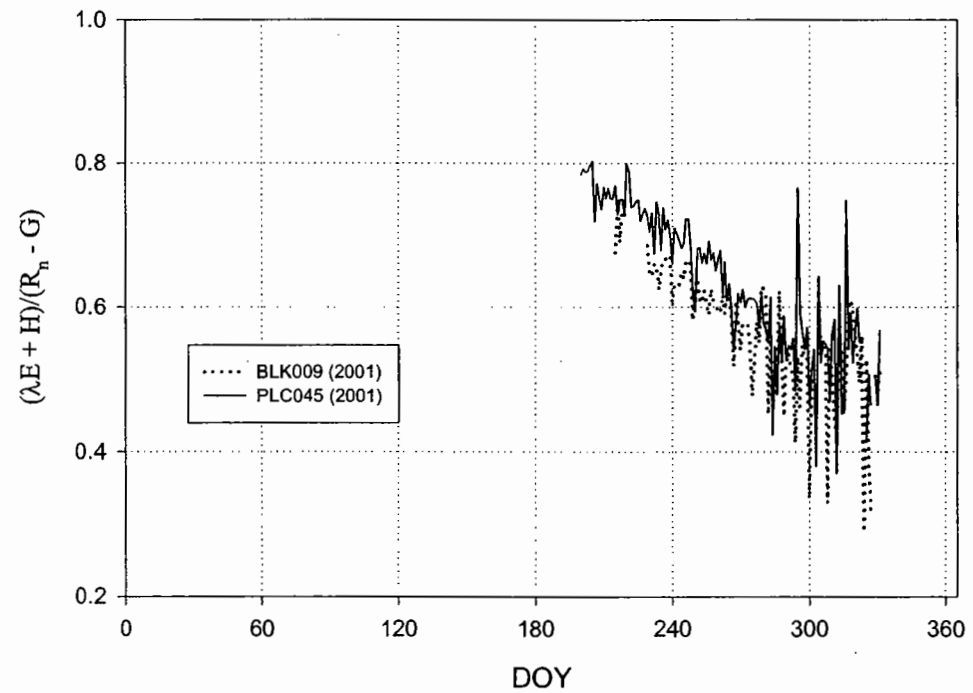

Figure 38. *EB* for BLK009 and BLK045 in 2001.

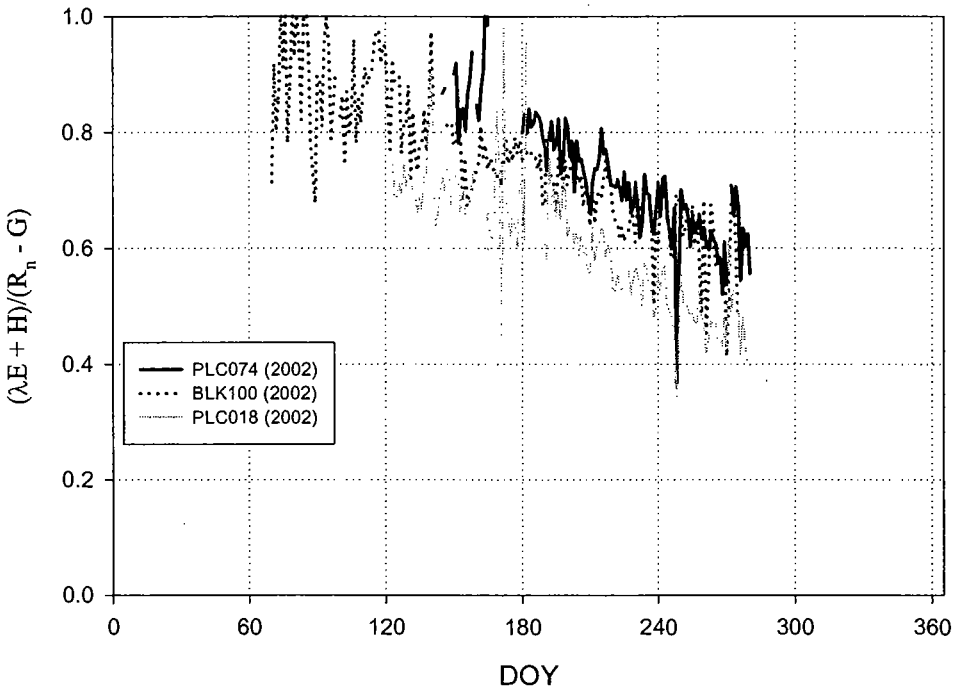

Figure 39. *EB* for PLC018, PLC074 and BLK100 in 2002.

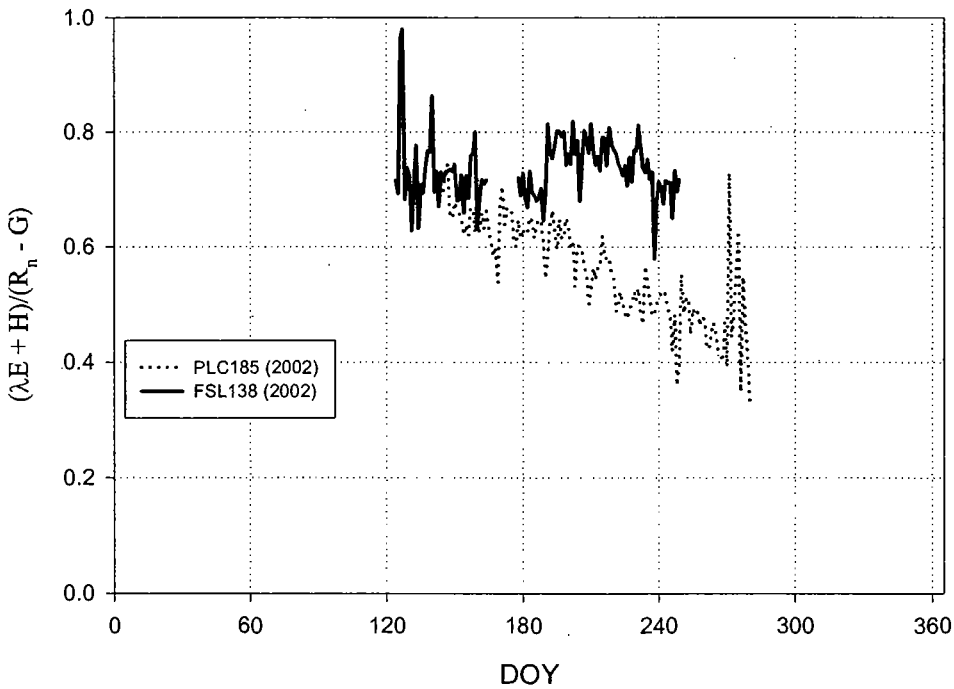

Figure 40. *EB* for PLC185 and FSL138 in 2002.

(84>DOY>288) when all the fluxes were relatively small. Generally, the closure error was least early in the growing season and increased approximately 20% by the end of the season. The increase in closure error usually began about midsummer (DOY 186) and was not evident before or after the growing season. Changes in EB seem related to H or λE individually or in combination rather than calibration drift, but the relationship is not understood. Interestingly, the EB trend at FSL138 was not similar to trends evident at other sites. The closure error at FSL138 was relatively stable except for a sharp decrease about DOY 191 that corresponded with a sudden decrease in λE suggesting the closure error was related to λE. At other sites, however, the late summer increase in the closure error was more gradual and increased as λE decreased.

Failure of EC systems to achieve EB closure has been observed in other studies, and various instrumental or theoretical explanations have been put forth. Zeller et al. (1989) and Massman et al. (1990) examined sources of error in EC turbulent flux measurements due to mismatches in sensor response times, sensor volume or line averaging effects, flow distortion around sensors and mounting structures, spatial separation of sensors, and sampling rate (aliasing) effects. Each source of error tends to reduce the covariance measured by the EC system, thereby causing the turbulent fluxes to be underestimated. After implementing corrections for each of these sources of error, their energy balance still failed to achieve closure, which they attributed to inaccuracy of the measurement of R_n and G.

In the event of non-closure of the energy balance, there are various strategies to correct the EC fluxes. Besides the formal frequency domain transfer function corrections used by Zeller et al. (1989) and Massman et al. (1990), several simple ad hoc corrections based on Equation 3

can be made, the choice of which depends on the suspected source of error. If the error is in the measurement of available energy, then no correction is necessary to the turbulent fluxes. If the error due to the hygrometer, energy balance can be achieved by assuming all the error is in the latent heat term. If the error is due to the sonic anemometer or due to a loss of covariance that affects H and λE in similar proportions, the turbulent fluxes can be corrected by assuming that β is measured correctly and adjusting the magnitude of the turbulent fluxes such that energy balance is achieved.

Examination of the EB from other EC systems operated as part of this project revealed that EB closure errors of similar magnitude as occur at sites with minimal ET (e.g. PLC018, Figure 39) suggesting that both turbulent fluxes are underestimated. Also, ET measured by the EC system at all sites was near 0 W m^{-2} during nighttime, as would be expected for the dry soil surface present at the site. Therefore, though the error may have been partly due to the hygrometer, ascribing the EB error solely to the λE term was unwarranted.

β measured with the BR and EC systems agrees during daylight hours, except at times when the BR system produced large erratic values (Figure 41). The β values are comparable between the two systems during the morning hours, climbing to a midday peak of ~1.7, then during the afternoon hours BR β often grow very large while the EC β smoothly decline from their midday peak. The large afternoon β sometimes measured by the BR system are considered erroneous, because the clear dry conditions during the measurement period should produce smoothly varying β during daylight hours. The cause of these erroneous measurements is unknown. During periods of afternoon winds, the BR system often yielded unstable large

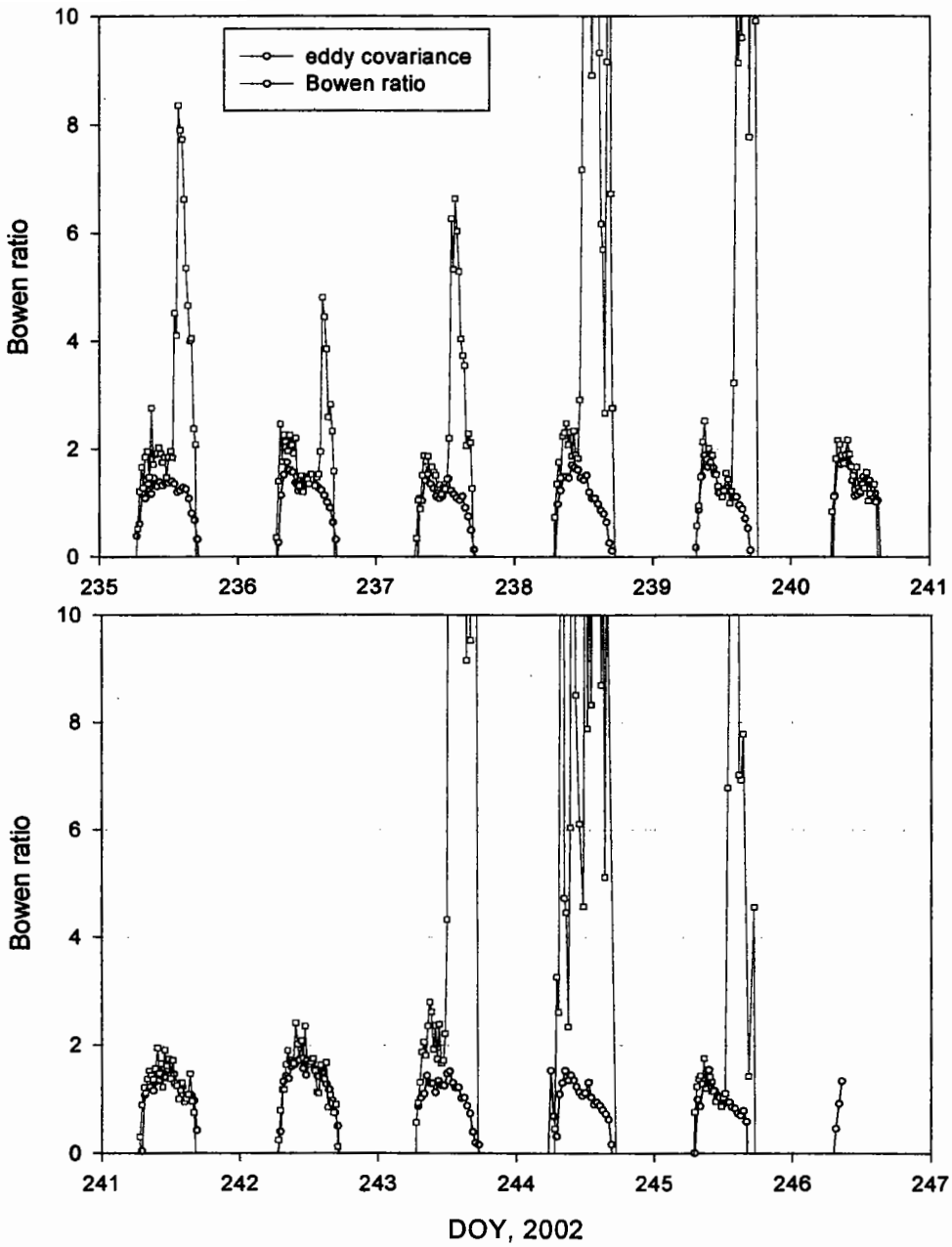

Figure 41. Daytime Bowen ratio ($H/\lambda E$) at BLK100 measured with eddy covariance and Bowen Ratio instruments in 2002. Only daytime β are shown because for either system, nighttime β tended to be highly erratic due to the small magnitude and variable sign of λE.

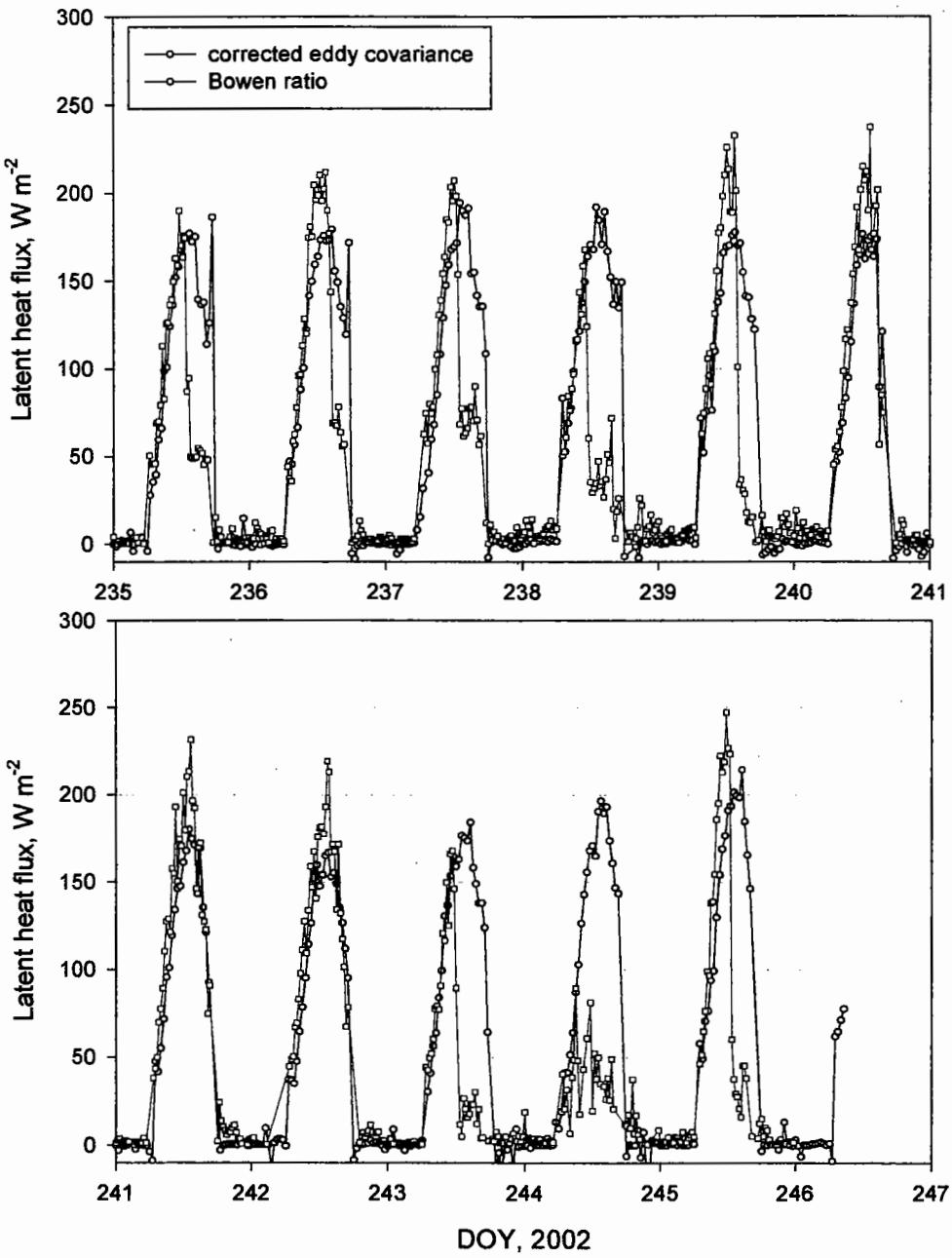

Figure 42. Latent heat flux at BLK 100 measured with eddy covariance and Bowen Ratio instruments in 2002. EC latent heat flux has been corrected using Equation 18.

Bowen ratios. Additionally, values of β produced by the EC system followed a smoothly varying pattern repeated each day of increase from negative values in the early morning to a midday maxima followed by decrease to negative values in the evening. Thus, use of β measured by the EC system is probably the most reliable way to correct the EC turbulent fluxes. The correction is applied as,

$$\lambda E_{corrected} = ET_{corr} = \frac{R_n - G}{\beta + 1} \tag{18}$$

Of course, when Equation 18 is used to correct the EC measurements, the computed flux is no longer independent of the energy balance measurements. Additionally, measurements at dawn and dusk when β is near -1 must either be discarded, similar to the processing of BR measurements, or not be corrected. Periods when β is near -1 have little influence on daily or seasonal ET estimates, because ET is usually low during the time of day when this condition prevails. Prior to the application of Equation 18, the only corrections applied the EC measurement were the oxygen and air density corrections. Using β as the correction factor thus assumes that other sources of error affect the turbulent fluxes in equal proportion (i.e., multiplicatively). When λE measured with the EC system is corrected using Equation 18, it produces similar results to λE measured with the BR system during periods when β produced by each system was similar (Figure 42). During periods when β measured with the BR system was erroneously large (e.g. at night), the corrected ET was greater than that measured with the BR system.

The corrected ET is usually, but not exclusively, greater than the uncorrected EC

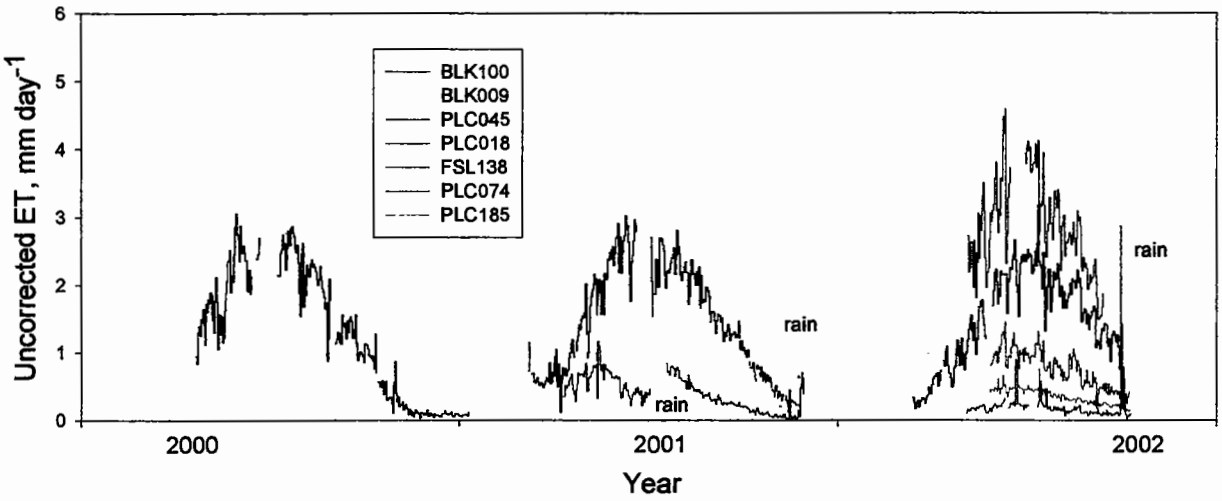

Figure 43. All uncorrected ET measured by EC systems.

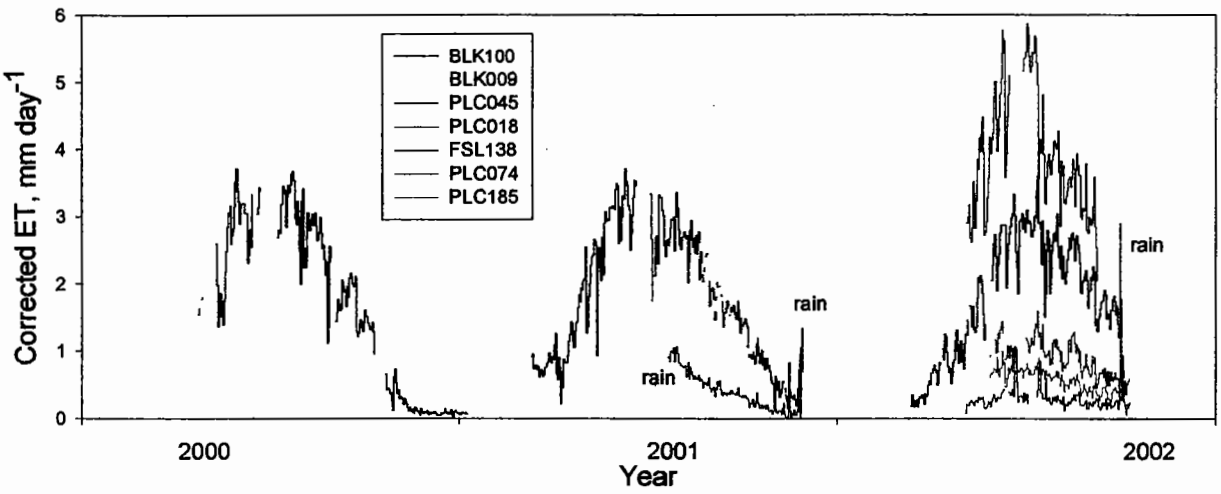

Figure 44. All corrected ET measured by EC systems.

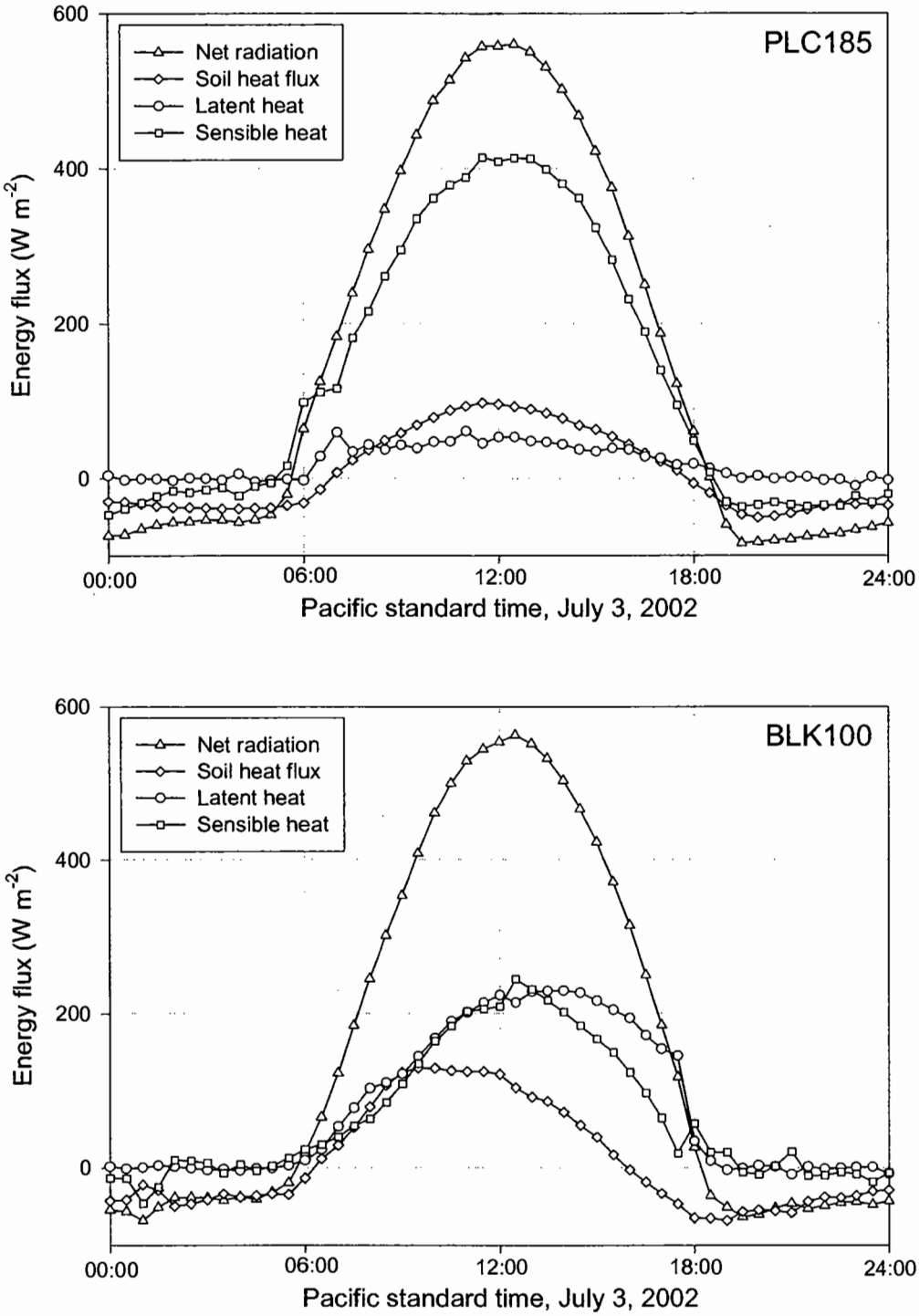

Figure 45. Half-hourly energy balance components measured at PLC185 (top graph) and BLK100 (bottom graph). Latent heat flux has been corrected for EB.

measurement. The correction (Equation 18) increased ET estimates a few tenths of mm day $^{-1}$ up to 1 mm day^{-1} depending on the site (Figures 43 and 44). One disadvantage was the shorter record of corrected ET because there were fewer days when all instruments were functioning. The disadvantage was particularly acute at BLK009 and PLC045 where datalogger problems prevented collection of *Rn* and *G* for the first half of the growing season. As described above, this problem was partially alleviated by fitting the Fourier model to the available ET_{corr} data.

Eddy covariance results

Eddy covariance ET measurements were obtained for most of growing season at all sites (Table 7 and Appendix A). Two examples of the diurnal fluxes typical of summer conditions of the Owens Valley at sites with dry and wet soils are shown in Figure 45 where daytime surface heating due to solar radiation is partitioned into positive daytime sensible and latent heat fluxes. At night, net radiation was negative due to cooling of the land surface, latent heat flux was near zero due to the cessation of plant transpiration, and sensible heat flux was small and negative. Soil heat flux was a relatively small component of the energy balance and changed sign from negative to positive in mid-morning and from positive to negative in late evening. Note the different relative magnitudes of latent heat and sensible heat flux between sites with wet and dry soils. Latent heat flux accounted for a greater proportion of the available energy at wetter sites.

The Fourier model coefficients and fitting statistics are given in Table 10 and shown in Figures 46-54. The low r^2 for PLC018 and PLC185 (Table 9) was due in large part to the low and relatively flat seasonal ET trend (small variance). Visual inspection of Figures 52 and 54 suggests the agreement between the data and Fourier model was acceptable for the purpose of integration. ET_{corr} during the growing season ranged between 50 and 700mm (ETr was greater

Table 10. ET_{corr} Fourier model coefficients and r^2 for each site-year.

Year	Site	mean	A(1)	A(2)	B(1)	B(2)	r^2
		mm day^{-1}					
2000	BLK 100	1.37	-1.62	0.26	-0.12	0.06	0.93
2001	BLK 100	1.33	-1.56	0.27	-0.13	-0.12	0.90
	BLK 9	1.43	-1.65	0.31	-0.14	-0.17	0.95
	PLC 45	0.50	-0.50	0.12	0.15	-0.08	0.85
2002	BLK 100	1.12	-1.33	0.30	-0.27	0.03	0.98
	FSL 138	1.94	-2.28	0.50	0.10	-0.20	0.70
	PLC 18	0.18	-0.14	0.01	-0.03	-0.02	0.54
	PLC 74	0.60	-0.49	0.02	0.06	-0.004	0.63
	PLC 185	0.35	-0.33	0.05	0.05	-0.05	0.57

than 1500mm) depending on water table depth and plant attributes (Table 11).

ET seasonal trends corresponded with the expected trends in evaporative demand throughout the summer and usually were greatest in late June or early July. The sharp decline in ET at FSL138 on July 11 (Figure 51) corresponded with termination of soil water decline at depths above 1 m and with the deepest water table depth (2.05 m). This site had the shallowest water table of all sites, and the ET decline may reflect a decrease in surface E derived from the soil and/or decrease in T as the water table approached the bottom of the saltgrass root zone of approximately 2m. Direct evaporation from the water table was neglible as discussed below in Section III. LAI began to decline steadily after the measurement on July 9 suggesting that curtailed transpiration constituted some fraction of the observed reduction in ET. Most of the decline in LAI was due to decline in DISP2, but vegetation at this site had a significant component of beardless wildrye, *Leymus triticoides*, and minor amounts of *Juncus sp.* It is not known if differing physiology of these species contributed to the observed ET step change.

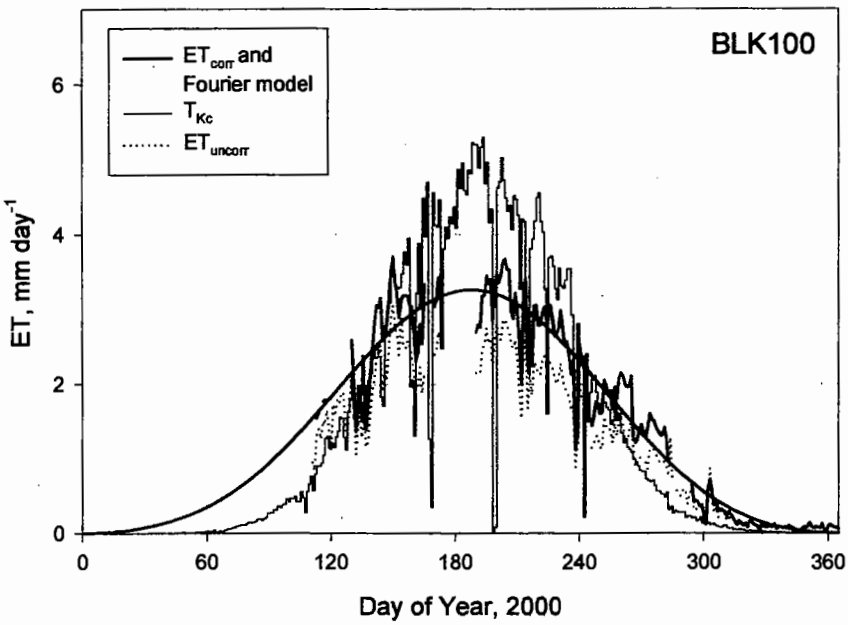

Figure 46. ET at BLK100 in 2000 measured with the EC system and estimated using field measurements and transpiration coefficients (Equation 17). EC measurements corrected and uncorrected for energy balance closure error are presented.

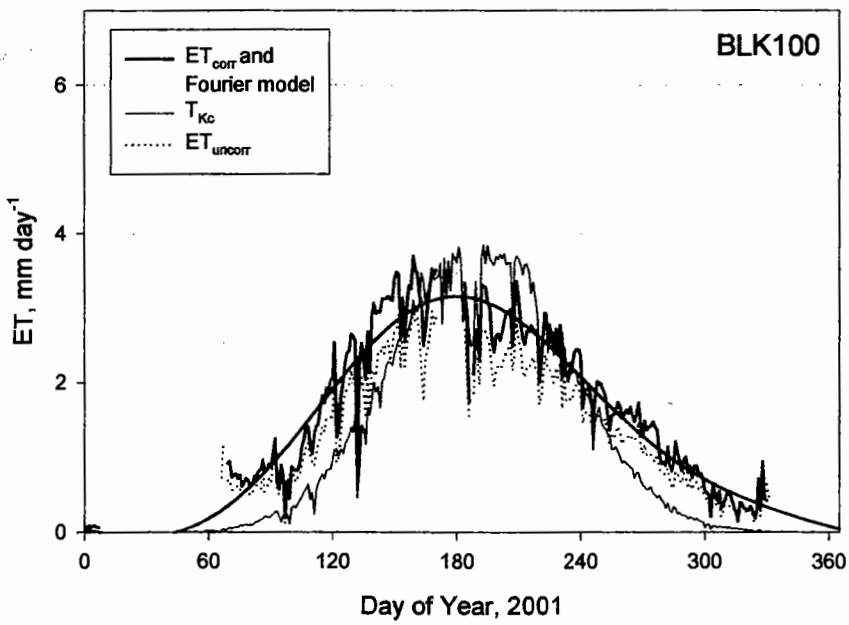

Figure 47. ET at BLK100 in 2001 measured with the EC system and estimated using field measurements and transpiration coefficients (Equation 17). EC measurements corrected and uncorrected for energy balance closure error are presented.

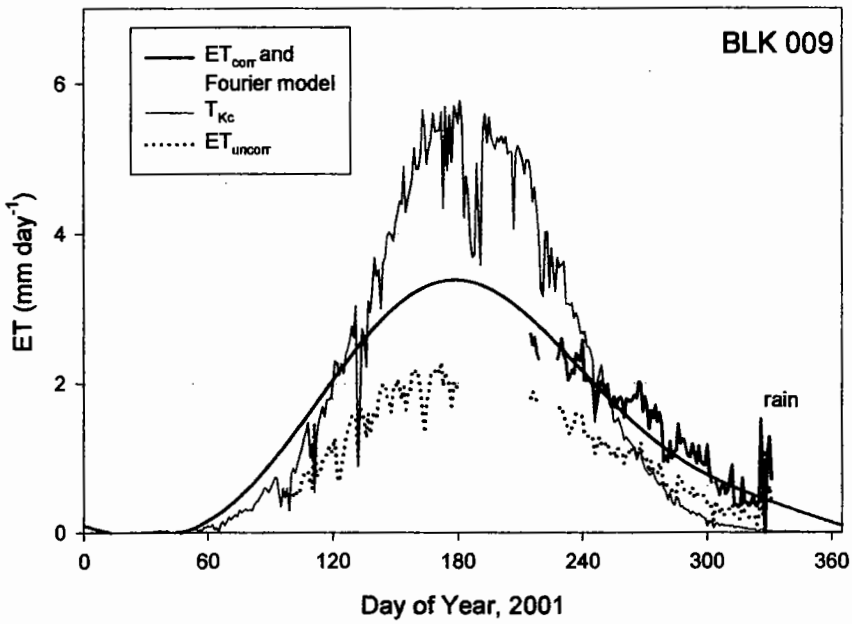

Figure 48. ET at BLK009 in 2001 measured with the EC system and estimated using field measurements and transpiration coefficients (Equation 17). EC measurements corrected and uncorrected for energy balance closure error are presented.

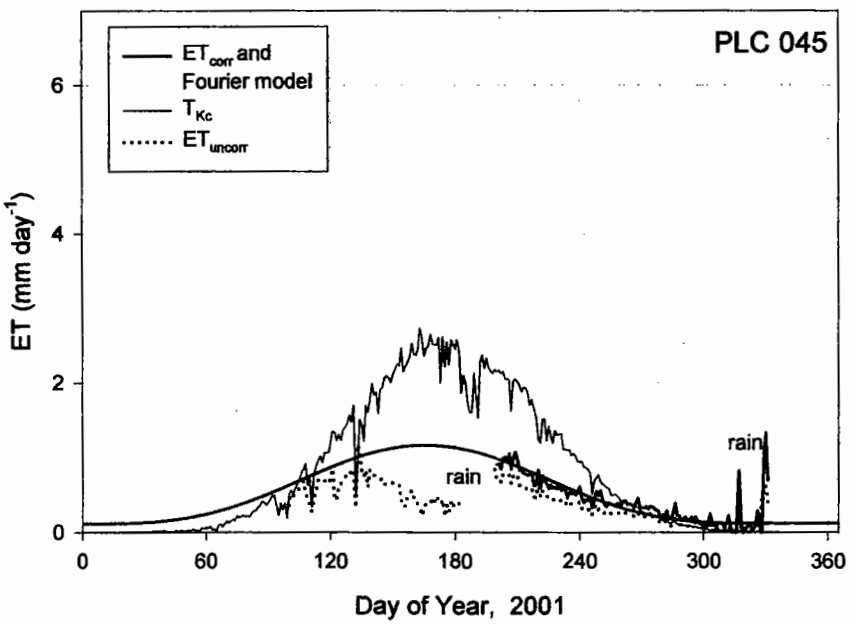

Figure 49. ET at PLC045 in 2001 measured with the EC system and estimated using field measurements and transpiration coefficients (Equation 17). EC measurements corrected and uncorrected for energy balance closure error are presented.

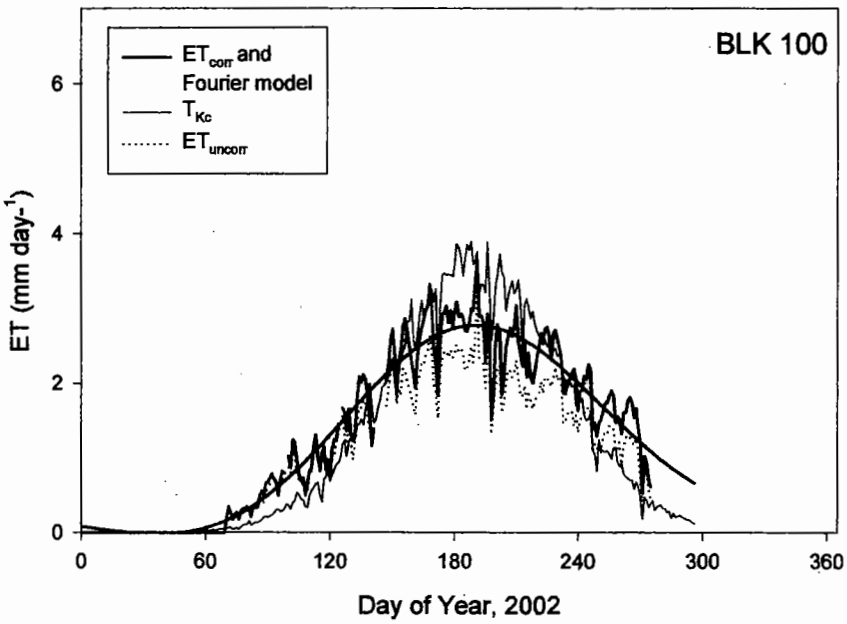

Figure 50. ET at BLK100 in 2002 measured with the EC system and estimated using field measurements and transpiration coefficients (Equation 17). EC measurements corrected and uncorrected for energy balance closure error are presented.

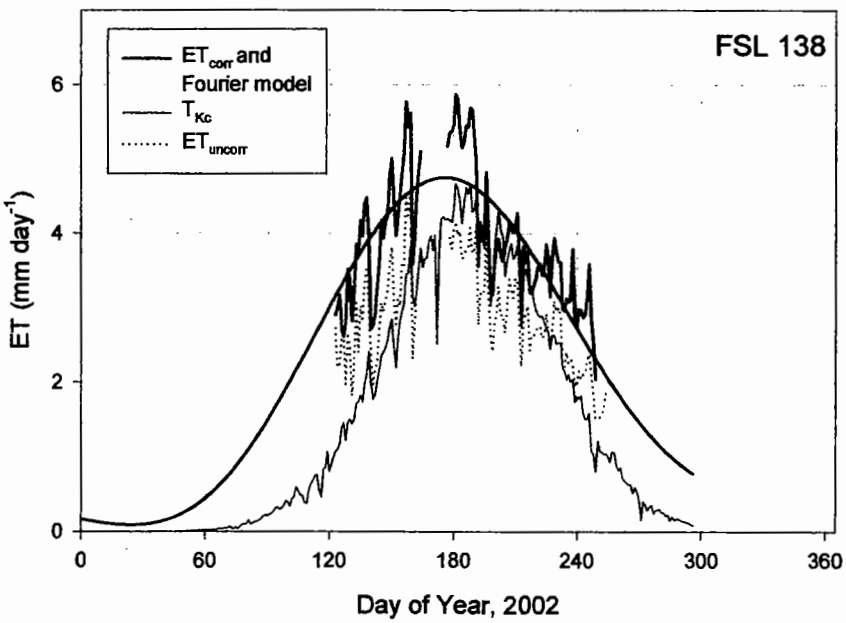

Figure 51. ET at FSL138 in 2003 measured with the EC system and estimated using field measurements and transpiration coefficients (Equation 17). EC measurements corrected and uncorrected for energy balance closure error are presented.

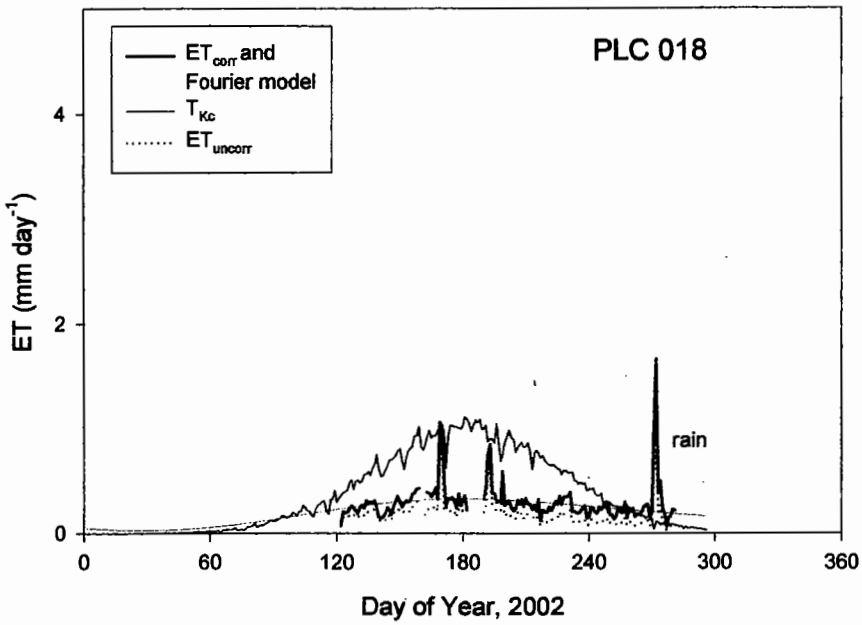

Figure 52. ET at PLC018 in 2002 measured with the EC system and estimated using field measurements and transpiration coefficients (Equation 17). EC measurements corrected and uncorrected for energy balance closure error are presented.

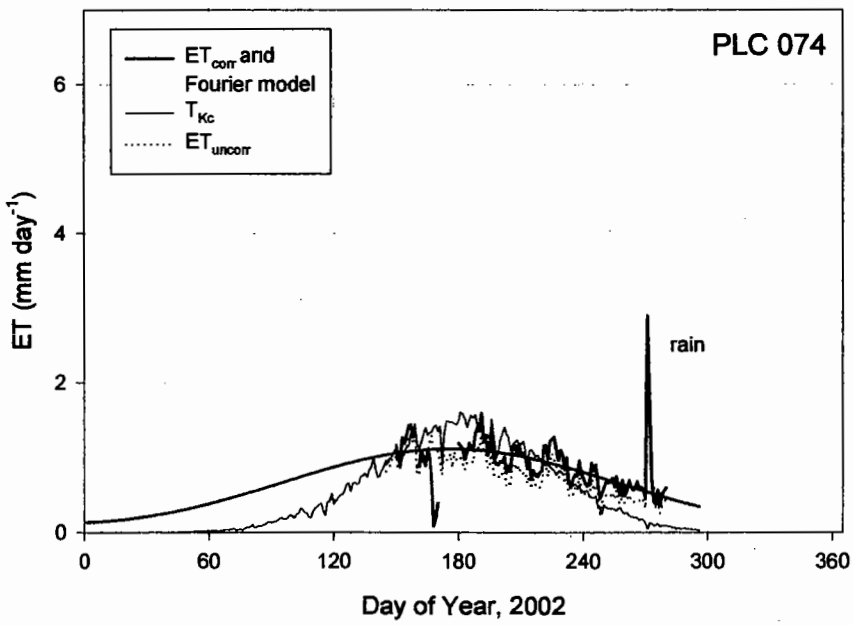

Figure 53. ET at PLC074 in 2002 measured with the EC system and estimated using field measurements and transpiration coefficients (Equation 17). EC measurements corrected and uncorrected for energy balance closure error are presented.

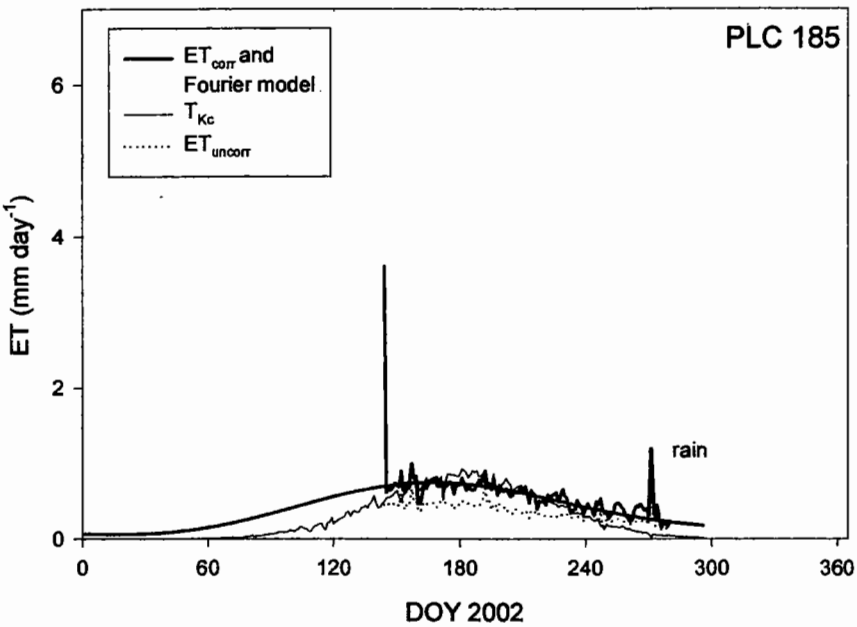

Figure 54. ET at PLC185 in 2002 measured with the EC system and estimated using field measurements and transpiration coefficients (Equation 17). EC measurements corrected and uncorrected for energy balance closure error are presented.

Comparison of EC and T_{Kc} results

Performance of the Kc models and vegetation measurements was evaluated to address three questions: 1) Did T_{Kc} approximate seasonal trends in ET measured by the EC stations? 2) Did the seasonal estimates of T_{Kc} compare favorably with measured seasonal totals? and 3) Did the LAI models for dominant species used to construct the Kc models agree with field measurements?

Daily values of ET measured by EC methods and corrected for the energy imbalance are presented in Figures 46 to 54 along with the daily T_{Kc} estimated using transpiration coefficients and LAI measurements (Steinwand, 1999b; Steinwand et al., 2001). Seasonal trends in T_{Kc} were

Table 11: Eddy covariance ET corrected for energy balance closure and T estimated from Kc models and measured *LAI* and ETr_i. Vegetation measurements taken nearest the date of maximum LAI for the dominant species in Kc models were used (Table 9). Measured and predicted fluxes are the sum of daily totals for the period with available corrected eddy covariance measurements and integrated for the entire growing season using the fitted Fourier model (March 25-October 15).

Year	Site	ET_{corr}	T_{Kc}	T_{Kc} RMSE †	Growing season ET_{corr}	Growing season T_{Kc}	Growing season T_{Kc} RMSE
		mm	mm	mm day^{-1}	mm	mm	mm day^{-1}
2000	BLK 100	337	355	0.80	460	472	0.71
2001	BLK 100	434	341	0.66	446	384	0.72
	BLK 9	152	127	0.78	471	593	0.74
	PLC 45	55	85	0.53	165	266	0.49
2002	BLK 100	347	337	0.54	377	362	0.51
	FSL 138	450	328	1.27	646	414	1.48
	PLC 18	45	89	0.31	53	107	0.25
	PLC 74	112	101	0.42	177	147	0.40
	PLC 185	77	68	0.20	108	82	0.19

†: RMSE = $[\sum(ET_{corr}\text{-model})^2/n]^{0.5}$

similar to trends in ET_{corr} at BLK100 (all years), PLC074, and PLC185. At these sites (and FSL138), T_{Kc} tended to underestimate early and late season ET_{corr} but overestimated midsummer ET. Seasonal trends in T_{Kc} compared less favorably at BLK009, FSL138, PLC045, and PLC018. At FSL138, PLC045, and PLC018, the failure may be due to failure of site conditions to meet model assumptions. At PLC 045 and PLC 018, the water table was at or below the maximum rooting depth for saltbush and rabbitbrush and the upper 4 to 5 meters of soil was near limiting water content. The Kc models were developed from data collected at sites with sufficient soil water, and therefore, it was not surprising that T_{Kc} overestimated ET_{corr}. The decline in LAI and

ET (inferred from decline in uncorrected *ET*) during June at PLC045 corresponded with the exhaustion of available soil water within the monitored soil depth (3.2m) by June 21. Subsequently, leaf area and ET_{corr} at this site responded to approximately 2 cm rain in early July (Figure 49). The T_{Kc} and Fourier models cannot accommodate the bimodal response exhibited at this site. As described above, the fraction of E from the soil may have been sizeable at FSL138 due to the shallow water table and moist soils near the surface. T_{Kc} doesn't include soil E which could account for part of the underestimation. Failure of the models at BLK009 was not easily attributable to nonnegligible soil surface evaporation or plant water stress, and the failure may reflect an inherent inability of the models to estimate ET of the dominant species, CHNA2. This discrepancy, should be investigated further.

The model agreement with daily ET_{corr} was evaluated by calculating the root mean squared error (RMSE) between T_{Kc} or T_{GB} and measured daily ET_{corr}. The root mean squared error (RMSE) of T_{Kc} model and measured daily ET ranged from 0.23 to 1.45 mm d^{-1} (Table 11). The low RMSE for BLK009 and PLC045 was deceptive, however, because the period with available ET_{corr} was limited to after late July. At both sites, values for ET_{corr} were not available for first half of the season and the differences were not included in the RMSE calculation (Figures 48 and 49).

The comparison of the daily ET measurements and T_{Kc} estimates are presented in Table 11. As shown above, the seasonal trends in T_{Kc} and ET_{corr} did not agree at some sites making the comparison of total ET based only the days for which data are available dependant on which portion of the growing season was measured. That problem also prevents site to site comparisons or for BLK100, year to year comparisons without relying on a model to integrate

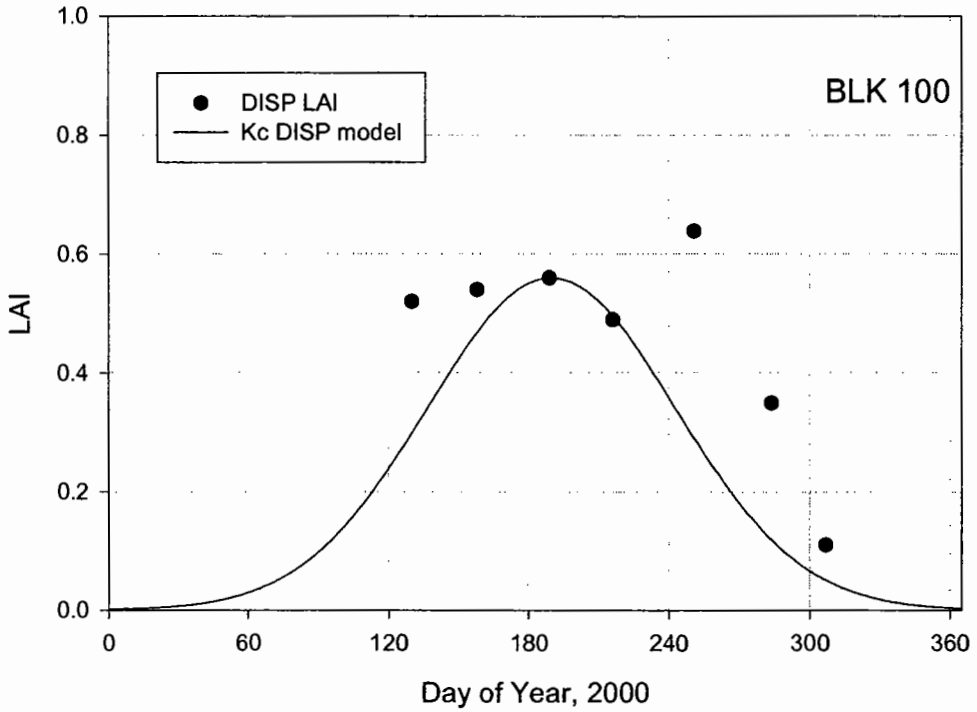

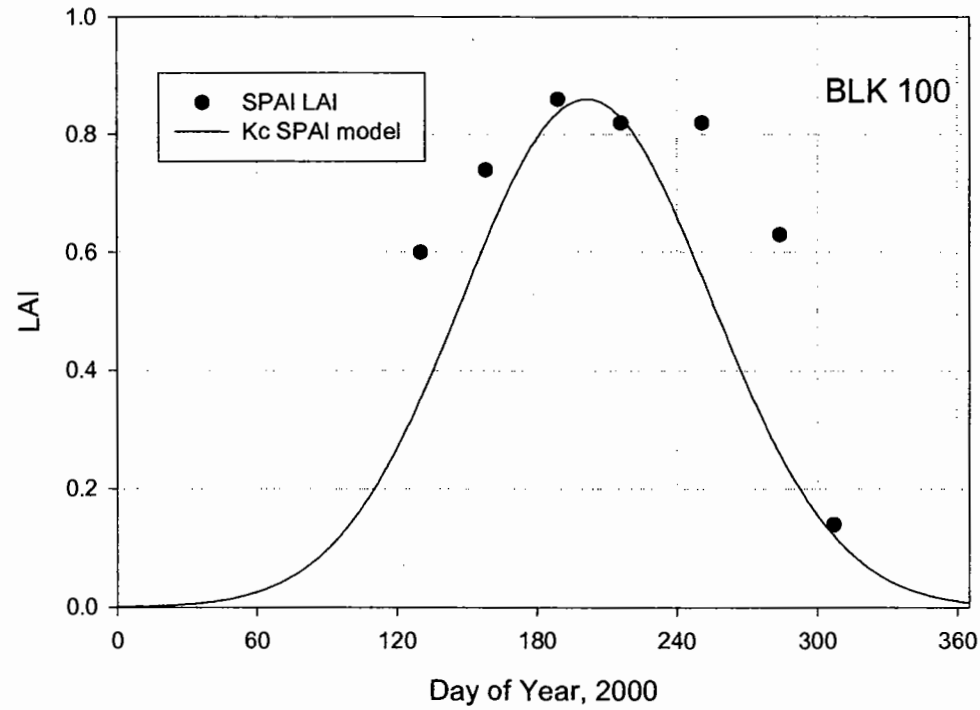

Figure 55. Measured LAI for dominant species at BLK100 in 2000 and LAI model in the Kc model scaled to the LAI used to calculate T_{Kc} LAI is the mean of the four transects.

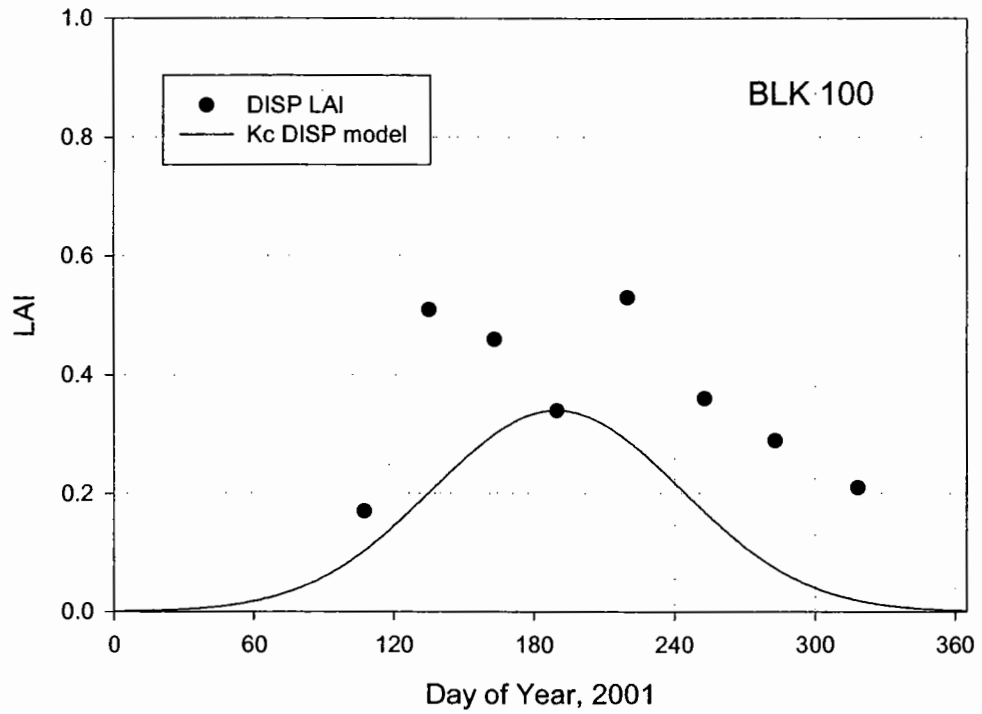

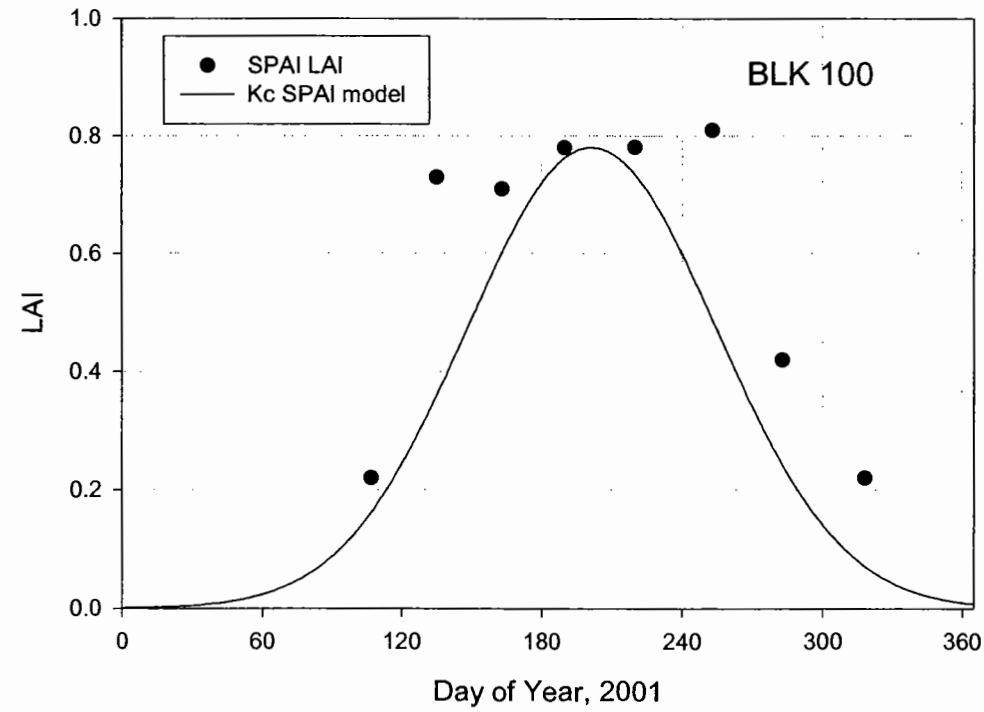

Figure 56. Measured LAI for dominant species at BLK100 in 2001 and LAI model in the Kc model scaled to the LAI used to calculate T_{Kc}. LAI is the mean of the four transects.

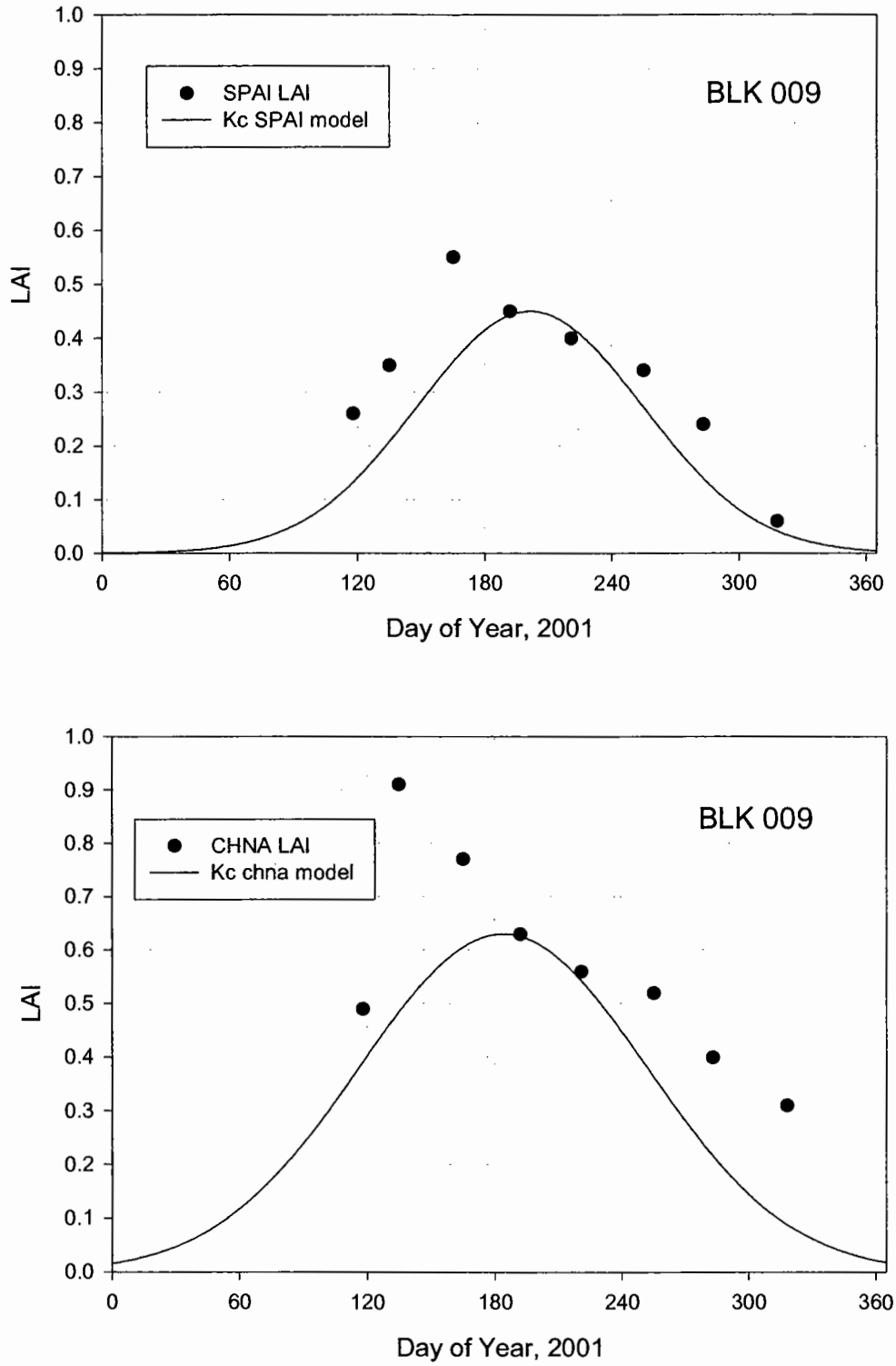

Figure 57. Measured LAI for dominant species at BLK009 in 2001 and LAI model in the Kc model scaled to the LAI used to calculate T_{Kc}. LAI is the mean of the four transects.

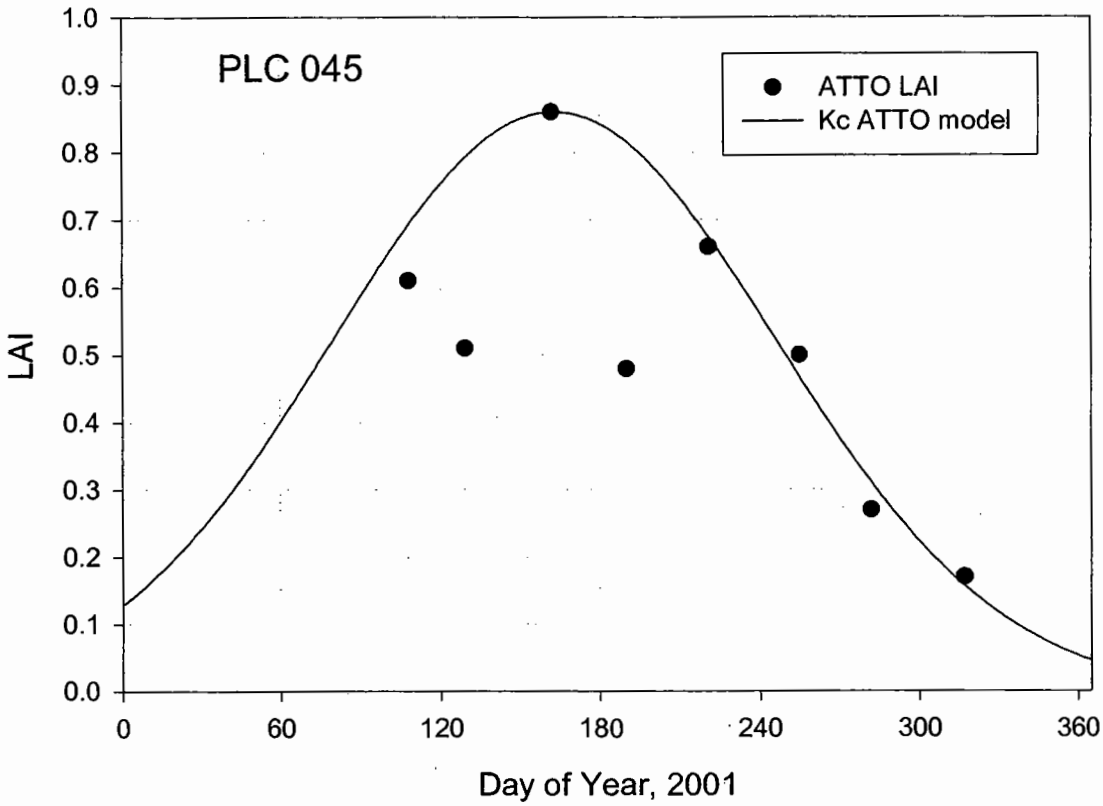

Figure 58. Measured LAI for dominant species at PLC045 in 2001 and LAI model in the Kc model scaled to the LAI used to calculate T_{Kc}. LAI is the mean of the four transects.

the seasonal total between uniform integration limits. The growing season values agreed best at well at BLK100 (all years) PLC074, and PLC185. The values were not expected to compare well for PLC046 and PLC018 for reason described above. Finally, T_{Kc} varies several centimeters if the LAI measurements bracketing the selected date for peak LAI are applied in Equation 16 indicating that reliance on a single midsummer measurement to represent the maximum LAI is a potentially large source of error if the peak LAI doesn't correspond with the sampling date because of site-specific or variable weather conditions.

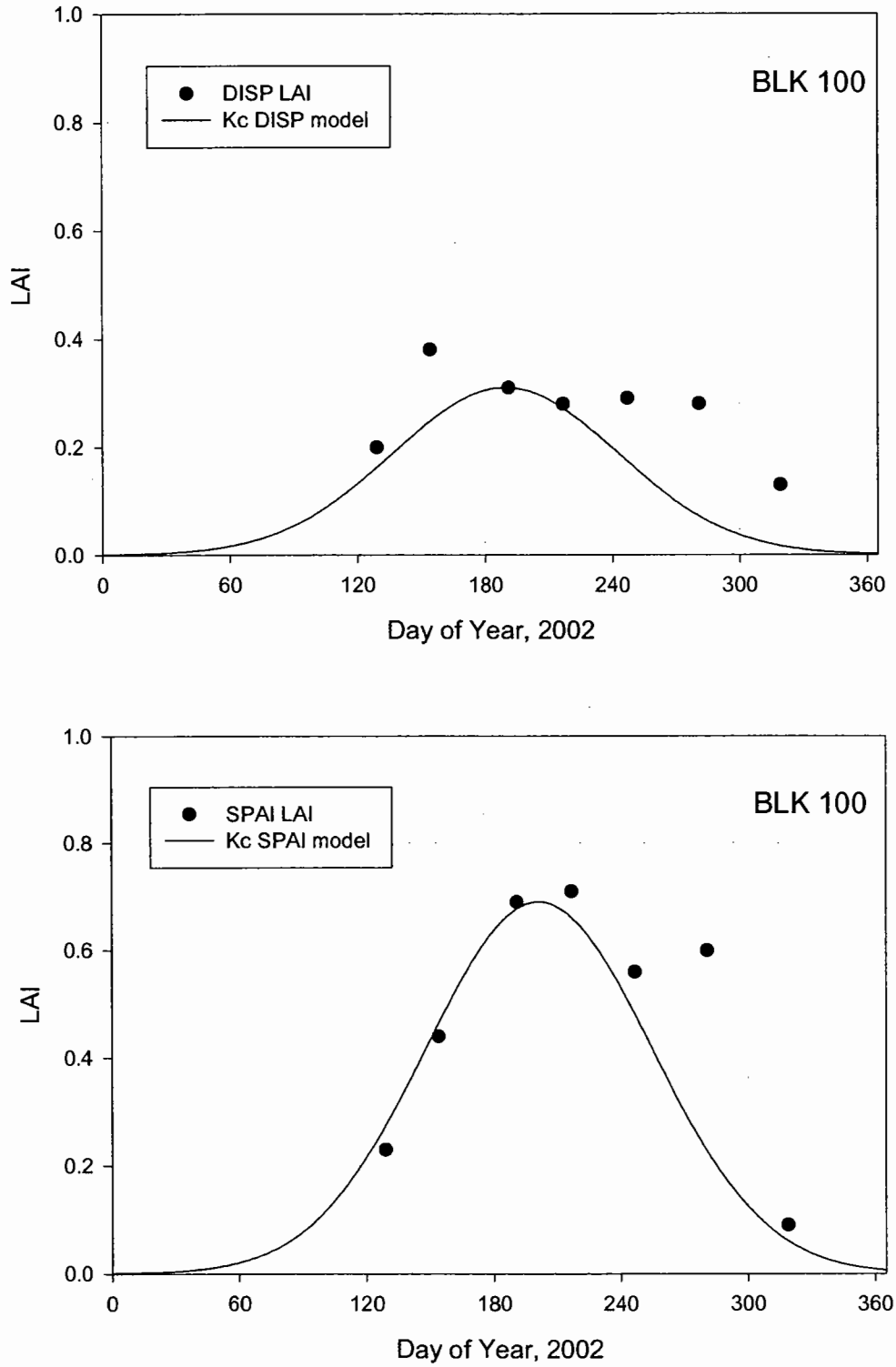

Figure 59. Measured LAI for dominant species at BLK100 in 2002 and LAI model in the Kc model scaled to the LAI used to calculate T_{Kc}. LAI is the mean of the four transects.

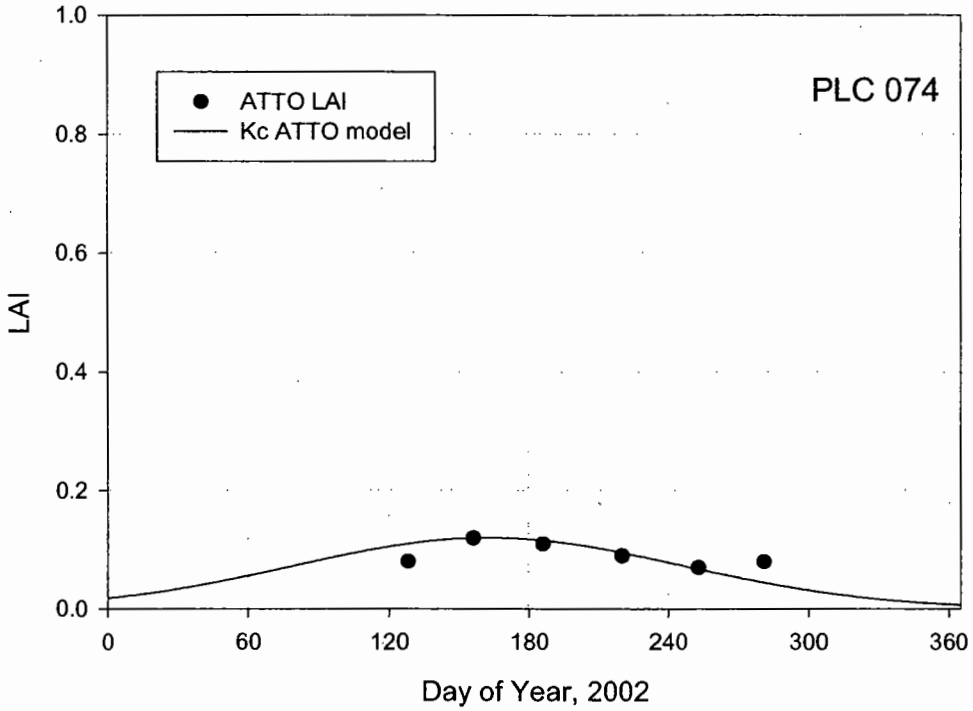

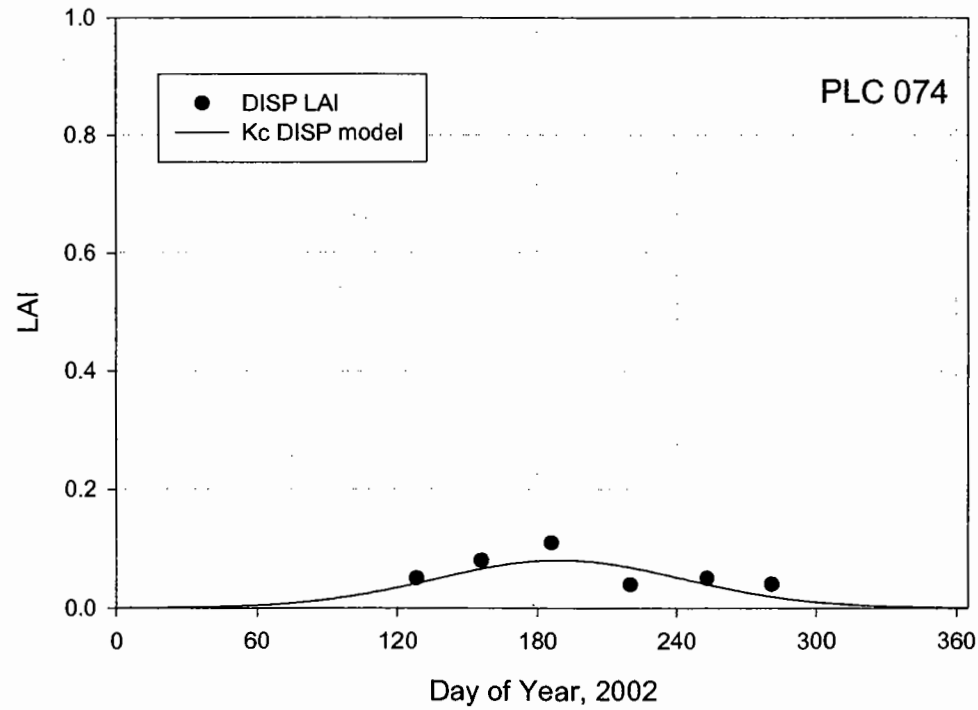

Figure 60. Measured LAI for dominant species at PLC074 in 2002 and LAI model in the Kc model scaled to the LAI used to calculate T_{Kc}. LAI is the mean of the four transects.

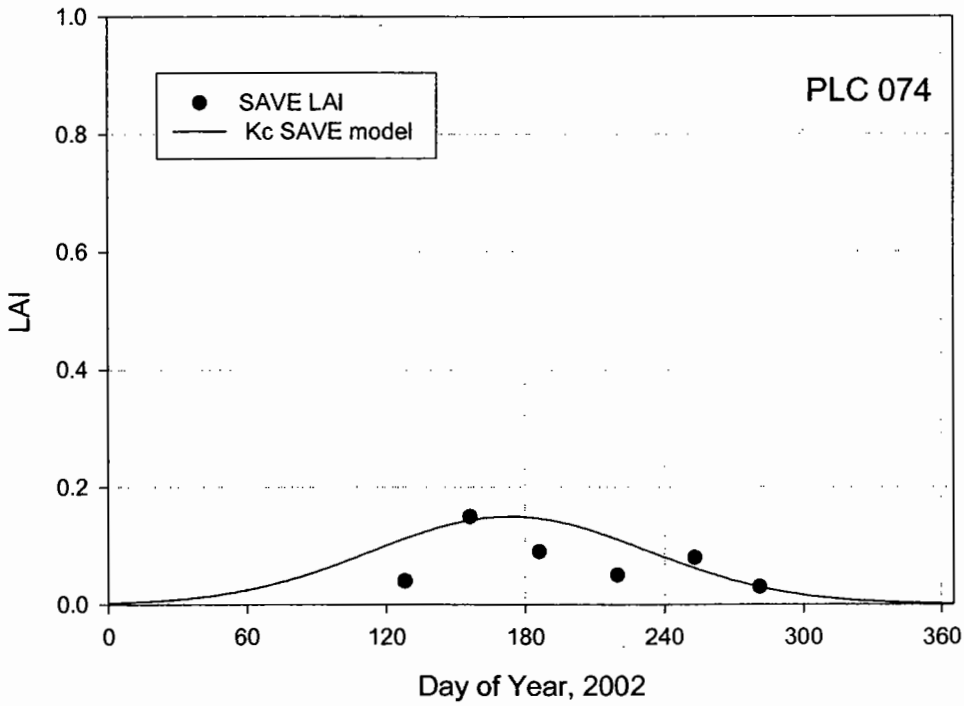

Figure 61. Measured LAI for dominant species at PLC074 in 2002 and LAI model in the Kc model scaled to the LAI used to calculate T_{Kc}. LAI is the mean of the four transects.

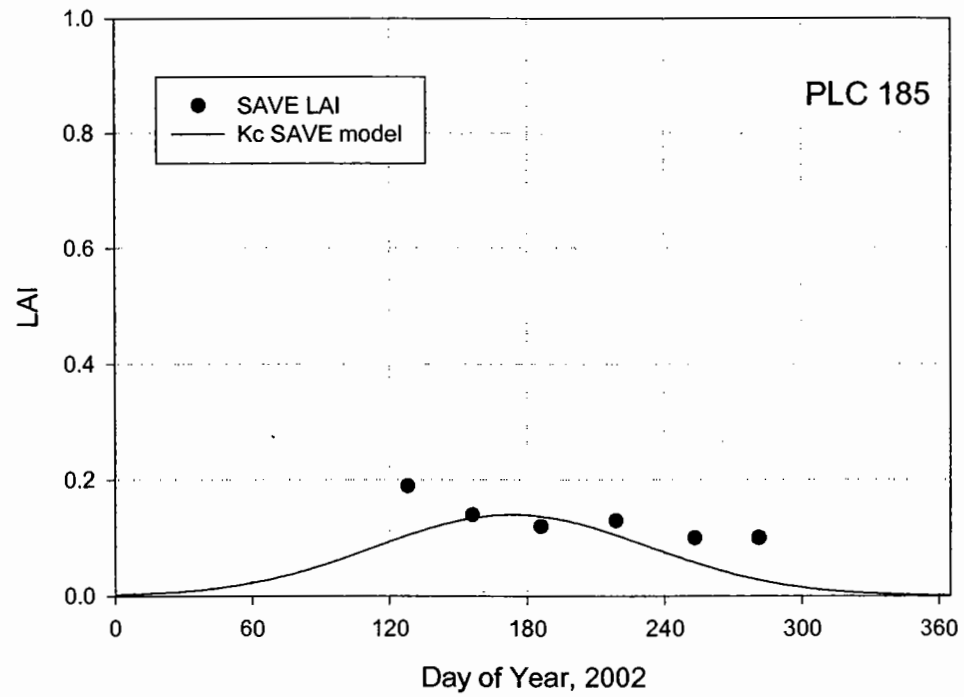

Figure 62. Measured LAI for dominant species at PLC185 in 2002 and LAI model in the Kc model scaled to the LAI used to calculate T_{Kc}. LAI is the mean of the four transects.

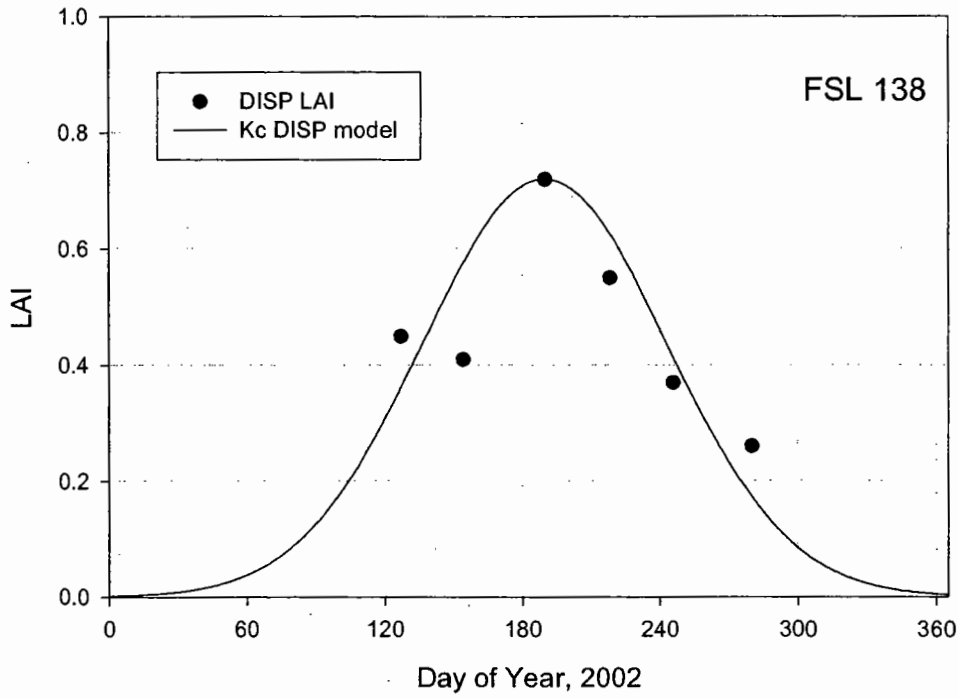

Figure 63. Measured LAI for dominant species at FSL138 in 2002 and LAI model in the Kc model scaled to the LAI used to calculate T_{Kc}. LAI is the mean of the four transects.

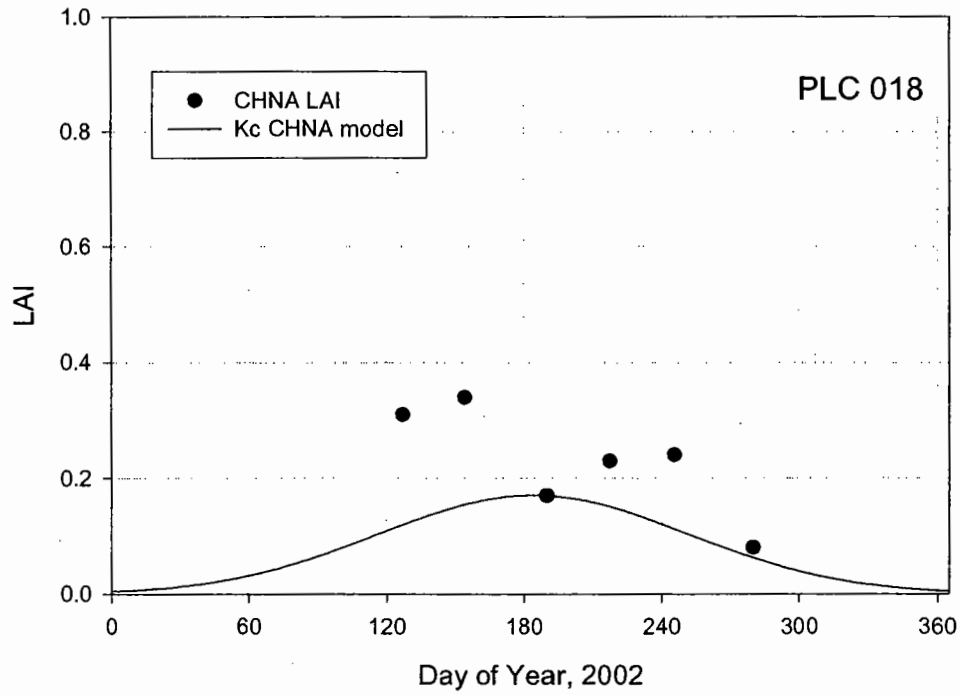

Figure 64. Measured LAI for dominant species at PLC018 in 2002 and LAI model in the Kc model scaled to the LAI used to calculate T_{Kc}. LAI is the mean of the four transects.

LAI of the dominant species at the EC sites was variable during the June-July period (midsummer). LAI for individual species generally showed fair correspondence between the observed maximum LAI and the timing of peak LAI in the Kc LAI models (Figures 55 to 64). Again, measured LAI used was the date nearest the average maximum LAI in the original Kc development. Examples of poor agreement were DISP2 at BLK100 in 2001, CHNA2 at BLK009 and PLC018, ATTO at PLC045. At these sites, the correspondence of the model and data could be improved considerably by better relying on vegetation measurements data collected on another date to fix the maximum *LAI*. Generally the shape of the model corresponded with field measurements; however, the models reflected trends in the data poorly and underestimated LAI for dominant species at BLK100, BLK009 and PLC018.

Conclusions

Turbulent fluxes measured by the EC system did not account for approximately one-third of the available energy. Similar discrepancies have been observed in other studies using EC methods. During periods when the BR system obtained stable measurements, the Bowen ratios measured by the two systems substantially agreed. It is recommended that EC measurements of λE be corrected by using the Bowen ratio measured by the EC system to account for all the available energy. Total ET corrected for the energy balance was measured by eddy covariance at seven sites with growing season totals ranged between 50 and 700mm (ETr greater than 1500mm) depending on water table depth and plant attributes. Seasonal total ET_{corr} generally agreed with estimates derived from Kc models and LAI measurements when the site conditions met assumptions of the Kc models. Variability in LAI among species during the peak months of the growing season (early June to early July) and the sensitivity of T_{Kc} estimates on correctly

sampling the peak LAI, however, is suggests that a single sampling date may be unacceptable.

III. Task 2: Vadose Zone model

This task was composed of two subtasks, field investigation of the soil water balance components and revision of a previously constructed vadose zone model that combined plant water use, soil water storage, and water table fluctuations to predict future water storage and plant water availability (Or and Groeneveld, 1994).

Field investigation

Introduction

Phreatophytes are known to utilize groundwater, but quantifying the portion of ET during the growing season drawn from groundwater is difficult. Plant uptake (T) largely drives changes in stored soil water and possibly depth to water table in the absence of hydrologic manipulations. Understanding the partitioning of T between soil water and groundwater sources, therefore, is essential to prepare an accurate model of the vadose zone water balance for phreatophytes. Field experiments were conducted to provide an accounting of the depths and magnitudes of water uptake by plant roots at sites instrumented with EC stations. The purpose of this task was collect field data to examine sources of plant uptake necessary to examine conceptualization of specific components of the vadose zone water balance model.

Materials and Methods

Site selection and instrumentation

Monitoring locations distributed vertically and laterally through the vadose zone near the

EC stations were visited periodically during this project. Detailed measurements of soil water content were conducted using a combination of time domain reflectometry (TDR), neutron probe access tubes, and gravimetric sampling. In the original proposal, matric potential monitoring was planned to support detailed numerical soil water modeling. The purpose of that effort was to assist parameterization of groundwater uptake in the vadose zone water balance model, but the intensity of that field and modeling effort was deemed infeasible and unnecessary. That methodology was replaced by the combination of soil hydraulic property measurements and simpler analytical models described below. The site selection and instrumentation are described in Section II

Soil characterization

Particle-size analyses by the hydrometer method (Gee and Bauder, 1986) were completed on sixty-five soil samples collected during access tube installation. Samples were selected to represent obvious textural differences observed during field sampling. Samples were analyzed for all sites except PLC074. Soil characterization data for PLC074 were available from previous research conducted at this site by LADWP, Inyo County, and Natural Resources Conservation Service (Appendix B).

Soil water retention measurements were collected on intact core samples collected at approximately 0.3m depth near each access tube. Retention measurements were collected using pressure cell methods (Dane and Hopmans, 2002). Parametric models of van Genuchten (1980) and Maulem (1976) and the retention curve data were used to derive parameters necessary to perform analytic modeling for the vadose zone model development. These results are given in Appendix B.

Saturated paste extracts were prepared to measure salinity of surface samples at BLK009, BLK100, and PLC045 (Rhoades, 1982). These data were used to assess the possibility for successful TDR measurements. TDR instruments often fail if soil salinity is greater than 5 dS/m.

TDR measurements were made of the surface soil layer in conjunction with the gravimetric samples to determine the potential of using TDR for routine measurements of θ. Surface TDR measurements are less destructive and quicker than the gravimetric samples. Surface (0-12 cm) measurements were collected using a Hydrosense TDR system (Campbell Scientific) after calibration using soils from Owens Valley several sites. The instrument was most reliable at sites with dry sandy soils (PLC074, PLC185) and least reliable at BLK100 when the soil was moist, probably due to soil salinity. Data from gravimetric sampling was used when the TDR failed.

Soil Water Balance (SWB) and Partitioning

This study determined the partitioning of ET between groundwater (ET_{gw}) and soil water (ET_{soil}) sources by measuring or estimating the water balance components and closure of the water balance,

$$\text{(i) } ETa = ET_{soil} + ET_{gw}, \quad \text{(ii) } ET_{soil} = P + \Delta S, \quad \text{(iii) } ET_{gw} = E_{gw} + T_{gw} \qquad (19)$$

$$\text{(iv) } T_{gw} = ETa - E_{gw} - P - \Delta S$$

where ET_{corr} is as defined previously, ΔS is change in soil water storage, P is precipitation, and T_{gw} and E_{gw} are transpiration and evaporation derived from groundwater, respectively. Runon, runoff, and deep percolation of precipitation were neglible. Partitioning calculations were made for the growing season (March 25 to October 15) because of vegetation phenology and

availability of field ET measurements. This period encompassed the majority of annual ET because vegetation is senesced during the winter. Determination of the each component of the water balance is described in the sections below.

ET_{corr}, Actual ET. ET_{corr} was the derived by summing the daily ET_{corr} values of the Fourier model. Please refer to Section II for a description of the EC methods and model fitting.

E_{gw}, Evaporation from Water Table. Under the arid conditions of Owens Valley, with relatively fine-textured soils in some of the sites, and in the presence of relatively shallow water table (<2 m) this component of the water balance may represent a significant contribution to the seasonal water balance. Availability of continuous eddy covariance measurements allowed us to estimate the magnitude of direct evaporation from the water table through the soil when plants were not actively transpiring, i.e. at night. E_{gw} was determined by summing nighttime ET_{corr}. This should be a generous estimate because it discounts soil E and leakage through plant stomata. To test whether this procedure gave realistic estimates, we compared nighttime ET_{corr} at BLK100 with theoretical predictions. BLK100 was chosen because it had the longest period of record and the finest textured soil (Appendix B), i.e. the greatest capillarity above the water table. Gardner (1958) derived an analytical expression for relating the maximum evaporation flux from a dry soil surface (E_{gw} [m/h]) as a function of soil properties (saturated hydraulic conductivity Ks [m/h], and an extinction parameter α [1/m])) and water table depth L [m],

$$E_{gw} = \frac{Ks}{\exp^{(\alpha L)} - 1} \tag{20}$$

The expression shows that for a water table depth of zero (at the soil surface) the soil-controlled rate of evaporation would be the saturated hydraulic conductivity. For a deep water table (large

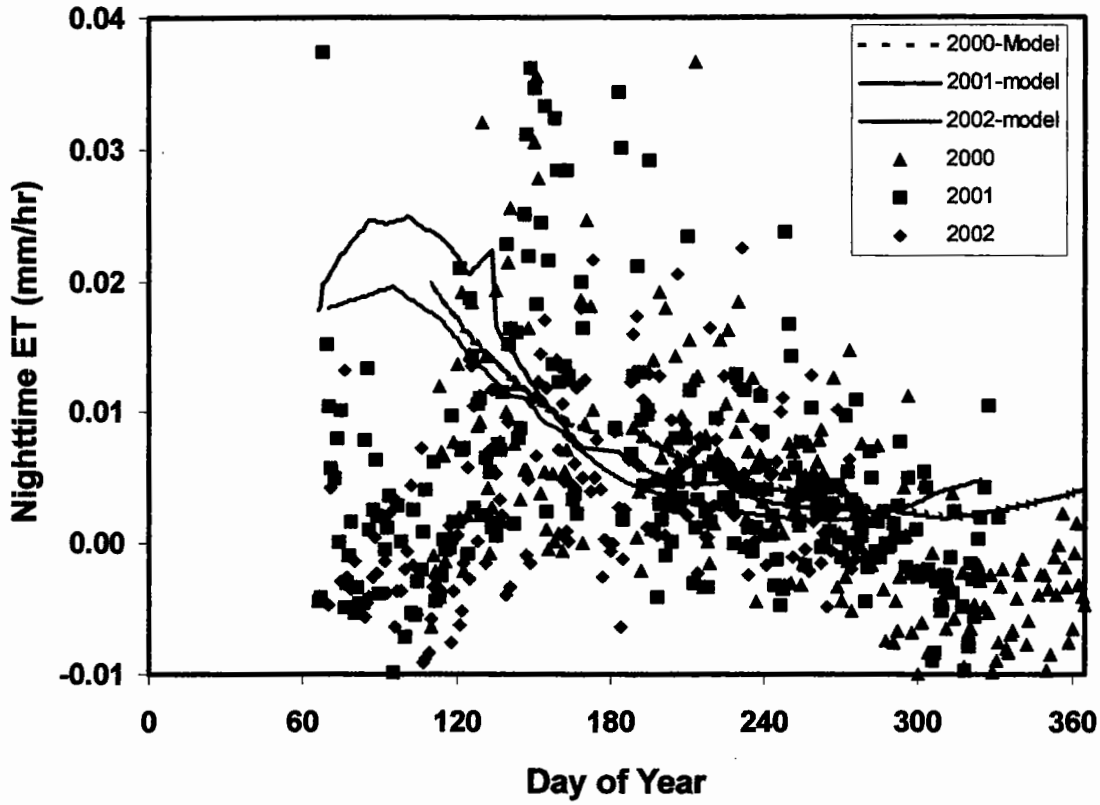

Figure 65. Nighttime soil evaporation measured by EC method at BLK100. Note the strong seasonal trend. Lines represent model predictions based on water table depth (Equation 20).

L) the direct evaporation would be zero. The analytical model results and nighttime ET_{corr} for BLK100 are presented in Figure 65. The results for show that for measured Ks of 8.5 mm/h (from soil water retention curve measurements), and water table range of depths from 2000 to 2500 mm, the best fit to the EC data was obtained with an estimated α=0.0027 [1/mm] which was consistent for the fine textured soil at this site. The magnitudes of theoretical E_{gw} and nighttime ET_{corr} were similar except for the early growing season (about DOY 90-130) when the water table was shallowest. The poor agreement for these months is not unusual because the

Gardner model only considers soil factors controlling evaporation rate and ignores that evaporation demand early in the growing season is small. The similarity of the two estimates for most of the growing season, however, and the small magnitudes of estimates derived using either method suggest that summing nighttime ET provided an acceptable and conservative (high) value for E_{gw}.

ΔS, Change in Stored Soil Water. Methods for neutron and gravimetric soil water measurements are described in Section II . Soil water stored in the soil (S) (cm/soil depth) was calculated according to,

$$S_{tube} = \sum \theta_i \Delta z_i \tag{21}$$

where θ_i is volumetric water content depth i and Δz_i is the thickness of the soil interval represented by θ_i. The storage calculation was calculated for the entire monitoring depth or for specific portions of the root zone to differentiate uptake groundwater from soil water uptake and then averaged to derive S. The change in soil water was taken as the maximum change observed between a measurement in the spring (usually the time S is greatest) and a measurement in the late summer or fall when S was smallest.

P, Precipitation. Precipitation was measured after each event by Inyo County or daily by the National Oceanic and Atmospheric Administration (NOAA). Rain gauges assigned to the sites were: Inyo County RG-6: BLK100, BLK009; Bishop Airport NOAA: PLC045, PLC074, PLC018; Inyo County RG-3: PLC185; Inyo County RG-1: FSL138. Equation 19 assumed that all P is utilized by vegetation. This assumption was probably inaccurate as some P evaporates directly back into the atmosphere and contributes to ET_{corr}. This will have no effect on

Table 12: Soil water balance components and calculation of T_{gw} for EC sites. The values represent growing season totals (March 25 to October 15.

Year	Site	T_{gw}	ET_{corr}	P	ΔS_{max}	E_{gw}	T_{gw}/ET_{corr}
		(mm)	(mm)	(mm)	(mm)	(mm)	
2000	BLK 100	338	460	11	99	12	0.73
2001	BLK 100	310	446	15	104	17	0.70
	BLK 9	310	471	15	131	15	0.66
	PLC 45	96	165†	35	34	0	0.58
2002	BLK 100	294	377	1	68	14	0.78
	FSL 138	490	646	2	97	57	0.76
	PLC 18	13	53	3	37††	0	0.25
	PLC 74	102	177	3	72	0	0.57
	PLC 185	36	108	3	69††	0	0.33

†: As described in the test this value may be exaggerated slightly because of the poor correspondance with actual ET trends and shape of the Fourier model.
††:Initial soil water measurement was 1 month into growing season and soil was near limiting suggesting maximum was ΔS_{max} underestimated. ΔS_{max} determined by adding winter precipitation depleted before first S measurement: PLC18, 35mm+2mm, PLC185, 35mm+34mm.

calculation of T_{gw} because the fraction of P contributing directly to ET_{corr} would have to be subtracted from variables on the same side of the equation (Equation 19iv). Double counting of P that infiltrated into the soil was avoided by defining S as the difference between measurements early and late in the growing season and ignoring P-driven increases in S during the summer.

Results and Discussion

Soil Water Balance (SWB) and Partitioning

All components of the seasonal soil water balance are given in Table 12. The portion of T derived from the water table was estimated from the water balance as the difference between ET_{corr}, soil water depletion, precipitation, and evaporation. The component of E derived from the water table was a negligible fractions of the SWB for all sites. P was neglible for all sites

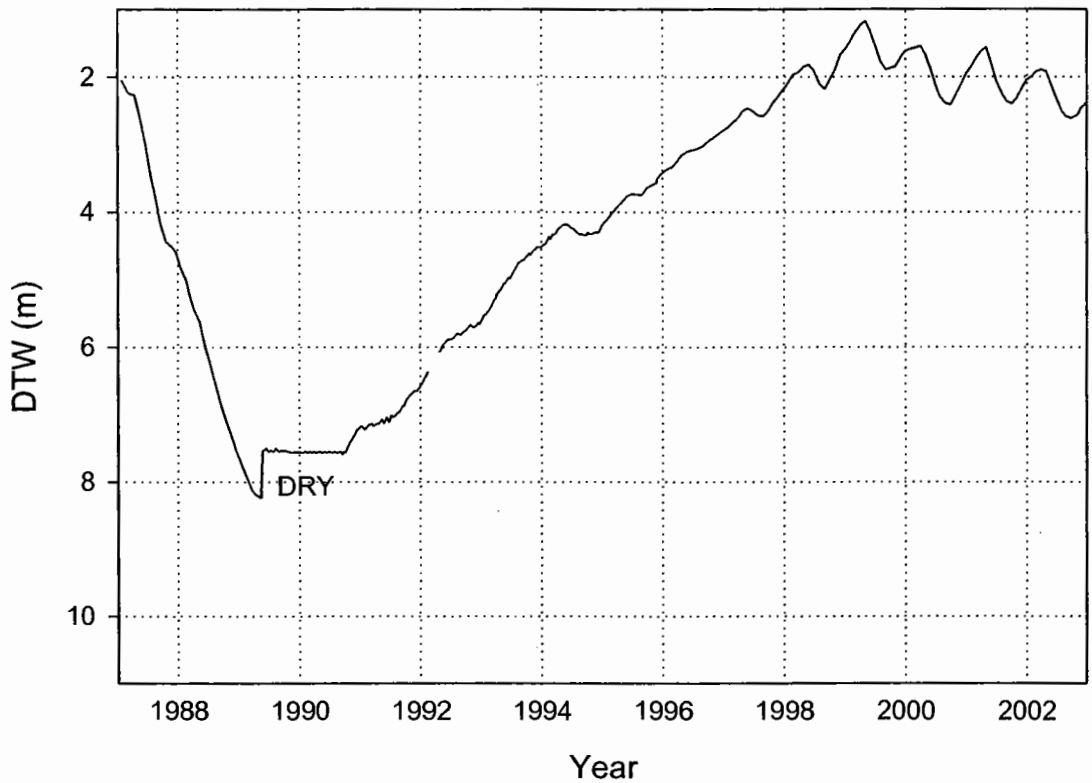

Figure 66. Hydrograph for monitoring well 419T. The magnitude of the intra-annual fluctuations do not correspond with pumping 1991 to 2003 and increase when the water is near the root zone (2m).water table to well below the root zone (approximately 2 m).

except PLC045. Direct uptake accounted for 66 to 80% of ET_{corr} for high cover sites with water table depths of 1 to 3 m. The site with the lowest contribution from the water table was PLC018. This site probably wasn't coupled to groundwater (DTW >5 m) suggesting this is the limit on the precision of our estimate of T_{gw}.

Determination of T_{gw} as the residual in the SWB lumps error for each component into the estimate. Because of this uncertainty, it was important to compare the results with an

independent estimate of T_{gw}. An important hydrologic signature that could assist quantification of plant uptake from groundwater is the rate and magnitude of water table drawdown (Freeze and Cherry, 1979). Evidence from recent water table recovery in a monitoring well, 419T, in an alkali meadow plant community (Figure 66) provides an example of the expected signature of vegetation uptake on seasonal water table fluctuations. The dramatic water level decline from 1987 to 1990 corresponded with a period of heavy pumping in this wellfield which lowered the Beginning in 1991, pumping was curtailed substantially with all occurring from one or two wells greater than 4.6 km from 419T. Notice that during the recovery from 1990 to 1997 when water levels were deeper than 3.0 m there was practically no seasonal variations in water table depths (other than those influenced by regional hydrological processes). In contrast, from 1997 to 2002 a clear seasonal fluctuation is evident that starts every year near the beginning of April coinciding with the onset of significant plant activity. Seasonal fluctuations in 419T did not correspond with pumping suggesting that ET may be controlling the intra-annual fluctuations.

We examined the relationship between plant water uptake and water table fluctuations to establish independent support for the values of T_{gw} derived from water balance closure. A key step to establishing that plants indeed drive the observed fluctuations in water table depth, was to measure water table depth at high temporal resolution and differentiate between behavior during the day time when plants transpire and during nighttime when T is substantially reduced. Results of high temporal water table depth measurement at BLK100 and PLC074 are depicted in Figures 67 and 68. In contrast to a relatively constant water table drawdown during the day (when plants are transpiring), during the night, there was practically no change in water table depth. Daily water table drawdown and concurrent related ET_{corr} results are summarized in

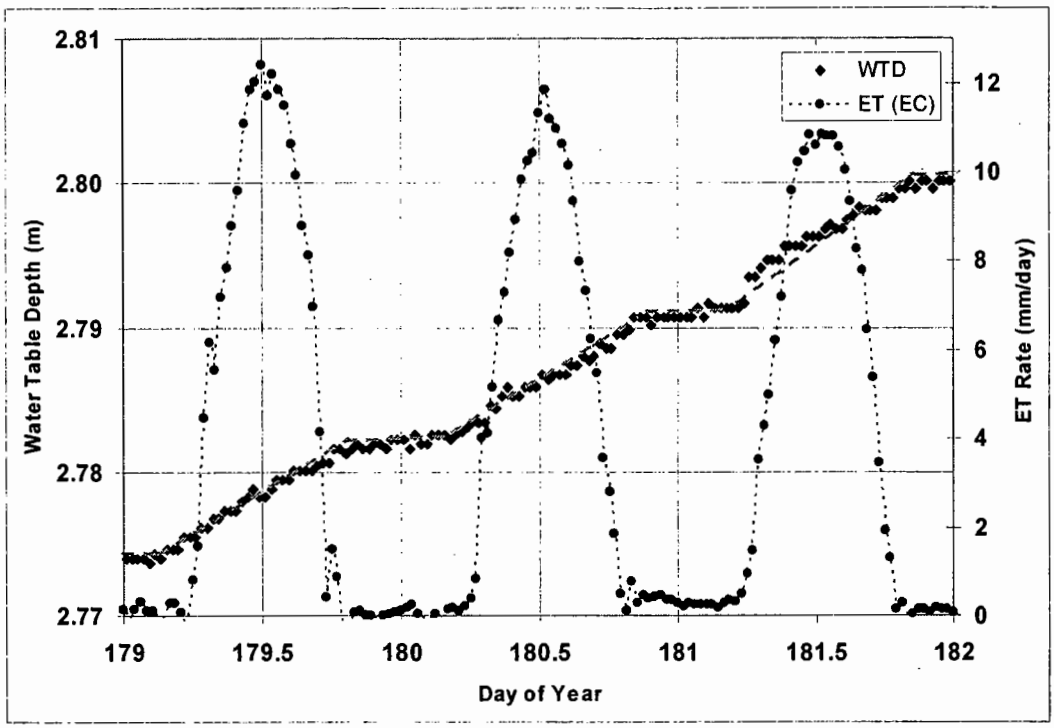

Figure 67. Diurnal fluctuations in water table depth (WTD) near EC station in BLK100 (well 850T). Notice a reduction in drawdown rate (smaller slope) during nighttime. ET(EC)=ET_{corr}.

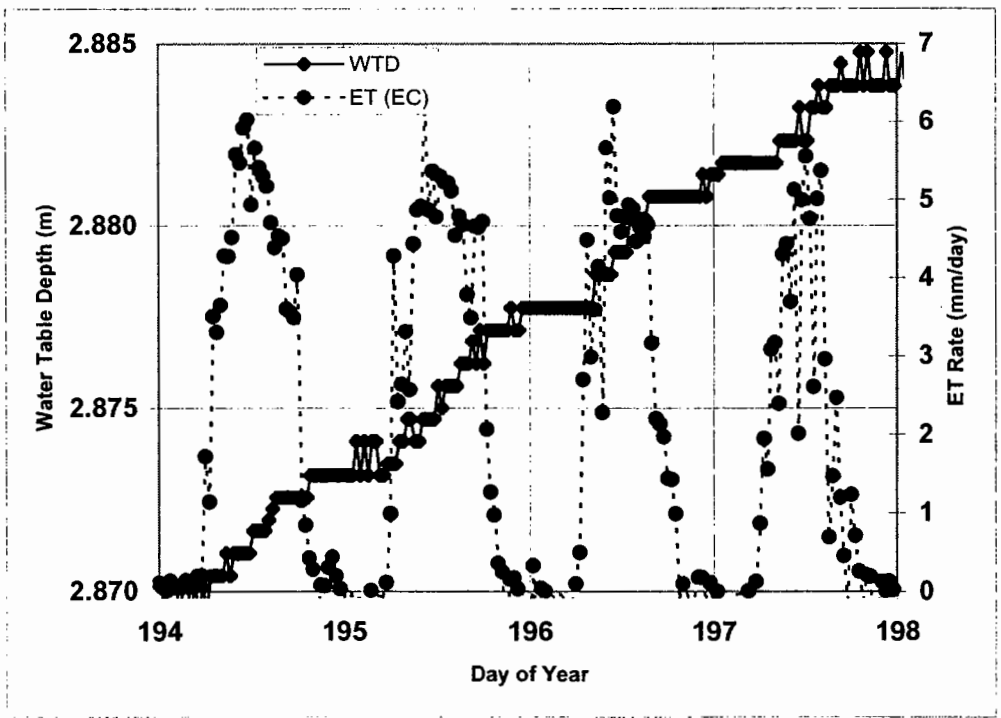

Figure 68. Diurnal fluctuations in water table depth (WTD) near EC station in PLC074 (well 012UT). Notice a reduction in drawdown rate (smaller slope) during nighttime. ET(EC)=ET_{corr}.

Table 13. Measured diurnal changes in water table depths, daily ET (eddy covariance method), and estimated specific yield for BLK 100 during summer of 2003 (Specific yield is estimated assuming ET was a result of uptake from water table only).

Site	Day of Year	Diurnal Change in WTD (mm)	Daily ET (mm)	Specific yield (-)
BLK100	178	8.84	4.07	0.46
	179	8.24	4.13	0.50
	180	8.53	4.00	0.47
	181	9.45	3.96	0.42
	182	10.0	3.96	0.40
	183	8.24	3.89	0.47
	184	8.84	3.88	0.44
	185	7.62	4.03	0.53
	186	7.62	4.27	0.56
	187	8.84	4.11	0.46
	188	8.23	4.09	0.49
	189	9.46	3.93	0.41
	mean	***8.66***	***4.03***	***0.47***
PLC074	193	4.27	2.3	0.54
	194	3.97	2.32	0.58
	195	3.65	2.3	0.63
	196	3.97	1.9	0.48
	197	2.44	1.43	0.59
	198	2.44	1.62	0.66
	mean	***3.46***	***1.98***	***0.58***

Table 13. Assuming that the entire drawdown was driven by ET_{corr} (primarily plant transpiration) that was independently measured by the EC station, we estimated an effective yield for the site by taking the ratio of daily ET to daily water table drawdown distance (r),

$$S_y = \frac{ET_{gw}}{r} \tag{22}$$

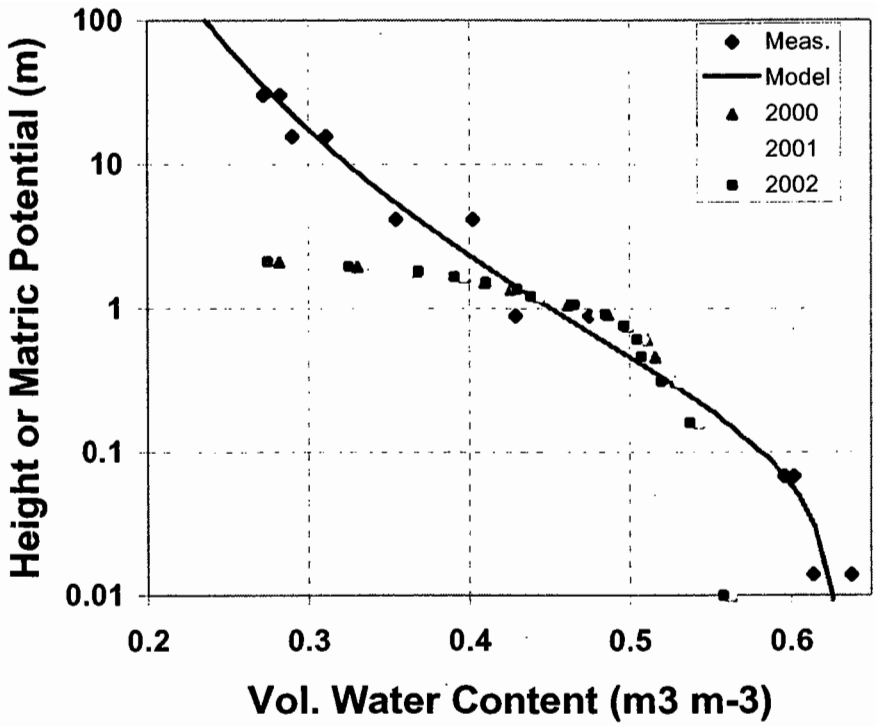

Figure 69. Soil water characteristic for BLK100 soil measured in the lab (and fitted model) and inferred from measured water content vs. height above the water table during April of 2000, 2001, and 2002.

The resulting value of specific yield for BLK100 was 0.47 and was 0.58 for PLC074. These values are considerably higher than expected for a profile under hydrostatic conditions. Freeze and Cherry (1979) suggested that the specific yield for unsaturated soil profiles with fluctuating shallow water table should be less than the drainable porosity for the soil, and could be estimated from a soil water characteristic curve. The primary flaw with this argument is that in the presence of plant uptake the soil profile is far from the quasi-equilibrium state expected for gravity drainage of a hydrostatic profile. The change in water table depth is brought about by

direct uptake through a soil profile that is much drier than a hydrostatic profile. The processes can be viewed as one of a propagating drying front induced by plant roots. At shallow depths, plants preferentially take up soil water due to presence of nutrients and typically higher root densities. An example from BLK100 is illustrated in Figure 69 showing water content measurements vs. height above the water table at it's shallowest position in early April for three consecutive years. Notice the strong divergence of the water content profile from a hydrostatic one based on the measured soil water retention curve that occur at an elevation of about 1 m above water table.

Extrapolating for the period between high and low DTW measurements, seasonal plant water uptake was estimated using Equation 22 and the mean S_y for BLK100 and PLC074. At BLK100, the calculated seasonal ET from these fluctuations between DOY 90 and 260 resulted in ET_{gw} of 383 mm, and ET of 393 mm in 2001 and 2002, respectively. For PLC074, ET_{gw} estimated from water table change for the period DOY112 to 246 as 133mm. These values based on seasonal water table fluctuations include E and T_{soil} and should overestimate T_{gw} by ~0.71 and 0.80 at BLK100 and ~0.57 at PLC074 if the T_{gw} estimates from the SWB are accurate. Multiplying the values derived from groundwater fluctuations by the fractions in Table 12 gave: 272 mm at BLK100 (2001), 314 mm at BLK100 (2002), and 75 mm at PLC074. Comparable values of T_{gw} for the same period determined by water balance closure were 293 mm in 2001 and 277 mm in 2002 at BLK100 and 59 mm at PLC074. Given the similarity of the values and the imprecision of the unrelated methods, we concluded that SWB estimates of T_{gw} were reliable for these shallow water table sites. This method was not tested for sites like PLC185 or PLC018 with deep water tables because of the absence of DTW monitoring.

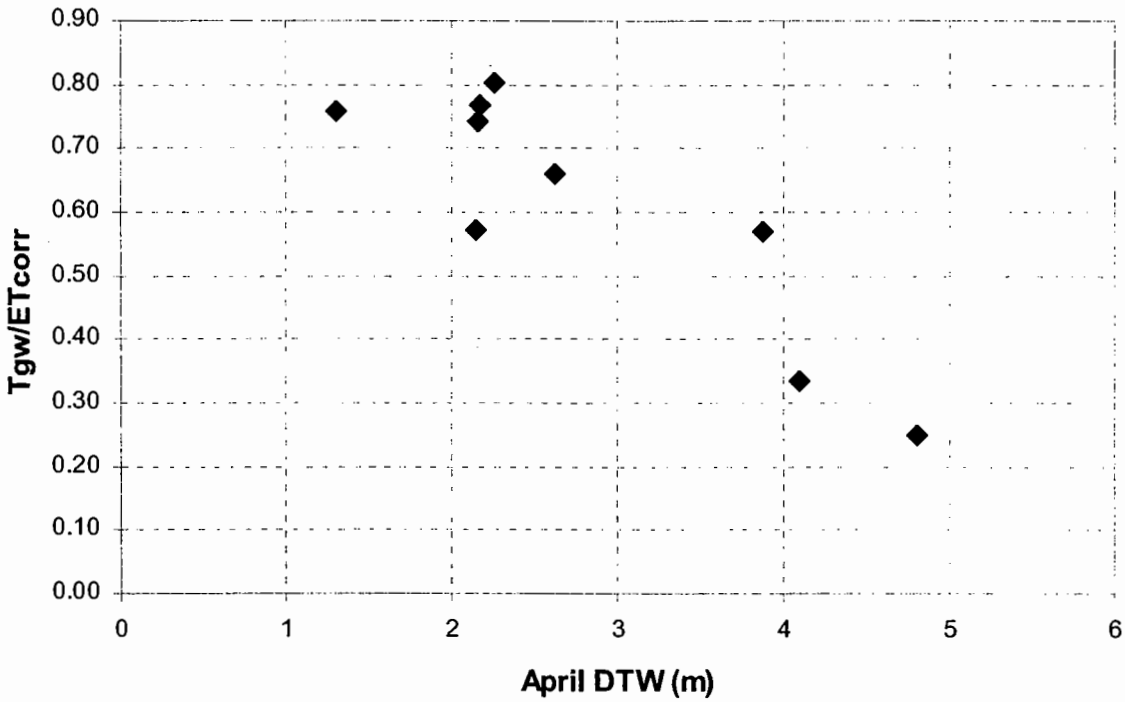

Figure 70. Fraction of ET supplied by direct uptake from the water table as a function of DTW at the beginning of the growing season. DTW values for PLC018 is an estimate and could be deeper (i.e. >4.8m). DTW for PLC185 was determined at the time of access tube installation.

Analysis of the water balance closure quantified the contribution to ET_{corr} from the water table when the root zone and the water table were "coupled". Groundwater pumping may lower the water table and "decouple" the water table from the root zone. Under such conditions, it would be expected that the contribution from the water table would decrease and reliance on stored soil water would increase (and/or T would decrease). Thus, modeling the soil water balance also requires an expression to reduce T_{gw} as the water table declines. Also, an expression is needed to describe the expected reduction in T as water table decline induces plant stress.

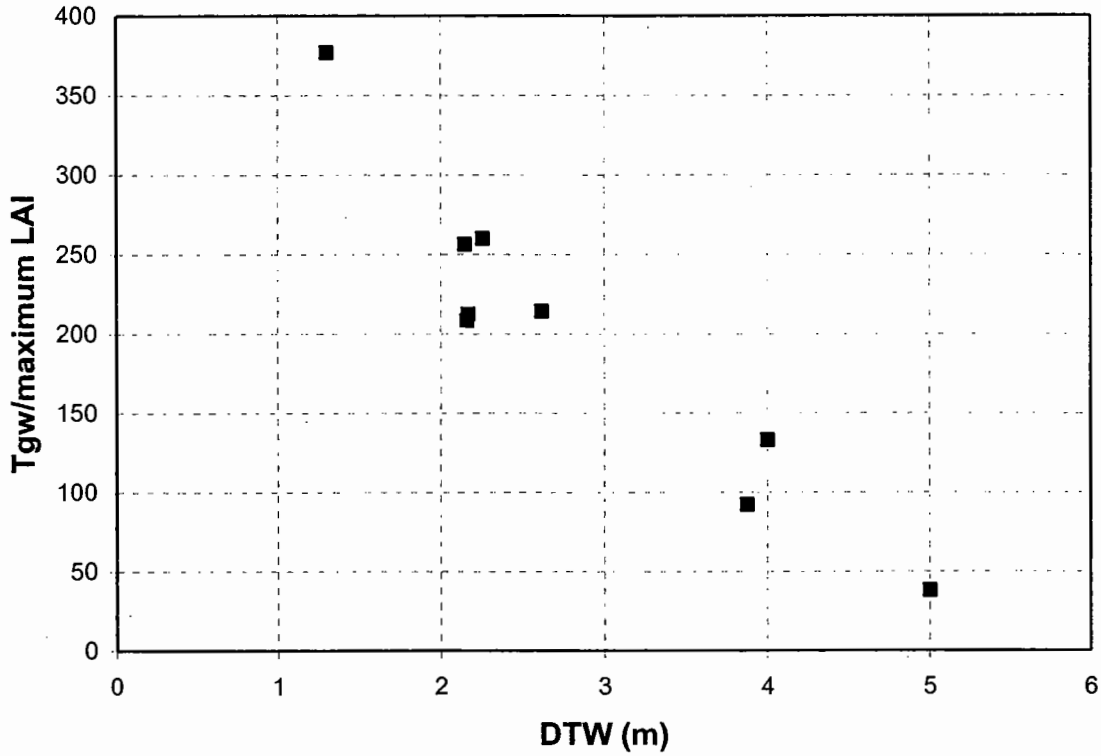

Figure 71. T_{gw} scaled by maximum LAI as a funtion of DTW. DTW values for PLC018 is an estimate and could be deeper (i.e. >5.0m). DTW for PLC185 was determined at the time of access tube installation.

The vadose model currently contains a parameter to account for water table uptake as a function of DTW, (KW, see below), but the parameter is related to maximum rooting depth and not well quantified. This study did not artificially lower the water table during the growing season preventing direct observation of this function. The study sites, however, included a range of water table and vegetation conditions including coupled and decoupled sites. The fraction of ET supplied by water table uptake (T_{gw}/ET_{corr}) was related to DTW as shown in Figure 70.

Alternatively, simple inspection suggested that T_{gw} was related to LAI and/or DTW (the latter are weakly correlated for this set of locations). The relationship between T_{gw}, LAI, and DTW is presented in Figure 71. Normalizing T_{gw} by peak LAI accounted for inherent site differences in plant community due to other soil factors or stress induced reduction in leaf area. Depending on the method to derive ET estimates (if based on LAI for example) this function may be able to accommodate the groundwater uptake for coupled sites and for sites affected by pumping. Further experimentation with the vadose zone model is necessary to determine which function is most applicable to reformulate the KW model parameter.

Conclusions

At sites with high leaf area and shallow water tables, 70-80 % of the ET_{corr} was derived from the water table directly and is not reflected in changes is soil water content. Quantifying this value has direct bearing on the parameterization of the vadose zone water balance model. Additionally, multiple functions relating T_{gw}, LAI and DTW were prepared to guide future conceptualization of the vadose zone model.

Vadose Zone KF model development/improvements

Introduction

Previous studies cooperatively conducted by the County and LADWP developed a mass balance model to determine changes in water storage in the vadose zone (Or and Groeneveld, 1994). The model uses transpiration coefficients, precipitation, and changes in water table depth to account for changes in vadose water storage and Kalman filtering to optimally update predictions as data become available. The Kalman filter utilizes uncertainty in both measurements and model predictions to determine the overall uncertainty in predicted soil water

storage. An important characteristic of the existing model is that the ET, water table fluctuation, and water table contribution to plant uptake can be modified, updated, or replaced without reference to the other model components. Key to the success of the model is proper accounting of sources for water uptake, groundwater or soil water by phreatophytes based on the depth to the water table.

The simplified soil water balance between two time periods, i and i+1 is,

$$SW_{i+1} = SW_i + P + \Delta SW_{DTW} - ETa \tag{23}$$

where, SW is soil water stored in the soil layer of interest, P is precipitation, ΔSW_{DTW} is change is soil water caused by change in DTW, and ETa is actual ET (ET_{corr} in this study). ΔSW_{DTW} is only calculated when the water table is within the root zone. The water balance model of Or and Groeneveld (1994) estimates the ETa by the following expression:

$$ETa = KC \cdot KW \cdot ETr \tag{24}$$

where ETr is potential evapotranspiration as determined by atmospheric-climatic conditions (e.g., Penman's equation); Kc is a transpiration coefficient which provides the ratio of ETa to potential evapotranspiration ETr (Equation 15). KW is a coefficient based on water table depth which partitions some of the ETa to direct uptake from the water table without depletion of stored soil water. When KW is 1 or greater, all ETa is drawn from the soil. The dominance of T_{gw} in the soil water balance when the water table was shallow pointed the need to focus on how to construct KW before making extensive revisions or tests of the model.

The objective of this task was to revise the vadose water balance model to update its components based on results obtained in this study.

Materials and Methods

Modeling was conducted using data collected at BLK100 because that site had the longest record. Because of the predominance of T_{gw}, model runs were primarily to evaluate the KW component by relying on measured ET, DTW and soil water information. All data used for this portion of the project were collected during the field investigation of the water balance closure described above.

Results and Discussion

Specific changes or improvements to the model are described in the sections below.

CIMIS ETr model

The vadose zone model requires predictions of plant water demand (*Kc*) that are adjusted for weather conditions using ETr. A stochastic model for generating synthetic *ETr* sequences for Owens Valley, CA was estimated from a 19 years (1983-2001) sequence of *ETr* based on observations collected at Bishop, California (CIMIS, 2002). A modified Penman equation was used to compute daily ETr, from which mean daily ETr and a corresponding standard deviation (STD) were obtained using the available data set (Figure 72). A clear seasonal trend existed in the ETr time series which was removed prior to fitting a stochastic model. A Fourier series was fitted to the daily ETr using procedures described by Salas et al., (1980). The first two harmonics series is given by,

$$\overline{ETr(i)} = < ETr > + \sum_{j=1}^{2} \left[A(j)\,\mathrm{COS}\left(\frac{2\pi ij}{365}\right) + B(j)\,\mathrm{SIN}\left(\frac{2\pi ij}{365}\right) \right] \qquad (25)$$

where i is the day of year, <ETr> is mean daily *ETr* for the entire year (4.12 mm/day), A(1)=-2.73; A(2)=-0.112; B(1)=0.187; and B(2)=0.097. We used the first harmonic only as it was

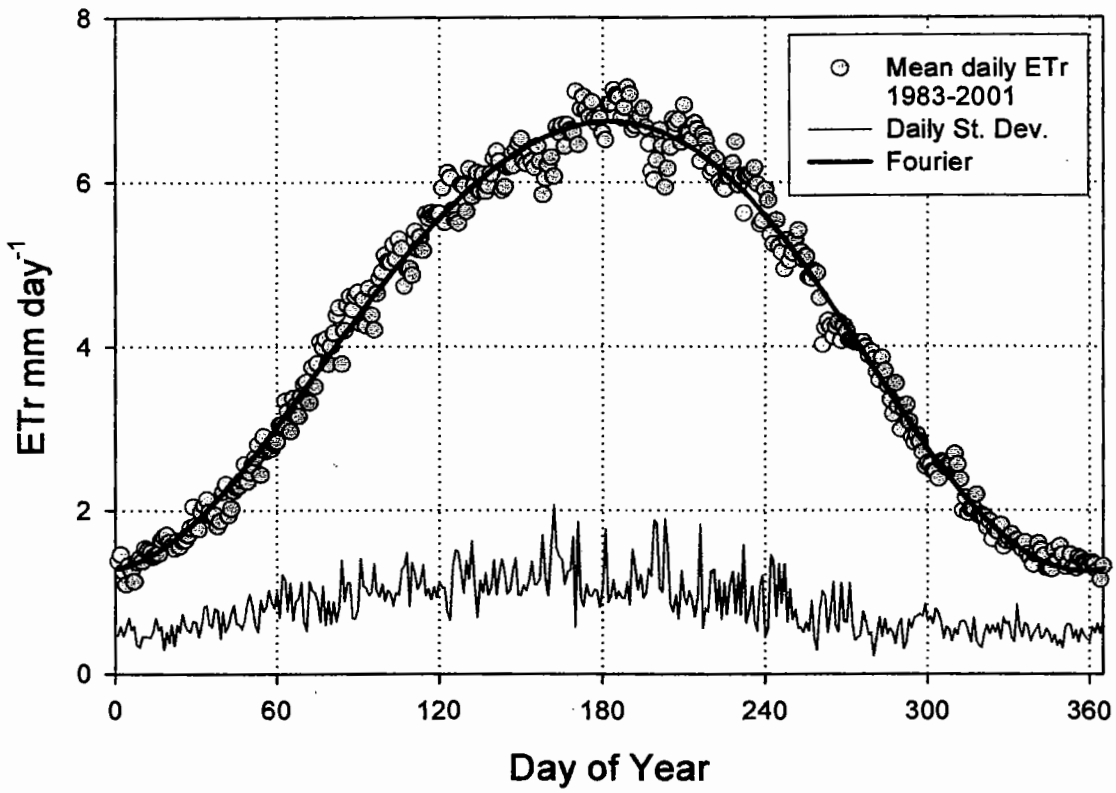

Figure 72: Mean daily *ETr* and its standard deviation (STD) estimated by the modified Penman equation from climatic data collected at Bishop, California (CIMIS, 2002, station #35).

capable of explaining more than 98% of the variance in average daily *ETr* indicating a strong seasonal (periodic) trend as evident from the data.

An approach based on classic time-series analysis was adopted for fitting a stochastic model to the residuals of mean daily *ETr* series, i.e., after removing the deterministic trend. Several possible ARMA(p,q) stochastic models were tested based on criteria of best fit and parsimony. Estimated parameters by the maximum likelihood method, statistics, and tests of the

Table 14. Estimated model parameters for standardized mean daily ETr series for 1983-2001 in Bishop, California. Data are from CIMIS Station #35).

ARMA(p,q) Model Order				
Parameters		AR(1)	AR(2)	ARMA(1,1)
ψ_1		0.438	0.421	0.506
ψ_2			0.031	
θ_1				0.085
Goodness-of-Fit and Parsimony Tests				
Residuals variance σ^2_ε		0.050	0.055	0.050
Porte Manteau Test - $Q_{L=90}$		98.8	97.0	97.2
AIC		-1088	-1086	-1087

residuals are given in Table 14. An ARMA(1,1) model was selected as the best model for the daily *ETr* data based on goodness-of-fit test results (Table 14), and capability to be reduced into a predictive model for ETr as shown next. The ARMA(1,1) model is given by,

$$ET_i = \phi_1 ET_{i-1} - \theta_1 \varepsilon_{i-1} + \varepsilon_i \qquad (26)$$

where φ_1 is an autoregression parameter, θ_1 is a moving average parameter, and ε_i is a normally distributed zero mean term with variance equal to σ^2_ε. The adequacy of the ARMA(1,1) was also confirmed by its best-fit to the autocorrelation of ETr residuals.

We adopted a method proposed by Graupe and Krause (1973) for improving the *ETr* model by transforming the ARMA(1,1) of ET_i estimates which are based on inaccurate measurements that include error into a first order autoregressive model, AR(1) of the

unobservable "true" state,

$$\widetilde{ET}_{i+1} = \varphi_1 \widetilde{ET}_i + u_i \quad (27)$$

where $ET_i=ET_i+v_i$, and $\sigma^2_u=\sigma^2_\varepsilon[1+\theta^2_1-\theta_1/\varphi_1-\theta_1\varphi_1]$ ($\sigma^2_u=0.06$). An estimate of the measurement variance is given by: $\sigma^2_v=\sigma^2_\varepsilon[\theta_1/\varphi_1]$ (with $\sigma^2_v=0.0084$).

Site-Scale Transpiration Coefficients

Initially we planned to use detailed information on vegetation cover and composition for each study site, coupled with vegetation based Kc to derive estimates for diurnal and seasonal transpiration fluxes. The Kc models were a subject of this study. Therefore, the vadose zone model was revised to rely on site-specific Kc derived from eddy covariance and *ETr* measurements rather than the approach described in the original proposal. This was necessary to insolate the investigation of *KW* from variability introduced by less direct estimates of ET. Site-scale Kc were derived from the eddy covariance ET_{corr}, CIMIS *ETr* measurements, and Equation 15. Although the data set is fragmentary, daily Kc from three measurement seasons at BLK100 (2000-2002), revealed a clear and repeatable trend (Figure 73). Subsequently, we fitted a Fourier series to mean daily Kc with some patching of missing periods in January and February when the instruments were being calibrated with linear trends depicted by the continuous line on Figure 73.

KW evaluation and model simulation

The water balance model estimates the actual evapotranspiration by Equation (24) given above. The relative portion of ETa satisfied by uptake directly from the water table (*KW*) was computed by three methods assuming that: (i) the uptake is proportional to the depth occupied by

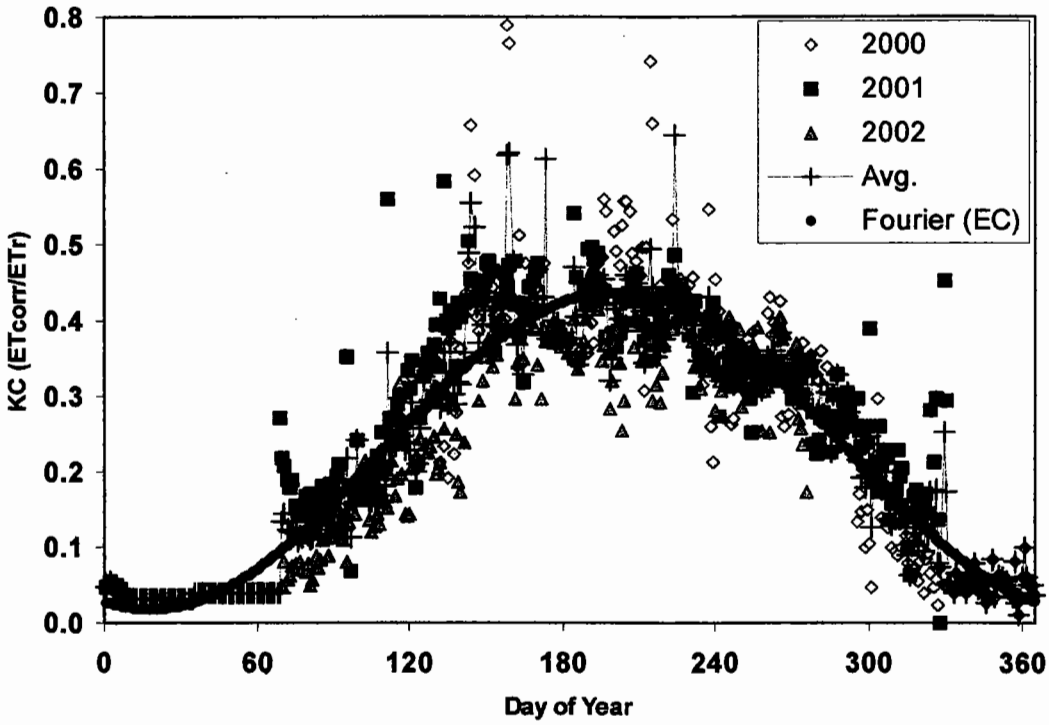

Figure 73. Site-scale Kc data, average, and fitted Fourier model for BLK100. Fourier model coeffcients: A(1) -0.20, B(1)-0.064, A(2) and B(2) 0.0; $r^2 = 0.91$.

the water table within the rooting zone (Or and Groeneveld, 1994); (ii) a newly-developed expression proposing that uptake is proportional to the depth occupied by the water table raised to a power (4>b>2); and (iii) the uptake follows a pattern of exponential-decay with depth given below by,

$$(i)\quad KW_i = \frac{DTW_i}{RTD_{\max}};\quad (ii)\quad KW_i = \left(\frac{DTW_i}{RTD_{\max}}\right)^b;\quad (iii)\quad KW_i = 1 - exp\left(-\frac{a \bullet DTW_i}{RTD_{\max}}\right) \qquad (28)$$

where RTD_{max} is the maximum rooting depth and all other variables as defined previously. All variables are expressed in units of equivalent water depth. Unfortunately, the short time frame of

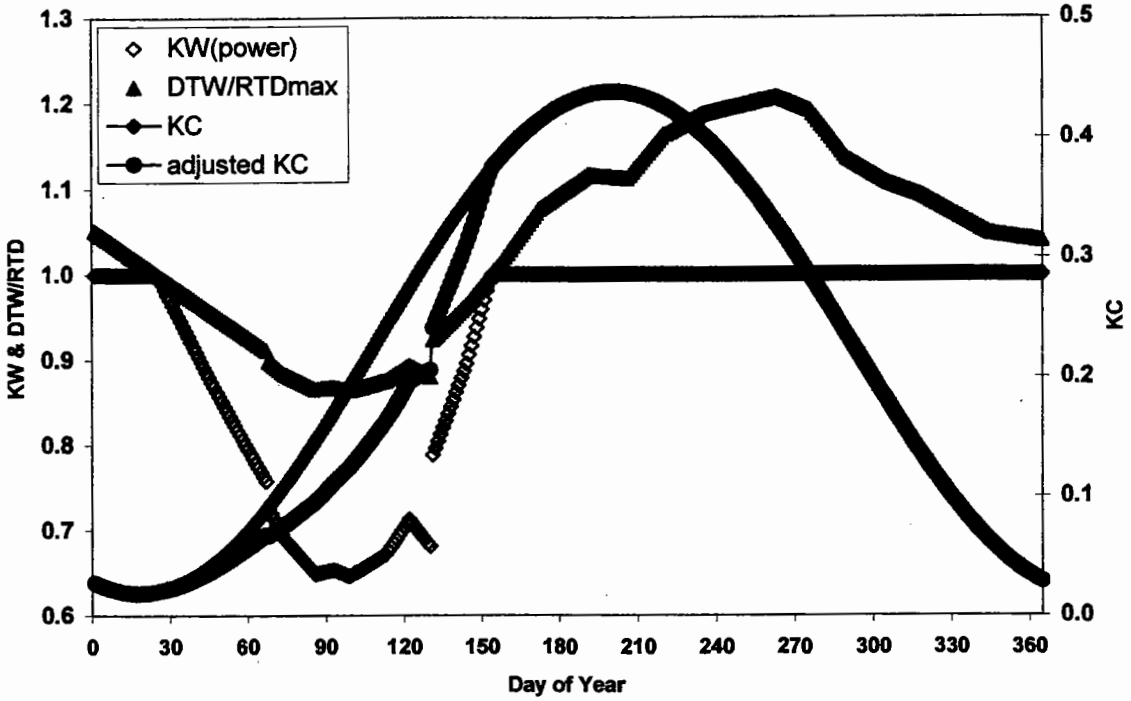

Figure 74. Changes in relative water table depth (DTW/RTD, where *RTDmax*=2500 mm) in BLK100 during 2001. *KW* was based on the power function with b=3, and the site Kc adjusted by the water table contribution as reflected by KW [calculated as: adjusted KC = (1-KW)*Kc(EC). The area between the Kc curves reflects the contribution of direct uptake from water table to site *ETcorr*.

the study did not allow for relying on function derived from the SWB. In previous studies we have used (iii) with a=2 (Or and Groeneveld, 1994). In this study we use (ii) with b=3 based weight for greater uptake of water from the water table when it was located within the rooting zone based on the field investigation results (Figure 74). This version gave the highest fraction of groundwater uptake, but still was lower than suggested by the SWB.

For all versions, $KW \geq 1$ for $DTW_i > RTD_{max}$. *RTDmax* was set at the multi-year water

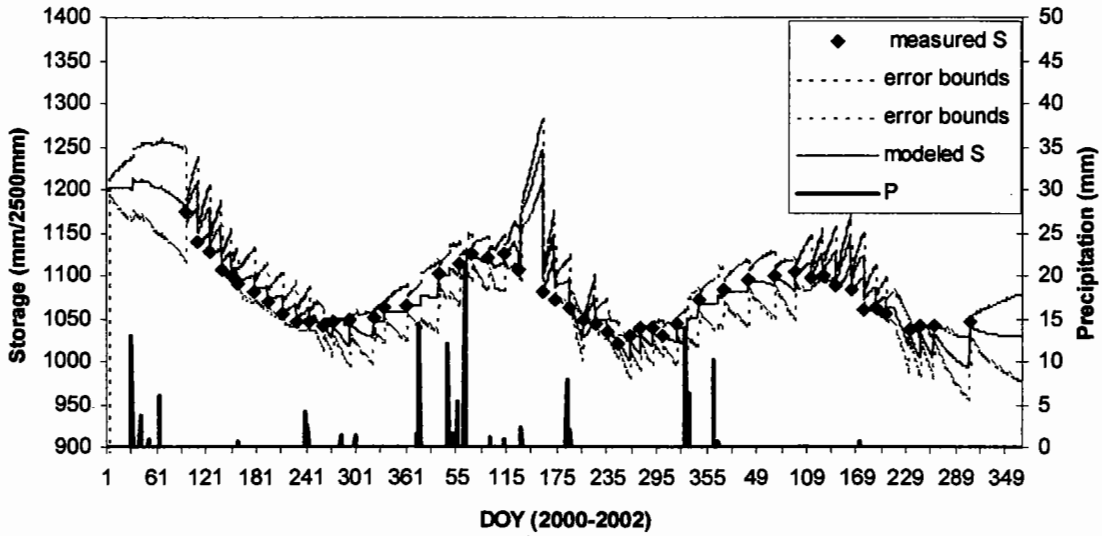

Figure 75. Measured and modeled changes in S at BLK100 for 2000-2002 using the revised water table uptake expresssion.

table average depth of about 2.5m. Conveniently this was the measurement depth for calculation of *S*. This site had fine-textured soils (Appendix B), and the saturated zone extended above the water table and into the active root zone (<2.5m).

An example of simulation results of the vadose zone model with the power version of KW is given in Figure 75. The model overestimated soil water content the during the growing season (especially in April and May) and underestimated the soil water content as the water table rose each winter. The SWB showed that groundwater uptake occurred after DOY 160 after the water table dropped below the RTDmax used for the simulations (2.5m). The model assumed that groundwater uptake ceased after DOY 160 (i.e. $KW = 1$). The model needs further refinement to determine the best formulation of the KW based on the SWB results. The

relationship between KW and RTD_{max} will be particularly important to refine.

Conclusions

Starting from the model reported by Or and Groeneveld (1994) we performed the following updates and key modifications: (1) the ETr stochastic model was updated by incorporating additional 10 years of ETr data obtained from the CIMIS station in Bishop, CA; (2) our estimates were improved on the amount of water taken up directly from the water table in sites with different water table depths to refine the partitioning function between uptake from vadose water and groundwater (3) the water balance model was revised to make use of these new functions.

IV. Public Outreach and Technical Presentations

Inyo County Water Department published an annual report called the *Monitor* to present summaries of significant policy developments, monitoring results of the environmental conditions in the Valley and to provide updates on current research by science staff including work performed for this project. The Monitor was produced in June 2003, and a copy is attached. The Water Department maintains a web site (www. inyowater.org) where reports and publications arising from this project will be posted. Drs. Harrington and Steinwand presented results from this project at national meetings in 2002 of the American Geophysical Union and Soil Science Society of America (SSSA). References for these presentations are given below. Drs. Steinwand and Or are scheduled to present a results of this study in a poster entitled: *Water Balance Closure for Owens Valley Phreatophytes Combining Water Table, Eddy Covariance,*

and Soil Water Measurements at the SSSA meetings in November 2003. Two internal Inyo County reports related to this project have been completed. Copies of those are attached to this report.

Presentations

Harrington, R.F., and A.L. Steinwand. 2002. Regional groundwater discharge estimated using micrometeorological measurements, plot-scale measurements of vegetation cover, and remotely-sensed vegetation cover. American Geophysical Union

Steinwand, A.L., R.F. Harrington, P.J. Hubbard, and D. Martin. 2002. Transpiration coefficients and eddy covariance estimates of evapotranspiration of Great Basin phreatophytes. In Agronomy Abstracts, ASA, Madison, WI.

V. References

Allen, R.G., L.S. Pereira, D. Raes, and M. Smith. 1998. Crop Evapotranspiration: Guidelines for Computing Crop Water Requirements. United Nations FAO, Irrigation and Drainage Paper 56. Rome, Italy. 300 p.

Arya, S.P. 2001. Introduction to Micrometeorology, Second Edition, Academic Press.

Ball, J.T., J.B. Picone, and P.D. Ross. 1994. Evapotranspiration by riparian vegetation along the lower Colorado River. Final report to U.S. Bureau of Reclamation. 188pp.

Bastiaanssen, W.G.M., M. Menenti, R.A. Feddes, and A.A. M. Holtslag. 1998a. A remote sensing surface energy balance algorithm for land (SEBAL). Part 1: Formulation. J. of Hydrology 198-212.

Bastiaanssen, W.G.M., H. Pelgrum, J. Wang, Y. Ma, J.F. Moreno, G.J. Roerink, R.A. Roebeling, and T. van der Wal. 1998b. A remote sensing surface energy balance algortithm for land (SEBAL). Part 2: Validation. J. of Hydrology 212-213:213-229.

Bastiaanssen, W.G.M. 2000. SEBAL-based sensible and latent heat fluxes in the irrigated Gediz Basin, Turkey. J. of Hydrology 229:87-100.

Bastiaanssen, W.G.M., M.D. Ahmad and Y. Chemin. 2002. Satellite surveillance of evaporative depletion across the Indus Basin. Water Resources Research 38, no. 12, 1273. 9 p.

Berger, D.L., M.J. Johnson, and M.L. Tumbusch. 2001.Estimates of Evapotranspiration from the Ruby Lake National Wildlife Refuge Area, Ruby Valley, Northeastern Nevada, May 1999-October 2000. USGS Water Resources Investigations Report 01-4234.

Bidlake, W.R. 2001. Evapotranspiration from a Bulrush-Dominated Wetland in the Klamath Basin, Oregon. J. of Amer. Water Res. Assoc. 36(6), 1309-1320.

Bidlake, W.R. 2002. Evapotranspiration from Selected Fallowed Fields on the Tule Lake National Wildlife Refuge, California, During May to October 2000, USGS Water Resources Investigations Report 02-4055.

Blaney, H.F. 1954. Consumptive use of groundwater by phreatophytes and hydrophytes. Pub. no. 37. de l'Association Internationale d'Hydrologic. Presented at the Tenth General Assembly of the Int'l. Union of Geology and Geophysics, Rome, Italy. September 1954.

Branson, F. A., R. F. Miller, and I. S. McQueen. 1976. Moisture relationships in twelve northern desert shrub communities near Grand Junction, Colorado. Ecology. 57:1104-1124.

Brutsaert, W. 1982. Evaporation into the atmosphere. D. Reidel.

Campbell Scientific Inc. 1998a. CSAT Three Dimensional Sonic Anemometer Instruction Manual, Revision 3/98.

Campbell Scientific Inc. 1998b. Eddy Covariance System Operator's Manual CA27 and KH20, Revision 7/98.

Campbell Scientific Inc. 1989. KH20 Krypton Hygrometer, Revision 11/89.

Campbell Scientific Inc. 1996. Q-7.1 Net Radiometer, Revision 5/96.

Campbell Scientific Inc. 1996.CS615 Water Content Reflectometer Instruction Manual, Version 8221-07, Revision 10/96.

Campbell Scientific Inc. 1999. HFT3 Soil Heat Flux Plate, Revision 2/99.

Campbell, G.S., and J.M. Norman. 1998. An Introduction to Environmental Biophysics, Second Edition, Springer.

Cheatham, N. H. and J. R. Haller. 1975. An annotated list of California habitat types. Unpublished mimeograph.

CIMIS, California Irrigation Management Information System. 2002. Agric. Water Conservation Section, Dept. of Water Resources, Sacramento, CA.

Danskin, W.R. 1998. Evaluation of the Hydrologic System and Selected Water-Management Alternatives in the Owens Valley, California, U.S. Geological Survey Water-Supply Paper 2370-H.

Dane, J.H. and J.W. Hopmans. 2002. Water Retention and Storage. pp. 671-796 *In.* J.H.Dane and G.C. Topp (eds.) Methods of soil analysis, Part 4. Soil Sci. Soc. Am. Book 5. SSSA. Madison, WI.

Duell, L.F.W. 1990. Estimates of Evapotranspiration in Alkaline Scrub and Meadow Communities of Owens Valley, California, Using the Bowen-Ratio, Eddy-Correlation, and Penman-Combination Methods. USGS Water Supply Paper 2370-E.

Duell, L. F. W. 1992. Eddy-correlation measurements at site L, Chapter D, USGS WRI 91459.

Elmore, A.J., J.F. Mustard, S.J. Manning, and D.B. Lobell. 2000. Quantifying vegetation change in semiarid environments: Precision and accuracy of spectral mixture analysis and the normalized difference vegetation index. Remote Sens. Environ. 73:87-102.

Farah, H.O. 2001. Estimation of regional evaporation under different weather conditions from satellite and meteorological data. A case study in the Naivasha Basin, Kenya. Doctoral Thesis Wageningen University and ITC.

Franks, S.W. and K.J. Beven. 1997. Estimation of evapotranspiration at the landscape scale: a fuzzy disaggregation approach. Water Resour. Res. 33:2929-2938.

Freeze, R.A., and J.A. Cherry. 1979. Groundwater. Prentice-Hall, Englewook Cliffs, New Jersey.

Gardner, W.R. 1958. Some steady state solutions of the unsaturated moisture flow equation with applications to evaporation from a water table Soil Sci. 85:228-232.

Gash, J.H.C. 1986. A not on estimating the effect of a limited fetch on micrometeorological evaporation measurements. Bound.-Layer Met. 35:409-413.

Gay, L. W. 1992. Bowen ratio measurements at sites C and L, Chapter A, USGS WRI 91-4159.

Gay, L.W. and L.J. Fritschen. 1979. An energy budget analysis of water use by saltcedar. Wat. Res. Res. 15:1589-1592.

Gee, G.W., and J.W. Bauder. 1986. Particle-size analysis. pp. 383-411 *In.* A.Klute (ed.) Methods of soil analysis, Part 1. 2nd ed. Agron. Monogr. 9. ASA and SSSA. Madison, WI.

Goodall, D. W. 1952. Some considerations in the use of point quadrats for the analysis of vegetation. Australian Journal of Scientific Research. 5:1-41.

Graupe, D. and D.I. Krause. 1973. On the identification of input-output noise models. Int. J. Syst. Sci. 4:617-621.

Groeneveld, D.P. 1997. Vertical point quadrat sampling and an extinction factor to calculate leaf area index. J. Arid Env. 36:475-485.

Hendrickx, J.M.H., S.-H. Hong, T. Miller, E. Small, P. Neville, J. Cleverly, and W.G.M. Bastiaanssen. 2002. Abstract. Actual ET rates derived by SEBAL in the Middle Rio Grande Valley Annual Meeting of American Geophysical Union, San Francisco, December 6-10.

Holland, R. F. 1986. Preliminary descriptions of the terrestrial natural communities of California. Unpublished mimeograph.

Hollett, K.J., W.R. Danskin, W.F. McCaffrey, and C.L. Walti. 1991. Geology and Water Resources of Owens Valley, California. USGS WSP 2370-B.

Iqbal, M. 1983. An introduction to solar radiation. Academic Press, Toronto.

Kuchler, A. W. 1967. Vegetation Mapping. New York, Ronald Press Co. 472 pp.

Kustas, W.P. and J.M. Norman. 1996. Use of remote sensing for evapotranspiration monitoring over land surfaces. Hydrol. Science J. 41;495-515.

Laczniak, R.J., G.A. DeMeo, S.R. Reiner, J.LaRue Smith, and W.E. Nylund. 1999. Estimates of ground-water discharge as determined from measurements of evapotranspiration, Ash Meadows area, Nye County, Nevada. U.S.G.S Water-Res. Invest. Rep. 99-4079.

Lee, C.H. 1912. An intensive study of the water resources of a part of the Owens Valley, California. USGS Water Supply Pap. 294.

Manning, S.J, J.F. Mustard and A.J. Elmore. 1999. Patterns of vegetation response to groundwater pumping detected with field monitoring and LandSat TM data. Ecological Society of America. August 1999. Spokane, WA. Ecological Society of America abstracts vol. 84.

Massman, W.J., D.G. Fox, K.F. Zeller, and D. Lukens, Verifying Eddy Correlation Measurements of Dry Deposition: A Study of the Energy Balance Components of the Pawnee Grasslands. USDA Rocky Mountain Forest and Range Experiment Station Research Paper RM-288, 1990.

Maulem, Y. 1976. A new model for predicting the hydraulic conductivity of unsaturated porous media. Water Resour. Res. 12:513-522.

Miller, R.F. 1988. Comparison of water use by *Artemisia tridentata* spp. *wyomingensis* and *Chrysothamnus viscidiflorus* spp. *viscidiflorus*. J. Range Manage. 41:58-62.

Miller, R.F., F.A. Branson, I.S. McQueen, and C.T. Snyder. 1982. Water relations in soils as related to plant communities in Ruby Valley, Nevada. J. Range Manage. 35:462-468.

Nichols, W.D. 2000. Regional ground-water evapotranspiration and ground-water budgets, Great Basin, Nevada. U.S.G.S. Prof. Pap. 1628.

Or, D., and D.P. Groeneveld. 1994. Stochastic estimation of plant-available soil water under fluctuating water table depths. J. Hydrol. 163:43-64.

Pelgrum, H. and W.B.M. Bastiaanssen. 1996. An intercomparison of techniques to determine the area-averaged latent heat flux from individual in-situ observations: a remote sensing approach using the European Field Experiment in a Desertification-Threatened Area data. Water Res. Res. 32:2775-2786.

Robinson, T.W. 1970. Evapotranspiration by woody phreatophytes in the Humboldt River

Valley near Winnemucca, Nevada. U.S.G.S. Prof. Paper 491-D.

Roerink, G.J. et al. 1997. Relating crop water consumption to irrigation water supply by remote sensing. Water Resources Management 11:445-465.

Salas, J.D., W. Delleur, V. Yevjevich, and W.L. Lane. 1980. Applied modeling of hydrologic time series. Water Resource Publications, Fort Collins, Co.

Schillinger, W.F. and F.L. Young. 2000. Soil water use and growth of Russian thistle after wheat harvest. Agron. J. 92:167-172.

Shuttleworth, W. J., 1993. Evaporation, *In* D. R. Maidment (ed.) Handbook of Hydrology, McGraw-Hill.

Snedecor, G. W. and W. G. Cochran. 1980. Statistical Methods, Iowa State University Press, Ames, Ia..

Stannard, D. I.. 1992. Bowen ratio measurements at sites C and F, Chapter B, USGS WRI 91-4159.

Steinwand, A.L. 1998. Evaluation of methods to calculate vegetation water requirements for the Owens Valley, Ca. Report to the Inyo/Los Angeles Technical Group, February 28, 1998. 55pp.

Steinwand, A.L. 1999a. Transpiration coefficients for three Great Basin shrubs. Report to the Inyo/Los Angeles Technical Group, May 12, 1999. 41pp.

Steinwand, A.L. 1999b. Transpiration coefficients for two Great Basin phreatophytic grasses. Report to the Inyo/Los Angeles Technical Group, November 24, 1999. 91pp.

Steinwand, A.L., R.F. Harrington, and D.P. Groeneveld. 2001. Transpiration coefficients for three Great Basin shrubs. J. Arid Env. 49:555-567.

Sumner, D.M., Evapotranspiration from Successional Vegetation in a Deforested Area of the Lake Wales Ridge, Florida. USGS Water Resources Investigations Report 96-4244, 1996.

Van den Hurk, B.J.J.M., W.G.M. Bastiaanssen, H. Pelgrum, and E. van Meijgaard. 1997. A new methodology for assimilation of initial soil moisture fields in weather prediction models using Meteosat and NOAA data. J. of Applied Meteorology 36:1271-1283.

van Genuchten, M.Th. 1980. A closed-form equation for predicting the hydraulic conductivity of unsaturated soils. Soil Sci. Soc. Am. J. 44:892-898.

Wang, J., W.G.M Bastiaanssen, Y. Ma, and H. Pelgrum. 1998. Aggregation of land surface parameters in the oasis-desert systems of Northwest China. Hydr. Processes 12:2133-2147.

Webb, E. K., G. I. Pearman, and R. Leuning. 1980. Correction of flux measurements for density effects due to heat and water vapor transfer. Quart. J. R. Meteorol. Soc., 106, 85-100.

Zeller, K.F., W. Massman, D. Stocker, D.G. Fox, D. Stedman, and D. Hazlett. 1989. Initial Results from the Pawnee Eddy Correlation System for Dry Acid Deposition Research. USDA Rocky Mountain Forest and Range Experiment Station Research Paper RM-282.

VI. Summary of Costs and Disbursements

Inyo County Salaries and Benefits	$75,686
Consultants	$78,605
Equipment	$60,721
General Operating	$13,507
Total Expense	$228, 519
Total Disbursement from DWR	$242,975

Appendix A: Daily eddy covariance, energy balance component, and transpiration model results.

Table A1: Daily eddy covariance, energy balance component, and transpiration model results at BLK100 in 2000.

DOY	LE	H	Rn	G	Ta	e	Ts	θ	wind speed	λE_{uncorr}	res	LE_{corr}	H_{corr}	β	λE_{corr}	T_{Kc}	T_{GB}	EC Fourier
	Wm^{-2}	Wm^{-2}	Wm^{-2}	Wm^{-2}	°C	kPa	°C	m^3m^{-3}	$m\ s^{-1}$	$mm\ day^{-1}$	Wm^{-2}	Wm^{-2}	Wm^{-2}		$mm\ day^{-1}$	$mm\ day^{-1}$	$mm\ day^{-1}$	$mm\ day^{-1}$
1																0.000	0.000	0.004
2																0.000	0.000	0.004
3																0.000	0.000	0.005
4																0.000	0.000	0.005
5																0.000	0.000	0.006
6																0.000	0.000	0.007
7																0.000	0.000	0.008
8																0.000	0.000	0.009
9																0.000	0.000	0.010
10																0.000	0.000	0.012
11																0.000	0.000	0.014
12																0.000	0.000	0.016
13																0.000	0.000	0.018
14																0.001	0.000	0.020
15																0.001	0.000	0.022
16																0.001	0.000	0.025
17																0.001	0.000	0.028
18																0.001	0.000	0.031
19																0.001	0.000	0.034
20																0.001	0.000	0.037
21																0.001	0.000	0.040
22																0.001	0.000	0.044
23																0.001	0.000	0.048
24																0.001	0.000	0.052
25																0.001	0.000	0.056
26																0.002	0.000	0.060
27																0.002	0.000	0.065
28																0.002	0.000	0.070
29																0.002	0.000	0.075
30																0.002	0.000	0.080
31																0.003	0.000	0.085
32																0.003	0.000	0.091
33																0.003	0.000	0.097
34																0.003	0.000	0.103
35																0.004	0.000	0.109
36																0.004	0.000	0.116
37																0.004	0.000	0.122
38																0.005	0.000	0.130
39																0.005	0.000	0.137
40																0.006	0.000	0.144
41																0.006	0.000	0.152
42																0.007	0.000	0.160
43																0.007	0.000	0.169
44																0.008	0.000	0.177
45																0.009	0.000	0.186
46																0.010	0.000	0.195
47																0.010	0.000	0.205

Table A1: Daily eddy covariance, energy balance component, and transpiration model results at BLK100 in 2000.

DOY	LE	H	Rn	G	Ta	e	Ts	θ	wind speed	λE_{uncorr}	res	LE_{corr}	H_{corr}	β	λE_{corr}	T_{Kc}	T_{GB}	EC Fourier
	Wm^{-2}	Wm^{-2}	Wm^{-2}	Wm^{-2}	°C	kPa	°C	m^3m^{-3}	$m\ s^{-1}$	$mm\ day^{-1}$	Wm^{-2}	Wm^{-2}	Wm^{-2}		$mm\ day^{-1}$	$mm\ day^{-1}$	$mm\ day^{-1}$	$mm\ day^{-1}$
48																0.011	0.000	0.215
49																0.012	0.000	0.225
50																0.013	0.000	0.235
51																0.015	0.000	0.246
52																0.016	0.000	0.257
53																0.017	0.000	0.269
54																0.019	0.000	0.280
55																0.020	0.000	0.292
56																0.022	0.000	0.305
57																0.024	0.000	0.318
58																0.025	0.000	0.331
59																0.028	0.000	0.344
60																0.030	0.000	0.358
61																0.032	0.000	0.372
62																0.035	0.000	0.387
63																0.037	0.001	0.402
64																0.040	0.001	0.417
65																0.043	0.002	0.433
66																0.047	0.002	0.449
67																0.050	0.003	0.465
68																0.054	0.004	0.482
69																0.058	0.005	0.499
70																0.063	0.006	0.517
71																0.067	0.008	0.535
72																0.072	0.010	0.553
73																0.077	0.012	0.572
74																0.083	0.014	0.591
75																0.089	0.017	0.610
76																0.095	0.019	0.630
77																0.102	0.022	0.651
78																0.109	0.026	0.671
79																0.116	0.030	0.692
80																0.124	0.034	0.714
81																0.132	0.038	0.736
82																0.141	0.043	0.758
83																0.150	0.049	0.781
84																0.160	0.054	0.804
85																0.170	0.061	0.827
86																0.181	0.068	0.851
87																0.193	0.075	0.875
88																0.205	0.083	0.900
89																0.217	0.092	0.925
90																0.231	0.102	0.950
91																0.245	0.112	0.976
92																0.259	0.123	1.001
93																0.275	0.135	1.028
94																0.291	0.148	1.054

Table A1: Daily eddy covariance, energy balance component, and transpiration model results at BLK100 in 2000.

DOY	LE	H	Rn	G	Ta	e	Ts	θ	wind speed	λE_{uncorr}	res	LE_{corr}	H_{corr}	β	λE_{corr}	T_{Kc}	T_{GB}	EC Fourier
	Wm^{-2}	Wm^{-2}	Wm^{-2}	Wm^{-2}	°C	kPa	°C	m^3m^{-3}	$m\ s^{-1}$	$mm\ day^{-1}$	Wm^{-2}	Wm^{-2}	Wm^{-2}		$mm\ day^{-1}$	$mm\ day^{-1}$	$mm\ day^{-1}$	$mm\ day^{-1}$
95																0.308	0.162	1.081
96																0.326	0.176	1.109
97																0.344	0.192	1.136
98																0.363	0.209	1.164
99																0.384	0.227	1.192
100																0.405	0.246	1.221
101																0.427	0.266	1.250
102																0.450	0.287	1.279
103																0.474	0.310	1.308
104																0.498	0.334	1.338
105																0.524	0.360	1.367
106																0.551	0.387	1.397
107																0.579	0.415	1.428
108																0.608	0.446	1.458
109																0.638	0.477	1.489
110																0.669	0.511	1.520
111	26.74	78.36	-1969.81	3.92	13.93	0.47	17.35	0.1	2.25	0.946				2.93		0.701	0.546	1.551
112	23.78	41.56	-18730	5.56	15.07	0.484	17.44	0.099	3.07	0.841				1.75		0.735	0.583	1.582
113	36.84	54.01	118.58	7.98	17.64	0.448	19.96	0.098	3.43	1.303	19.76	43.69	66.91	1.47	1.543	0.769	0.621	1.613
114	39.38	42.61	115.2	6.42	17.39	0.304	19.89	0.096	3.43	1.393	26.79	46.15	62.64	1.08	1.629	0.805	0.662	1.645
115	35.51	55.2	-1973.3	5.81	16.87	0.362	20.61	0.094	3.89	1.256				1.55		0.842	0.704	1.676
116	42.51	56.03	127.41	6.89	18.89	0.387	21.16	0.083	2.28	1.504	21.99	50.01	70.52	1.32	1.771	0.880	0.748	1.708
117	41	55.8	129.62	7.66	20.38	0.477	21.76	0.076	2.59	1.451	25.17	50.59	71.37	1.36	1.796	0.919	0.794	1.740
118	46.5	50.46	-4055.87	8.86	21.7	0.391	22.1	0.075	3.59	1.645				1.09		0.959	0.842	1.772
119	39.9	55.12	-18719.6	1.07	19.56	0.296	21.13	0.074	5.14	1.412				1.38		1.001	0.892	1.804
120	31.64	52.21	-10345.3	2.92	15.83	0.275	20.31	0.074	4.4	1.119				1.65		1.043	0.944	1.836
121	48.86	53.72	127.33	8.15	17.99	0.274	21.54	0.073	2.6	1.729	16.59	55.08	64.09	1.1	1.949	1.087	0.998	1.868
122	45.58	48.08	-10340.3	9.53	20.57	0.369	21.66	0.073	3.07	1.613				1.05		1.132	1.054	1.900
123	50.53	45.87	-4054.41	11.32	22.99	0.465	24.06	0.072	3.33	1.788				0.91		1.178	1.113	1.932
124	49.05	55.65	-10330.9	10.2	22.01	0.61	24.21	0.071	2.36	1.735				1.13		1.226	1.173	1.964
125	53.52	48.88	-10338.3	10.19	22.75	0.539	24.13	0.071	2.81	1.894				0.91		1.274	1.235	1.996
126	52.54	46.44	-20798	10.86	24.11	0.519	25.33	0.07	3.17	1.859				0.88		1.324	1.299	2.028
127	42.17	47.48	-14534.4	8.63	21.23	0.507	24.35	0.07	3.77	1.492				1.13		1.375	1.366	2.060
128	36.69	43.19	-22890.2	6.4	21.36	0.703	24.47	0.07	5.11	1.298				1.18		1.427	1.434	2.091
129	50.1	52.27	-10329.4	10.32	21.32	0.614	25.52	0.069	2.97	1.773				1.04		1.480	1.505	2.123
130	59.95	53.66	156.65	10.92	22.41	0.525	25.48	0.067	2087.04	2.121	32.13	73.02	72.71	0.9	2.591	1.534	1.577	2.155
131	49.86	68.59	135.5	-2.39	19.36	0.303	23.81	0.068	7.42	1.764	19.44	56.04	81.86	1.38	1.978	1.590	1.651	2.186
132	29.75	66.8	130.77	-1.91	10.29	0.199	20.16	0.068	2088.18	1.053	36.13	38.97	93.71	2.25	1.365	1.646	1.728	2.218
133	39.44	78.72	143.63	4.65	12.94	0.233	20.38	0.068	3.1	1.395	20.82	46.31	92.67	2	1.629	1.703	1.806	2.249
134	44.18	72.4	151.19	8.24	17.01	0.297	21.42	0.068	3.15	1.563	26.38	52.55	90.4	1.64	1.856	1.761	1.886	2.280
135	36.25	46.17	103.19	3.93	18.74	0.332	20.81	0.067	3.95	1.283	16.85	43.01	56.25	1.27	1.519	1.821	1.967	2.311
136	43.49	78.37	152.55	4.88	16.75	0.353	21.44	0.067	4.43	1.539	25.8	49.45	98.22	1.8	1.745	1.881	2.051	2.341
137	32.67	59.4	118.24	2.26	13.18	0.482	20.44	0.067	3.59	1.156	23.91	39.63	76.35	1.82	1.391	1.942	2.136	2.371
138	34.66	44.89	133.85	11.89	18.94	0.608	22.57	0.067	4.74	1.226	42.41	49.69	72.27	1.3	1.754	2.004	2.222	2.402
139	45.98	51.73	146.79	10.93	20.02	0.653	24.64	0.066	2.74	1.627	38.15	61.66	74.2	1.13	2.181	2.066	2.310	2.431
140	53.44	33.33	134.86	12.94	22.34	0.577	25.09	0.066	2.82	1.891	35.16	69.99	51.94	0.62	2.481	2.130	2.399	2.461
141	58.19	36.59	149.12	12.11	24.17	0.517	26.74	0.065	2.75	2.059	42.23	79.86	57.15	0.63	2.838	2.194	2.490	2.490

Table A1: Daily eddy covariance, energy balance component, and transpiration model results at BLK100 in 2000.

DOY	LE	H	Rn	G	Ta	e	Ts	θ	wind speed	λE_{uncorr}	res	LE_{corr}	H_{corr}	β	λE_{corr}	T_{Kc}	T_{GB}	EC Fourier
	Wm^{-2}	Wm^{-2}	Wm^{-2}	Wm^{-2}	°C	kPa	°C	m^3m^{-3}	$m\ s^{-1}$	$mm\ day^{-1}$	Wm^{-2}	Wm^{-2}	Wm^{-2}		$mm\ day^{-1}$	$mm\ day^{-1}$	$mm\ day^{-1}$	$mm\ day^{-1}$
142	66.38	32.21	152.5	13.85	25.77	0.496	27.69	0.064	2.69	2.349	40.06	85.87	52.78	0.49	3.057	2.258	2.582	2.519
143	66.92	35.33	151.02	13.37	26.68	0.63	27.8	0.063	2.2	2.368	35.4	84.85	52.8	0.53	3.027	2.324	2.675	2.548
144	71.16	29.61	154.8	17.56	28.79	0.714	29.29	0.063	2086.71	2.518	36.47	88.46	48.77	0.42	3.157	2.389	2.768	2.576
145	53.67	29.78	132.27	7.41	26.36	0.806	28.57	0.062	3.87	1.899	41.42	72.95	51.92	0.55	2.594	2.456	2.863	2.604
146	60.4	46.23	152.78	12.36	24.08	0.783	28.29	0.062	2.86	2.137	33.79	76.62	63.8	0.77	2.722	2.522	2.958	2.632
147	57.88	45.34	158.64	9.61	24.28	0.682	28.82	0.062	3.08	2.048	45.81	79.29	69.73	0.78	2.818	2.589	3.054	2.659
148	69.37	55.02	177.6	13.02	26.15	0.687	28.72	0.061	2.82	2.454	40.2	88.1	76.48	0.79	3.141	2.656	3.150	2.686
149	81.03	31.08	161.68	15.61	28.19	0.509	29.75	0.061	3.61	2.867	33.96	98.65	47.41	0.38	3.519	2.724	3.247	2.712
150	86.25	37.08	172.37	10.73	27.48	0.409	30.65	0.059	2.6	3.052	38.31	104.17	57.47	0.43	3.714	2.791	3.343	2.738
151	77.78	30.4	150.01	9.44	25.73	0.348	29.57	0.059	3.26	2.752	32.4	94.91	45.66	0.39	3.378	2.859	3.440	2.763
152	75.82	29.67	142.2	10.62	24.2	0.287	29.15	0.058	3.38	2.683	26.09	90.59	40.99	0.39	3.218	2.927	3.536	2.788
153	66.41	48.43	155	7.42	22.94	0.366	28.63	0.058	3.91	2.350	32.74	81.49	66.09	0.73	2.893	2.994	3.632	2.813
154	81.37	55.92	165.16	8.29	23.41	0.42	27.84	0.058	2.71	2.879	19.58	88.27	68.6	0.69	3.139	3.061	3.728	2.837
155	71.01	47.51	166.24	9.91	24.08	0.447	28.21	0.058	2.6	2.512	37.81	89.6	66.74	0.67	3.191	3.128	3.822	2.860
156	69.92	48.36	166.01	10.22	25.61	0.473	28.17	0.058	3.36	2.474	37.51	89.57	66.22	0.69	3.194	3.195	3.916	2.883
157	72.81	51.08	163.75	8.41	24.09	0.455	28.36	0.058	2.5	2.576	31.45	89.56	65.78	0.7	3.188	3.261	4.009	2.905
158	70.31	49.46	164.77	11.17	23.86	0.46	28.04	0.057	3.25	2.488	33.83	85.82	67.78	0.7	3.053	3.327	4.101	2.927
159	66.85	47.08	159.16	7.16	23.99	0.51	27.76	0.058	5.46	2.365	38.08	85.62	66.39	0.7	3.045	3.392	4.191	2.948
160																3.456	4.280	2.969
161	54.1	77.68	169.85	8.43	16.49	0.666	23.61	0.061	2.52	1.914	29.65	65.37	96.06	1.44	2.307	3.519	4.367	2.989
162	54.93	62.07	158.22	6.91	20.34	0.543	24.97	0.06	2.95	1.943	34.31	68.48	82.83	1.13	2.427	3.582	4.452	3.008
163	62.88	60.8	173.21	11.12	22.34	0.5	26.64	0.059	2.81	2.225	38.42	78.98	83.12	0.97	2.805	3.644	4.535	3.027
164	52.94	27.04	128.61	8.62	24.52	0.624	27.24	0.059	2.22	1.873	40.01	71.52	48.48	0.51	2.544	3.704	4.616	3.045
165	60.02	26.1	166.77	15.69	28.23	0.736	29.3	0.058	4.54	2.124	64.96	93.46	57.62	0.43	3.333	3.764	4.694	3.062
166																3.822	4.770	3.079
167																3.879	4.843	3.095
168																3.935	4.914	3.111
169																3.989	4.981	3.126
170	67.56	59.59	179.68	10.21	26	0.861	29.67	0.056	3.76	2.390	42.33	85.29	84.19	0.88	3.039	4.042	5.045	3.140
171	69.4	44.94	169	11.87	25.34	0.761	30.46	0.056	2.28	2.455	42.79	88.29	68.84	0.65	3.142	4.092	5.105	3.153
172	76.2	37.51	165.24	10.86	26.58	0.565	31.2	0.055	2.76	2.696	40.67	96.31	58.07	0.49	3.430	4.142	5.162	3.165
173	73.26	32.48	161.77	13.42	27.85	0.576	31.14	0.055	3.2	2.592	42.62	95.11	53.25	0.44	3.394	4.189	5.216	3.177
174																4.235	5.266	3.188
175																4.278	5.311	3.199
176																4.320	5.353	3.208
177																4.359	5.391	3.217
178																4.397	5.425	3.225
179																4.432	5.455	3.233
180																4.464	5.480	3.239
181																4.495	5.501	3.245
182																4.523	5.518	3.250
183																4.549	5.530	3.254
184																4.572	5.537	3.257
185																4.593	5.541	3.260
186																4.611	5.539	3.262
187																4.626	5.533	3.263
188																4.639	5.523	3.263

Table A1: Daily eddy covariance, energy balance component, and transpiration model results at BLK100 in 2000.

DOY	LE	H	Rn	G	Ta	e	Ts	θ	wind speed	λE_{uncorr}	res	LE_{corr}	H_{corr}	β	λE_{corr}	T_{Kc}	T_{GB}	EC Fourier
	Wm^{-2}	Wm^{-2}	Wm^{-2}	Wm^{-2}	°C	kPa	°C	m^3m^{-3}	$m\ s^{-1}$	$mm\ day^{-1}$	Wm^{-2}	Wm^{-2}	Wm^{-2}		$mm\ day^{-1}$	$mm\ day^{-1}$	$mm\ day^{-1}$	$mm\ day^{-1}$
189																4.650	5.508	3.262
190	60.59	55.5	165.18	7.02	23.4	0.533	28.79	0.056	4.05	2.144	42.06	75.79	82.36	0.92	2.692	4.657	5.489	3.261
191	60.19	57.22	170.15	7.41	23.75	0.615	29.28	0.056	3.38	2.130	45.32	78.76	83.98	0.95	2.800	4.662	5.466	3.259
192	60.47	51.97	158.92	8.17	23.72	0.71	29.64	0.056	2.52	2.139	38.32	77.56	73.19	0.86	2.758	4.664	5.438	3.256
193	69.95	47.2	167.73	9.04	25.22	0.609	29.9	0.056	3.01	2.475	41.53	89.34	69.35	0.67	3.182	4.664	5.406	3.252
194	71.16	50.17	167.88	7.25	25.9	0.468	29.49	0.056	3.28	2.518	39.3	89.57	71.06	0.7	3.193	4.661	5.369	3.247
195	77.63	40.64	167.96	11.28	27.56	0.475	30.23	0.055	2.91	2.747	38.41	96.86	59.81	0.52	3.456	4.655	5.329	3.242
196	71.82	42.25	169.8	8.52	26.01	0.534	30.61	0.055	2.64	2.541	47.21	93.83	67.45	0.59	3.348	4.647	5.284	3.236
197	73.85	42.14	172.98	14.02	27.76	0.667	31.5	0.055	2.62	2.613	42.97	95.29	63.67	0.57	3.400	4.636	5.236	3.229
198	62.85	37.5	151.53	8.54	27.51	0.744	31.95	0.055	2.88	2.224	42.64	79.91	63.08	0.6	2.847	4.622	5.184	3.221
199	72.07	41	167.38	6.55	26.23	0.539	30.89	0.055	2.83	2.550	47.75	92.36	68.47	0.57	3.291	4.605	5.128	3.212
200	79.23	36.15	160.56	8.25	26.63	0.41	30.83	0.054	2.79	2.803	36.93	97.19	55.12	0.46	3.464	4.586	5.069	3.203
201	73.59	32.03	162.91	9.41	26.63	0.388	30.73	0.053	2.43	2.604	47.89	94.17	59.33	0.44	3.359	4.565	5.006	3.193
202	73.16	35.6	167.58	8.86	28	0.469	31.14	0.053	3.06	2.588	49.95	97.2	61.52	0.49	3.472	4.541	4.940	3.182
203	80.34	34.64	169.7	8.59	28.05	0.471	30.91	0.053	2.7	2.842	46.13	101.78	59.33	0.43	3.638	4.514	4.871	3.170
204	81.02	36.39	166.54	9.39	27.64	0.399	31.02	0.053	2.11	2.867	39.74	102.86	54.29	0.45	3.678	4.485	4.798	3.158
205	78.27	27.41	162.1	12.17	29.28	0.545	31.78	0.053	2.5	2.769	44.25	98.9	51.03	0.35	3.536	4.453	4.723	3.145
206	76.83	26.98	160.04	11.42	30.43	0.608	32.9	0.052	2.41	2.718	44.81	98.84	49.78	0.35	3.535	4.420	4.645	3.131
207	71.61	30.11	147.26	8.01	-10.63	0.249	32	0.053	2.76	2.534	37.54	87.34	51.92	0.42	2.971	4.383	4.565	3.117
208	70.01	53.97	159.8	8.28	-5.75	0.309	31.46	0.053	2.42	2.477	27.54	83.1	68.42	0.77	2.878	4.345	4.482	3.101
209	73.18	37.29	156.88	6.52	26.82	0.514	30.92	0.053	2.67	2.589	39.88	90.37	59.99	0.51	3.224	4.304	4.398	3.085
210	65.71	32.03	146	6.58	26.99	0.462	30.09	0.053	2.84	2.325	41.68	83.54	55.88	0.49	2.981	4.262	4.311	3.069
211	53.08	20	121.69	8.04	27.46	0.623	29.77	0.053	2.23	1.878	40.57	69.86	43.79	0.38	2.493	4.217	4.222	3.051
212	43.45	-0.76	80.25	3.7	28.32	0.769	29.08	0.054	1.81	1.537	33.87	55.94	20.62	-0.02	1.998	4.170	4.132	3.033
213	69.5	14.28	142.42	14.7	30.89	0.861	31.23	0.054	2.49	2.459	43.94	90.09	37.63	0.21	3.227	4.122	4.040	3.015
214	73.89	23.18	154.28	12.54	31.59	1.047	33.36	0.053	2.74	2.614	44.67	95.28	46.46	0.31	3.410	4.071	3.947	2.995
215	47.31	14.15	115.63	7.01	29.57	1.019	32.17	0.054	2.7	1.674	47.16	62.61	46	0.3	2.242	4.019	3.853	2.975
216	60.39	1.42	90.28	2.29	27.66	1.143	30.09	0.056	3.46	2.137	26.18	70.87	17.12	0.02	2.522	3.965	3.758	2.955
217	52.31	30.85	129.76	5.55	26.12	1.03	29.88	0.056	2.17	1.851	41.05	63.08	61.14	0.59	2.246	3.910	3.662	2.934
218	64.82	37.81	160.1	8.56	27.84	0.772	30.71	0.055	2.72	2.293	48.91	85.48	66.06	0.58	3.053	3.853	3.565	2.912
219	63.24	34.89	160	8.83	28.03	0.814	31.09	0.054	3.11	2.237	53.04	85.56	65.61	0.55	3.057	3.794	3.468	2.889
220	60.09	44.59	157.01	6.65	26.78	0.723	30.31	0.054	3.3	2.126	45.68	78.19	72.17	0.74	2.788	3.735	3.371	2.866
221	60.26	42.48	153.61	6.52	26.15	0.595	30.02	0.054	3.55	2.132	44.34	78.28	68.81	0.7	2.788	3.674	3.274	2.843
222	65.43	42.2	155.9	3.69	26.09	0.56	30.02	0.054	2.63	2.315	44.58	82.88	69.33	0.64	2.955	3.612	3.176	2.819
223	67.06	39.64	155.62	4.86	25.35	0.379	28.92	0.054	2.86	2.373	44.06	85.1	65.66	0.59	3.034	3.548	3.079	2.794
224	64.04	31.85	148.99	7.54	26.11	0.436	29.73	0.054	2.95	2.266	45.57	80.58	60.88	0.5	2.871	3.484	2.983	2.769
225	65.13	32.59	153.3	7.58	27.08	0.431	29.62	0.053	2.53	2.304	48	84.19	61.52	0.5	3.005	3.419	2.886	2.743
226	64.22	35.13	156.28	6.72	27.11	0.5	30.02	0.053	2.47	2.272	50.2	85.58	63.97	0.55	3.056	3.354	2.791	2.717
227	62.34	32.64	150.31	9.43	27.98	0.576	30.24	0.053	2.73	2.206	45.9	79.94	60.93	0.52	2.853	3.287	2.696	2.691
228	58.84	32.94	136.13	6	27.72	0.764	30.47	0.053	2.23	2.082	38.35	74	56.13	0.56	2.642	3.220	2.602	2.664
229	56.56	31.09	140.89	6.98	27.52	0.754	30.19	0.054	2.15	2.001	46.27	74.53	59.39	0.55	2.660	3.152	2.509	2.636
230	58.67	31.51	145.04	6.29	28.65	0.801	30.51	0.054	2.78	2.076	48.58	77.26	61.49	0.54	2.758	3.084	2.417	2.608
231	64.32	22.43	144.5	5.94	26.87	0.415	29.9	0.054	2.87	2.276	51.81	83.87	54.69	0.35	2.989	3.016	2.326	2.580
232	58.78	45.39	150.35	1.46	24.05	0.374	28.58	0.055	2.34	2.080	44.72	77.39	71.5	0.77	2.754	2.947	2.237	2.551
233	55.12	41.82	149.2	3.99	23.23	0.407	27.68	0.055	2.6	1.950	48.27	70.9	74.3	0.76	2.524	2.879	2.149	2.522
234	53.72	43.93	149.98	3.66	23.52	0.406	27.54	0.055	2.78	1.901	48.68	72.18	74.15	0.82	2.569	2.810	2.063	2.493
235	51.44	51.37	152.43	3.58	23.84	0.468	27.09	0.055	3.33	1.820	46.04	66.28	82.57	1	2.359	2.741	1.979	2.463

Table A1: Daily eddy covariance, energy balance component, and transpiration model results at BLK100 in 2000.

DOY	LE	H	Rn	G	Ta	e	Ts	θ	wind speed	λE_{uncorr}	res	LE_{corr}	H_{corr}	β	λE_{corr}	T_{Kc}	T_{GB}	EC Fourier
	Wm^{-2}	Wm^{-2}	Wm^{-2}	Wm^{-2}	°C	kPa	°C	m^3m^{-3}	$m\ s^{-1}$	$mm\ day^{-1}$	Wm^{-2}	Wm^{-2}	Wm^{-2}		$mm\ day^{-1}$	$mm\ day^{-1}$	$mm\ day^{-1}$	$mm\ day^{-1}$
236	46.52	52.7	149.19	5.24	25.62	0.59	28.23	0.055	4.14	1.646	44.73	59.93	84.02	1.13	2.132	2.672	1.896	2.433
237	49.17	43.64	146.9	10.15	25.06	0.745	28.31	0.055	2.65	1.740	43.95	65.17	71.58	0.89	2.321	2.603	1.814	2.402
238	24.93	11.31	62.65	2.1	25.15	1.202	27.63	0.056	2.1	0.882	24.31	31.54	29.01	0.45	1.120	2.535	1.735	2.372
239	34.1	25.06	85.27	-3.04	23.2	1.507	27.16	0.073	1.94	1.206	29.14	38.3	50.01	0.73	1.358	2.467	1.657	2.341
240	59.17	29.57	129.85	1.34	24.41	1.195	24.6	0.086	2.32	2.093	39.76	71.79	56.71	0.5	2.552	2.399	1.582	2.309
241	50.15	28.03	115.31	3.94	23.95	1.183	25.07	0.074	2.6	1.774	33.18	65.49	45.87	0.56	2.327	2.332	1.508	2.278
242		-1.3	60.38	-4.4	19.34	-60415.4	23.66	0.071						-0.23		2.265	1.437	2.246
243			128.83	-1	20.28	-99999	24.38	0.075						-0.23		2.199	1.367	2.214
244			154.06	-5.27	19.09	-45831.3	20.99	0.078						-0.23		2.133	1.299	2.182
245		49.31	123.22	-5.48	16.58	-45832.5	20.96	0.07						0		2.068	1.234	2.150
246	32.23	68.48	143	1.22	16.14	0.702	20.94	0.067	2.71	1.140	41.07	40.99	100.8	2.12	1.446	2.004	1.171	2.118
247	33.9	58.75	140.66	1	18.95	0.697	22.19	0.065	3.28	1.199	47.01	44.42	95.25	1.73	1.571	1.941	1.109	2.085
248	36.73	56.96	138.73	-2.23	19.83	0.524	22.39	0.064	3.37	1.300	47.27	49.98	90.97	1.55	1.771	1.878	1.050	2.053
249	36.47	47.69	131.34	3.35	18.27	0.399	22.07	0.062	3.26	1.290	43.83	47.91	80.08	1.31	1.694	1.817	0.993	2.020
250	32.62	48.44	131.53	-0.82	18.26	0.467	23.27	0.061	3.56	1.154	51.3	45.33	87.03	1.49	1.602	1.756	0.938	1.987
251	31.88	37.24	118.09	1.45	19.72	0.471	22.27	0.061	2.19	1.128	47.52	45.83	70.81	1.17	1.625	1.696	0.885	1.954
252	44.03	45.41	135.65	4.58	22.68	0.518	24.02	0.06	2.3	1.558	41.63	57.82	73.25	1.03	2.055	1.638	0.834	1.921
253	40.36	38.6	129.95	2.65	21.45	0.422	23.66	0.06	2.41	1.428	48.35	55.48	71.83	0.96	1.971	1.580	0.785	1.888
254	40.59	49.19	132.23	1.09	21.25	0.421	23.59	0.059	2.51	1.436	41.36	52.92	78.22	1.21	1.879	1.524	0.738	1.855
255	38.89	36.58	127.9	3.12	21.25	0.411	23.54	0.059	2.38	1.376	49.31	53.73	71.05	0.94	1.909	1.468	0.693	1.822
256	34.24	32.5	112.96	3.08	21.54	0.415	23.48	0.06	1.98	1.211	43.14	46.81	63.07	0.95	1.664	1.414	0.650	1.789
257	41.48	27.1	116.18	5.22	24.38	0.489	25.08	0.059	2.15	1.468	42.38	54.93	56.03	0.65	1.957	1.361	0.609	1.756
258	36.85	34.02	128.1	7.51	26.44	0.701	25.41	0.059	3.71	1.304	49.72	50.62	69.97	0.92	1.805	1.309	0.570	1.724
259	42.29	32.68	125.34	0.53	24.93	0.524	25.16	0.059	3.29	1.496	49.84	58.42	66.39	0.77	2.082	1.258	0.533	1.691
260	43.24	24.78	122.96	4.89	25.29	0.457	24.95	0.059	3.06	1.530	50.06	60.26	57.82	0.57	2.151	1.209	0.497	1.658
261	41.49	19.83	120.46	7.45	25.82	0.541	25.88	0.058	2.56	1.468	51.69	59.06	53.95	0.48	2.106	1.161	0.464	1.626
262	34.67	16.61	118.34	3.8	26.12	0.59	26.84	0.058	3.44	1.227	63.27	56.22	58.32	0.48	2.002	1.114	0.432	1.593
263	34.32	16.15	118.17	6.35	26.8	0.603	26.55	0.058	2.91	1.214	61.35	55.05	56.78	0.47	1.962	1.068	0.401	1.561
264	37.59	15.14	115.49	7	27.74	0.758	27.63	0.058	3.52	1.330	55.76	55.12	53.37	0.4	1.964	1.023	0.372	1.528
265	44	7.98	110.74	4.39	27.25	0.594	27.1	0.058	3.82	1.557	54.37	59.12	47.22	0.18	2.106	0.980	0.345	1.496
266	32.28	46.62	113.34	-2.51	19.19	0.595	24.14	0.058	3.84	1.142	36.97	36.33	79.52	1.44	1.286	0.938	0.319	1.464
267	25.02	44.92	110.08	-3.95	16.94	0.613	23.13	0.059	2.99	0.885	44.08	34.47	79.56	1.8	1.216	0.897	0.295	1.433
268	26.57	44.61	111.28	-2.79	16.39	0.473	21.83	0.059	2.58	0.940	42.9	35.73	78.34	1.68	1.261	0.858	0.272	1.401
269	28.43	46.5	113.2	-2.87	16.02	0.42	20.56	0.06	2.03	1.006	41.14	39.43	76.64	1.64	1.394	0.819	0.251	1.370
270	28.34	39.61	112.05	-1.56	16.6	0.332	20.16	0.06	1.97	1.003	45.65	41.17	72.44	1.4	1.458	0.782	0.230	1.339
271	27.67	37	108.46	3.07	18.87	0.463	20.78	0.059	2.57	0.979	40.72	37.89	67.51	1.34	1.343	0.746	0.211	1.308
272	26.79	41.26	109.94	0.65	19.25	0.585	22.04	0.059	2.4	0.948	41.23	36.56	72.73	1.54	1.296	0.712	0.193	1.277
273	24.24	16.38	105.77	3.95	21.56	0.532	21.94	0.059	3.28	0.858	61.2	40.01	61.8	0.68	1.420	0.678	0.177	1.247
274	31.97	24.09	103.04	1.98	22.5	0.501	23.42	0.059	2.92	1.131	45	45.21	55.86	0.75	1.607	0.646	0.161	1.217
275	31.69	30.27	106.52	-0.36	20.34	0.427	21.83	0.059	2.05	1.121	44.91	42.94	63.93	0.96	1.526	0.615	0.147	1.187
276	31.44	23.91	100.96	3.85	22.16	0.432	21.8	0.059	2.59	1.112	41.77	42.36	54.75	0.76	1.504	0.585	0.133	1.157
277	29.7	28.76	99.97	0.32	21.27	0.509	22.35	0.059	2.35	1.051	41.18	39.7	59.95	0.97	1.408	0.556	0.121	1.128
278	27.19	27.79	100.8	0.41	20.2	0.492	22.06	0.059	2.02	0.962	45.42	38.34	62.06	1.02	1.360	0.528	0.109	1.099
279	26.62	30.68	101.11	0.89	20.42	0.516	21.84	0.059	2.4	0.942	42.92	37.03	63.19	1.15	1.314	0.501	0.098	1.070
280	25.79	31.87	101.49	0.37	19.17	0.527	21.38	0.059	1.97	0.912	43.48	37.09	64.04	1.24	1.315	0.476	0.088	1.042
281	26.99	30.44	100.84	0.72	19.84	0.488	21.48	0.059	2.25	0.955	42.69	40.05	60.07	1.13	1.421	0.451	0.079	1.014
282	24.84	24.77	94.27	-0.84	19.31	0.438	20.51	0.06	2.56	0.879	45.5	36.09	59.03	1	1.280	0.428	0.070	0.987

Table A1: Daily eddy covariance, energy balance component, and transpiration model results at BLK100 in 2000.

DOY	LE	H	Rn	G	Ta	e	Ts	θ	wind speed	λE_{uncorr}	res	LE_{corr}	H_{corr}	β	λE_{corr}	T_{Kc}	T_{GB}	EC Fourier
	Wm^{-2}	Wm^{-2}	Wm^{-2}	Wm^{-2}	°C	kPa	°C	m^3m^{-3}	$m\ s^{-1}$	$mm\ day^{-1}$	Wm^{-2}	Wm^{-2}	Wm^{-2}		$mm\ day^{-1}$	$mm\ day^{-1}$	$mm\ day^{-1}$	$mm\ day^{-1}$
283	21.52	25.46	81.69	1.32	19.01	0.559	19.64	0.06	4.34	0.761	33.38	26.88	53.48	1.18	0.951	0.405	0.062	0.959
284	35.99	17.09		-12.91	11.05	0.634	16.46	0.08	2.55	1.273				0.47		0.383	0.055	0.932
285	19.81	44.11		-7.97	8.86	0.566	13.48	0.075	2.95	0.701				2.23		0.363	0.048	0.906
286		32.04		-9.73	9.24	0.643	14.12	0.072	2.04					4.17		0.343	0.042	0.880
287	16.04	37.12		-2.46	10.44	-2082.78	13.37	0.068	1.86	0.568				2.31		0.324	0.037	0.854
288	15.49	34.93		-2.86	12.95	0.622	15.16	0.065	2.6	0.548				2.25		0.306	0.032	0.829
289	13.86	31.41		-4.38	11.59	0.546	14.62	0.064	1.73	0.490				2.27		0.288	0.027	0.804
290	16.31	34.74		-2.52	13.14	0.475	14.96	0.063	1.83	0.577				2.13		0.272	0.023	0.779
291	16.52	29.05		-0.75	14.4	0.41	15.39	0.063	2.15	0.584				1.76		0.256	0.019	0.755
292	10.85	18.39		-4.54	13.58	0.445	15.26	0.063	1.51	0.384				1.7		0.241	0.016	0.731
293	15.19	22.04		-0.61	14.7	0.48	15.89	0.062	1.72	0.537				1.45		0.227	0.013	0.707
294	16.23	11.82	47.12	5.5	17.11	0.484	16.42	0.062	3.3	0.574	13.57	18.54	23.08	0.73	0.655	0.214	0.010	0.684
295	8.37	16.4	41.16	-7.62	13.35	0.481	16.08	0.062	5.75	0.296	24	11.97	36.81	1.96	0.420	0.201	0.008	0.662
296	8.98	26.09	55.1	-6.41	9.56	0.316	13.56	0.062	5.7	0.318	26.43	12.59	48.91	2.9	0.440	0.189	0.006	0.640
297	9.11	27.6	56.82	-1.06	12.8	0.483	15.1	0.061	4.33	0.322	21.17	12.08	45.8	3.03	0.424	0.177	0.005	0.618
298	9.61	38.75	56.46	-1.59	10.74	0.73	14.71	0.062	2.05	0.340	9.69	10.26	47.79	4.03	0.361	0.167	0.004	0.597
299	9.66	25.66	49.71	-0.64	13.44	0.66	15.24	0.063	4.87	0.342	15.02	10.74	39.61	2.66	0.378	0.156	0.003	0.576
300	6.94	27.92	39.96	-2.45	11.43	0.664	14.92	0.063	4.12	0.246	7.54	7.29	35.11	4.02	0.255	0.146	0.002	0.555
301	2.98	4.86	46.13	-11.43	7.43	-2082.6	13.09	0.068	4168.16	0.105	49.72	3.38	54.18	1.63	0.120	0.137	0.002	0.535
302	15.75	35.82	63.73	-1.43	8.61	0.599	11.05	0.069	2.47	0.557	13.59	17.64	47.51	2.27	0.618	0.128	0.001	0.516
303	24.49	16.07	36.92	-5.77	11.56	0.633	12.28	0.068	3.98	0.866	2.13	20.79	21.9	0.66	0.728	0.120	0.001	0.496
304	11.25	20.04	46.89	-5.28	8.39	0.443	11.52	0.067	3.47	0.398	20.88	15.1	37.07	1.78	0.527	0.112	0.000	0.478
305	7.63	11.17	38.39	-6.07	9.47	0.375	10.83	0.067	4.37	0.270	25.67	10.6	33.87	1.46	0.371	0.105	0.000	0.459
306	9.68	21.55	39.23	-5.24	9.15	0.275	11.13	0.066	2.78	0.342	13.23	11.93	32.53	2.23	0.418	0.098	0.000	0.441
307	5.84	20.5	48.48	-0.46	10.11	-2082.93	11	0.065	2.86	0.207	22.6	8.49	40.45	3.51	0.298	0.092	0.000	0.424
308	6.47	17.2	39.25	-6.19	10.77	0.405	12.5	0.065	3.31	0.229	21.77	9.22	36.22	2.66	0.324	0.086	0.000	0.407
309	6.62	21.16	37.9	-7.2	8	0.32	10.72	0.065	2.6	0.234	17.32	8.6	36.5	3.2	0.302	0.080	0.000	0.390
310	7.61	24.52	38.88	-2.37	8.62	0.276	10.15	0.065	1.9	0.269	9.12	8.19	33.07	3.22	0.287	0.075	0.000	0.374
311	4.31	18.44	40.07	-4.61	8.54	0.374	10.33	0.065	4.66	0.152	21.93	6.05	38.64	4.27	0.212	0.069	0.000	0.358
312	5.2	-3.2	30	-6.78	8.8	0.265	10.03	0.064	5.53	0.184	34.78	8.31	28.47	-0.62	0.291	0.065	0.000	0.343
313	6.52	16.9	33.23	-4.27	6.74	0.222	8.38	0.065	2.75	0.231	14.08	7.04	30.45	2.59	0.246	0.060	0.000	0.328
314	5.15	12.4	27.47	-6.85	8.67	0.245	9.86	0.064	4.59	0.182	16.77	6.04	28.29	2.41	0.211	0.056	0.000	0.313
315	4.56	27.91	30.35	-9.14	2.13	0.267	7.41	0.065	2.29	0.161	7.02	4.54	34.94	6.12	0.158	0.052	0.000	0.299
316	2.31	7.12	15.82	-9.87	1.29	0.253	5.93	0.066	3.56	0.082	16.26	3.24	22.45	3.09	0.113	0.048	0.000	0.286
317	4.57	25.52	27.62	-11.52	0.05	0.215	5.15	0.066	2.16	0.162	9.06	4.77	34.38	5.58	0.166	0.045	0.000	0.272
318	3.85	29.18	31.33	-7.25	0.66	0.178	3.52	0.066	2.68	0.136	5.55	3.77	34.81	7.57	0.131	0.042	0.000	0.259
319	1.99	5.48	12.35	-8.2	3.66	0.204	4.86	0.066	3.64	0.070	13.08	2.88	17.67	2.75	0.101	0.039	0.000	0.247
320	3.26	23.6	27.68	-10.54	0.07	0.192	3.44	0.066	1.91	0.115	11.36	3.89	34.33	7.24	0.135	0.036	0.000	0.235
321	1.65	14.63	25.86	-5.06	1.55	-2083.05	3.81	0.066	2.65	0.058	14.64	2.31	28.61	8.87	0.081	0.034	0.000	0.223
322	3.03	5.48	21.04	-4.38	4.27	0.229	4.71	0.066	3.98	0.107	16.91	4.69	20.73	1.81	0.164	0.031	0.000	0.211
323	4.21	16.62	18.52	-7.91	4.29	0.125	5.61	0.066	2.49	0.149	5.6	4.53	21.9	3.94	0.159	0.029	0.000	0.200
324	3.33	20.94	21.97	-8.79	1.74	0.112	3.6	0.066	1.47	0.118	6.48	3.55	27.21	6.29	0.124	0.027	0.000	0.190
325	3.07	22.12	27.74	-3.44	3.12	0.135	3.87	0.066	1.47	0.109	5.99	3.05	28.13	7.19	0.107	0.025	0.000	0.179
326	2.65	14.45	16.82	-7.98	4.24	0.166	4.09	0.066	1.86	0.094	7.7	2.5	22.3	5.46	0.088	0.023	0.000	0.169
327	1.05	-2.66	14.93	1.57	7.74	0.281	5.88	0.066	4.32	0.037	14.97	1.42	11.94	-2.53	0.050	0.021	0.000	0.160
328	3.17	9.6	20.25	-4.37	8.05	0.251	7.57	0.065	3.02	0.112	11.85	4.06	20.56	3.03	0.142	0.020	0.000	0.151
329	2.95	21.76	26.24	-2.39	7.7	0.288	7.15	0.065	1.6	0.104	3.91	2.67	25.96	7.38	0.094	0.018	0.000	0.142

Table A1: Daily eddy covariance, energy balance component, and transpiration model results at BLK100 in 2000.

DOY	LE	H	Rn	G	Ta	e	Ts	θ	wind speed	λE_{uncorr}	res	LE_{corr}	H_{corr}	β	λE_{corr}	T_{Kc}	T_{GB}	EC Fourier
	Wm^{-2}	Wm^{-2}	Wm^{-2}	Wm^{-2}	°C	kPa	°C	m^3m^{-3}	$m\ s^{-1}$	mm day^{-1}	Wm^{-2}	Wm^{-2}	Wm^{-2}		mm day^{-1}	mm day^{-1}	mm day^{-1}	mm day^{-1}
330	2.66	22.37	26.7	-4.68	6.45	0.381	6.89	0.065	1.78	0.094	6.35	2.17	29.21	8.42	0.077	0.017	0.000	0.133
331	2.26	14.61	21.71	-4.47	5.56	0.359	6.44	0.066	1.61	0.080	9.31	2.48	23.71	6.46	0.087	0.016	0.000	0.125
332	3.06	22.22	26.69	-3.18	6.19	0.373	6.67	0.066	1.54	0.108	4.6	2.9	26.98	7.25	0.102	0.014	0.000	0.117
333	2.67	18.99	23.14	-1.62	6.9	-2082.92	6.96	0.066	1.9	0.094	3.1	2.41	22.35	7.11	0.085	0.013	0.000	0.110
334	4.23	17.31	20.79	-1	11.51	0.322	7.76	0.065	3.66	0.150	0.25	3.18	18.6	4.09	0.113	0.012	0.000	0.102
335	1.89	16.83	19.76	-9.25	5.47	0.302	6.59	0.066	1.63	0.067	10.29	1.71	27.3	8.91	0.060	0.011	0.000	0.095
336	1.78	9.52	15.7	-4.44	4.38	0.327	5.97	0.066	1.3	0.063	8.83	2.37	17.78	5.34	0.083	0.011	0.000	0.089
337	2.91	21.45	20.53	-6.94	4.45	0.332	5.66	0.066	1.37	0.103	3.1	2.52	24.94	7.36	0.088	0.010	0.000	0.082
338	2.32	17.35	19.63	-6.2	3.84	0.301	4.68	0.066	1.5	0.082	6.15	1.95	23.88	7.47	0.069	0.009	0.000	0.076
339	2.31	12.66	17.01	-2.46	5.11	0.286	5.04	0.066	1.37	0.082	4.5	2.4	17.07	5.47	0.084	0.008	0.000	0.071
340	1.34	-0.58	3.4	-8.85	4.21	0.244	5.03	0.066	1.55	0.047	11.49	2.13	10.11	-0.43	0.075	0.008	0.000	0.065
341	2.62	10.01	14.81	-3.09	3.26	0.216	3.92	0.067	1.21	0.093	5.26	3	14.89	3.82	0.104	0.007	0.000	0.060
342	2.09	10.16	18.01	-2.08	6.32	0.26	6.27	0.066	1.18	0.074	7.83	2.43	17.65	4.86	0.085	0.007	0.000	0.055
343	2.1	14.68	19.64	-5.58	4.75	0.31	5.46	0.066	1.27	0.074	8.45	1.97	23.25	7	0.069	0.006	0.000	0.050
344	1.92	20.46	20.63	-6.18	3.45	0.408	4.71	0.067	1.41	0.068	4.43	1.65	25.16	10.68	0.058	0.006	0.000	0.046
345	1.9	18.28	16.45	-6.4	3.12	0.424	4.38	0.067	1.46	0.067	2.67	1.28	21.57	9.64	0.045	0.005	0.000	0.042
346	1.4	15.78	18.97	-4.45	1.3	0.327	3.13	0.067	1.82	0.050	6.24	1.22	22.2	11.26	0.043	0.005	0.000	0.038
347	1.37	8.35	17.21	-3.76	4.98	0.393	5.45	0.067	3.4	0.048	11.26	1.47	19.51	6.08	0.052	0.005	0.000	0.034
348	2.64	17.86	18.36	-4.27	2.4	0.328	4.35	0.067	1.83	0.093	2.13	2.35	20.28	6.75	0.082	0.004	0.000	0.031
349	2.64	11.22	11.17	-2.82	4.73	0.349	5.16	0.067	1.85	0.093	0.13	2.01	11.98	4.26	0.070	0.004	0.000	0.027
350	2.74	12.84	17.93	-2.35	5.99	0.353	5.59	0.067	1.63	0.097	4.69	2.61	17.66	4.69	0.091	0.004	0.000	0.024
351	3.83	6.97	10.59	-6.55	6.14	0.226	5.69	0.067	2.52	0.136	6.34	4.02	13.13	1.82	0.141	0.003	0.000	0.022
352	2.79	3.03	6.16	-1.63	5.97	0.203	4.31	0.067	2.57	0.099	1.97	2.58	5.21	1.09	0.090	0.003	0.000	0.019
353	2.44	16.17	9.95	-12.29	1.89	0.181	3.52	0.067	1.55	0.086	3.62	2.01	20.23	6.62	0.070	0.003	0.000	0.017
354	2.61	19.31	17.09	-7.23	-0.09	0.132	1.97	0.067	1.34	0.092	2.4	2.57	21.75	7.4	0.089	0.003	0.000	0.015
355	2.43	20.44	22.06	-5.17	1.36	0.148	2.27	0.067	1.41	0.086	4.37	2.28	24.94	8.42	0.080	0.002	0.000	0.013
356	2.59	15.48	14.52	-1.8	5.53	0.175	3.21	0.067	2.28	0.092	-1.75	1.92	14.4	5.97	0.067	0.002	0.000	0.011
357	3.34	-2.66	4.33	-0.81	12.27	0.154	6.39	0.066	2.84	0.118	4.47	3.62	1.52	-0.8	0.127	0.002	0.000	0.009
358	1.96	17.59	14.15	-6.73	3.51	0.2	3.9	0.067	1.78	0.069	1.33	1.54	19.34	8.98	0.054	0.002	0.000	0.008
359	1.36	8.53	10.69	-0.27	4.9	0.259	3.91	0.067	2.56	0.048	1.06	0.63	10.33	6.26	0.022	0.002	0.000	0.007
360	1.87	-8.35	1.05	-4.16	6.3	0.231	5.44	0.066	5.12	0.066	11.69	2.71	2.49	-4.46	0.095	0.002	0.000	0.006
361	2.68	-0.94	2.95	-9.13	4.5	0.137	4.45	0.066	3.44	0.095	10.35	3.32	8.76	-0.35	0.116	0.002	0.000	0.005
362	2.62	11.86	9.23	-7.82	1.21	0.101	1.93	0.067	1.51	0.093	2.58	2.66	14.4	4.53	0.093	0.001	0.000	0.005
363	2.46	18.91	18.77	-6.09	2.58	0.126	1.79	0.067	1.79	0.087	3.49	2.27	22.59	7.7	0.079	0.001	0.000	0.004
364	2.25	16.28	17.21	-4.67	3.45	0.147	2.24	0.067	1.31	0.080	3.36	2.25	19.63	7.24	0.079	0.001	0.000	0.004
365	1.76	16.31	13.68	-7.51	1.83	0.159	1.87	0.067	1.45	0.062	3.12	1.66	19.53	9.27	0.058	0.001	0.000	0.004

Table A2: Daily eddy covariance, energy balance component, and transpiration model results at BLK100 in 2001.

DOY	LE	H	Rn	G	Ta	e	Ts	θ	wind speed	λE_{uncorr}	res	LE_{corr}	H_{corr}	β	λE_{corr}	T_{Kc}	T_{GB}	EC Fourier
	Wm^{-2}	Wm^{-2}	Wm^{-2}	Wm^{-2}	°C	kPa	°C	m^3m^{-3}	$m\ s^{-1}$	$mm\ day^{-1}$	Wm^{-2}	Wm^{-2}	Wm^{-2}		$mm\ day^{-1}$	$mm\ day^{-1}$	$mm\ day^{-1}$	$mm\ day^{-1}$
1	1.51	-1.01	12.68	-1.62	4.61	0.162	2.3	0.067	2.21	0.053	13.8	2.17	12.13	-0.67	0.076	0.000	0.000	0.039
2	2.24	2.49	6.68	-6.37	5.94	0.154	3.99	0.066	2.70	0.079	8.32	2.54	10.51	1.11	0.089	0.000	0.000	0.033
3	2.09	14.08	13.54	-5.92	3.49	0.089	1.93	0.067	1.67	0.074	3.29	2.14	17.33	6.74	0.075	0.000	0.000	0.026
4	2.4	16.26	17.18	-5.85	3.2	0.091	1.75	0.067	1.44	0.085	4.37	2.14	20.89	6.78	0.075	0.000	0.000	0.020
5	2.47	22.37	19.06	-5.66	1.89	0.096	1.5	0.067	1.34	0.087	-0.12	2.52	22.2	9.04	0.088	0.000	0.000	0.015
6	2.25	17.29	18.96	-5.34	2.22	0.101	1.47	0.067	1.45	0.080	4.77	1.97	22.33	7.69	0.069	0.000	0.000	0.009
7	1.9	9.63	15.55	0.73	3.85	0.127	2.41	0.067	1.79	0.067	3.3	1.86	12.96	5.08	0.065	0.000	0.000	0.003
8	3.22	5.8	9.84	2.67	6.54	0.522	5.42	0.067	8336	0.114	-1.85					0.000	0.000	-0.002
9																0.000	0.000	-0.007
10																0.000	0.000	-0.012
11																0.000	0.000	-0.016
12																0.000	0.000	-0.021
13																0.000	0.000	-0.025
14																0.000	0.000	-0.029
15																0.001	0.000	-0.033
16																0.001	0.000	-0.036
17																0.001	0.000	-0.039
18																0.001	0.000	-0.042
19																0.001	0.000	-0.045
20																0.001	0.000	-0.047
21																0.001	0.000	-0.050
22																0.001	0.000	-0.051
23																0.001	0.000	-0.053
24																0.001	0.000	-0.054
25																0.001	0.000	-0.055
26																0.001	0.000	-0.055
27			27.35	-5.6	3.44	-99999	4.24	0.163	99999		32.94					0.002	0.000	-0.055
28			32.56	-8.41	3.01	-77082	3.33	0.159	99999		40.97					0.002	0.000	-0.055
29			34.86	-2.35	2.47	-70832	2.58	0.155	99999		37.21					0.002	0.000	-0.054
30																0.002	0.000	-0.053
31																0.002	0.000	-0.052
32																0.002	0.000	-0.050
33																0.003	0.000	-0.048
34																0.003	0.000	-0.046
35																0.003	0.000	-0.043
36																0.003	0.000	-0.039
37																0.004	0.000	-0.035
38																0.004	0.000	-0.031
39																0.005	0.000	-0.026
40																0.005	0.000	-0.021
41																0.005	0.000	-0.015
42																0.006	0.000	-0.009
43																0.006	0.000	-0.003
44																0.007	0.000	0.005
45																0.007	0.000	0.012
46																0.008	0.000	0.020

Table A2: Daily eddy covariance, energy balance component, and transpiration model results at BLK100 in 2001.

DOY	LE	H	Rn	G	Ta	e	Ts	θ	wind speed	λE_{uncorr}	res	LE_{corr}	H_{corr}	β	λE_{corr}	T_{Kc}	T_{GB}	EC Fourier
	Wm^{-2}	Wm^{-2}	Wm^{-2}	Wm^{-2}	°C	kPa	°C	m^3m^{-3}	$m\ s^{-1}$	mm day^{-1}	Wm^{-2}	Wm^{-2}	Wm^{-2}		mm day^{-1}	mm day^{-1}	mm day^{-1}	mm day^{-1}
47																0.009	0.000	0.029
48			66	-1.47	2.03	-99999	3.81	0.273	99999		67.48					0.010	0.000	0.038
49			33.15	-2.33	3.59	-99999	4.55	0.265	99999		35.48					0.010	0.000	0.047
50			8.93	-6.78	3.66	-99999	3.48	0.265	99999		15.72					0.011	0.000	0.058
51			74.36	-0.15	4.18	-99999	4.79	0.271	99999		74.51					0.012	0.000	0.068
52			63.65	-1.74	3.81	-99999	4.95	0.258	99999		65.38					0.013	0.000	0.079
53			49.64	-4.95	4.16	-87499	4.81	0.247	99999		54.59					0.014	0.000	0.091
54			65.36	-8.06	2.53	-58332	3.81	0.231	99999		73.41					0.016	0.000	0.103
55			11.95	-9.59	-0.16	-99999	2.06	0.273	99999		21.53					0.017	0.000	0.116
56			46.51	2.67	1.89	-99999	3.49	0.315	99999		43.84					0.018	0.000	0.130
57			35.79	-0.52	4.72	-99999	5.15	0.333	99999		36.31					0.020	0.000	0.143
58			75.16	0.94	6.92	-95832	6.58	0.303	99999		74.22					0.021	0.000	0.158
59			68.44	-6.15	2.91	-77082	5.25	0.273	99999		74.59					0.023	0.000	0.173
60			76.4	0.29	3.31	-77082	5.38	0.254	99999		76.11					0.025	0.000	0.188
61			54.59	-1.99	5.21	-97916	6.12	0.245	99999		56.58					0.027	0.000	0.204
62			76.16	0.76	5.24	-85416	6.15	0.233	99999		75.4					0.029	0.000	0.221
63			13.93	-5.39	5.81	-99999	5.89	0.249	99999		19.32					0.031	0.001	0.238
64			60.55	6.48	8.29	-99999	7.32	0.344	99999		54.07					0.033	0.001	0.256
65			11.11	-4.29	5.74	-99999	6.87	0.378	99999		15.41					0.036	0.001	0.274
66	20.57	18.09	97.81	5.16	8.8	-49999	8.34	0.321	52084	0.728	53.99					0.038	0.001	0.293
67	32.54	40.09	97.5	5.27	9.39	0.646	8.99	0.286	1.99	1.151	19.59					0.041	0.002	0.312
68		49.14	94.85	2.24	7.45	-2083	9.13	0.266	3.52		21021.82					0.044	0.003	0.332
69	19.22	34.51	82.41	-3.01	7.85	0.491	8.95	0.249	5.75	0.680	31.68	26.37	59.05	1.80	0.920	0.048	0.004	0.353
70	19.69	38.55	91.25	-2.07	8.9	0.357	8.62	0.234	5.66	0.697	35.08	27.19	66.13	1.96	0.950	0.051	0.005	0.374
71	15.95	47.91	91.61	-1.7	7.89	0.344	8.37	0.221	3.41	0.564	29.46	21.03	72.29	3.00	0.734	0.055	0.006	0.395
72	15.57	41.75	92.73	1.09	11.7	0.346	9.26	0.212	3.50	0.551	34.32	21.89	69.74	2.68	0.769	0.059	0.008	0.417
73	16.84	40.27	88.48	3.27	11.8	0.279	9.41	0.203	2.70	0.596	28.09	22.29	62.92	2.39	0.783	0.063	0.010	0.440
74	17.71	51.9	89.59	3.67	10.72	0.362	10.12	0.196	3.05	0.627	16.31	20.61	65.31	2.93	0.722	0.067	0.011	0.463
75	15.92	40.65	94.82	3.17	12.44	0.383	10.89	0.189	3.82	0.563	35.07	21.9	69.75	2.55	0.769	0.072	0.014	0.486
76	14.64	54.12	93.54	5.08	11.55	0.461	11.75	0.183	1.91	0.518	19.7	17.49	70.98	3.70	0.614	0.077	0.016	0.510
77	14.81	54.66	101.4	7.63	13.31	0.618	12.75	0.178	1.81	0.524	24.31	18.71	75.06	3.69	0.659	0.082	0.019	0.535
78	15.67	54.56	101.04	8.2	14.7	0.645	13.56	0.172	2.25	0.554	22.61	20.53	72.3	3.48	0.723	0.088	0.021	0.560
79	15.29	48.09	90.71	5.15	15.53	0.660	14.25	0.167	1.98	0.541	22.18	19.78	65.77	3.15	0.697	0.093	0.025	0.586
80	13.63	42.71	81.95	5.43	15.2	0.607	14.27	0.162	1.94	0.482	20.17	17.65	58.87	3.13	0.622	0.100	0.028	0.612
81	14.74	44.5	85.47	5.39	14.32	0.636	14.57	0.156	2.22	0.522	20.85	18.33	61.76	3.02	0.646	0.106	0.032	0.638
82	16.33	51.45	101.44	4.66	14.57	0.594	15.2	0.151	2.53	0.578	29.01	21.3	75.49	3.15	0.750	0.113	0.036	0.665
83	17.57	59.05	99.43	1.14	15	0.489	14.6	0.146	2.71	0.622	21.66	21.63	76.65	3.36	0.763	0.120	0.041	0.693
84	17.34	53.87	103.21	4.28	14.87	0.389	14.53	0.142	2.02	0.614	27.72	23.11	75.81	3.11	0.815	0.128	0.046	0.721
85	16.07	44.5	105.63	2.03	16.21	0.379	15.09	0.136	4.09	0.569	43.04	24.03	79.57	2.77	0.847	0.136	0.051	0.749
86	23.97	38.52	105.22	4.83	17.14	0.357	15.32	0.131	4.16	0.848	37.89	27.55	72.84	1.61	0.971	0.145	0.057	0.778
87	15.28	46.27	114.71	3.54	16.95	0.506	15.78	0.128	3.15	0.541	49.62	23.76	87.41	3.03	0.841	0.154	0.064	0.807
88	16.06	48.57	110.19	3.91	16.93	0.489	15.94	0.124	4.01	0.568	41.65	23.4	82.88	3.02	0.825	0.163	0.071	0.837
89	19.97	51.95	107.8	4.59	15.93	0.452	16.58	0.121	2.65	0.707	31.29	25.98	77.23	2.60	0.916	0.173	0.079	0.867
90	18.47	56.74	110.89	4.9	16.65	0.555	16.84	0.118	2.72	0.653	30.77	24.56	81.43	3.07	0.867	0.183	0.087	0.897
91	26.54	63.01	120.35	7.84	17.32	0.524	17.28	0.116	3.86	0.939	22.96	30.85	81.66	2.37	1.089	0.194	0.096	0.928
92	29.47	43.94	104.07	-0.75	18.09	0.214	17.36	0.113	5.24	1.043	31.42	35.54	69.28	1.49	1.253	0.206	0.105	0.959

Table A2: Daily eddy covariance, energy balance component, and transpiration model results at BLK100 in 2001.

DOY	LE	H	Rn	G	Ta	e	Ts	θ	wind speed	λE_{uncorr}	res	LE_{corr}	H_{corr}	β	λE_{corr}	T_{Kc}	T_{GB}	EC Fourier
	Wm^{-2}	Wm^{-2}	Wm^{-2}	Wm^{-2}	°C	kPa	°C	m^3m^{-3}	$m\ s^{-1}$	mm day^{-1}	Wm^{-2}	Wm^{-2}	Wm^{-2}		mm day^{-1}	mm day^{-1}	mm day^{-1}	mm day^{-1}
93	16.26	77.04	108.15	-6.78	9.41	0.246	14.62	0.111	3.68	0.575	21.63	18.65	96.28	4.74	0.653	0.218	0.115	0.991
94	13.98	63.53	96.22	-1.82	7.65	0.306	13.69	0.111	2.76	0.495	20.53	16.41	81.63	4.54	0.573	0.230	0.127	1.022
95	23.5	24.67	80.46	-7.47	6.67	0.574	13.19	0.113	2.40	0.831	39.76	25.89	62.03	1.05	0.901	0.243	0.138	1.055
96	18.78	54.5	94.53	2.89	8.98	0.463	12.95	0.114	2.67	0.664	18.37	21.57	70.07	2.90	0.755	0.257	0.151	1.087
97	3.39	62.26	125.91	-4.03	7.72	0.419	13.82	0.113	4.89	0.120	64.3	6.28	123.66	18.38	0.222	0.271	0.165	1.120
98	16.88	66.94	99.11	-4.35	5.44	0.237	12.12	0.113	3.49	0.597	19.64	19.49	83.97	3.96	0.679	0.286	0.179	1.153
99	21.79	34.45	40.49	-10.73	3.33	-2083	9.87	0.112	3.87	0.771	-5.02	13.11	38.11	1.58	0.455	0.302	0.195	1.186
100	19.07	68.55	129.3	-1.11	7.43	0.307	11.35	0.113	4.30	0.675	42.79	25.13	105.28	3.60	0.877	0.318	0.211	1.219
101	21.52	87.26	136.81	5.14	8.23	0.334	12.76	0.111	4.17	0.761	22.88	23.93	107.74	4.05	0.838	0.335	0.229	1.253
102	18.66	63.03	116.76	3.01	8.28	0.365	13.98	0.109	3.16	0.660	32.07	23.63	90.12	3.38	0.826	0.353	0.247	1.287
103	20.37	76.06	116.03	0.28	10.49	0.414	13.74	0.108	3.11	0.721	19.32	23.53	92.22	3.73	0.825	0.372	0.267	1.321
104	20.97	62.14	116.83	3.96	11.56	0.309	14.41	0.106	3.19	0.742	29.76	26.38	86.49	2.96	0.926	0.391	0.288	1.356
105	26.2	66.51	127.45	5.55	12.99	0.386	15.49	0.104	2.36	0.927	29.18	32.58	89.31	2.54	1.147	0.411	0.310	1.390
106	28.15	72.71	136.03	3.88	15.3	0.353	16.09	0.101	2.88	0.996	31.3	35.22	96.93	2.58	1.244	0.431	0.334	1.425
107	32.11	59.75	126.8	5.31	16.91	0.286	16.47	0.099	2.58	1.136	29.63	40.53	80.96	1.86	1.432	0.453	0.358	1.459
108	33.7	63.84	127.81	4.32	15.74	0.284	16.48	0.097	4.50	1.192	25.95	39.83	83.65	1.89	1.406	0.475	0.384	1.494
109	28.47	57.61	104.31	-0.26	13.88	0.376	16.38	0.096	3.89	1.007	18.48	32.58	71.99	2.02	1.144	0.498	0.412	1.529
110	26.36	72.74	123.8	3.34	11.08	0.351	16.45	0.095	4.40	0.933	21.36	29.95	90.5	2.76	1.048	0.522	0.441	1.564
111	24.76	49.45	113.94	-11.93	7.95	0.551	13.06	0.107	5.57	0.876	51.68	37.27	88.61	2.00	1.301	0.547	0.471	1.599
112	28.95	61.92	140.17	5.1	11.71	0.438	14.53	0.107	2.60	1.024	44.19	40.37	94.7	2.14	1.417	0.573	0.503	1.634
113	33.28	71.25	145.1	8.07	13.77	0.510	16.38	0.1	1.91	1.177	32.49	40.93	96.1	2.14	1.442	0.599	0.537	1.669
114	35.2	59.03	142.59	9.75	16.38	0.578	18.29	0.094	1.70	1.245	38.61	46.53	86.31	1.68	1.645	0.626	0.572	1.705
115	39.86	56.91	143.63	9.55	18.63	0.567	19.47	0.092	2.22	1.410	37.32	51.76	82.32	1.43	1.833	0.654	0.609	1.740
116	37.89	52.3	131.16	6.51	19.24	0.555	19.97	0.089	2.65	1.341	34.46	48.78	75.88	1.38	1.727	0.684	0.647	1.775
117	42.44	58.23	148.3	7.66	19.67	0.571	20.63	0.088	2086	1.502	39.98	54.62	86.03	1.37	1.934	0.713	0.687	1.810
118	43.47	68.45	160.4	7.49	18.54	0.446	20.43	0.086	3.76	1.538	41	53.97	98.95	1.57	1.909	0.744	0.729	1.845
119	42.99	52.87	143.48	4.33	17.91	0.401	21.01	0.084	2.84	1.521	43.29	57.69	81.46	1.23	2.039	0.776	0.772	1.879
120	44.98	64.74	156.45	7.61	19.62	0.527	21.19	0.082	2.46	1.591	39.12	58.4	90.45	1.44	2.070	0.809	0.818	1.914
121	56.93	35.2	132.15	11.73	22.33	0.484	22.56	0.081	2.64	2.014	28.29	71.54	48.88	0.62	2.542	0.842	0.865	1.949
122	26.01	66.09	125.59	-7.66	13.64	0.281	19.62	0.08	6.76	0.920	41.15	36.22	97.03	2.54	1.269	0.877	0.914	1.983
123	28.2	64.66	126.53	-0.96	12.32	0.251	18.2	0.08	4.88	0.998	34.62	38.74	88.74	2.29	1.359	0.912	0.964	2.017
124	36.98	56.26	130.99	4.07	15.32	0.287	19.14	0.079	2.70	1.308	33.68	51.32	75.6	1.52	1.811	0.948	1.016	2.052
125	47.75	58.64	135.88	8.08	17.91	0.416	20.67	0.078	1.98	1.689	21.41	56.59	71.21	1.23	2.003	0.985	1.071	2.085
126	51.77	47.93	134.07	8.93	20.08	0.411	21.9	0.076	2.47	1.832	25.44	64.24	60.89	0.93	2.276	1.023	1.127	2.119
127	53.99	44.99	137.37	10.33	22.49	0.547	23.38	0.075	2.53	1.910	28.06	67.58	59.46	0.83	2.401	1.062	1.184	2.152
128	55.09	45.55	139.69	10.07	23.54	0.601	24.02	0.074	2.66	1.949	28.98	68.31	61.3	0.83	2.430	1.101	1.244	2.185
129	60.99	35.62	130.91	10.55	24.55	0.510	24.88	0.072	3.04	2.158	23.74	74.63	45.73	0.58	2.654	1.142	1.305	2.218
130	57.52	36.12	135.63	8.77	24.57	0.567	25.44	0.071	3.26	2.035	33.21	73.94	52.92	0.63	2.629	1.183	1.368	2.251
131	58.99	52.18	144.6	7.43	23.83	0.542	25.08	0.07	2.78	2.087	26	72.15	65.02	0.88	2.566	1.225	1.433	2.283
132	24.91	0.35	26.86	-9.01	16.07	0.959	20.28	0.08	2.73	0.881	10.61	26.35	9.51	0.01	0.929	1.268	1.499	2.315
133	58	25.94	101.76	-3.11	15.02	0.917	18.49	0.095	1.95	2.052	20.93	63.34	41.53	0.45	2.231	1.311	1.567	2.346
134	58.69	59.54	155.43	10.41	19.37	0.678	20.14	0.088	2.67	2.077	26.79	71.48	73.54	1.01	2.532	1.356	1.637	2.377
135	53.55	39.17	124.07	9.57	22.56	0.731	22.53	0.081	2.35	1.895	21.79	65.59	48.91	0.73	2.329	1.401	1.708	2.408
136	44.22	20.65	94.25	8.26	24.01	0.909	23.84	0.076	2.65	1.565	21.13	57.62	28.36	0.47	2.046	1.447	1.781	2.438
137	58.02	47.12	149.78	8.35	22.98	0.660	24.57	0.074	2.99	2.053	36.3	75.67	65.76	0.81	2.686	1.493	1.855	2.468
138	44.15	28.72	111.47	4.3	21.57	0.680	23.34	0.072	3.15	1.562	34.3	60.2	46.97	0.65	2.134	1.540	1.930	2.498

Table A2: Daily eddy covariance, energy balance component, and transpiration model results at BLK100 in 2001.

DOY	LE	H	Rn	G	Ta	e	Ts	θ	wind speed	λE_{uncorr}	res	LE_{corr}	H_{corr}	β	λE_{corr}	T_{Kc}	T_{GB}	EC Fourier
	Wm^{-2}	Wm^{-2}	Wm^{-2}	Wm^{-2}	°C	kPa	°C	m^3m^{-3}	$m\ s^{-1}$	mm day^{-1}	Wm^{-2}	Wm^{-2}	Wm^{-2}		mm day^{-1}	mm day^{-1}	mm day^{-1}	mm day^{-1}
139	61.38	39.74	148.08	8.88	22.88	0.596	24.76	0.071	2.64	2.172	38.08	81.57	57.63	0.65	2.896	1.588	2.006	2.527
140	60.04	27.67	141.73	9.76	25.53	0.450	25.53	0.069	3.98	2.124	44.27	86.34	45.63	0.46	3.071	1.636	2.084	2.555
141	58.86	35.15	145.53	7.86	24.89	0.596	26.72	0.067	3.04	2.083	43.65	82.39	55.28	0.60	2.929	1.684	2.163	2.583
142	67.25	35.86	143.77	9.74	24.75	0.568	26.84	0.066	2.34	2.379	30.93	83.2	50.83	0.53	2.961	1.733	2.243	2.611
143	66.86	35.46	142.59	9.67	25.5	0.679	27.21	0.065		2.366	30.59	82.63	50.29	0.53	2.945	1.783	2.324	2.638
144	70.22	31.16	143.46	11.99	27.5	0.708	28.23	0.065	2.77	2.484	30.09	87.8	43.66	0.44	3.130	1.833	2.406	2.664
145	67.5	37.85	149.81	9.51	27.05	0.708	28.2	0.064	3.32	2.388	34.96	87.62	52.69	0.56	3.123	1.883	2.488	2.690
146	71.23	40.11	151.8	7.93	24.71	0.637	28.04	0.064	2.45	2.520	32.53	87.97	55.9	0.56	3.130	1.934	2.571	2.715
147	72.37	33.33	146.02	10.57	25.34	0.544	28.32	0.063	3.39	2.561	29.75	88.85	46.6	0.46	3.158	1.985	2.654	2.740
148	64.6	34.82	148.45	6.35	24.74	0.555	28.45	0.062	3.35	2.286	42.69	87.79	54.31	0.54	3.118	2.036	2.738	2.764
149	69.76	37.85	150.42	10.11	25.11	0.526	28.12	0.062	2.75	2.468	32.7	87.23	53.07	0.54	3.103	2.087	2.822	2.787
150	75.98	22.38	144.35	10.85	27.72	0.543	29.06	0.061	3.10	2.688	35.14	95.35	38.15	0.29	3.397	2.138	2.907	2.810
151	76.71	28.19	153.41	10.66	27.91	0.613	29.8	0.06	3.01	2.714	37.85	97.82	44.92	0.37	3.488	2.190	2.991	2.832
152	82	22.79	138.59	9.9	29.11	0.625	29.59	0.06	3.60	2.901	23.91	96.74	31.96	0.28	3.451	2.241	3.075	2.854
153	61.81	7.96	97.53	2.58	25.59	0.387	27.56	0.059	5.46	2.187	25.18	73.2	21.75	0.13	2.597	2.292	3.158	2.875
154	76.51	34.11	142.53	9.71	22.97	0.336	28.03	0.059	3.68	2.707	22.19	88.5	44.32	0.45	3.139	2.343	3.241	2.895
155	61.52	50.75	147.56	5.2	20.47	0.368	27.71	0.058	4.53	2.177	30.1	74.69	67.68	0.82	2.640	2.394	3.324	2.914
156	70.06	47.32	156.32	11.04	23.46	0.602	28.07	0.058	2.79	2.479	27.9	83.85	61.43	0.68	2.981	2.445	3.406	2.933
157	74.95	34.4	151.99	10.31	25.75	0.666	29.91	0.057	2.58	2.652	32.33	92.84	48.83	0.46	3.306	2.495	3.487	2.951
158	76.99	23.57	137.52	10.12	27.86	0.595	29.53	0.057	3.31	2.724	26.85	91.44	35.96	0.31	3.260	2.545	3.567	2.969
159	85.35	17.74	143.99	9.8	27.75	0.433	29.98	0.056	3.17	3.020	31.1	103.97	30.22	0.21	3.707	2.595	3.645	2.985
160	79.8	29.51	150.78	8.8	26.71	0.458	29.98	0.056	3.31	2.823	32.67	98.8	43.19	0.37	3.519	2.643	3.723	3.001
161	81.18	36.25	156.97	9.87	26.03	0.495	29.8	0.055	2.73	2.872	29.67	97.32	49.78	0.45	3.465	2.692	3.799	3.017
162	74.24	28.18	139.87	9.58	25.75	0.472	30.04	0.055	3.62	2.627	27.87	88.76	41.54	0.38	3.156	2.740	3.873	3.031
163	61.01	30.93	149.57	6.91	24.61	0.534	29.52	0.055	3.88	2.159	50.72	87.13	55.53	0.51	3.095	2.787	3.945	3.045
164	49.63	44.17	148.05	1.33	20.38	0.306	27.32	0.055	5.11	1.756	52.93	70.72	76	0.89	2.499	2.833	4.016	3.058
165	65.81	59.37	156.79	7.17	20.9	0.408	28.11	0.055	2.85	2.328	24.44	77.24	72.37	0.90	2.737	2.878	4.084	3.070
166	68.81	51.85	163.8	9.09	23.94	0.502	28.31	0.054	3.21	2.435	34.05	84.87	69.84	0.75	3.019	2.923	4.150	3.081
167	74.77	45.53	162.52	10.45	25.81	0.559	29.42	0.054	2.85	2.645	31.77	92.05	60.02	0.61	3.281	2.966	4.213	3.092
168	83.5	33.56	157.07	10.17	27.05	0.529	30.19	0.054	2.84	2.954	29.84	99.04	47.86	0.40	3.532	3.009	4.275	3.102
169	78.81	33.75	154.14	8.91	26.96	0.486	30.48	0.053	3.27	2.788	32.67	97	48.22	0.43	3.457	3.050	4.333	3.111
170	81.27	32.92	156.73	9.69	27.44	0.529	30.76	0.053	2.89	2.875	32.85	98.65	48.39	0.41	3.518	3.090	4.389	3.119
171																3.129	4.441	3.126
172																3.167	4.491	3.133
173																3.203	4.538	3.139
174																3.238	4.581	3.144
175																3.272	4.621	3.148
176																3.304	4.657	3.152
177																3.334	4.690	3.155
178																3.363	4.720	3.157
179																3.390	4.745	3.158
180																3.416	4.767	3.158
181																3.440	4.785	3.158
182																3.462	4.800	3.156
183																3.482	4.810	3.154
184	76.42	16.9	141.88	15.62	32.33	0.984	33.14	0.051	3.21	2.704	32.94	93.16	33.1	0.22	3.334	3.500	4.817	3.152

Table A2: Daily eddy covariance, energy balance component, and transpiration model results at BLK100 in 2001.

DOY	LE	H	Rn	G	Ta	e	Ts	θ	wind speed	λE_{uncorr}	res	LE_{corr}	H_{corr}	β	λE_{corr}	T_{Kc}	T_{GB}	EC Fourier
	Wm^{-2}	Wm^{-2}	Wm^{-2}	Wm^{-2}	°C	kPa	°C	m^3m^{-3}	$m\ s^{-1}$	mm day^{-1}	Wm^{-2}	Wm^{-2}	Wm^{-2}		mm day^{-1}	mm day^{-1}	mm day^{-1}	mm day^{-1}
185	57.99	14.51	114.19	9.88	30.31	1.198	32.82	0.051	2.80	2.052	31.82	74.57	29.75	0.25	2.661	3.516	4.819	3.148
186	43.36	5.47	71.64	2.39	26.93	1.327	30.38	0.052	3.15	1.534	20.41	49.04	20.21	0.13	1.745	3.531	4.818	3.144
187			45.56	-7.12	19.74	1.862	25.15	0.115			87.21		77.82	0.37		3.543	4.813	3.139
188	52.58	27.34	97.72	-0.96	20.78	1.717	23.98	0.14	1.86	1.860	18.77	59.91	38.78	0.52	2.118	3.554	4.804	3.133
189	67.19	41.21	141.13	5.1	23.16	1.377	25.32	0.125	1.80	2.377	27.63	75.86	60.18	0.61	2.690	3.563	4.791	3.126
190	64.68	22.55	117.29	1.67	24.37	1.026	24.94	0.108	3.05	2.288	28.39	76.19	39.43	0.35	2.709	3.569	4.774	3.119
191	55.69	24.54	111.47	0.18	23.96	1.140	25.16	0.095	2.60	1.970	31.06	64.44	46.85	0.44	2.288	3.574	4.753	3.111
192	76	47.57	169.01	4.2	24.84	0.893	25.33	0.087	3.21	2.689	41.23	93.27	71.54	0.63	3.319	3.576	4.729	3.102
193	74.87	48.08	163.18	3.03	25.09	0.591	26.42	0.076	2.85	2.649	37.19	92.32	67.83	0.64	3.286	3.577	4.701	3.093
194	75.94	41.95	161.73	4.63	26.18	0.545	26.98	0.069	3.12	2.687	39.21	92.23	64.88	0.55	3.286	3.575	4.669	3.082
195	73.29	48.1	159.1	4.61	25.08	0.554	27.8	0.065	2.51	2.593	33.1	86.72	67.76	0.66	3.087	3.572	4.633	3.072
196	70.88	44.87	154.26	5	25.36	0.560	28.7	0.062	3.41	2.508	33.5	84.81	64.44	0.63	3.016	3.566	4.594	3.060
197	60.57	61.97	160.78	3.45	22.99	0.604	28.05	0.059	3.08	2.143	34.79	72.35	84.98	1.02	2.569	3.559	4.552	3.048
198	55.24	63.82	156.99	5.19	22.68	0.711	28.11	0.058	2.92	1.954	32.75	67.88	83.93	1.16	2.409	3.549	4.507	3.035
199	61.77	58.12	159.82	6.82	23.9	0.778	28.88	0.057	2.96	2.185	33.1	73.94	79.06	0.94	2.627	3.537	4.458	3.021
200	62.53	58.93	159.27	4.49	23.44	0.642	28.82	0.056	3.06	2.212	33.31	74.72	80.05	0.94	2.656	3.524	4.406	3.007
201	61.44	63.01	159.77	5.72	23.34	0.639	28.53	0.055	2.95	2.174	29.59	72.27	81.77	1.03	2.568	3.508	4.351	2.992
202	63.14	52.74	155.15	7.12	23.83	0.662	29.23	0.054	2.71	2.234	32.15	75.18	72.85	0.84	2.673	3.491	4.293	2.977
203	65.56	48.61	156.83	7.07	24.95	0.592	29.36	0.054	2.86	2.320	35.6	79.39	70.38	0.74	2.825	3.471	4.233	2.961
204	67.71	45.21	156.04	6.45	24.62	0.593	29.8	0.053	2.31	2.396	36.68	82.98	66.61	0.67	2.954	3.450	4.169	2.944
205	69.27	47.74	155.52	6.58	24.72	0.479	29.41	0.052	2.44	2.451	31.94	82.77	66.17	0.69	2.949	3.427	4.104	2.927
206	71.91	40.71	149.79	8.27	25.53	0.493	29.89	0.052	2.37	2.544	28.9	83.67	57.85	0.57	2.983	3.402	4.036	2.909
207	60.95	36.58	132.5	7.25	26.06	0.643	29.86	0.052	1.94	2.156	27.72	69.91	55.35	0.60	2.494	3.375	3.966	2.891
208	68.84	39.7	153.89	10.69	28.1	0.716	30.83	0.052	2.17	2.436	34.66	84.15	59.05	0.58	3.006	3.347	3.894	2.872
209	79.25	28.45	152.67	8.91	28.66	0.552	31.23	0.051	2.71	2.804	36.06	93.94	49.82	0.36	3.358	3.317	3.820	2.853
210	72.46	34.28	150.24	7.25	27.5	0.541	31.15	0.051	2.97	2.564	36.25	87.48	55.51	0.47	3.122	3.285	3.744	2.833
211	69.32	43.24	145.16	9.6	26.67	0.530	31.01	0.05	3.13	2.453	23.01	78.69	56.88	0.62	2.802	3.252	3.666	2.812
212	60.72	40.53	144.01	8.64	26.29	0.715	31.73	0.05	3.81	2.148	34.12	72.57	62.8	0.67	2.583	3.217	3.588	2.792
213	58.44	51.08	151.21	7.69	26.07	0.860	31.25	0.05	3.24	2.068	34	70.51	73.01	0.87	2.513	3.181	3.508	2.770
214	61.98	38.28	144.71	9.92	27.89	0.838	31.71	0.05	3.28	2.193	34.53	75.49	59.3	0.62	2.692	3.143	3.426	2.749
215	61.85	45.58	149.99	6.77	28.06	0.779	31.27	0.05	3.72	2.188	35.79	75.49	67.73	0.74	2.694	3.104	3.344	2.726
216	64.05	40.87	145.94	4.27	25.15	0.465	30.44	0.05	2.07	2.266	36.73	77.76	63.9	0.64	2.771	3.064	3.261	2.704
217	66.09	46.38	150.36	5.49	24.54	0.439	29.45	0.05	2.79	2.338	32.41	76.29	68.58	0.70	2.720	3.022	3.178	2.681
218	61.91	49.46	152.54	11.05	27.2	0.669	30.78	0.05	2.49	2.190	30.11	74.7	66.79	0.80	2.668	2.980	3.093	2.657
219	61.62	42.5	149.04	9.13	28.43	0.874	31.92	0.049	2.35	2.180	35.78	75.84	64.06	0.69	2.711	2.936	3.009	2.634
220	48.28	21.86	103.64	8.53	28.76	0.969	30.98	0.05	2.54	1.708	24.96	56.39	38.71	0.45	2.013	2.891	2.924	2.609
221	51.73	25.61	114.72	6.69	28.62	1.034	31.59	0.05	2.57	1.830	30.7	65.09	42.94	0.50	2.323	2.845	2.839	2.585
222	61.42	38.27	145.3	7.75	28.65	0.877	31.53	0.05	2.37	2.173	37.87	78.19	59.37	0.62	2.793	2.798	2.754	2.560
223	66.98	34.08	143.33	7.71	28.81	0.699	31.61	0.049	2086	2.370	34.56	82.14	53.48	0.51	2.936	2.751	2.670	2.535
224	61.35	32.18	130.66	5.31	28.21	0.655	30.66	0.05	2.76	2.171	31.81	74.41	50.93	0.52	2.661	2.702	2.585	2.510
225	61.06	49.41	147.19	5.74	25.95	0.682	30.37	0.05	2.14	2.160	30.98	71.37	70.08	0.81	2.546	2.653	2.502	2.484
226	59.28	42.53	144.19	7.73	26.62	0.665	30.39	0.049	2.44	2.097	34.65	74.92	61.55	0.72	2.675	2.603	2.418	2.458
227	56.52	29.34	126.65	5.47	27.57	0.651	30.44	0.049	2.35	2.000	35.33	68.79	52.39	0.52	2.457	2.553	2.336	2.432
228	62.07	36.9	142.55	7.07	27.46	0.615	30.45	0.049	2.44	2.196	36.51	76.05	59.43	0.59	2.717	2.502	2.254	2.406
229	57.36	33	132.51	8.38	28.64	0.699	30.88	0.049	2.04	2.029	33.78	68.14	56	0.58	2.435	2.451	2.173	2.379
230	63.85	32.51	136.55	6.3	28.77	0.659	30.96	0.049	2.39	2.259	33.88	77.49	52.76	0.51	2.772	2.399	2.093	2.352

Table A2: Daily eddy covariance, energy balance component, and transpiration model results at BLK100 in 2001.

DOY	LE	H	Rn	G	Ta	e	Ts	θ	wind speed	λE_{uncorr}	res	LE_{corr}	H_{corr}	β	λE_{corr}	T_{Kc}	T_{GB}	EC Fourier
	Wm^{-2}	Wm^{-2}	Wm^{-2}	Wm^{-2}	°C	kPa	°C	m^3m^{-3}	$m\ s^{-1}$	$mm\ day^{-1}$	Wm^{-2}	Wm^{-2}	Wm^{-2}		$mm\ day^{-1}$	$mm\ day^{-1}$	$mm\ day^{-1}$	$mm\ day^{-1}$
231	46.83	26.7	105.45	3.7	27.68	0.654	29.45	0.049	2.63	1.657	28.23	57.84	43.92	0.57	2.064	2.347	2.014	2.325
232	60.4	38.49	137.29	7.01	26.82	0.599	29.93	0.049	2.77	2.137	31.4	69.14	61.15	0.64	2.467	2.295	1.936	2.298
233	49.16	40.18	125.58	0.81	23.85	0.461	28.94	0.049	2.31	1.739	35.43	59.94	64.82	0.82	2.132	2.243	1.860	2.271
234	49.54	45.17	127.89	4.26	23.62	0.526	27.93	0.049	2.80	1.753	28.91	57.05	66.57	0.91	2.030	2.190	1.785	2.244
235	50.38	43.85	130.82	3.86	23.01	0.526	27.95	0.049	2.69	1.782	32.73	61.42	65.54	0.87	2.186	2.138	1.711	2.216
236	49.71	41.02	131.62	4.99	24.25	0.563	28.4	0.049	2.05	1.759	35.9	62.73	63.9	0.83	2.234	2.085	1.639	2.189
237	55.36	33.6	130.94	6.99	25.56	0.519	28.61	0.049	2.45	1.959	34.99	67.66	56.28	0.61	2.414	2.033	1.568	2.161
238	55.4	33.72	132.8	7.61	27.32	0.649	29.58	0.049	2.54	1.960	36.07	68.46	56.73	0.61	2.446	1.980	1.499	2.133
239	53.98	28.18	126.97	6.72	28.6	0.701	30.21	0.049	2.48	1.910	38.1	68.35	51.9	0.52	2.444	1.928	1.432	2.105
240	51.72	22.98	117.51	6.37	28.8	0.637	29.83	0.049	2.44	1.830	36.44	66.11	45.03	0.44	2.364	1.876	1.366	2.078
241	41.19	33.58	107.8	3.01	26.19	0.698	28.63	0.049	2.80	1.457	30.01	46.71	58.09	0.82	1.666	1.825	1.302	2.050
242	44.92	50.73	127.47	2.82	24.24	0.688	27.94	0.05	3.15	1.589	28.99	53.51	71.14	1.13	1.904	1.774	1.240	2.022
243	45.37	45.44	124.5	3.43	23.14	0.642	27.51	0.05	2.76	1.605	30.25	53.58	67.49	1.00	1.906	1.723	1.180	1.994
244	45.1	45.41	127.18	4.34	23.96	0.618	27.49	0.05	2.67	1.596	32.33	54.43	68.41	1.01	1.937	1.672	1.121	1.966
245	41.45	39.94	120.22	7.66	25.04	0.854	28.31	0.05	2.47	1.467	31.16	49.75	62.82	0.96	1.771	1.622	1.064	1.938
246	36.33	31.11	89.86	3.22	24.89	1.037	28.12	0.05	2.30	1.285	19.2	41.09	45.55	0.86	1.461	1.573	1.009	1.910
247	41.6	46.69	124.62	4.48	23.04	1.019	28.26	0.05	1.87	1.472	31.85	50.82	69.33	1.12	1.806	1.524	0.956	1.883
248	44.25	28.86	118.91	5.06	25.78	0.788	28.33	0.05	3.13	1.566	40.74	56.61	57.24	0.65	2.015	1.476	0.904	1.855
249	43.73	23.22	110.02	1.72	24.2	0.398	27.57	0.05	3.80	1.547	41.35	56.48	51.82	0.53	2.006	1.429	0.855	1.828
250	43.69	30.9	113.6	1.88	23.13	0.390	26.86	0.05	2.53	1.546	37.14	55.25	56.48	0.71	1.963	1.382	0.807	1.800
251	41.19	34.89	115.73	1.8	23.53	0.441	26.5	0.05	2.89	1.457	37.85	53.35	60.57	0.85	1.896	1.336	0.761	1.773
252	42.79	42.33	118.32	1.1	21.99	0.388	25.31	0.05	3.02	1.514	32.1	51.14	66.08	0.99	1.817	1.290	0.717	1.745
253	37.35	50.23	120.12	4.81	22.37	0.543	25.33	0.05	3.01	1.321	27.73	44.51	70.8	1.34	1.581	1.246	0.675	1.718
254	32.93	43.82	106.07	3.18	24	0.595	26.09	0.05	4.09	1.165	26.14	38.29	64.61	1.33	1.359	1.202	0.634	1.691
255	36.48	42.86	109.5	0.46	23.05	0.468	25.72	0.051	3.73	1.291	29.7	44.02	65.02	1.17	1.563	1.159	0.595	1.664
256	35.16	36.63	110.46	1.58	21.09	0.538	24.89	0.051	2.79	1.244	37.09	44.27	64.61	1.04	1.571	1.117	0.558	1.638
257	37.31	46.12	114.96	0.2	20.84	0.495	24.34	0.051	2.38	1.320	31.32	45.89	68.86	1.24	1.630	1.076	0.523	1.611
258	39.97	33.98	109.65	3	22.29	0.414	24.2	0.051	2.50	1.414	32.7	49.02	57.62	0.85	1.742	1.036	0.489	1.585
259	38.23	31.96	108.32	4.05	22.71	0.510	24.93	0.051	2.77	1.353	34.08	47.42	56.84	0.84	1.684	0.996	0.456	1.559
260	33.23	32.4	106.65	2.2	22.44	0.655	25.76	0.051	2.85	1.176	38.81	43.27	61.17	0.98	1.536	0.958	0.426	1.533
261	35.18	34.08	107.16	3.39	22.78	0.614	25.12	0.051	2.49	1.245	34.5	44.51	59.25	0.97	1.582	0.920	0.396	1.507
262	35.96	30.83	104.71	2.76	22.59	0.570	25.03	0.051	2.32	1.272	35.16	46.18	55.76	0.86	1.642	0.883	0.369	1.481
263	35.89	35.24	106.01	2.73	22.87	0.630	25	0.051	2.34	1.270	32.15	44.74	58.54	0.98	1.591	0.848	0.342	1.456
264	36.83	36.86	107.87	0.66	22.07	0.577	24.67	0.051	1.86	1.303	33.52	47.09	60.12	1.00	1.675	0.813	0.318	1.431
265	34.53	29.03	97.27	1.49	21.47	0.518	23.85	0.051	2.16	1.222	32.22	43.77	52.02	0.84	1.555	0.779	0.294	1.406
266	34.73	25.46	90.67	0.68	22.11	0.494	23.33	0.051	2.34	1.229	29.81	41.51	48.48	0.73	1.476	0.746	0.272	1.381
267	35.8	30.12	103.7	5.91	23.27	0.490	24.2	0.051	3.13	1.267	31.87	44.36	53.43	0.84	1.577	0.714	0.251	1.357
268	41.39	29.97	106.07	2.32	26.86	0.496	26.55	0.05	4.27	1.464	32.39	48.71	55.04	0.72	1.736	0.683	0.231	1.333
269	33.13	42.21	101.9	-0.34	20.65	0.456	23.3	0.051	2.29	1.172	26.89	40.96	61.28	1.27	1.454	0.653	0.213	1.309
270	29.59	29.19	95.3	2.58	22.56	0.531	23.12	0.051	3.35	1.047	33.95	35.79	56.94	0.99	1.273	0.624	0.195	1.285
271	33.18	34.24	100.46	-0.67	21.32	0.480	22.94	0.051	2.23	1.174	33.71	41.9	59.22	1.03	1.488	0.596	0.179	1.262
272	29.19	26.67	95.08	-0.16	21.32	0.485	23.12	0.051	3.05	1.033	39.39	38.66	56.58	0.91	1.372	0.569	0.163	1.239
273	30.32	27.4	95.57	2.64	21.46	0.499	22.71	0.052	2.38	1.073	35.21	39.53	53.4	0.90	1.406	0.542	0.149	1.216
274	29.05	24.5	99.12	3.02	23.06	0.525	23.25	0.051	2.71	1.028	42.55	40.03	56.07	0.84	1.424	0.517	0.136	1.193
275	27.84	14.83	90.27	0.93	23.14	0.516	23.14	0.051	2086	0.985	46.67	41.62	47.73	0.53	1.481	0.492	0.123	1.171
276	26.3	16.2	91.79	1.93	22.76	0.498	23.1	0.051	2.58	0.931	47.37	39.76	50.1	0.62	1.414	0.469	0.112	1.149

Table A2: Daily eddy covariance, energy balance component, and transpiration model results at BLK100 in 2001.

DOY	LE	H	Rn	G	Ta	e	Ts	θ	wind speed	λE_{uncorr}	res	LE_{corr}	H_{corr}	β	λE_{corr}	T_{Kc}	T_{GB}	EC Fourier
	Wm^{-2}	Wm^{-2}	Wm^{-2}	Wm^{-2}	°C	kPa	°C	m^3m^{-3}	$m\ s^{-1}$	$mm\ day^{-1}$	Wm^{-2}	Wm^{-2}	Wm^{-2}		$mm\ day^{-1}$	$mm\ day^{-1}$	$mm\ day^{-1}$	$mm\ day^{-1}$
277	29.23	26.51	92.15	2.04	21.9	0.574	22.72	0.051	2.00	1.034	34.36	38.35	51.76	0.91	1.364	0.446	0.101	1.127
278	24.28	24.85	82.11	0.02	19.93	0.583	22.18	0.052	2.87	0.859	32.95	29.61	52.47	1.02	1.050	0.424	0.091	1.106
279	22.29	42.9	84.44	-4.17	15.6	0.633	20.33	0.052	1.78	0.789	23.41	25.82	62.79	1.92	0.912	0.403	0.082	1.085
280	21.78	36.71	85.11	-1.99	15.6	0.609	19.59	0.053	1.87	0.771	28.61	26.59	60.52	1.69	0.940	0.382	0.073	1.064
281	21.82	35.33	76.59	-0.91	16.34	0.600	19.41	0.053	1.58	0.772	20.35	25.18	52.32	1.62	0.890	0.363	0.065	1.043
282	24.03	13.19	75.79	-2.14	17.13	0.347	19.02	0.053	3.54	0.850	40.7	32.38	45.54	0.55	1.143	0.344	0.058	1.023
283	20.33	25.86	73.63	-5.14	14.72	0.321	18.17	0.053	2.86	0.719	32.59	25.41	53.36	1.27	0.896	0.326	0.051	1.003
284	17.27	14.73	58.02	0.63	15.24	0.379	16.93	0.054	2.19	0.611	25.39	23.1	34.28	0.85	0.815	0.309	0.045	0.983
285	16.3	14.67	78.59	-0.66	18.4	0.486	19.26	0.053	4.83	0.577	48.27	26.28	52.97	0.90	0.928	0.292	0.039	0.964
286	22.81	16.65	79.04	-1.18	18.08	0.354	17.9	0.054	2.31	0.807	40.76	34.26	45.96	0.73	1.215	0.277	0.034	0.945
287	22.27	17.72	74.01	-1.18	18.61	0.411	19.44	0.053	2.35	0.788	35.2	29.94	45.25	0.80	1.060	0.262	0.029	0.926
288	19.58	19.61	67.39	-0.54	17.43	0.379	17.82	0.054	2.11	0.693	28.73	26.8	41.12	1.00	0.949	0.247	0.025	0.907
289	18.34	19.36	62.25	-2.51	16.92	0.382	17.52	0.054	2.02	0.649	27.05	23.16	41.59	1.06	0.819	0.233	0.021	0.889
290	22.2	27.2	72.77	-2.52	16.31	0.379	17.36	0.054	1.96	0.785	25.88	27.49	47.8	1.23	0.972	0.220	0.018	0.871
291	20.37	19.05	73.59	-0.54	17.59	0.401	17.86	0.054	2.48	0.721	34.71	28.48	45.65	0.93	1.008	0.208	0.015	0.853
292	16.36	16.08	57.08	-0.74	17.07	0.429	17.24	0.054	1.92	0.579	25.38	22.53	35.3	0.98	0.796	0.196	0.012	0.836
293	19.7	17.55	63.5	0.72	17.37	0.429	17.4	0.054	1.81	0.697	25.53	25.08	37.7	0.89	0.886	0.184	0.009	0.819
294	16.03	-0.28	45.72	1.2	20.07	0.464	18.88	0.054	2.92	0.567	28.76	20.58	23.94	-0.02	0.728	0.174	0.007	0.802
295	18.8	24.29	70.83	-3.78	16.46	0.436	17.88	0.054	2.63	0.665	31.52	25.2	49.41	1.29	0.891	0.163	0.005	0.785
296	18.78	14.67	67.26	2.08	16.89	0.433	16.99	0.054	2.49	0.664	31.72	25.21	39.97	0.78	0.892	0.154	0.004	0.769
297	16.4	20.96	63.88	-5.43	14.51	0.359	16.96	0.054	2.45	0.580	31.96	21.3	48.01	1.28	0.751	0.144	0.003	0.753
298	17.82	31.11	71.05	-4.75	13.35	0.334	15.4	0.055	1.80	0.630	26.87	22.34	53.46	1.75	0.788	0.136	0.003	0.737
299	15.82	28.06	68.04	-2.97	13.17	0.330	14.42	0.055	2.05	0.560	27.14	19.73	51.28	1.77	0.696	0.127	0.002	0.721
300	12.91	12.74	47.76	-0.69	15.21	0.410	15.13	0.055	2.21	0.457	22.8	16.04	32.4	0.99	0.566	0.119	0.002	0.706
301	12.32	28.63	63.78	-3.47	13.36	0.520	14.82	0.055	2.20	0.436	26.29	14.8	52.44	2.32	0.522	0.112	0.001	0.691
302	11.96	22.47	52.42	-1.06	13.16	0.508	14.41	0.056	2.12	0.423	19.05	14.26	39.22	1.88	0.502	0.105	0.001	0.676
303	6.28	-1.22	13.9	-2.1	14.16	0.779	14.9	0.056	2.69	0.222	10.94	5.91	10.09	-0.19	0.207	0.098	0.000	0.661
304	14.33	32.75	63.26	-7.09	11.13	0.600	14.02	0.057	1.59	0.507	23.27	17.89	52.46	2.29	0.628	0.092	0.000	0.647
305	11.11	29.24	61.94	-4.54	9.99	-2083	12.49	0.057	1.61	0.393	26.13	14.44	52.05	2.63	0.507	0.086	0.000	0.633
306	9.45	23.08	53.13	-4.56	9.99	0.523	12.15	0.057	1.58	0.334	25.18	11.99	45.71	2.44	0.422	0.081	0.000	0.619
307	11.89	24.57	60.98	-2.36	11.73	0.516	12.83	0.057	1.84	0.421	26.87	15.64	47.7	2.07	0.551	0.075	0.000	0.605
308	5.67	0.65	26.14	-0.93	12.29	0.554	12.81	0.057	2.17	0.201	20.75	9.05	18.02	0.11	0.318	0.070	0.000	0.592
309	7.99	11.31	37.14	-4.58	12.11	0.639	12.75	0.058	1.61	0.283	22.42	10.54	31.18	1.42	0.371	0.066	0.000	0.578
310	10.74	33.98	60.81	-3.01	12.28	0.667	12.55	0.058	1.91	0.380	19.09	12.36	51.45	3.16	0.435	0.061	0.000	0.565
311	10.07	17.09	56.19	-3.34	13.36	0.520	12.51	0.058	2.32	0.356	32.37	15.23	44.3	1.70	0.537	0.057	0.000	0.552
312	9.77	11.41	51.87	-4.67	12.89	0.381	12.23	0.058	2.60	0.346	35.36	15.59	40.95	1.17	0.549	0.053	0.000	0.540
313	10.12	28.36	53.65	-9.95	7.51	0.228	9.32	0.059	1.66	0.358	25.12	12.54	51.06	2.80	0.440	0.050	0.000	0.527
314	8.41	28.47	53.86	-1.69	9.08	0.342	9.54	0.059	1.74	0.298	18.67	9.7	45.85	3.38	0.340	0.046	0.000	0.515
315	6.99	38.57	61	1.93	13.18	0.761	12.56	0.058	2.70	0.247	13.52	7.39	51.68	5.52	0.260	0.043	0.000	0.503
316	3.33	24.03	48.03	-0.54	10.76	0.826	12.28	0.058	4.03	0.118	21.21	4.22	44.35	7.22	0.148	0.040	0.000	0.491
317	7.37	24.37	53.41	-10.49	8.25	0.450	10.43	0.059	2.31	0.261	32.16	11.45	52.46	3.30	0.401	0.037	0.000	0.479
318	8.15	24.59	50.57	-3.87	9.15	0.496	10.03	0.059	1.59	0.288	21.7	10.87	43.57	3.02	0.382	0.035	0.000	0.467
319	8.33	33.57	52.08	-3.88	8.97	0.536	9.79	0.059	1.80	0.295	14.06	9.24	46.72	4.03	0.324	0.032	0.000	0.456
320	7.64	30.06	50.48	-3.26	9.27	0.583	10.19	0.059	1.80	0.270	16.04	8.72	45.02	3.93	0.306	0.030	0.000	0.445
321	7.36	25.84	44.62	-6.02	8.53	0.531	9.55	0.059	2.02	0.260	17.43	8.35	42.29	3.51	0.293	0.028	0.000	0.433
322	7.33	17.83	43.34	-7.62	7.93	0.349	8.29	0.06	1.82	0.259	25.8	9.82	41.14	2.43	0.345	0.026	0.000	0.422

Table A2: Daily eddy covariance, energy balance component, and transpiration model results at BLK100 in 2001.

DOY	LE	H	Rn	G	Ta	e	Ts	θ	wind speed	λE_{uncorr}	res	LE_{corr}	H_{corr}	β	λE_{corr}	T_{Kc}	T_{GB}	EC Fourier
	Wm^{-2}	Wm^{-2}	Wm^{-2}	Wm^{-2}	°C	kPa	°C	m^3m^{-3}	$m\ s^{-1}$	mm day^{-1}	Wm^{-2}	Wm^{-2}	Wm^{-2}		mm day^{-1}	mm day^{-1}	mm day^{-1}	mm day^{-1}
323	6.5	20.5	39.69	-2.22	7.99	0.329	7.95	0.06	1.54	0.230	14.91	8.14	33.77	3.15	0.285	0.024	0.000	0.411
324	3.53	3.88	16.44	-9.42	7.04	0.365	8.15	0.06	1.68	0.125	18.44	5.59	20.26	1.10	0.195	0.022	0.000	0.401
325	6.44	12.45	33.85	4.44	9.96	0.416	9.44	0.06	1.93	0.228	10.51	7.3	22.1	1.93	0.256	0.021	0.000	0.390
326	18.36	12.28	50.17	0.62	12.76	0.462	12.12	0.059	3.25	0.650	18.9	20.52	29.03	0.67	0.721	0.019	0.000	0.379
327	5.91	7.05	34.28	-8.17	8.4	0.248	9.74	0.06	3.12	0.209	29.49	9.26	33.19	1.19	0.324	0.018	0.000	0.369
328	26.95	-23.2	-15.72	-10.38	6.95	0.614	8.17	0.205	14586	0.954	-9.1	27.15	-32.49	-0.86	0.945	0.016	0.000	0.359
329	19.64	-1.6	1.56	-18.77	2.7	0.508	6.22	0.27	1.73	0.695	2.28	12.93	7.39	-0.08	0.449	0.015	0.000	0.349
330	18.19	3.68	5.64	-18.25	2.02	0.355	3.31	0.228	3.19	0.644	2.02	12.2	11.69	0.20	0.423	0.014	0.000	0.339
331	12.17	4.89	-0.98	-18.25	0.7	0.296	2.1	0.211	3.43	0.431	0.21					0.013	0.000	0.329
332		7.45	-2005.9	-12.47	-0.73	-47916	1.09	0.194	45834		6536.32					0.012	0.000	0.319
333			-1.02	-12.01	-0.03	-99999	2.33	0.227	99999		11					0.011	0.000	0.309
334			25.78	-12.74	-1.08	-99999	1.11	0.274	99999		38.52					0.010	0.000	0.299
335			15.13	-0.02	3.32	-99999	3.68	0.309	99999		15.14					0.010	0.000	0.290
336			18.58	1.82	7.45	-99999	6.07	0.292	99999		16.77					0.009	0.000	0.280
337			24.68	-10.46	7.03	-99999	5.81	0.264	99999		35.14					0.008	0.000	0.271
338			9.02	-18.8	1.91	-79166	3.04	0.237	99999		27.81					0.008	0.000	0.262
339			3.68	-12.92	0	-99999	1.37	0.213	99999		16.6					0.007	0.000	0.253
340			13.8	-9.03	2.1	-99999	1.87	0.212	99999		22.83					0.007	0.000	0.243
341			-7.73	-2.81	8.08	-62499	3.23	0.215	99999		-4.93					0.006	0.000	0.234
342			-4.01	-10.34	3.36	-81249	3.03	0.206	99999		6.33					0.006	0.000	0.226
343			-8.92	-7.01	3.71	-85416	2.51	0.199	99999		-1.91					0.005	0.000	0.217
344			-15.68	-9.33	3.51	-99999	3.06	0.196	99999		-6.35					0.005	0.000	0.208
345																0.004	0.000	0.199
346																0.004	0.000	0.191
347																0.004	0.000	0.182
348																0.004	0.000	0.174
349																0.003	0.000	0.165
350			13.91	-10.52	-0.25	-72916	1.26	0.167	99999		24.42					0.003	0.000	0.157
351			1.1	-11.08	-1.39	-89582	0.25	0.162	99999		12.17					0.003	0.000	0.149
352			11.38	-11.02	-1.84	-99999	-0.15	0.158	99999		22.4					0.003	0.000	0.141
353			11.57	-9.89	-0.83	-99999	-0.4	0.156	99999		21.47					0.002	0.000	0.133
354			14.75	1.58	5.71	-64582	1.92	0.163	99999		13.17					0.002	0.000	0.125
355			7.03	-7.87	3.05	-89582	2.67	0.16	99999		14.89					0.002	0.000	0.117
356			2	-4.06	2.16	-99999	1.62	0.156	99999		6.06					0.002	0.000	0.109
357			-2.13	-3.85	5.6	-91666	3.86	0.155	99999		1.72					0.002	0.000	0.102
358			-6.99	-11.32	1.33	-85416	2.26	0.151	99999		4.33					0.002	0.000	0.094
359			8.73	-7.39	0.71	-72916	1.07	0.146	99999		16.12					0.002	0.000	0.087
360			13.29	-2.01	3.86	-74999	2.42	0.146	99999		15.3					0.001	0.000	0.080
361			6.65	-2.69	4.72	-89582	3.5	0.144	99999		9.35					0.001	0.000	0.073
362			4.72	-2.49	5.05	-99999	3.96	0.142	99999		7.21					0.001	0.000	0.066
363			10.62	-0.61	4.41	-99999	5.16	0.258	99999		11.24					0.001	0.000	0.059
364			10.09	1.11	5.29	-99999	5.99	0.299	99999		8.98					0.001	0.000	0.052
365																0.001	0.000	0.045

Table A3: Daily eddy covariance, energy balance component, and transpiration model results at BLK009 in 2001.

DOY	LE	H	Rn	G	Ta	e	Ts	θ	wind speed	λE_{uncorr}	res	LE_{corr}	H_{corr}	β	$\lambda E_{corr.}$	T_{Kc}	T_{GB}	EC Fourier
	Wm^{-2}	Wm^{-2}	Wm^{-2}	Wm^{-2}	°C	kPa	°C	m^3m^{-3}	$m\ s^{-1}$	$mm\ day^{-1}$	Wm^{-2}	Wm^{-2}	Wm^{-2}		$mm\ day^{-1}$	$mm\ day^{-1}$	$mm\ day^{-1}$	$mm\ day^{-1}$
1																0.001	0.000	0.087
2																0.001	0.000	0.079
3																0.001	0.000	0.071
4																0.001	0.000	0.063
5																0.001	0.000	0.055
6																0.002	0.000	0.048
7																0.002	0.000	0.040
8																0.002	0.000	0.033
9																0.002	0.000	0.026
10																0.002	0.000	0.019
11																0.002	0.000	0.013
12																0.002	0.000	0.006
13																0.003	0.000	0.000
14																0.003	0.000	-0.006
15																0.003	0.000	-0.012
16																0.003	0.000	-0.017
17																0.004	0.000	-0.022
18																0.004	0.000	-0.027
19																0.004	0.000	-0.032
20																0.005	0.000	-0.036
21																0.005	0.000	-0.040
22																0.005	0.000	-0.044
23																0.006	0.000	-0.047
24																0.006	0.000	-0.050
25																0.007	0.000	-0.052
26																0.008	0.000	-0.055
27																0.008	0.000	-0.057
28																0.009	0.000	-0.058
29																0.010	0.000	-0.059
30																0.010	0.000	-0.060
31																0.011	0.000	-0.060
32																0.012	0.000	-0.060
33																0.013	0.000	-0.059
34																0.014	0.000	-0.058
35																0.015	0.000	-0.056
36																0.017	0.000	-0.054
37																0.018	0.000	-0.052
38																0.019	0.000	-0.048
39																0.021	0.000	-0.045
40																0.022	0.000	-0.041
41																0.024	0.000	-0.036
42																0.026	0.000	-0.031
43																0.028	0.000	-0.025
44																0.030	0.000	-0.019
45																0.032	0.000	-0.012
46																0.035	0.000	-0.005
47																0.037	0.000	0.003

Table A3: Daily eddy covariance, energy balance component, and transpiration model results at BLK009 in 2001.

DOY	LE	H	Rn	G	Ta	e	Ts	θ	wind speed	λE_{uncorr}	res	LE_{corr}	H_{corr}	β	λE_{corr}	T_{Kc}	T_{GB}	EC Fourier
	Wm^{-2}	Wm^{-2}	Wm^{-2}	Wm^{-2}	°C	kPa	°C	m^3m^{-3}	$m\ s^{-1}$	$mm\ day^{-1}$	Wm^{-2}	Wm^{-2}	Wm^{-2}		$mm\ day^{-1}$	$mm\ day^{-1}$	$mm\ day^{-1}$	$mm\ day^{-1}$
48																0.040	0.000	0.012
49																0.043	0.000	0.021
50																0.046	0.000	0.031
51																0.049	0.000	0.041
52																0.053	0.000	0.052
53																0.057	0.000	0.064
54																0.061	0.000	0.076
55																0.065	0.000	0.089
56																0.069	0.000	0.102
57																0.074	0.000	0.116
58																0.079	0.001	0.131
59																0.085	0.001	0.146
60																0.090	0.001	0.162
61																0.096	0.002	0.179
62																0.103	0.002	0.196
63																0.109	0.002	0.214
64																0.116	0.003	0.233
65																0.124	0.004	0.252
66																0.132	0.004	0.272
67																0.140	0.005	0.292
68																0.149	0.006	0.313
69																0.158	0.008	0.335
70																0.168	0.009	0.358
71																0.178	0.011	0.381
72																0.189	0.012	0.404
73																0.200	0.014	0.428
74																0.212	0.017	0.453
75																0.225	0.019	0.479
76																0.238	0.022	0.505
77																0.251	0.025	0.531
78																0.266	0.028	0.558
79																0.281	0.032	0.586
80																0.296	0.036	0.615
81																0.313	0.040	0.643
82																0.330	0.045	0.673
83																0.348	0.050	0.703
84																0.367	0.055	0.733
85																0.386	0.061	0.764
86																0.406	0.068	0.796
87																0.428	0.075	0.828
88																0.450	0.083	0.860
89																0.472	0.091	0.893
90																0.496	0.100	0.927
91																0.521	0.109	0.960
92																0.547	0.119	0.995
93																0.573	0.130	1.029
94																0.601	0.142	1.064

Table A3: Daily eddy covariance, energy balance component, and transpiration model results at BLK009 in 2001.

DOY	LE	H	Rn	G	Ta	e	Ts	θ	wind speed	λE_{uncorr}	res	LE_{corr}	H_{corr}	β	λE_{corr}	T_{Kc}	T_{GB}	EC Fourier
	Wm^{-2}	Wm^{-2}	Wm^{-2}	Wm^{-2}	°C	kPa	°C	m^3m^{-3}	$m\ s^{-1}$	mm day^{-1}	Wm^{-2}	Wm^{-2}	Wm^{-2}		mm day^{-1}	mm day^{-1}	mm day^{-1}	mm day^{-1}
95																0.629	0.155	1.100
96																0.659	0.168	1.135
97																0.690	0.183	1.171
98																0.721	0.198	1.208
99																0.754	0.214	1.244
100																0.788	0.232	1.281
101	14.18	109.21			12.05	0.3			3.55	0.502				7.70		0.823	0.250	1.319
102	13.03	93.42			8.98	0.34			2.07	0.461				7.17		0.859	0.270	1.356
103	16.1	99.4			10.34	0.38			2.01	0.570				6.17		0.896	0.290	1.394
104	15.23	84.67			12.03	0.29			2.65	0.539				5.56		0.934	0.312	1.432
105	19.19	92.45			13.35	0.34			2.04	0.679				4.82		0.974	0.335	1.470
106	21.93	88.96			15.29	0.33			2.5	0.776				4.06		1.014	0.360	1.508
107	22.98	81.39			16.57	0.26			2.13	0.813				3.54		1.056	0.386	1.546
108	23.47	82.38			15.92	0.27			3.15	0.830				3.51		1.099	0.413	1.585
109	19.05	68.78			13.88	0.35			2.87	0.674				3.61		1.143	0.441	1.623
110	16.47	81.21			9.88	0.34			2.54	0.583				4.93		1.188	0.471	1.662
111	41.32	56.62			8.72	0.54			4.27	1.462				1.37		1.235	0.503	1.701
112	20.93	93.12			11.68	0.41			1.84	0.741				4.45		1.282	0.536	1.740
113	22.68	106.81			13.46	0.48			1.49	0.802				4.71		1.331	0.571	1.779
114	23.02	97.48			15.98	0.55			1.27	0.814				4.24		1.381	0.607	1.817
115	27.31	91.15			18.13	0.53			1.77	0.966				3.34		1.431	0.645	1.856
116	27.72	78.29			18.91	0.53			1.93	0.981				2.82		1.484	0.684	1.895
117	29.8	87.39			19.42	0.56			2.17	1.054				2.93		1.537	0.726	1.934
118	32.08	105.87			18.59	0.44			2.56	1.135				3.30		1.591	0.769	1.972
119	29.88	84.07			18.27	0.36			2.17	1.057				2.81		1.646	0.813	2.011
120	32.68	91.14			19.52	0.49			2.05	1.156				2.79		1.703	0.860	2.049
121	35.67	71.33			22.26	0.44			2.23	1.262				2.00		1.760	0.908	2.087
122	21.39	92.57			13.3	0.26			5.03	0.757				4.33		1.819	0.958	2.125
123	19.18	89.11			12.09	0.23			3.4	0.679				4.65		1.878	1.010	2.163
124	24.88	94.26			14.94	0.25			2.02	0.880				3.79		1.939	1.064	2.200
125	30.54	93.84			18.07	0.37			1.69	1.081				3.07		2.000	1.119	2.238
126	35.86	89.88			19.28	0.38			1.91	1.269				2.51		2.062	1.176	2.275
127	38.59	84.11			22.19	0.5			1.72	1.365				2.18		2.126	1.235	2.312
128	40.83	69.82			24.01	0.56			2.39	1.445				1.71		2.190	1.296	2.348
129	43.84	78.66			23.3	0.51			2.14	1.551				1.79		2.255	1.358	2.384
130	43.22	80.42			23.91	0.55			2.12	1.529				1.86		2.320	1.422	2.420
131	43.89	73.68			23.73	0.5			2.39	1.553				1.68		2.387	1.488	2.455
132	28.44	21.76			17.43	0.78			16640	1.006				0.77		2.454	1.556	2.490
133	47.82	67.17			17.37	0.82			8321	1.692				1.41		2.521	1.625	2.525
134	45.41	85.71			20.22	0.66			2.43	1.607				1.89		2.589	1.696	2.559
135	42.38	64.3			22.64	0.68			1.85	1.499				1.52		2.658	1.768	2.593
136	35.9	66.77			22.61	0.92			1.73	1.270				1.86		2.727	1.842	2.626
137	45	83.11			22.41	0.69			2.1	1.592				1.85		2.797	1.917	2.658
138	37.31	50			21.31	0.67			2.34	1.320				1.34		2.867	1.993	2.691
139	43.18	82.9			22.27	0.58			1.84	1.528				1.92		2.937	2.071	2.722
140	45.19	64.05			24.82	0.45			2.99	1.599				1.42		3.008	2.149	2.753
141	43.61	80.1			24.63	0.56			2.21	1.543				1.84		3.079	2.229	2.784

Table A3: Daily eddy covariance, energy balance component, and transpiration model results at BLK009 in 2001.

DOY	LE	H	Rn	G	Ta	e	Ts	θ	wind speed	λE_{uncorr}	res	LE_{corr}	H_{corr}	β	λE_{corr}	T_{Kc}	T_{GB}	EC Fourier
	Wm^{-2}	Wm^{-2}	Wm^{-2}	Wm^{-2}	°C	kPa	°C	m^3m^{-3}	$m\ s^{-1}$	$mm\ day^{-1}$	Wm^{-2}	Wm^{-2}	Wm^{-2}		$mm\ day^{-1}$	$mm\ day^{-1}$	$mm\ day^{-1}$	$mm\ day^{-1}$
142	51.36	80.69			24.26	0.55			1.89	1.817				1.57		3.150	2.310	2.814
143	54.38	72.49			25.65	0.67			2.14	1.924				1.33		3.220	2.392	2.843
144	56.25	82.57			26.84	0.71			2.03	1.990				1.47		3.291	2.474	2.872
145	55.88	74.15			26.65	0.69			2.52	1.977				1.33		3.362	2.558	2.900
146	51.14	81.21			24.57	0.61			2.33	1.809				1.59		3.432	2.641	2.927
147	50.37	72.31			24.58	0.55			2.36	1.782				1.44		3.503	2.726	2.954
148	45.56	79.46			24.15	0.53			1.97	1.612				1.74		3.573	2.810	2.980
149	54.54	79.54			24.25	0.51			2.04	1.930				1.46		3.642	2.895	3.005
150	54.3	70.13			26.54	0.54			1.97	1.921				1.29		3.711	2.980	3.030
151	57.97	79.98			27.3	0.6			1.79	2.051				1.38		3.780	3.064	3.053
152	54.78	47.2			27.77	0.63			3.4	1.938				0.86		3.848	3.149	3.077
153	50.37	31.11			25.24	0.36			2.95	1.782				0.62		3.915	3.233	3.099
154	55.12	78.78			21.93	0.33			2.69	1.950				1.43		3.981	3.317	3.120
155	46.43	86			20.75	0.34			3.02	1.643				1.85		4.047	3.400	3.141
156	52.59	90.81			23.22	0.59			1.89	1.861				1.73		4.111	3.482	3.161
157	52.55	72.93			25.75	0.63			1.92	1.859				1.39		4.175	3.563	3.180
158	60.4	77.01			27.2	0.58			2.27	2.137				1.28		4.237	3.644	3.199
159	59.45	66.07			26.72	0.42			2.71	2.103				1.11		4.299	3.722	3.216
160	61.67	69.74			26.13	0.44			2.51	2.182				1.13		4.359	3.800	3.233
161	59.68	71.47			25.81	0.49			2.1	2.112				1.20		4.417	3.876	3.249
162	53.44	71.05			24.58	0.48			2.15	1.891				1.33		4.474	3.950	3.264
163	45.32	75.47			23.35	0.5			2.5	1.603				1.67		4.530	4.023	3.278
164	37.78	78.72			20.15	0.28			3.86	1.337				2.08		4.584	4.093	3.292
165	49.61	91.7			20.76	0.37			2.2	1.755				1.85		4.637	4.162	3.304
166	52.74	82.18			23.13	0.48			2.53	1.866				1.56		4.687	4.228	3.316
167	59.29	74.2			25.52	0.51			2.31	2.098				1.25		4.736	4.291	3.326
168	61.51	78.62			26.71	0.53			1.99	2.176				1.28		4.783	4.352	3.336
169	60.99	71.4			26.79	0.45			2.27	2.158				1.17		4.828	4.411	3.345
170	62.43	70.05			27.29	0.5			2.15	2.209				1.12		4.871	4.466	3.353
171	60.49	65.13			26.52	0.45			2.03	2.140				1.08		4.912	4.519	3.360
172	64.57	78.64			43.22	1.71			2.04	2.285				1.22		4.951	4.568	3.367
173	55.61	70.99			27.59	0.78			2.23	1.968				1.28		4.988	4.614	3.372
174	60.79	80.22			27.83	0.77			2.29	2.151				1.32		5.023	4.657	3.377
175	57.33	66.43			26.3	0.59			2.25	2.028				1.16		5.055	4.697	3.380
176	56.29	75.17			24.33	0.44			2.91	1.992				1.34		5.085	4.733	3.383
177	47.93	68.57			25.29	0.61			2.91	1.696				1.43		5.112	4.766	3.385
178	56.77	71.59			26.11	0.63			3.35	2.009				1.26		5.137	4.795	3.386
179	54.71	76.09			25.11	0.6			2.45	1.936				1.39		5.160	4.820	3.386
180	57.18	61.54			26.61	0.65			2.1	2.023				1.08		5.180	4.841	3.385
181																5.197	4.859	3.383
182																5.212	4.873	3.381
183																5.225	4.883	3.377
184																5.235	4.889	3.373
185																5.242	4.891	3.368
186																5.246	4.889	3.362
187																5.248	4.883	3.355
188																5.247	4.874	3.348

Table A3: Daily eddy covariance, energy balance component, and transpiration model results at BLK009 in 2001.

DOY	LE	H	Rn	G	Ta	e	Ts	θ	wind speed	λE_{uncorr}	res	LE_{corr}	H_{corr}	β	λE_{corr}	T_{Kc}	T_{GB}	EC Fourier
	Wm^{-2}	Wm^{-2}	Wm^{-2}	Wm^{-2}	°C	kPa	°C	m^3m^{-3}	$m\ s^{-1}$	mm day^{-1}	Wm^{-2}	Wm^{-2}	Wm^{-2}		mm day^{-1}	mm day^{-1}	mm day^{-1}	mm day^{-1}
189																5.244	4.860	3.339
190																5.238	4.843	3.330
191																5.229	4.821	3.320
192																5.217	4.796	3.309
193																5.203	4.767	3.298
194																5.186	4.735	3.286
195																5.167	4.699	3.273
196																5.145	4.659	3.259
197																5.121	4.616	3.244
198																5.094	4.570	3.229
199																5.064	4.521	3.213
200																5.033	4.468	3.196
201																4.998	4.412	3.179
202																4.962	4.354	3.161
203																4.923	4.293	3.143
204																4.882	4.229	3.123
205																4.839	4.163	3.104
206																4.793	4.094	3.083
207			160.58	4.75				0.078								4.746	4.023	3.062
208			184.66	6.55				0.077								4.696	3.951	3.041
209			181.97	6.19				0.077								4.645	3.876	3.019
210			180.28	5.79				0.077								4.592	3.799	2.996
211			172.05	4.95				0.077								4.537	3.721	2.973
212			178.15	6.58				0.076								4.480	3.642	2.949
213			185.62	5.88				0.077								4.421	3.561	2.925
214			182.8	6.06	28.92	0.78		0.076	2.93					-1.92		4.361	3.479	2.901
215	50.96	67.74	181.44	5.83	27.53	0.73		0.076	2.9	1.803		75.39		1.33	2.667	4.300	3.396	2.876
216	53.53	77.49	178.9	4.9	25.15	0.46		0.077	1.52	1.894		71.09		1.45	2.515	4.237	3.313	2.851
217	51.09	71.27	181.65	4.3	24.69	0.42		0.077	2.4	1.808		74.05		1.40	2.620	4.173	3.228	2.825
218	50.04	84.17	189.44	6.33	26.69	0.66		0.076	2.03	1.770		68.27		1.68	2.416	4.108	3.143	2.799
219			178.63	6.81	22.8	0.91		0.076	1.49			65.85		1.61	2.330	4.041	3.058	2.772
220			133.17	5.11				0.076								3.974	2.973	2.745
221			139.35	5.72				0.076								3.905	2.887	2.718
222			158.17	5.53				0.076								3.836	2.802	2.691
223			176.08	6.32				0.076								3.766	2.716	2.663
224			164.58	5.07				0.076								3.695	2.631	2.635
225			180.88	4.81				0.076								3.624	2.547	2.607
226			174.1	5.11				0.076								3.551	2.463	2.578
227			162.38	5.19				0.076								3.479	2.379	2.549
228			173.99	5.09	32.5	0.59		0.076	2.27			65.65		1.57	2.323	3.406	2.297	2.521
229	47.17	60.13	161.66	5.2	28.07	0.69		0.076	1.63	1.669		68.78		1.28	2.434	3.333	2.215	2.492
230	47.82	53.95	161.73	5.23	29.01	0.65		0.076	2.56	1.692		73.54		1.13	2.602	3.259	2.134	2.462
231	43.11	44.98	142.04	4.99	28.22	0.65		0.076	2.28	1.525		67.07		1.04	2.373	3.186	2.055	2.433
232	42.81	68.98	173.11	3.65	26.09	0.55		0.076	2.72	1.515		64.89		1.61	2.296	3.112	1.976	2.403
233	38.11	62.16	155.62	3.58	23.72	0.43		0.076	1.62	1.348		57.79		1.63	2.045	3.039	1.899	2.374
234	37.1	59.46	157.41	2.94	23.6	0.52		0.077	2.42	1.313		59.35		1.60	2.100	2.965	1.823	2.344
235	40	62.58	161.42	3.46	23.67	0.49		0.077	2.4	1.415		61.59		1.56	2.179	2.892	1.749	2.314

Table A3: Daily eddy covariance, energy balance component, and transpiration model results at BLK009 in 2001.

DOY	LE	H	Rn	G	Ta	e	Ts	θ	wind speed	λE_{uncorr}	res	LE_{corr}	H_{corr}	β	λE_{corr}	T_{Kc}	T_{GB}	EC Fourier
	Wm^{-2}	Wm^{-2}	Wm^{-2}	Wm^{-2}	°C	kPa	°C	m^3m^{-3}	$m\ s^{-1}$	mm day^{-1}	Wm^{-2}	Wm^{-2}	Wm^{-2}		mm day^{-1}	mm day^{-1}	mm day^{-1}	mm day^{-1}
236	40.24	66.96	164.59	3.8	23.77	0.52		0.077	1.69	1.424		60.36		1.66	2.135	2.819	1.676	2.285
237	45.3	59.49	161.39	4.23	25.49	0.49		0.076	2.17	1.603		67.94		1.31	2.404	2.746	1.605	2.255
238	44.73	63.03	164.9	4.91	26.44	0.61		0.076	2.12	1.583		66.41		1.41	2.350	2.674	1.535	2.225
239	43.74	57.39	155.97	5.44	27.82	0.68		0.076	1.84	1.548		65.11		1.31	2.304	2.602	1.467	2.195
240	43.86	45.74	154.33	5.33	28.45	0.61		0.076	2.09	1.552		72.94		1.04	2.581	2.531	1.400	2.165
241	36.57	47.03	135.33	3.35	26.3	0.69		0.076	2.42	1.294		57.73		1.29	2.043	2.460	1.335	2.135
242	36.34	63.85	161.65	2.94	24.14	0.65		0.077	2.49	1.286		57.57		1.76	2.037	2.390	1.272	2.106
243	36.51	61.9	158.78	2.87	23.45	0.59		0.077	2.25	1.292		57.84		1.70	2.047	2.321	1.211	2.076
244	37.13	65.74	161.45	2.94	23.26	0.59		0.077	2.2	1.314		57.21		1.77	2.024	2.252	1.152	2.046
245	34.98	61.25	154.43	4.05	24.88	0.84		0.077	2.11	1.238		54.66		1.75	1.934	2.184	1.094	2.017
246	29.77	49.59	122.81	2.93	24.7	1.02		0.077	1.8	1.053		44.97		1.67	1.591	2.117	1.038	1.987
247	33.05	69.92	157.86	3.51	23.7	1.01		0.077	1.61	1.169		49.54		2.12	1.753	2.051	0.984	1.958
248	36.07	61.08	151.65	3.81	24.99	0.8		0.077	2.04	1.276		54.89		1.69	1.942	1.986	0.932	1.929
249	33.41	47.68	141.49	2.18	23.21	0.4		0.077	2.35	1.182		57.40		1.43	2.031	1.922	0.882	1.900
250	34.79	54.97	146.02	2.49	22.27	0.37		0.077	1.9	1.231		55.63		1.58	1.968	1.858	0.834	1.871
251	33.3	61.23	149.66	1.99	22.22	0.43		0.078	1.69	1.178		52.02		1.84	1.840	1.796	0.787	1.842
252	34.25	55.58	148.96	1.6	21.36	0.38		0.078	2.5	1.212		56.18		1.62	1.988	1.735	0.742	1.814
253	29.88	61.2	152.25	1.92	21.56	0.54		0.078	2.45	1.057		49.32		2.05	1.745	1.675	0.699	1.785
254	29.73	50.53	131.21	2.46	23.19	0.55		0.077	3.08	1.052		47.69		1.70	1.687	1.617	0.658	1.757
255	31.07	48.21	133.49	2.02	22.04	0.44		0.078	2.46	1.099		51.52		1.55	1.823	1.559	0.618	1.729
256	27.96	54.28	141.33	1.86	20.59	0.52		0.078	2.29	0.989		47.42		1.94	1.678	1.502	0.580	1.701
257	31.71	56.47	142.81	1.78	20.83	0.46		0.078	2.16	1.122		50.72		1.78	1.794	1.447	0.544	1.674
258	31.19	53.64	141.17	1.57	21.05	0.42		0.078	2	1.104		51.33		1.72	1.816	1.393	0.510	1.647
259	30.16	50.59	136.32	2.22	21.7	0.51		0.078	2.06	1.067		50.09		1.68	1.772	1.341	0.477	1.620
260	26	55.48	139.6	2.75	21.08	0.66		0.078	1.55	0.920		43.67		2.13	1.545	1.289	0.445	1.593
261	29.97	47.46	133.41	2.47	22.51	0.59		0.078	2.18	1.060		50.68		1.58	1.793	1.239	0.415	1.566
262	30.93	50.64	134.13	1.96	21.71	0.55		0.078	1.99	1.094		50.12		1.64	1.773	1.190	0.387	1.540
263	29.37	49.77	136.14	2.3	22.03	0.61		0.078	2.08	1.039		49.67		1.70	1.757	1.142	0.360	1.514
264	31.6	51.68	135.33	2.14	22.13	0.56		0.078	1.66	1.118		50.54		1.64	1.788	1.096	0.335	1.489
265	31.65	46.78	130.7	1.6	21.51	0.49		0.078	1.97	1.120		52.10		1.48	1.843	1.051	0.310	1.463
266	29.7	40.76	121.97	0.93	20.57	0.45		0.079	2.03	1.051		51.02		1.37	1.805	1.007	0.288	1.438
267	29.64	33.62	124.29	2.23	22.82	0.47		0.078	2.74	1.049		57.19		1.13	2.023	0.964	0.266	1.414
268	34	38.64	123.35	4.08	26.96	0.47		0.077	3.26	1.203		55.83		1.14	1.975	0.923	0.246	1.389
269	26.73	47.05	127.5	1.08	20.52	0.48		0.079	2.21	0.946		45.80		1.76	1.620	0.883	0.227	1.365
270	27.84	39.19	125.38	1.46	22.01	0.51		0.079	2.68	0.985		51.47		1.41	1.821	0.844	0.209	1.341
271	27.29	42.94	123.06	0.96	21.06	0.44		0.079	2.09	0.966		47.45		1.57	1.679	0.806	0.192	1.318
272	22.75	47.5	122.9	1.41	20.41	0.5		0.079	1.73	0.805		39.34		2.09	1.392	0.770	0.176	1.295
273	26.77	44.13	124	1.67	21.04	0.49		0.079	1.98	0.947		46.19		1.65	1.634	0.735	0.161	1.272
274	23.81	31.64	102.94	1.58	22.67	0.53		0.079	2.05	0.842		43.52		1.33	1.540	0.701	0.147	1.249
275	23.02	33.06	119.52	2	22.42	0.51		0.078	1.8	0.814		48.24		1.44	1.707	0.668	0.134	1.227
276	21.8	38.62	118.08	1.62	21.77	0.49		0.079	1.85	0.771		42.02		1.77	1.487	0.636	0.122	1.205
277	26.3	38.6	113.84	1.83	21.94	0.56		0.079	1.81	0.931		45.39		1.47	1.606	0.606	0.111	1.184
278	22.84	33.37	103.15	1.12	20.58	0.56		0.079	2.48	0.808		41.46		1.46	1.467	0.577	0.100	1.163
279	16.97	55.36	113.8	-1.17	15.3	0.58		0.08	1.45	0.600		26.97		3.26	0.954	0.548	0.091	1.142
280	18.08	51.35	110.15	-0.81	16.13	0.6		0.08	1.64	0.640		28.89		2.84	1.022	0.521	0.082	1.121
281	16.61	45.25	98.97	-1.19	15.53	0.58		0.081	1.18	0.588		26.89		2.72	0.952	0.495	0.073	1.101
282	15.64	30.46	100.7	-1.27	16.55	0.36		0.081	2.31	0.553		34.59		1.95	1.224	0.470	0.066	1.081

Table A3: Daily eddy covariance, energy balance component, and transpiration model results at BLK009 in 2001.

DOY	LE	H	Rn	G	Ta	e	Ts	θ	wind speed	λE_{uncorr}	res	LE_{corr}	H_{corr}	β	λE_{corr}	T_{Kc}	T_{GB}	EC Fourier
	Wm^{-2}	Wm^{-2}	Wm^{-2}	Wm^{-2}	°C	kPa	°C	m^3m^{-3}	$m\ s^{-1}$	$mm\ day^{-1}$	Wm^{-2}	Wm^{-2}	Wm^{-2}		$mm\ day^{-1}$	$mm\ day^{-1}$	$mm\ day^{-1}$	$mm\ day^{-1}$
283	15.78	40.75	98.5	-2.18	13.14	0.3		0.082	1.79	0.558		28.10		2.58	0.994	0.446	0.059	1.062
284	14.08	20.03	72.01	-1.8	15.3	0.41		0.082	1.9	0.498		30.47		1.42	1.078	0.423	0.052	1.042
285	15.21	33.41	101.17	0.29	17.84	0.47		0.081	3.36	0.538		31.56		2.20	1.117	0.401	0.046	1.024
286	21.13	30.23	99.29	-0.66	18.17	0.35		0.082	2.19	0.748		41.12		1.43	1.455	0.379	0.041	1.005
287	21.08	41.29	100.61	0.49	17.68	0.39		0.081	1.66	0.746		33.84		1.96	1.197	0.359	0.036	0.987
288	18.69	32.01	95.82	-0.46	17.23	0.35		0.081	1.95	0.661		35.49		1.71	1.256	0.340	0.031	0.969
289	15.85	19.57	78.13	-0.73	16.81	0.36		0.081	1.98	0.561		35.29		1.24	1.249	0.321	0.027	0.951
290	16.61	32.26	93.06	-0.71	15.79	0.38		0.082	1.78	0.588		31.87		1.94	1.128	0.304	0.023	0.934
291	15.6	35.41	94.56	-0.44	16.96	0.4		0.082	1.74	0.552		29.05		2.27	1.028	0.287	0.020	0.917
292	14.69	25.75	77.48	-1.13	15.87	0.42		0.082	1.63	0.520		28.56		1.75	1.010	0.271	0.017	0.900
293	16.99	24.71	81.97	-0.35	17.58	0.41		0.082	1.74	0.601		33.54		1.45	1.187	0.255	0.014	0.884
294	12.51	7.85	49.39	-0.01	17.63	0.46		0.081	1.77	0.443		30.35		0.63	1.074	0.241	0.011	0.867
295	13.95	36.91	94.61	-1.16	15.16	0.43		0.082	1.8	0.494		26.27		2.65	0.929	0.227	0.009	0.852
296	15.15	24.82	85.79	-0.61	16.93	0.44		0.082	2.35	0.536		32.75		1.64	1.159	0.214	0.007	0.836
297	14.83	32.16	84.43	-1.46	14.22	0.32		0.082	1.91	0.525		27.11		2.17	0.959	0.201	0.006	0.821
298	13.78	37.23	93.98	-2.38	12.72	0.32		0.083	1.62	0.488		26.03		2.70	0.921	0.189	0.005	0.806
299	13.52	38.72	95.98	-2.68	12.14	0.32		0.084	1.72	0.478		25.53		2.86	0.903	0.178	0.004	0.791
300	11.09	7.53	54.26	-1.33	14.87	0.42		0.083	1.99	0.392		33.11		0.68	1.171	0.167	0.003	0.776
301	11.6	32.6	89.01	-0.88	14.09	0.49		0.083	2.18	0.410		23.59		2.81	0.835	0.157	0.002	0.762
302	9.58	26.49	69.34	-2.11	12.78	0.49		0.083	1.51	0.339		18.98		2.77	0.671	0.147	0.002	0.748
303	4.32	-3.54	18.47	-1.12	13.48	0.74		0.083	2.24	0.153				-0.82		0.138	0.001	0.734
304	11.84	47.91	93.49	-2.97	9.98	0.56		0.084	1.18	0.419		19.11		4.05	0.676	0.129	0.000	0.720
305	9.01	38.17	84.85	-3.72	9.17	0.46		0.085	1.6	0.319		16.91		4.24	0.598	0.121	0.000	0.707
306	7.74	28.19	62.53	-3.32	9.11	0.49		0.085	1.43	0.274		14.19		3.64	0.502	0.114	0.000	0.694
307	9.67	37.35	83.32	-2.33	11.14	0.48		0.085	1.73	0.342		17.61		3.86	0.623	0.106	0.000	0.681
308	6.12	5.11	32.32	-1.82	11.82	0.52		0.084	1.84	0.217		18.61		0.84	0.658	0.100	0.000	0.668
309	7.96	18.94	47.36	-1.81	11.1	0.61		0.084	1.32	0.282		14.55		2.38	0.515	0.093	0.000	0.655
310	8	31.65	77.07	-2.3	12.49	0.65		0.085	1.96	0.283		16.01		3.96	0.567	0.087	0.000	0.643
311	9.25	23.17	71.29	-1.78	13.13	0.51		0.085	2.09	0.327		20.85		2.50	0.738	0.081	0.000	0.631
312	10.7	17.8	66.1	-2.03	13.09	0.36		0.085	2.5	0.379		25.58		1.66	0.905	0.076	0.000	0.619
313	6.24	38.76	72.78	-5.2	7.53	0.23		0.087	1.35	0.221		10.81		6.21	0.383	0.071	0.000	0.607
314	5.52	36.09	73.96	-4.04	8.06	0.32		0.087	1.7	0.195		10.35		6.54	0.366	0.066	0.000	0.595
315	4.47	28.7	70.64	-0.96	13.33	0.74		0.085	2.39	0.158		9.65		6.42	0.341	0.062	0.000	0.583
316	5.2	29.34	66.78	-2.45	9.93	0.8		0.086	2.74	0.184		10.42		5.64	0.369	0.058	0.000	0.572
317	12.26	35.32	75.39	-4.38	7.59	0.44		0.087	1.48	0.434		20.55		2.88	0.727	0.054	0.000	0.561
318	7.2	39.66	73.23	-3.57	8.77	0.47		0.087	1.23	0.255		11.80		5.50	0.418	0.050	0.000	0.550
319	6.83	39.22	73.55	-3.5	8.17	0.51		0.087	1.59	0.242		11.43		5.74	0.404	0.047	0.000	0.538
320	5.65	35.26	69.91	-2.9	8.74	0.56		0.087	1.52	0.200		10.06		6.24	0.356	0.043	0.000	0.528
321	5.97	28.22	59.89	-3.58	7.9	0.52		0.087	1.69	0.211		11.08		4.72	0.392	0.040	0.000	0.517
322	6.9	26.09	62.43	-4.1	7.44	0.34		0.088	1.75	0.244		13.92		3.78	0.492	0.038	0.000	0.506
323	6.07	31	62.34	-3.78	7.77	0.31		0.088	1.29	0.215		10.83		5.11	0.383	0.035	0.000	0.495
324	2.84	3.59	18.63	-3.58	6.34	0.35		0.087	1.38	0.100		9.81		1.26	0.347	0.032	0.000	0.485
325	6.7	27.78	63.83	-1.44	9.74	0.39		0.087	1.34	0.237		12.68		4.14	0.449	0.030	0.000	0.474
326	17.43	-5.78	27.92	-0.86	11.4	0.42		0.086	1.92	0.617		43.06		-0.33	1.523	0.028	0.000	0.464
327	6.48	10.79	50.6	-4.33	8.08	0.23		0.088	2.22	0.229		20.61		1.67	0.729	0.026	0.000	0.454
328	31.18	-47.52	-5.06	-5.48	6.42	0.54		0.155	13260	1.103		-0.80		-1.52	-0.028	0.024	0.000	0.443
329	14.43	13.75	45.86	-9.94	2.17	0.51		0.226	1.3	0.511		28.57		0.95	1.011	0.022	0.000	0.433

Table A3: Daily eddy covariance, energy balance component, and transpiration model results at BLK009 in 2001.

DOY	LE	H	Rn	G	Ta	e	Ts	θ	wind speed	λE_{uncorr}	res	LE_{corr}	H_{corr}	β	λE_{corr}	T_{Kc}	T_{GB}	EC Fourier
	Wm^{-2}	Wm^{-2}	Wm^{-2}	Wm^{-2}	°C	kPa	°C	m^3m^{-3}	$m\ s^{-1}$	$mm\ day^{-1}$	Wm^{-2}	Wm^{-2}	Wm^{-2}		$mm\ day^{-1}$	$mm\ day^{-1}$	$mm\ day^{-1}$	$mm\ day^{-1}$
330	17.53	13.85	51.97	-12.96	1.78	0.35		0.215	2.87	0.620		36.27		0.79	1.283	0.021	0.000	0.423
331	10.33	21.28	49.12	-12.62	-0.06	0.3		0.207	2.23	0.365		20.18		2.06	0.714	0.019	0.000	0.413
332																0.018	0.000	0.403
333																0.017	0.000	0.393
334																0.015	0.000	0.383
335																0.014	0.000	0.373
336																0.013	0.000	0.363
337																0.012	0.000	0.354
338																0.011	0.000	0.344
339																0.011	0.000	0.334
340																0.010	0.000	0.324
341																0.009	0.000	0.315
342																0.009	0.000	0.305
343																0.008	0.000	0.295
344																0.007	0.000	0.286
345																0.007	0.000	0.276
346																0.006	0.000	0.267
347																0.006	0.000	0.257
348																0.005	0.000	0.248
349																0.005	0.000	0.238
350																0.005	0.000	0.229
351																0.004	0.000	0.220
352																0.004	0.000	0.210
353																0.004	0.000	0.201
354																0.004	0.000	0.192
355																0.003	0.000	0.183
356																0.003	0.000	0.174
357																0.003	0.000	0.165
358																0.003	0.000	0.156
359																0.003	0.000	0.147
360																0.002	0.000	0.138
361																0.002	0.000	0.129
362																0.002	0.000	0.120
363																0.002	0.000	0.112
364																0.002	0.000	0.103
365																0.002	0.000	0.095

Table A4: Daily eddy covariance, energy balance component, and transpiration model results at PLC045 in 2001.

DOY	LE	H	Rn	G	Ta	e	Ts	θ	wind speed	λE_{uncorr}	res	LE_{corr}	H_{corr}	β	λE_{corr}	T_{Kc}	T_{GB}	EC Fourier
	Wm^{-2}	Wm^{-2}	Wm^{-2}	Wm^{-2}	°C	kPa	°C	m^3m^{-3}	$m\ s^{-1}$	mm day^{-1}	Wm^{-2}	Wm^{-2}	Wm^{-2}		mm day^{-1}	mm day^{-1}	mm day^{-1}	mm day^{-1}
1																0.001	0.000	0.120
2																0.001	0.000	0.120
3																0.001	0.000	0.120
4																0.001	0.000	0.119
5																0.001	0.000	0.119
6																0.001	0.000	0.119
7																0.002	0.000	0.119
8																0.002	0.000	0.119
9																0.002	0.000	0.119
10																0.002	0.000	0.119
11																0.002	0.000	0.119
12																0.002	0.000	0.119
13																0.002	0.000	0.119
14																0.003	0.000	0.119
15																0.003	0.000	0.120
16																0.003	0.000	0.120
17																0.003	0.000	0.120
18																0.004	0.000	0.121
19																0.004	0.000	0.121
20																0.004	0.000	0.122
21																0.005	0.000	0.122
22																0.005	0.000	0.123
23																0.005	0.000	0.124
24																0.006	0.000	0.125
25																0.006	0.000	0.126
26																0.007	0.000	0.127
27																0.007	0.000	0.128
28																0.008	0.000	0.129
29																0.008	0.000	0.131
30																0.009	0.000	0.132
31																0.010	0.000	0.134
32																0.010	0.000	0.135
33																0.011	0.000	0.137
34																0.012	0.000	0.139
35																0.013	0.000	0.141
36																0.014	0.000	0.143
37																0.015	0.000	0.146
38																0.016	0.000	0.148
39																0.017	0.000	0.151
40																0.019	0.000	0.154
41																0.020	0.000	0.157
42																0.021	0.000	0.160
43																0.023	0.000	0.163
44																0.025	0.000	0.167
45																0.026	0.000	0.170
46																0.028	0.000	0.174
47																0.030	0.000	0.178

Table A4: Daily eddy covariance, energy balance component, and transpiration model results at PLC045 in 2001.

DOY	LE	H	Rn	G	Ta	e	Ts	θ	wind speed	λE_{uncorr}	res	LE_{corr}	H_{corr}	β	λE_{corr}	T_{Kc}	T_{GB}	EC Fourier
	Wm^{-2}	Wm^{-2}	Wm^{-2}	Wm^{-2}	°C	kPa	°C	m^3m^{-3}	$m\ s^{-1}$	$mm\ day^{-1}$	Wm^{-2}	Wm^{-2}	Wm^{-2}		$mm\ day^{-1}$	$mm\ day^{-1}$	$mm\ day^{-1}$	$mm\ day^{-1}$
48																0.032	0.000	0.182
49																0.035	0.000	0.186
50																0.037	0.000	0.191
51																0.039	0.000	0.195
52																0.042	0.000	0.200
53																0.045	0.000	0.205
54																0.048	0.000	0.210
55																0.051	0.000	0.216
56																0.054	0.000	0.221
57																0.058	0.000	0.227
58																0.061	0.000	0.233
59																0.065	0.000	0.239
60																0.069	0.000	0.245
61																0.074	0.001	0.252
62																0.078	0.001	0.258
63																0.083	0.001	0.265
64																0.088	0.002	0.272
65																0.093	0.002	0.280
66																0.099	0.003	0.287
67																0.105	0.003	0.295
68																0.111	0.004	0.302
69																0.117	0.004	0.310
70																0.124	0.005	0.318
71																0.131	0.006	0.327
72																0.138	0.007	0.335
73																0.146	0.008	0.344
74																0.154	0.009	0.353
75																0.162	0.010	0.362
76																0.171	0.012	0.371
77																0.180	0.013	0.381
78																0.190	0.015	0.390
79																0.199	0.016	0.400
80																0.210	0.018	0.410
81																0.220	0.021	0.420
82																0.231	0.023	0.430
83																0.243	0.025	0.440
84																0.255	0.028	0.451
85																0.267	0.031	0.461
86																0.280	0.034	0.472
87																0.293	0.038	0.483
88																0.307	0.042	0.494
89																0.321	0.046	0.505
90																0.336	0.050	0.516
91																0.351	0.055	0.527
92																0.367	0.060	0.539
93																0.383	0.065	0.550
94																0.399	0.071	0.562

Table A4: Daily eddy covariance, energy balance component, and transpiration model results at PLC045 in 2001.

DOY	LE	H	Rn	G	Ta	e	Ts	θ	wind speed	λE_{uncorr}	res	LE_{corr}	H_{corr}	β	λE_{corr}	T_{Kc}	T_{GB}	EC Fourier
	Wm^{-2}	Wm^{-2}	Wm^{-2}	Wm^{-2}	°C	kPa	°C	m^3m^{-3}	$m\ s^{-1}$	mm day^{-1}	Wm^{-2}	Wm^{-2}	Wm^{-2}		mm day^{-1}	mm day^{-1}	mm day^{-1}	mm day^{-1}
95																0.417	0.077	0.573
96																0.434	0.084	0.585
97																0.452	0.091	0.597
98																0.471	0.099	0.609
99																0.490	0.107	0.621
100	9.99	49.82			9.37	0.250			1.67	0.353				4.99		0.510	0.115	0.632
101	14.54	106.47			7.7	0.360			2.23	0.514				7.33		0.530	0.124	0.644
102	13.61	91.78			8.84	0.320			1.85	0.482				6.74		0.551	0.134	0.657
103	14.46	84.38			9.77	0.340			2.07	0.512				5.84		0.572	0.144	0.669
104	14.65	91.95			11.03	0.270			2.28	0.518				6.28		0.594	0.155	0.681
105	16.67	86.88			13.27	0.320			1.93	0.590				5.21		0.616	0.166	0.693
106	17.66	92.88			14.49	0.310			2.02	0.625				5.26		0.639	0.178	0.705
107	19.24	88.73			15.53	0.210			1.93	0.681				4.61		0.662	0.191	0.717
108	15.01	101.48			13.3	0.230			2.31	0.531				6.76		0.686	0.204	0.729
109	12.54	77.1			11.1	0.360			2.26	0.444				6.15		0.710	0.218	0.741
110	10.78	82.85			9.68	0.310			2.20	0.381				7.68		0.734	0.233	0.753
111	7.94	50.56			7.33	0.500			3.76	0.281				6.37		0.760	0.248	0.765
112	12.77	104.3			11.28	0.410			1.38	0.452				8.17		0.785	0.265	0.777
113	15.23	101.96			13.87	0.470			1.53	0.539				6.70		0.811	0.282	0.789
114	19.76	101.37			16.54	0.520			1.61	0.699				5.13		0.838	0.299	0.801
115	18.8	96.6			17.89	0.510			1.56	0.665				5.14		0.865	0.318	0.813
116	19	81.68			18.52	0.510			1.62	0.672				4.30		0.892	0.337	0.824
117	19.27	97.24			17.94	0.510			1.55	0.682				5.05		0.920	0.358	0.836
118	19.38	100.77			16.8	0.380			2.13	0.686				5.20		0.948	0.379	0.848
119	18.27	98.56			17.62	0.340			1.57	0.646				5.40		0.976	0.401	0.859
120	20.41	99.64			18.83	0.460			1.56	0.722				4.88		1.005	0.423	0.870
121	23.81	82			20.63	0.390			1.80	0.842				3.44		1.034	0.447	0.882
122	12.11	116.33			12.65	0.230			4.73	0.428				9.61		1.063	0.472	0.893
123	12.35	120.7			10.76	0.230			2.82	0.437				9.77		1.093	0.497	0.904
124	17.79	101.78			15.47	0.240			1.88	0.629				5.72		1.123	0.523	0.915
125	18.31	94.42			17.75	0.340			1.17	0.648				5.16		1.153	0.550	0.926
126	19.79	101.15			18.78	0.390			1.45	0.700				5.11		1.184	0.578	0.936
127	20.33	97.34			21.11	0.520			1.20	0.719				4.79		1.214	0.607	0.947
128	22.63	77.55			21.98	0.540			1.43	0.801				3.43		1.245	0.637	0.957
129	22.84	94.08			22.27	0.470			1.51	0.808				4.12		1.276	0.668	0.967
130	22.05	97.95			22.7	0.520			1.27	0.780				4.44		1.307	0.699	0.977
131	23.4	103.35			22.25	0.470			1.90	0.828				4.42		1.338	0.731	0.987
132	9.32	38.71			15.04	0.830			37944	0.330				4.15		1.369	0.765	0.996
133	32.9	55.48			15.38	0.900			41784	1.164				1.69		1.400	0.799	1.005
134	31.06	99.79			19	0.580			1.65	1.099				3.21		1.432	0.833	1.015
135	23.32	83.34			22.36	0.710			1.36	0.825				3.57		1.463	0.869	1.023
136	20.92	72.59			21.67	0.880			1.25	0.740				3.47		1.494	0.905	1.032
137	23.29	103.17			21.27	0.630			1.45	0.824				4.43		1.525	0.942	1.041
138	17.01	81.07			20.77	0.610			1.92	0.602				4.77		1.556	0.979	1.049
139	23.27	108.33			21.39	0.510			1.35	0.823				4.66		1.587	1.017	1.057
140	21.2	94.86			23.57	0.430			2.43	0.750				4.47		1.617	1.056	1.065
141	21.4	101.61			24.39	0.490			1.74	0.757				4.75		1.647	1.095	1.072

Table A4: Daily eddy covariance, energy balance component, and transpiration model results at PLC045 in 2001.

DOY	LE	H	Rn	G	Ta	e	Ts	θ	wind speed	λE_{uncorr}	res	LE_{corr}	H_{corr}	β	λE_{corr}	T_{Kc}	T_{GB}	EC Fourier
	Wm^{-2}	Wm^{-2}	Wm^{-2}	Wm^{-2}	°C	kPa	°C	m^3m^{-3}	$m\ s^{-1}$	$mm\ day^{-1}$	Wm^{-2}	Wm^{-2}	Wm^{-2}		$mm\ day^{-1}$	$mm\ day^{-1}$	$mm\ day^{-1}$	$mm\ day^{-1}$
142	20.92	106.62			23.6	0.530			1.31	0.740				5.10		1.678	1.135	1.079
143	20.71	93.15			24.87	0.660			1.64	0.733				4.50		1.707	1.175	1.086
144	19.64	97.87			25.61	0.670			1.57	0.695				4.98		1.737	1.216	1.093
145	20.22	105.3			25.46	0.640			1.86	0.715				5.21		1.766	1.257	1.100
146	17.96	95.43			23.81	0.540			1.60	0.635				5.31		1.795	1.298	1.106
147	18.2	102.29			24.89	0.490			2.07	0.644				5.62		1.823	1.340	1.112
148	17.69	108.94			24.16	0.470			1.75	0.626				6.16		1.851	1.381	1.117
149	17.83	112.34			23.98	0.470			1.31	0.631				6.30		1.878	1.423	1.123
150	18.67	101.54			26.56	0.480			1.61	0.661				5.44		1.905	1.465	1.128
151	18.18	108.69			26.94	0.550			1.48	0.643				5.98		1.931	1.507	1.132
152	17.31	80.19			27.03	0.530			2.12	0.612				4.63		1.957	1.548	1.137
153	17.91	91.63			23.53	0.340			2.30	0.634				5.12		1.982	1.590	1.141
154	11.9	114.66			21.56	0.280			2.36	0.421				9.63		2.006	1.631	1.145
155	9.46	122.25			19.99	0.290			2.31	0.335				12.92		2.029	1.673	1.148
156	9.86	117.26			22.18	0.550			1.59	0.349				11.89		2.052	1.713	1.152
157	13.27	105.25			25.46	0.590			1.33	0.470				7.93		2.075	1.754	1.155
158	15.01	91.76			26.29	0.500			1.63	0.531				6.12		2.096	1.793	1.157
159	15.67	106.36			26.09	0.330			1.89	0.554				6.79		2.116	1.833	1.159
160	12.65	108.14			26.09	0.370			1.89	0.448				8.55		2.136	1.871	1.161
161	12.4	112.01			25.25	0.430			1.62	0.439				9.03		2.155	1.909	1.163
162	10.18	102.59			24.2	0.430			1.88	0.360				10.08		2.173	1.946	1.164
163	9.21	118.33			24.09	0.430			3.43	0.326				12.85		2.190	1.982	1.165
164	6.24	121.35			19.66	0.240			4.05	0.221				19.45		2.206	2.017	1.166
165	8.7	127.32			20.51	0.330			2.10	0.308				14.63		2.221	2.052	1.166
166	10.84	124.57			23.73	0.430			2.25	0.384				11.50		2.235	2.085	1.166
167	11.75	114.61			25.95	0.440			2.23	0.416				9.76		2.248	2.117	1.166
168	10.92	108.4			26	0.450			1.50	0.386				9.93		2.260	2.147	1.165
169	13.16	109.51			25.84	0.380			1.55	0.466				8.32		2.271	2.177	1.164
170	11.75	110.68			26.47	0.460			1.39	0.416				9.42		2.281	2.205	1.163
171	13.64	100.4			26.18	0.430			1.70	0.483				7.36		2.290	2.231	1.161
172	11.39	107.69			26.96	0.470			1.93	0.403				9.46		2.298	2.256	1.159
173	10.6	80.83			27.42	0.750			1.84	0.375				7.63		2.305	2.280	1.157
174	12.23	110.59			27.2	0.750			1.50	0.433				9.04		2.310	2.302	1.155
175	6.05	86.05			24.78	0.520			1.36	0.214				14.23		2.315	2.322	1.152
176	10.3	124.82			23.99	0.380			2.84	0.364				12.12		2.318	2.341	1.148
177	7.67	109.75			24.81	0.570			2.42	0.271				14.31		2.320	2.358	1.145
178	11.66	122.13			25.85	0.600			2.78	0.413				10.47		2.321	2.373	1.141
179	9.74	114.16			25.84	0.530			2.30	0.345				11.72		2.321	2.387	1.137
180	11.5	114.94			27.66	0.590			2.30	0.407				10.00		2.320	2.398	1.132
181	11.29	116.02			29.19	0.500			1.84	0.399				10.27		2.318	2.408	1.128
182	10.68	103.07			28.33	0.650			1.19	0.378				9.65		2.314	2.416	1.123
183	13.02	108.31			25.26	0.770			1.21	0.461				8.32		2.309	2.422	1.117
184																2.304	2.426	1.112
185																2.297	2.428	1.106
186																2.289	2.428	1.100
187																2.280	2.426	1.093
188																2.269	2.423	1.086

Table A4: Daily eddy covariance, energy balance component, and transpiration model results at PLC045 in 2001.

DOY	LE	H	Rn	G	Ta	e	Ts	θ	wind speed	λE_{uncorr}	res	LE_{corr}	H_{corr}	β	λE_{corr}	T_{Kc}	T_{GB}	EC Fourier
	Wm^{-2}	Wm^{-2}	Wm^{-2}	Wm^{-2}	°C	kPa	°C	m^3m^{-3}	$m\ s^{-1}$	mm day^{-1}	Wm^{-2}	Wm^{-2}	Wm^{-2}		mm day^{-1}	mm day^{-1}	mm day^{-1}	mm day^{-1}
189																2.258	2.417	1.079
190																2.246	2.410	1.072
191																2.232	2.400	1.065
192																2.218	2.389	1.057
193																2.202	2.376	1.049
194																2.186	2.361	1.041
195																2.169	2.345	1.032
196																2.150	2.326	1.023
197																2.131	2.306	1.015
198																2.111	2.285	1.005
199	23.69	147.78			28.89	0.660		-0.187	3.13	0.838				6.24		2.090	2.261	0.996
200	20.11	112.39	175.29	6.37	23.98	0.650		-0.069	2.08	0.712		25.64		5.59	0.907	2.068	2.236	0.987
201	20.5	112.1	173.21	5.78	23.84	0.590		0.070	2.28	0.725		25.88		5.47	0.916	2.046	2.210	0.977
202	18.89	111.14	171.63	6.58	23.83	0.570		0.065	1.68	0.668		23.98		5.89	0.848	2.022	2.182	0.967
203	22.23	106.23	169.51	6.84	24.8	0.540		0.062	2.14	0.787		28.15		4.78	0.996	1.998	2.153	0.957
204	22.67	102.21	164.4	7.77	25.06	0.520		0.060	1.42	0.802		28.43		4.51	1.006	1.973	2.123	0.947
205	22.1	104.68	164.55	6.72	24.56	0.470		0.060	1.83	0.782		27.51		4.74	0.973	1.948	2.091	0.936
206	21.41	89.1	160.5	6.85	25.51	0.420		0.060	1.57	0.758		29.77		4.16	1.053	1.922	2.058	0.926
207	18.4	83.35	138.76	6.88	25.88	0.630		0.060	1.28	0.651		23.85		4.53	0.844	1.895	2.024	0.915
208	21.17	96.65	164.53	7.78	27.15	0.660		0.061	1.82	0.749		28.16		4.57	0.997	1.868	1.989	0.904
209	22.28	88.23	158.47	8.38	27.04	0.520		0.061	1.18	0.788		30.26		3.96	1.071	1.840	1.953	0.893
210	20.97	93.29	156.69	7.7	26.47	0.470		0.062	1.36	0.742		27.34		4.45	0.967	1.811	1.916	0.882
211	17.58	96.53	157.83	6.08	25.05	0.480		0.062	1.56	0.622		23.38		5.49	0.827	1.782	1.878	0.871
212	17.79	101.6	161.87	5.87	25.81	0.650		0.063	2.60	0.629		23.25		5.71	0.822	1.753	1.839	0.859
213	16.77	102.05	164.51	6.37	26.98	0.670		0.063	2.97	0.593		22.32		6.09	0.790	1.723	1.800	0.848
214	16.45	99.32	161.13	6.95	28.11	0.690		0.062	2.87	0.582		21.91		6.04	0.775	1.693	1.760	0.836
215	16.55	103.95	163.15	6.37	27.72	0.700		0.063	2.76	0.586		21.53		6.28	0.762	1.663	1.720	0.825
216	16.05	90.11	150.98	5.37	25.33	0.490		0.063	1.08	0.568		22.01		5.62	0.779	1.632	1.679	0.813
217	16.57	100	159.32	3.74	24.97	0.390		0.064	2.56	0.586		22.12		6.04	0.782	1.601	1.638	0.801
218	13.18	96.8	151.9	5.37	26.75	0.600		0.063	1.95	0.466		17.56		7.34	0.621	1.570	1.597	0.789
219	13.13	93.17	154.19	7.92	28.47	0.890		0.062	1.63	0.465		18.07		7.10	0.639	1.539	1.555	0.777
220	18.89	69.05	114.84	4.94	26.62	1.040		0.064	1.47	0.668		23.61		3.66	0.835	1.507	1.513	0.765
221	13.2	68.94	108.27	4.08	26.02	1.040		0.064	1.22	0.467		16.74		5.22	0.592	1.475	1.471	0.753
222	15.91	93.52	153.35	5.29	27.71	0.840		0.063	1.62	0.563		21.53		5.88	0.762	1.444	1.429	0.741
223	14.61	98.18	158.92	6.6	28.49	0.620		0.063	1.65	0.517		19.73		6.72	0.698	1.412	1.387	0.729
224	13.77	96.1	153.76	6.8	28.09	0.620		0.063	1.64	0.487		18.42		6.98	0.652	1.380	1.345	0.717
225	12.34	100.7	155.73	4.94	25.64	0.670		0.064	1.44	0.437		16.46		8.16	0.582	1.348	1.304	0.705
226	12.9	95.54	155.55	4.91	26.67	0.630		0.064	1.83	0.456		17.92		7.41	0.634	1.316	1.262	0.693
227	12.14	78.92	129.26	4.45	26.31	0.620		0.064	1.36	0.430		16.64		6.50	0.589	1.285	1.221	0.681
228	12.65	98.15	155.47	5.15	26.56	0.570		0.064	1.74	0.448		17.16		7.76	0.607	1.253	1.180	0.669
229	11.98	87.86	143.89	6.55	27.43	0.600		0.064	1.31	0.424		16.48		7.34	0.583	1.222	1.140	0.657
230	12.76	81.93	141.02	6.71	27.93	0.590		0.064	1.44	0.451		18.10		6.42	0.640	1.190	1.100	0.645
231	11.53	79.64	129.67	4.93	27.07	0.560		0.064	1.63	0.408		15.78		6.91	0.558	1.159	1.060	0.633
232	11.22	72.75	128.66	4.16	25.56	0.540		0.065	1.83	0.397		16.64		6.48	0.589	1.128	1.021	0.621
233	11.84	88.15	137.49	3.54	23.33	0.440		0.065	1.11	0.419		15.86		7.45	0.561	1.098	0.983	0.609
234	9.46	90.86	139.49	2.06	22.73	0.490		0.066	2.17	0.335		12.96		9.61	0.459	1.067	0.945	0.597
235	10.32	83.93	142.47	3.72	23.77	0.430		0.066	2.34	0.365		15.19		8.13	0.538	1.037	0.908	0.586

Table A4: Daily eddy covariance, energy balance component, and transpiration model results at PLC045 in 2001.

DOY	LE	H	Rn	G	Ta	e	Ts	θ	wind speed	λE_{uncorr}	res	LE_{corr}	H_{corr}	β	λE_{corr}	T_{Kc}	T_{GB}	EC Fourier
	Wm^{-2}	Wm^{-2}	Wm^{-2}	Wm^{-2}	°C	kPa	°C	m^3m^{-3}	$m\ s^{-1}$	mm day^{-1}	Wm^{-2}	Wm^{-2}	Wm^{-2}		mm day^{-1}	mm day^{-1}	mm day^{-1}	mm day^{-1}
236	10.81	89.87	141.37	4.92	24.77	0.470		0.065	1.61	0.382		14.65		8.32	0.518	1.007	0.872	0.574
237	10.58	89.07	145.43	4.71	25.3	0.470		0.065	2.01	0.374		14.94		8.42	0.529	0.978	0.836	0.562
238	10.17	90.46	145.04	5.54	26.4	0.560		0.064	1.55	0.360		14.10		8.90	0.499	0.949	0.801	0.551
239	10.93	78.35	133.45	6.1	27.48	0.660		0.064	1.33	0.387		15.59		7.17	0.552	0.920	0.767	0.539
240	11.46	76.24	138.46	6.26	27.78	0.600		0.064	1.37	0.405		17.27		6.66	0.611	0.891	0.733	0.528
241	9.06	84.1	135.64	4.46	26.44	0.640		0.065	2.56	0.321		12.76		9.28	0.451	0.863	0.701	0.517
242	7.89	86.72	138.02	3.07	24.84	0.610		0.065	2.73	0.279		11.25		10.99	0.398	0.836	0.669	0.506
243	8.6	82.51	134.54	3.17	24.43	0.560		0.065	2.38	0.304		12.40		9.59	0.439	0.809	0.638	0.494
244	8.21	86.57	141.61	2.7	23.66	0.510		0.066	2.37	0.290		12.03		10.55	0.426	0.782	0.608	0.484
245	8.99	86.4	142.69	4.14	24.84	0.730		0.065	1.95	0.318		13.06		9.61	0.462	0.756	0.579	0.473
246	6.76	51.84	82.78	1.64	23.51	0.970		0.066	1.57	0.239		9.36		7.67	0.331	0.730	0.551	0.462
247	8.94	90.69	141.58	3.64	23.42	0.930		0.066	1.30	0.316		12.38		10.14	0.438	0.705	0.523	0.452
248	10.6	77.24	132.68	4.12	24.41	0.720		0.065	1.57	0.375		15.51		7.29	0.549	0.680	0.497	0.441
249	8.64	68.97	127.29	2.05	22.88	0.340		0.066	2.24	0.306		13.94		7.98	0.493	0.656	0.471	0.431
250	9.42	64.22	126.3	2.36	23.06	0.350		0.066	1.66	0.333		15.85		6.82	0.561	0.633	0.447	0.421
251	8.28	76.6	127.46	2.92	23.64	0.360		0.066	1.62	0.293		12.15		9.25	0.430	0.609	0.423	0.411
252	6.91	85.83	136.64	0.74	20.99	0.350		0.067	2.33	0.244		10.13		12.42	0.358	0.587	0.400	0.401
253	6.44	84.39	138.3	1.05	21.52	0.500		0.067	2.40	0.228		9.73		13.09	0.344	0.565	0.378	0.391
254	7.51	66.49	111.31	1.66	23.59	0.520		0.067	3.49	0.266		11.13		8.85	0.394	0.543	0.356	0.382
255	7.09	76.92	128.26	1.11	21.76	0.400		0.067	2.38	0.251		10.73		10.85	0.380	0.522	0.336	0.372
256	7.2	82.27	130.18	0.81	19.89	0.500		0.067	1.61	0.255		10.41		11.43	0.368	0.501	0.317	0.363
257	6.6	81.05	132.53	0.92	19.8	0.430		0.067	1.94	0.234		9.91		12.28	0.351	0.481	0.298	0.354
258	7.38	78.35	128.1	1.16	20.33	0.400		0.067	1.30	0.261		10.93		10.62	0.387	0.462	0.280	0.345
259	7.07	73.74	125.73	1.62	20.88	0.490		0.067	1.09	0.250		10.86		10.43	0.384	0.443	0.263	0.337
260	6.95	75.48	125.72	2.16	20.91	0.640		0.067	1.14	0.246		10.42		10.86	0.369	0.425	0.246	0.328
261	7.96	77.24	127.33	1.77	21.57	0.560		0.067	1.79	0.282		11.73		9.71	0.415	0.407	0.231	0.320
262	7.28	67.03	123.34	2.2	21.99	0.500		0.067	1.77	0.258		11.87		9.20	0.420	0.390	0.216	0.312
263	7.04	74.71	125.67	2.36	21.98	0.550		0.067	1.79	0.249		10.62		10.61	0.376	0.373	0.202	0.304
264	6.5	66.39	122.1	2.44	22.21	0.510		0.067	1.46	0.230		10.67		10.21	0.378	0.357	0.189	0.296
265	6.52	65.17	115.19	1.76	21.54	0.440		0.067	1.72	0.231		10.32		9.99	0.365	0.341	0.176	0.288
266	6	50.3	93.99	-0.02	20.73	0.410		0.068	1.72	0.212		10.02		8.39	0.354	0.326	0.164	0.281
267	6.02	47.74	99.68	0.33	22.09	0.420		0.068	2.41	0.213		11.13		7.93	0.394	0.311	0.152	0.274
268	7.49	52.2	107.12	3.85	26.13	0.490		0.066	2.93	0.265		12.96		6.97	0.458	0.297	0.142	0.267
269	5.95	67.91	119.81	0.45	19.7	0.440		0.068	1.90	0.211		9.62		11.41	0.340	0.283	0.131	0.260
270	5.72	65.33	117.92	0.72	20.81	0.450		0.068	2.27	0.202		9.44		11.43	0.334	0.270	0.122	0.253
271	5.72	63.58	112.11	1.21	20.05	0.400		0.068	1.53	0.202		9.15		11.12	0.324	0.257	0.113	0.247
272	5.85	60.34	111.54	1.26	20.62	0.470		0.068	1.59	0.207		9.75		10.32	0.345	0.245	0.104	0.241
273	5.45	64.23	114.82	0.84	20.3	0.460		0.068	1.54	0.193		8.91		11.78	0.315	0.233	0.096	0.234
274	6.01	65.37	118.83	2.33	22.26	0.500		0.068	1.51	0.213		9.81		10.88	0.347	0.221	0.089	0.229
275	5.89	57.04	104.63	1.82	20.18	0.500		0.068	1.18	0.208		9.62		9.68	0.340	0.210	0.081	0.223
276	5.36	61.07	109.69	0.92	20.38	0.480		0.068	1.17	0.190		8.78		11.40	0.311	0.200	0.075	0.217
277	5.09	59.85	108.59	1.28	20.65	0.570		0.068	1.16	0.180		8.41		11.75	0.298	0.190	0.069	0.212
278	4.49	50.77	97.45	0.72	20.51	0.510		0.068	2.72	0.159		7.86		11.31	0.278	0.180	0.063	0.207
279	3.01	60.8	102.25	-0.41	17.17	0.510		0.069	1.80	0.106		4.84		20.17	0.171	0.171	0.057	0.202
280	3.84	55.68	101.89	-1.02	16.67	0.530		0.069	1.61	0.136		6.64		14.51	0.235	0.162	0.052	0.197
281	3.64	40.15	75.27	-1.7	16.73	0.540		0.070	1.10	0.129		6.40		11.04	0.226	0.153	0.048	0.192
282	4.48	47.37	92.49	-1.62	16.48	0.320		0.070	1.98	0.159		8.13		10.58	0.288	0.145	0.043	0.188

Table A4: Daily eddy covariance, energy balance component, and transpiration model results at PLC045 in 2001.

DOY	LE	H	Rn	G	Ta	e	Ts	θ	wind speed	λE_{uncorr}	res	LE_{corr}	H_{corr}	β	λE_{corr}	T_{Kc}	T_{GB}	EC Fourier
	Wm^{-2}	Wm^{-2}	Wm^{-2}	Wm^{-2}	°C	kPa	°C	m^3m^{-3}	$m\ s^{-1}$	$mm\ day^{-1}$	Wm^{-2}	Wm^{-2}	Wm^{-2}		$mm\ day^{-1}$	$mm\ day^{-1}$	$mm\ day^{-1}$	$mm\ day^{-1}$
283	3.14	56.07	93.17	-3.26	13.05	0.290		0.071	1.32	0.111		5.11		17.89	0.181	0.137	0.039	0.184
284	2.13	24.01	57.4	-4.39	14.06	0.400		0.072	1.97	0.075		5.03		11.27	0.178	0.130	0.036	0.180
285	4.03	47.98	95.1	-0.19	17.38	0.440		0.070	2.97	0.143		7.38		11.91	0.261	0.123	0.032	0.176
286	5.24	40.43	94.27	-0.98	17.3	0.330		0.071	1.93	0.185		10.93		7.72	0.387	0.116	0.029	0.172
287	3.75	44.74	84.05	-0.33	17	0.360		0.070	1.32	0.133		6.53		11.92	0.231	0.109	0.026	0.168
288	3.14	45.85	91.62	-1.16	16.72	0.320		0.071	1.73	0.111		5.95		14.59	0.210	0.103	0.023	0.165
289	2.65	43.39	76.78	-1.56	15.1	0.350		0.071	1.55	0.094		4.51		16.36	0.160	0.097	0.021	0.162
290	2.54	43.07	84.77	-1.57	14.79	0.340		0.071	1.42	0.090		4.81		16.95	0.170	0.092	0.019	0.159
291	3.13	45.01	87.64	-0.39	17.85	0.380		0.071	1.47	0.111		5.72		14.38	0.203	0.086	0.017	0.156
292	2.26	38.04	72.51	-1.87	14.75	0.390		0.071	1.43	0.080		4.17		16.86	0.148	0.081	0.015	0.153
293	2.81	47.94	90.8	-0.29	16.62	0.390		0.071	1.28	0.099		5.04		17.03	0.178	0.077	0.013	0.150
294	2.74	27.38	61.49	-0.69	17.26	0.430		0.071	1.41	0.097		5.66		10.00	0.200	0.072	0.011	0.148
295	3.11	65.57	87.87	-1.9	14.09	0.410		0.071	1.18	0.110		4.07		21.06	0.144	0.068	0.010	0.145
296	3.47	46.63	83.32	-1.44	15.49	0.410		0.072	1.86	0.123		5.87		13.45	0.208	0.064	0.009	0.143
297	2.66	41.48	76.22	-1.93	13.92	0.310		0.072	1.82	0.094		4.71		15.59	0.167	0.060	0.007	0.141
298	1.75	45.38	84.38	-2.63	12.34	0.300		0.072	1.39	0.062		3.23		25.87	0.114	0.056	0.006	0.139
299	1.73	46.25	80.37	-3.5	11.17	0.300		0.073	1.48	0.061		3.02		26.69	0.107	0.053	0.005	0.137
300	1.67	16.72	35	-4.63	11.14	0.360		0.073	1.02	0.059		3.60		10.03	0.127	0.049	0.004	0.135
301	1.01	34.7	65.96	-3.59	11	0.450		0.073	1.50	0.036		1.97		34.35	0.070	0.046	0.004	0.134
302	1.75	36.13	67.4	-2.52	12.14	0.450		0.073	1.65	0.062		3.23		20.66	0.114	0.043	0.003	0.132
303	2.63	6.05	19.22	-3.62	12.12	0.650		0.073	1.81	0.093		6.92		2.30	0.245	0.040	0.002	0.131
304	2.6	52.43	82.02	-3.55	8.48	0.460		0.074	1.03	0.092		4.04		20.19	0.143	0.038	0.002	0.130
305	1.37	42.26	79.38	-4.08	8.34	0.430		0.074	1.04	0.048		2.62		30.84	0.093	0.035	0.001	0.128
306	1.35	28.96	49.79	-5	7.79	0.470		0.075	0.85	0.048		2.44		21.38	0.086	0.033	0.001	0.127
307	1.88	43.01	78.74	-2.98	10.41	0.460		0.074	1.38	0.067		3.42		22.85	0.121	0.031	0.001	0.126
308	1.8	32.17	60.37	-2.17	11.32	0.500		0.073	1.54	0.064		3.31		17.88	0.117	0.029	0.001	0.125
309	1.42	26.5	56.76	-2.52	12.02	0.590		0.074	1.55	0.050		3.01		18.63	0.107	0.027	0.000	0.125
310	1.04	43.65	77.16	-2.05	11.21	0.610		0.074	1.58	0.037		1.84		41.94	0.065	0.025	0.000	0.124
311	2.42	42.56	74.09	-3.02	10.05	0.450		0.074	1.02	0.086		4.15		17.56	0.147	0.023	0.000	0.123
312	2.35	23.53	66.46	-3.34	11.06	0.350		0.074	1.94	0.083		6.34		10.03	0.224	0.022	0.000	0.123
313	1.12	43.89	66.46	-4.97	6.15	0.210		0.075	0.98	0.040		1.78		39.03	0.063	0.020	0.000	0.122
314	0.02	31.96	65.73	-4.87	8.29	0.320		0.076	1.75	0.001		0.04		1822	0.002	0.019	0.000	0.122
315	-0.41	33.43	72.21	-0.46	13.91	0.680		0.073	2.49	-0.015		-0.90		-82	-0.032	0.018	0.000	0.121
316	0.82	48.95	64.08	-2.47	10.75	0.760		0.074	3.35	0.029		1.10		59.92	0.039	0.016	0.000	0.121
317	12.66	25.71	67.85	-2.98	11.15	0.400		0.075	2.25	0.448		23.37		2.03	0.827	0.015	0.000	0.121
318	1.87	41.31	69.97	-3.03	9.02	0.410		0.075	0.95	0.066		3.16		22.10	0.112	0.014	0.000	0.121
319	-0.03	38.58	69.75	-3.94	7.95	0.460		0.075	1.29	-0.001		-0.06		-1231	-0.002	0.013	0.000	0.120
320	0.86	38.57	66.5	-3.21	8.21	0.520		0.075	1.28	0.030		1.52		45.06	0.054	0.012	0.000	0.120
321	1.3	40	64.69	-4.27	6.34	0.450		0.076	1.14	0.046		2.17		30.87	0.077	0.011	0.000	0.120
322	2	35.26	61.71	-5.71	6.08	0.290		0.077	1.20	0.071		3.62		17.64	0.128	0.011	0.000	0.120
323	0.91	37.03	63.74	-5.14	6.49	0.280		0.076	0.87	0.032		1.65		40.64	0.058	0.010	0.000	0.120
324	0.19	1.78	7.47	-6.04	4.94	0.340		0.077	1.00	0.007		1.30		9.30	0.046	0.009	0.000	0.120
325	1.22	14.21	32.99	-4.29	7.92	0.400		0.076	0.81	0.043		2.95		11.69	0.104	0.008	0.000	0.120
326	4.08	23.38	53.68	-0.49	11.28	0.390		0.074	2.53	0.144		8.05		5.73	0.285	0.008	0.000	0.120
327	1.64	27.57	59.98	-2.81	9.27	0.230		0.075	2.68	0.058		3.53		16.79	0.125	0.007	0.000	0.120
328	13.28	-22.2	-7.65	-9.8	5.25	0.540		0.122	25385	0.470		-3.20		-1.67	-0.113	0.007	0.000	0.120
329	15.13	14.22	39.23	-18.76	0.72	0.440		0.140	0.96	0.535		29.89		0.94	1.058	0.006	0.000	0.121

Table A4: Daily eddy covariance, energy balance component, and transpiration model results at PLC045 in 2001.

DOY	LE	H	Rn	G	Ta	e	Ts	θ	wind speed	λE_{uncorr}	res	LE_{corr}	H_{corr}	β	λE_{corr}	T_{Kc}	T_{GB}	EC Fourier
	Wm^{-2}	Wm^{-2}	Wm^{-2}	Wm^{-2}	°C	kPa	°C	m^3m^{-3}	$m\ s^{-1}$	mm day^{-1}	Wm^{-2}	Wm^{-2}	Wm^{-2}		mm day^{-1}	mm day^{-1}	mm day^{-1}	mm day^{-1}
330	17.54	23.23	70.22	-17.59	0.04	0.330		0.119	1.62	0.621		37.78		1.33	1.337	0.006	0.000	0.121
331	11.19	28.67	52.66	-17.56	-1.33	0.290		0.106	1.68	0.396		19.71		2.56	0.697	0.005	0.000	0.121
332																0.005	0.000	0.121
333																0.005	0.000	0.121
334																0.004	0.000	0.121
335																0.004	0.000	0.121
336																0.004	0.000	0.121
337																0.003	0.000	0.122
338																0.003	0.000	0.122
339																0.003	0.000	0.122
340																0.003	0.000	0.122
341																0.002	0.000	0.122
342																0.002	0.000	0.122
343																0.002	0.000	0.122
344																0.002	0.000	0.122
345																0.002	0.000	0.122
346																0.002	0.000	0.122
347																0.002	0.000	0.122
348																0.001	0.000	0.122
349																0.001	0.000	0.122
350																0.001	0.000	0.122
351																0.001	0.000	0.122
352																0.001	0.000	0.122
353																0.001	0.000	0.122
354																0.001	0.000	0.122
355																0.001	0.000	0.122
356																0.001	0.000	0.122
357																0.001	0.000	0.121
358																0.001	0.000	0.121
359																0.001	0.000	0.121
360																0.001	0.000	0.121
361																0.001	0.000	0.121
362																0.001	0.000	0.121
363																0.000	0.000	0.120
364																0.000	0.000	0.120
365																0.000	0.000	0.120

Table A5: Daily eddy covariance, energy balance component, and transpiration model results at BLK100 in 2002.

DOY	LE	H	Rn	G	Ta	e	Ts	θ	wind speed	λE_{uncorr}	res	LE_{corr}	H_{corr}	β	λE_{corr}	T_{Kc}	T_{GB}	EC Fourier
	Wm^{-2}	Wm^{-2}	Wm^{-2}	Wm^{-2}	°C	kPa	°C	m^3m^{-3}	$m\ s^{-1}$	$mm\ day^{-1}$	Wm^{-2}	Wm^{-2}	Wm^{-2}		$mm\ day^{-1}$	$mm\ day^{-1}$	$mm\ day^{-1}$	$mm\ day^{-1}$
1		0	17.05	-4.82	4.36	-99999	4.76	0.296	99999		21.87		21.87	0.00	0.000	0.000	0.000	0.081
2																0.000	0.000	0.077
3																0.000	0.000	0.073
4																0.000	0.000	0.069
5																0.000	0.000	0.065
6																0.000	0.000	0.061
7																0.000	0.000	0.057
8																0.000	0.000	0.054
9																0.000	0.000	0.050
10																0.000	0.000	0.046
11																0.000	0.000	0.042
12																0.000	0.000	0.039
13																0.000	0.000	0.035
14																0.001	0.000	0.032
15																0.001	0.000	0.028
16																0.001	0.000	0.025
17																0.001	0.000	0.022
18																0.001	0.000	0.019
19																0.001	0.000	0.016
20																0.001	0.000	0.013
21																0.001	0.000	0.010
22																0.001	0.000	0.007
23																0.001	0.000	0.005
24																0.001	0.000	0.002
25																0.001	0.000	0.000
26																0.002	0.000	-0.002
27																0.002	0.000	-0.004
28																0.002	0.000	-0.006
29																0.002	0.000	-0.008
30																0.002	0.000	-0.009
31																0.002	0.000	-0.011
32																0.003	0.000	-0.012
33																0.003	0.000	-0.013
34																0.003	0.000	-0.013
35																0.003	0.000	-0.014
36																0.004	0.000	-0.014
37																0.004	0.000	-0.014
38																0.004	0.000	-0.014
39																0.005	0.000	-0.014
40																0.005	0.000	-0.013
41																0.006	0.000	-0.012
42																0.006	0.000	-0.011
43																0.007	0.000	-0.010
44																0.007	0.000	-0.008
45																0.008	0.000	-0.006
46																0.009	0.000	-0.003
47																0.009	0.000	-0.001

Table A5: Daily eddy covariance, energy balance component, and transpiration model results at BLK100 in 2002.

DOY	LE	H	Rn	G	Ta	e	Ts	θ	wind speed	λE_{uncorr}	res	LE_{corr}	H_{corr}	β	λE_{corr}	T_{Kc}	T_{GB}	EC Fourier
	Wm^{-2}	Wm^{-2}	Wm^{-2}	Wm^{-2}	°C	kPa	°C	m^3m^{-3}	$m\ s^{-1}$	$mm\ day^{-1}$	Wm^{-2}	Wm^{-2}	Wm^{-2}		$mm\ day^{-1}$	$mm\ day^{-1}$	$mm\ day^{-1}$	$mm\ day^{-1}$
48																0.010	0.000	0.002
49																0.011	0.000	0.006
50																0.012	0.000	0.009
51																0.013	0.000	0.013
52																0.014	0.000	0.018
53		0	50.3	4.1	10.36	-58332	9.59	0.103	99999		46.19		46.20	0.00	0.000	0.015	0.000	0.023
54		0	42.14	4.9	14.81	-6248	10.85	0.100	99999		37.24		37.24	0.00	0.000	0.016	0.000	0.028
55		0	37	-2.79	11.22	-43749	10.53	0.098	99999		39.79		39.79	0.00	0.000	0.017	0.000	0.033
56		0	45.24	-1.03	10.01	-29165	9.37	0.097	99999		46.28		46.28	0.00	0.000	0.019	0.000	0.039
57		0	43.38	2.03	10.13	-10415	9.83	0.095	99999		41.34		41.34	0.00	0.000	0.020	0.000	0.045
58		0	34.39	-0.95	11.62	1.343	10.00	0.093	99999		35.35		35.35	0.00	0.000	0.022	0.000	0.052
59		0	40.85	4.8	11.35	-18749	10.28	0.092	99999		36.04		36.04	0.00	0.000	0.023	0.000	0.059
60		0	40.9	-10.75	5.7	-12499	8.90	0.090	99999		51.65		51.65	0.00	0.000	0.025	0.000	0.067
61		0	46.57	-7.3	4.12	-4166	6.76	0.090	99999		53.87		53.87	0.00	0.000	0.027	0.000	0.074
62		0	50.67	-3.14	2.7	-37499	6.33	0.090	99999		53.81		53.81	0.00	0.000	0.029	0.000	0.083
63		0	54.41	-1.91	4.34	-33332	6.73	0.089	99999		56.32		56.33	0.00	0.000	0.031	0.000	0.092
64		0	55.09	3.56	7.75	1.041	8.52	0.088	99999		51.53		51.53	0.00	0.000	0.034	0.001	0.101
65		0	34.79	0.61	6.74	-62499	8.17	0.088	99999		34.18		34.18	0.00	0.000	0.036	0.001	0.110
66		0	61.78	0.53	8.94	-66665	9.70	0.095	99999		61.25		61.25	0.00	0.000	0.039	0.001	0.120
67		0	50.66	-6.65	5.47	-12499	8.00	0.093	99999		57.31		57.31	0.00	0.000	0.042	0.002	0.131
68		0	62.54	-3.88	5.25	-37499	6.79	0.091	99999		66.42		66.42	0.00	0.000	0.045	0.002	0.142
69		0	32.61	4.82	10.97	-22915	8.33	0.090	99999		27.80		27.80	0.00	0.000	0.048	0.003	0.153
70		33.81	66.14	12.06	11	-39583	11.21	0.086	50001		15.45	5.28	48.79	7.03	0.186	0.051	0.005	0.165
71	9.33	50.33	77.29	12.34	14.01	0.427	12.90	0.081	2.63	0.330	5.29	9.97	54.98	5.39	0.351	0.055	0.006	0.178
72	7.32	39.35	52.07	-6.17	10.29	0.244	12.11	0.073	4.34	0.259	11.57	7.80	50.44	5.38	0.273	0.059	0.007	0.191
73	4.6	33.2	33.94	-10.08	2.62	0.269	7.90	0.074	3.91	0.163	6.23	4.98	39.04	7.22	0.173	0.063	0.009	0.204
74	6.91	53.75	57.3	-1.62	2.18	0.229	7.95	0.074	2.69	0.244	-1.73	6.29	52.63	7.78	0.219	0.067	0.010	0.218
75	8.02	47.41	59.5	-1.22	3.67	0.186	8.22	0.074	3.80	0.284	5.30	7.79	52.93	5.91	0.271	0.071	0.012	0.232
76	5.49	39.71	42.32	-2.77	2.67	0.250	7.78	0.074	3.04	0.194	-0.10	5.07	40.02	7.24	0.176	0.076	0.014	0.247
77	7.86	49.93	70.57	-3.01	4.5	0.215	7.83	0.074	5.03	0.278	15.78	8.33	65.25	6.35	0.290	0.081	0.017	0.262
78	8.16	45.96	67.64	6.32	10.4	0.243	10.60	0.072	2.47	0.289	7.20	9.16	52.16	5.63	0.322	0.087	0.019	0.278
79	9.1	58.53	71.15	4.64	10.73	0.298	11.69	0.071	2.54	0.322	-1.11	9.01	57.50	6.43	0.317	0.092	0.022	0.294
80	8.9	56.74	72.98	2.88	12.17	0.291	12.41	0.071	2.80	0.315	4.45	9.94	60.15	6.38	0.350	0.098	0.025	0.310
81	8.98	61.33	76.74	6.29	13.74	0.253	13.12	0.070	4.12	0.318	0.15	8.58	61.87	6.83	0.303	0.105	0.029	0.328
82	6.92	73.55	88.53	4.21	10.89	0.369	14.18	0.069	2.98	0.245	3.85	6.14	78.18	10.63	0.215	0.111	0.032	0.345
83	8.57	49.17	67.83	-2.45	9.07	0.346	12.67	0.068	3.35	0.303	12.54	10.29	59.98	5.74	0.361	0.118	0.037	0.363
84	9.78	62.9	76.05	2.97	8.75	0.384	12.83	0.068	2.69	0.346	0.39	9.37	63.70	6.43	0.329	0.126	0.041	0.382
85	10.51	61.61	70.15	0.05	9.83	0.328	12.82	0.067	1.85	0.372	-2.03	9.95	60.15	5.86	0.349	0.133	0.046	0.401
86	13.49	61.12	83.11	4.53	11.31	0.311	13.54	0.067	1.72	0.477	3.96	14.17	64.41	4.53	0.499	0.142	0.051	0.420
87	12.85	45.27	84	9.56	16.14	0.304	15.32	0.066	3.81	0.455	16.32	15.77	58.67	3.52	0.556	0.150	0.057	0.440
88	10.96	44.03	82.09	6.71	18.19	0.391	16.55	0.064	4.15	0.388	20.41	14.28	61.11	4.02	0.505	0.159	0.064	0.461
89	14.65	30.8	72.57	5.48	18.54	0.237	16.98	0.063	3.80	0.518	21.64	18.95	48.14	2.10	0.670	0.169	0.070	0.482
90	17.29	51	78.83	2.81	16.46	0.208	17.21	0.062	2.63	0.612	7.73	19.05	56.96	2.95	0.674	0.179	0.078	0.503
91	18.13	50.95	82.91	5.43	16.68	0.230	17.07	0.062	2.45	0.641	8.39	20.60	56.87	2.81	0.730	0.189	0.086	0.525
92	18.17	43.78	83.05	6.53	18.76	0.261	18.01	0.061	2.85	0.643	14.58	22.26	54.26	2.41	0.788	0.200	0.094	0.547
93	19.16	58.73	89.44	7.58	18.41	0.368	18.58	0.060	2.39	0.678	3.97	20.40	61.46	3.07	0.723	0.211	0.103	0.570
94	19.51	65.13	89.12	4.33	17.38	0.354	18.35	0.060	2.62	0.690	0.15	19.10	65.68	3.34	0.676	0.223	0.113	0.593

Table A5: Daily eddy covariance, energy balance component, and transpiration model results at BLK100 in 2002.

DOY	LE	H	Rn	G	Ta	e	Ts	θ	wind speed	λE_{uncorr}	res	LE_{corr}	H_{corr}	β	λE_{corr}	T_{Kc}	T_{GB}	EC Fourier
	Wm^{-2}	Wm^{-2}	Wm^{-2}	Wm^{-2}	°C	kPa	°C	m^3m^{-3}	$m\ s^{-1}$	$mm\ day^{-1}$	Wm^{-2}	Wm^{-2}	Wm^{-2}		$mm\ day^{-1}$	$mm\ day^{-1}$	$mm\ day^{-1}$	$mm\ day^{-1}$
95	14.16	62.14	83.49	3.08	14.75	0.296	16.83	0.060	3.47	0.501	4.11	14.07	66.34	4.39	0.496	0.236	0.124	0.616
96	16.37	57.31	97.55	4.09	15.51	0.392	17.68	0.059	3.07	0.579	19.78	20.06	73.40	3.50	0.707	0.249	0.135	0.640
97	20.45	52.97	94.73	7.71	16.65	0.429	18.79	0.059	2.63	0.724	13.60	23.32	63.70	2.59	0.823	0.263	0.147	0.664
98	20.31	56.4	92.17	7.55	18.02	0.463	19.85	0.058	2.74	0.719	7.92	22.56	62.06	2.78	0.797	0.277	0.160	0.689
99		64.18	109.6	11.64	19.12	-2083	20.97	0.058	3.05							0.292	0.174	0.714
100	24.66	52.87	102.53	8.91	19.73	0.466	22.47	0.057	2.56	0.872	16.10	29.00	64.62	2.14	1.025	0.307	0.189	0.740
101	22.46	45.38	87.41	8.87	19.87	0.527	21.74	0.057	2.88	0.795	10.70	24.59	53.95	2.02	0.870	0.323	0.204	0.766
102	28.49	36.57	94.46	6.97	21	0.451	22.19	0.056	3.21	1.008	22.43	35.13	52.36	1.28	1.245	0.340	0.221	0.792
103	30.63	50.86	100.13	6.56	20.1	0.373	22.15	0.055	2.49	1.084	12.09	34.19	59.39	1.66	1.212	0.357	0.239	0.818
104	22.72	27.84	70.18	6.95	21.09	0.502	20.80	0.056	3.24	0.804	12.67	27.49	35.74	1.23	0.975	0.375	0.257	0.845
105	19.72	70.07	103.84	-3.25	14.27	0.282	19.68	0.055	6.09	0.698	17.30	21.86	85.22	3.55	0.766	0.394	0.277	0.873
106	19.29	85.99	112.25	2.65	11.06	0.306	17.72	0.056	4.28	0.682	4.33	19.57	90.03	4.46	0.687	0.414	0.298	0.900
107	17.43	70.42	112.51	0.15	10.59	0.254	18.28	0.056	4.25	0.617	24.52	21.11	91.26	4.04	0.738	0.434	0.320	0.928
108	13.66	55.07	77.27	-2.83	6.46	0.257	15.32	0.056	4.62	0.483	11.37	14.83	65.26	4.03	0.518	0.455	0.344	0.956
109	15.5	68.76	102.67	-0.58	7.9	0.376	14.86	0.057	5.14	0.548	18.98	18.13	85.12	4.44	0.633	0.476	0.368	0.985
110	21.8	74.15	113	3.72	9.87	0.364	16.80	0.056	2.72	0.771	13.33	23.60	85.68	3.40	0.827	0.499	0.394	1.014
111	22.51	80.27	117.86	5.21	11.58	0.332	17.24	0.056	2.56	0.796	9.87	24.57	88.08	3.57	0.865	0.522	0.421	1.043
112	29.52	67.51	117.75	7.8	15.02	0.338	18.76	0.055	2.26	1.044	12.91	32.67	77.27	2.29	1.154	0.546	0.450	1.072
113	33.31	64.14	117.8	9.37	17.6	0.360	20.29	0.054	2.38	1.179	10.98	36.89	71.54	1.93	1.305	0.571	0.480	1.101
114	26.78	61.75	106.25	8.48	16.61	0.578	20.33	0.054	3.71	0.947	9.24	28.53	69.25	2.31	1.008	0.596	0.511	1.131
115	22.93	49.59	81.76	5.8	16.07	0.861	20.95	0.054	2.79	0.811	3.45	23.32	52.63	2.16	0.822	0.623	0.544	1.161
116	30.54	45.81	82.17	3.82	14.27	0.705	20.04	0.055	3.44	1.081	2.00	30.78	47.57	1.50	1.080	0.650	0.578	1.191
117	34.06	95.55	136.31	3.69	12.82	0.394	19.76	0.055	4.07	1.205	3.01	32.77	99.85	2.81	1.152	0.678	0.614	1.221
118	23.18	81.2	118.84	5.27	11.64	0.399	18.98	0.055	3.60	0.820	9.19	23.91	89.67	3.50	0.840	0.706	0.651	1.251
119	27.55	91.83	125.98	0.56	15.3	0.385	19.66	0.054	5.62	0.975	6.04	27.76	97.66	3.33	0.978	0.736	0.690	1.282
120	20.94	76.53	101.54	-1.43	9	0.275	16.53	0.055	3.96	0.741	5.50	20.90	82.07	3.65	0.732	0.766	0.730	1.313
121	27.38	67.51	122.18	10.29	11.31	0.295	18.39	0.054	3.65	0.969	17.00	31.49	80.40	2.47	1.105	0.798	0.772	1.343
122	28.66	60.46	122.59	6.87	15.73	0.470	20.69	0.053	2.68	1.014	26.61	35.47	80.25	2.11	1.250	0.830	0.816	1.374
123	33.57	86.21	137.59	8.27	15.86	0.484	21.46	0.053	2.51	1.188	9.54	35.07	94.25	2.57	1.238	0.862	0.861	1.405
124	37.79	69.4	132.36	11.68	17.86	0.472	22.23	0.053	2.35	1.337	13.48	41.30	79.38	1.84	1.460	0.896	0.908	1.436
125	40.13	66.35	131.71	-1033	19.61	0.553	23.82	0.052	2.53	1.420				1.65		0.930	0.956	1.467
126	43.81	62.75	130.11	11.03	20.58	0.536	23.98	0.051	3.38	1.550	12.52	47.12	71.95	1.43	1.669	0.965	1.006	1.498
127	37.12	55.19	127.82	6.96	19.45	0.377	23.93	0.051	5.39	1.313	28.55	45.70	75.17	1.49	1.616	1.001	1.058	1.529
128	33.32	69.34	128.76	3.35	14.86	0.265	22.72	0.051	4.14	1.179	22.74	38.63	86.77	2.08	1.359	1.038	1.111	1.560
129	40.35	65.19	141.74	12.42	18.23	0.347	23.41	0.051	3.48	1.428	23.78	46.88	82.44	1.62	1.657	1.075	1.166	1.591
130	34.41	79.63	132.49	3.13	17.39	0.302	23.20	0.050	5.01	1.217	15.32	37.22	92.15	2.31	1.311	1.114	1.222	1.622
131	27.47	67.36	136.07	3.3	14.93	0.407	21.78	0.051	4.47	0.972	37.95	36.11	96.67	2.45	1.271	1.152	1.280	1.653
132	33.58	48.59	106.52	8.11	17.41	0.318	22.43	0.050	2.82	1.188	16.25	38.15	60.26	1.45	1.347	1.192	1.339	1.684
133	41.55	51.61	133.89	12.61	20.49	0.388	24.19	0.050	2.86	1.470	28.12	50.37	70.91	1.24	1.785	1.232	1.400	1.715
134	47.24	42.78	134.9	12.14	22.21	0.427	25.87	0.049	3.39	1.671	32.73	58.93	63.83	0.91	2.090	1.273	1.462	1.746
135	47.11	50.91	137.08	11.44	22.6	0.488	26.76	0.049	3.34	1.667	27.63	56.92	68.73	1.08	2.019	1.315	1.525	1.776
136	49.56	48	135.77	11.34	23.1	0.543	27.23	0.048	3.50	1.753	26.88	59.67	64.75	0.97	2.118	1.357	1.590	1.806
137	50.11	62.26	145.62	11.9	23.73	0.550	27.26	0.048	3.37	1.773	21.34	57.76	75.96	1.24	2.053	1.399	1.656	1.836
138	42.44	52.45	131.63	7.83	22.9	0.499	26.60	0.048	3.57	1.502	28.89	52.28	71.52	1.24	1.856	1.443	1.723	1.866
139	39.46	73.25	142.95	6.5	21.91	0.477	25.95	0.048	6.81	1.396	23.75	43.55	92.90	1.86	1.543	1.486	1.792	1.896
140	34.87	85.99	120.56	-3.48	13.39	0.382	22.49	0.049	5.39	1.234	3.18	33.22	90.82	2.47	1.166	1.531	1.861	1.926
141	33.94	81.77	141.41	4.17	11.6	0.269	21.89	0.049	2.28	1.201	21.54	39.59	97.65	2.41	1.389	1.575	1.931	1.955

Table A5: Daily eddy covariance, energy balance component, and transpiration model results at BLK100 in 2002.

DOY	LE	H	Rn	G	Ta	e	Ts	θ	wind speed	λE_{uncorr}	res	LE_{corr}	H_{corr}	β	λE_{corr}	T_{Kc}	T_{GB}	EC Fourier
	Wm^{-2}	Wm^{-2}	Wm^{-2}	Wm^{-2}	°C	kPa	°C	m^3m^{-3}	$m\ s^{-1}$	$mm\ day^{-1}$	Wm^{-2}	Wm^{-2}	Wm^{-2}		$mm\ day^{-1}$	$mm\ day^{-1}$	$mm\ day^{-1}$	$mm\ day^{-1}$
142		83.9	143.47	6.03	13.06	-16665	22.65	0.049	2.79					0.01		1.620	2.003	1.984
143		63.3	139.91	9.11	16.81	-37498	23.77	0.048	3.26					0.12		1.666	2.075	2.013
144		54.36	-8195	-1.1E5	19.06	-22915	-20812	0.048	3.02					0.01		1.712	2.148	2.041
145		66.72	-1937	212.35	20.6	-37498	-6225	0.048	2.63					0.00		1.758	2.221	2.069
146		43.98	120.78	473.06	21.24	-31249	-16644	0.048	2086					0.00		1.804	2.295	2.097
147	47.85	58.85	142.09	10.69	21.46	0.601	26.24	0.047	2.96	1.693	24.70	57.61	73.79	1.23	2.044	1.851	2.370	2.125
148	54	62.88	152.43	9.13	21.89	0.518	27.09	0.047	2.63	1.911	26.41	63.98	79.31	1.16	2.272	1.897	2.445	2.152
149	61.39	54.19	153.64	12.4	24.15	0.440	27.75	0.047	2.65	2.172	25.65	72.81	68.43	0.88	2.593	1.944	2.520	2.178
150	62.86	44.19	152.25	14.45	26.55	0.463	29.01	0.046	2.78	2.224	30.75	76.49	61.31	0.70	2.729	1.991	2.595	2.205
151	57.62	39.46	137.19	12.61	27.61	0.640	29.77	0.046	3.87	2.039	27.50	67.21	57.37	0.68	2.396	2.038	2.670	2.230
152	48.5	39.08	104.84	3.53	23.69	0.685	27.71	0.046	3.01	1.716	13.73	53.37	47.94	0.81	1.894	2.085	2.745	2.256
153	54.7	55.42	150.14	11.87	22.36	0.637	28.42	0.046	3.61	1.935	28.14	64.35	73.92	1.01	2.281	2.131	2.820	2.281
154	51.75	40.94	145.2	9.49	23.92	0.490	28.33	0.046	3.52	1.831	43.01	68.85	66.86	0.79	2.443	2.178	2.894	2.305
155	62.1	41.77	149.74	12.43	25.3	0.465	29.86	0.045	2.47	2.197	33.44	77.48	59.83	0.67	2.756	2.224	2.968	2.330
156	60.78	30.91	150.05	13.89	27.95	0.664	31.04	0.045	2.64	2.150	44.47	80.35	55.80	0.51	2.866	2.270	3.041	2.353
157																2.316	3.113	2.376
158																2.361	3.184	2.399
159																2.406	3.255	2.421
160																2.450	3.324	2.442
161	44.43	59.03	145.24	6.74	18.9	0.367	27.09	0.045	3.58	1.572	35.04	54.80	83.70	1.33	1.936	2.494	3.391	2.463
162	57.71	60.03	154.62	9.56	21.44	0.447	28.43	0.045	3.36	2.042	27.32	66.67	78.38	1.04	2.363	2.538	3.457	2.483
163	58.94	52.43	157.68	10.83	23.58	0.446	29.04	0.044	2.85	2.085	35.48	72.70	74.14	0.89	2.586	2.580	3.522	2.503
164	63.57	52.92	160.9	11.53	25.38	0.484	29.97	0.044	2.99	2.249	32.87	76.87	72.50	0.83	2.738	2.622	3.585	2.522
165	62.89	47.72	161.14	10.83	25.61	0.533	30.62	0.043	2.42	2.225	39.69	79.98	70.33	0.76	2.850	2.663	3.646	2.541
166	66.92	45.01	159.1	10.94	26.54	0.536	30.85	0.043	3.04	2.368	36.23	83.41	64.75	0.67	2.975	2.703	3.705	2.558
167	68.91	40.86	157.88	10.86	26.58	0.467	30.95	0.043	2.78	2.438	37.25	85.15	61.86	0.59	3.039	2.742	3.762	2.576
168	75.02	25.4	153.25	15.02	28.89	0.469	32.02	0.043	3.34	2.654	37.82	93.26	44.98	0.34	3.330	2.780	3.816	2.592
169	66.94	35.48	154.1	12.8	29.09	0.661	32.77	0.042	4.53	2.368	38.88	84.33	56.98	0.53	3.009	2.818	3.868	2.608
170	56.13	35.57	138.83	12.28	27.97	0.809	32.89	0.042	3.89	1.986	34.86	69.53	57.02	0.63	2.475	2.854	3.918	2.623
171	53.21	29.69	121.28	4.21	26.8	0.819	31.08	0.043	3.39	1.883	34.16	63.24	53.82	0.56	2.250	2.889	3.965	2.638
172	43.23	29.74	94.6	0.64	22.89	0.818	27.83	0.045	2.70	1.530	20.99	52.21	41.75	0.69	1.850	2.923	4.010	2.652
173	60.84	56.66	160.29	11.38	23.45	0.690	29.88	0.044	3.10	2.153	31.41	71.71	77.20	0.93	2.549	2.955	4.051	2.665
174	65.52	50.82	165.91	9.9	25.7	0.536	30.70	0.044	2.89	2.318	39.67	82.10	73.91	0.78	2.925	2.986	4.090	2.678
175	68.16	45.77	160.37	12.15	27.18	0.528	31.39	0.043	3.00	2.412	34.29	82.63	65.59	0.67	2.947	3.016	4.126	2.689
176	68.9	40.78	158.29	12.14	27.84	0.501	32.06	0.043	3.15	2.438	36.47	85.13	61.03	0.59	3.038	3.045	4.158	2.701
177	66.22	46.01	149.6	7.86	26.55	0.585	31.93	0.043	2.66	2.343	29.51	78.84	62.91	0.69	2.812	3.072	4.188	2.711
178	69.03	43.17	158.07	11	26.67	0.611	32.23	0.043	2.50	2.442	34.87	83.34	63.73	0.63	2.974	3.097	4.214	2.721
179	66.14	44.01	150.72	10.61	26.83	0.661	32.17	0.043	2.75	2.340	29.96	77.35	62.77	0.67	2.759	3.121	4.237	2.729
180	67.33	46.08	162.83	12.27	27.64	0.729	33.03	0.042	2.92	2.382	37.15	82.73	67.83	0.68	2.954	3.144	4.256	2.738
181	70.99	41.82	159.73	12.3	29.39	0.665	33.45	0.042	3.32	2.512	34.62	86.48	60.96	0.59	3.091	3.165	4.273	2.745
182	67.98	36.12	147.34	11.23	29.84	0.610	33.14	0.042	3.99	2.405	32.01	81.06	55.05	0.53	2.897	3.184	4.285	2.752
183	69.08	42.6	157.49	10.18	28.08	0.472	33.31	0.042	3.52	2.444	35.63	82.18	65.13	0.62	2.931	3.201	4.295	2.758
184	68.54	44.47	156.91	9.25	26.46	0.574	33.16	0.042	2.48	2.425	34.65	81.09	66.57	0.65	2.891	3.217	4.301	2.763
185	61.11	47.44	152.41	8.54	26.94	0.751	32.51	0.042	3.16	2.162	35.31	75.85	68.02	0.78	2.707	3.231	4.303	2.767
186	62.01	48.31	155.62	9.86	27.35	0.683	32.38	0.042	3.24	2.194	35.45	75.51	70.25	0.78	2.694	3.244	4.302	2.771

Table A5: Daily eddy covariance, energy balance component, and transpiration model results at BLK100 in 2002.

DOY	LE	H	Rn	G	Ta	e	Ts	θ	wind speed	λE_{uncorr}	res	LE_{corr}	H_{corr}	β	λE_{corr}	T_{Kc}	T_{GB}	EC Fourier
	Wm^{-2}	Wm^{-2}	Wm^{-2}	Wm^{-2}	°C	kPa	°C	m^3m^{-3}	$m\ s^{-1}$	$mm\ day^{-1}$	Wm^{-2}	Wm^{-2}	Wm^{-2}		$mm\ day^{-1}$	$mm\ day^{-1}$	$mm\ day^{-1}$	$mm\ day^{-1}$
187	64.87	45.93	160.98	10.37	27.95	0.696	32.73	0.042	3.15	2.295	39.81	78.32	72.29	0.71	2.795	3.254	4.297	2.774
188	70.4	46.97	164.13	10.34	28.55	0.675	33.05	0.042	2.89	2.491	36.43	84.05	69.74	0.67	3.001	3.263	4.289	2.776
189	64.24	40.84	164.97	9.52	28.89	0.534	33.27	0.042	2086	2.273	50.38	83.29	72.17	0.64	2.978	3.270	4.278	2.778
190	73.74	25.68	161.31	13.49	31.09	0.517	34.26	0.041	2.68	2.609	48.39	94.46	53.36	0.35	3.384	3.275	4.263	2.778
191	89.44	22.36	155.63	14.68	32.6	0.582	35.53	0.041	2.24	3.164	29.15	100.36	40.59	0.25	3.600	3.278	4.244	2.778
192	66.19	33.48	145.7	11.22	30.31	1.056	34.93	0.041	3.44	2.342	34.81	81.14	53.34	0.51	2.899	3.280	4.223	2.777
193	64.72	38.27	155.51	11.74	30.72	1.113	35.58	0.042	2.66	2.290	40.79	81.27	62.51	0.59	2.907	3.279	4.197	2.776
194	63.79	30.86	142.37	9.3	30.78	0.956	35.35	0.042	3.05	2.257	38.42	78.68	54.39	0.48	2.814	3.277	4.169	2.773
195	54.59	22.59	123.33	7.46	29.86	0.889	33.64	0.042	2.75	1.931	38.69	63.92	51.95	0.41	2.285	3.273	4.138	2.770
196	69.72	41.63	155.67	9.19	28.76	0.724	33.37	0.042	2.74	2.467	35.13	82.05	64.43	0.60	2.932	3.267	4.103	2.767
197	63.75	34.88	140.35	9.91	27.95	0.719	33.49	0.042	2.40	2.256	31.81	72.57	57.87	0.55	2.591	3.259	4.065	2.762
198	37.23	15.97	73.21	-2.18	25.33	0.852	29.78	0.043	2.74	1.317	22.19	42.48	32.91	0.43	1.510	3.250	4.024	2.757
199	46.26	19.2	91.84	4.85	25.21	1.048	28.99	0.044	2.93	1.637	21.53	52.03	34.97	0.41	1.847	3.238	3.981	2.751
200	55.57	47.66	154.64	9.08	25.35	0.868	31.57	0.044	2.70	1.966	42.34	69.77	75.79	0.86	2.484	3.225	3.935	2.744
201	62.81	47	158.3	8.65	26.56	0.703	32.31	0.043	2.51	2.222	39.85	78.26	71.39	0.75	2.792	3.210	3.886	2.737
202	62.84	48.23	154.45	6.91	26.77	0.525	31.83	0.043	3.04	2.223	36.47	74.80	72.74	0.77	2.668	3.193	3.834	2.728
203	45.21	33.85	114.24	3.66	26.21	0.417	29.75	0.043	3.36	1.600	31.51	52.09	58.49	0.75	1.856	3.175	3.780	2.720
204	49.48	34.28	122.89	8.06	26.43	0.593	29.74	0.043	3.11	1.751	31.07	58.80	56.03	0.69	2.096	3.154	3.724	2.710
205	55.57	35.61	139.33	11.22	28.44	0.933	32.11	0.043	2.47	1.966	36.94	69.62	58.50	0.64	2.486	3.133	3.665	2.700
206	61.75	30.21	136.81	10.2	29.6	0.941	33.24	0.043	2.22	2.185	34.65	73.27	53.34	0.49	2.616	3.109	3.605	2.689
207	60.99	28.51	140.88	7.62	28.21	0.609	32.78	0.042	3.35	2.158	43.77	76.94	56.32	0.47	2.745	3.084	3.542	2.678
208	58.68	38.73	143.7	6.37	26.11	0.581	31.56	0.043	2.76	2.076	39.92	73.77	63.56	0.66	2.632	3.057	3.478	2.665
209	60.91	35.59	149.56	8.19	26.76	0.564	31.53	0.043	2.52	2.155	44.87	77.73	63.64	0.58	2.776	3.029	3.412	2.653
210	65.13	25.06	152.3	11.11	29.11	0.527	32.61	0.042	2.77	2.304	51.00	85.03	56.17	0.38	3.041	3.000	3.344	2.639
211	59.17	27.16	132.03	8.74	29.32	0.584	32.19	0.042	2.88	2.093	36.96	71.44	51.85	0.46	2.554	2.969	3.275	2.625
212	51.65	20.2	119.92	8.2	29.06	0.660	31.83	0.042	2.75	1.827	39.86	66.80	44.91	0.39	2.387	2.936	3.205	2.610
213	51.8	27.39	121.8	6.89	28.27	0.755	31.72	0.043	2.69	1.833	35.71	62.34	52.56	0.53	2.226	2.903	3.133	2.595
214	55.73	42.26	149.59	8.82	27.75	0.801	32.47	0.042	2.95	1.972	42.78	71.64	69.13	0.76	2.555	2.868	3.061	2.579
215	46.71	40.89	130.08	2.68	25.19	0.646	30.40	0.043	3.68	1.653	39.81	58.43	68.97	0.88	2.079	2.831	2.988	2.563
216	53.58	49.32	149.04	6.06	23.93	0.504	30.18	0.043	2.56	1.896	40.07	67.69	75.29	0.92	2.407	2.794	2.914	2.546
217	50.24	51.49	139.81	4.49	22.82	0.524	29.60	0.043		1.778	33.59	58.76	76.55	1.02	2.087	2.755	2.839	2.528
218	46.82	51.34	141.17	4.84	22.77	0.536	29.21	0.043	2.92	1.657	38.18	56.46	79.88	1.10	2.005	2.716	2.764	2.510
219	49.54	42.91	135.69	5.49	22.62	0.485	28.82	0.043	2.55	1.753	37.74	61.09	69.11	0.87	2.170	2.675	2.688	2.491
220	51.63	40.38	144.19	5.22	24.42	0.404	29.83	0.043	3.03	1.827	46.96	66.21	72.76	0.78	2.356	2.634	2.613	2.472
221	52.86	33.67	141.19	7.38	25.61	0.390	29.82	0.043	2.56	1.870	47.27	70.12	63.69	0.64	2.501	2.592	2.537	2.453
222	57.09	28.25	140.66	8.35	27.01	0.408	30.27	0.043	2.43	2.020	46.97	74.95	57.36	0.49	2.676	2.549	2.461	2.433
223	52.6	24.01	130.77	7.32	27.59	0.487	30.39	0.043	2.41	1.861	46.85	70.88	52.57	0.46	2.533	2.505	2.386	2.412
224	58.98	20.84	135.3	9.79	29.3	0.536	31.33	0.042	2.54	2.087	45.69	76.32	49.19	0.35	2.732	2.460	2.310	2.391
225	57.96	18.77	135.66	10.29	30.79	0.536	32.26	0.042	2.69	2.051	48.64	76.85	48.53	0.32	2.752	2.415	2.236	2.369
226	57.94	16.13	128.96	10.15	31.26	0.563	32.56	0.042	2.29	2.050	44.74	74.05	44.76	0.28	2.651	2.369	2.161	2.348
227	55.22	9.94	109.35	6.1	30.32	0.639	32.30	0.042	2.81	1.954	38.10	65.31	37.95	0.18	2.337	2.323	2.087	2.325
228	58.4	25.6	133.87	7.76	29.25	0.610	31.61	0.042	2.29	2.066	42.12	74.58	51.54	0.44	2.669	2.276	2.014	2.303
229	62.57	17.97	132.14	8.48	29.45	0.496	31.61	0.042	2.35	2.214	43.12	75.76	47.90	0.29	2.712	2.229	1.942	2.280
230	57.49	16.76	127.48	6.04	29.09	0.474	31.64	0.042	2.59	2.034	47.18	72.45	48.99	0.29	2.589	2.182	1.871	2.256
231	59.28	27.17	131.98	5.73	26.17	0.408	29.95	0.042	2.82	2.097	39.80	69.25	56.99	0.46	2.469	2.134	1.800	2.232
232	55.53	30.82	132.21	4.01	26.07	0.332	30.19	0.042	4.21	1.965	41.85	64.75	63.45	0.56	2.303	2.086	1.731	2.208
233	41.14	40.46	129.35	1.57	22.45	0.415	28.62	0.043	3.68	1.456	46.18	52.67	75.11	0.98	1.869	2.038	1.663	2.184

Table A5: Daily eddy covariance, energy balance component, and transpiration model results at BLK100 in 2002.

DOY	LE	H	Rn	G	Ta	e	Ts	θ	wind speed	λE_{uncorr}	res	LE_{corr}	H_{corr}	β	λE_{corr}	T_{Kc}	T_{GB}	EC Fourier
	Wm^{-2}	Wm^{-2}	Wm^{-2}	Wm^{-2}	°C	kPa	°C	m^3m^{-3}	$m\ s^{-1}$	$mm\ day^{-1}$	Wm^{-2}	Wm^{-2}	Wm^{-2}		$mm\ day^{-1}$	$mm\ day^{-1}$	$mm\ day^{-1}$	$mm\ day^{-1}$
234	41.94	52.05	135.73	3	22.15	0.426	27.25	0.043	2.47	1.484	38.75	52.46	80.28	1.24	1.862	1.990	1.596	2.159
235	44.9	48.83	136.88	3.12	22.17	0.436	27.82	0.043	1.86	1.589	40.03	57.08	76.68	1.09	2.028	1.942	1.530	2.134
236	46.26	44.11	134.82	4.63	23.58	0.464	27.75	0.043	2.83	1.637	39.82	57.72	72.47	0.95	2.053	1.894	1.466	2.109
237	45.8	40.68	134.66	3.68	23.86	0.448	27.60	0.043	2.43	1.620	44.50	59.85	71.13	0.89	2.132	1.846	1.402	2.084
238	40.33	22.19	131.17	6.6	25.84	0.410	28.05	0.043	3.24	1.427	62.05	61.70	62.87	0.55	2.198	1.798	1.341	2.058
239	44.35	29.27	123.88	6.26	25.3	0.438	28.80	0.043	2.98	1.569	44.01	57.60	60.02	0.66	2.048	1.751	1.281	2.032
240	37.92	26.46	111.11	3.16	24.66	0.534	28.33	0.043	3.31	1.342	43.57	46.10	61.86	0.70	1.639	1.703	1.222	2.006
241	42.67	38.03	127.45	6	23.72	0.570	28.05	0.043	2.69	1.510	40.75	53.26	68.19	0.89	1.894	1.656	1.165	1.980
242	43.59	42.68	130.47	3.46	23.8	0.561	27.80	0.044	3.10	1.542	40.74	53.53	73.49	0.98	1.903	1.609	1.109	1.953
243	45.36	43.54	132.6	1.31	22.29	0.402	26.87	0.044	1.86	1.605	42.40	58.90	72.40	0.96	2.095	1.563	1.055	1.927
244	45.51	36.48	127.04	6.2	24.48	0.507	27.36	0.044	1.95	1.610	38.85	57.63	63.20	0.80	2.054	1.517	1.003	1.900
245	47.6	26.95	127.88	6.72	25.97	0.573	28.48	0.043	2.35	1.684	46.61	63.21	57.95	0.57	2.255	1.472	0.952	1.873
246	46.62	23.31	127.79	7.3	27.75	0.574	28.78	0.043	2.92	1.649	50.55	61.03	59.45	0.50	2.177	1.427	0.903	1.846
247	30.33	17.72	84.39	2.5	26.08	0.752	27.86	0.044	3.02	1.073	33.85	38.95	42.94	0.58	1.384	1.382	0.855	1.820
248	33.47	27.37	90.33	2.68	24.23	0.863	26.81	0.044	3.50	1.184	26.81	41.44	46.21	0.82	1.472	1.338	0.809	1.792
249	31.55	30.43	87.41	-2.95	22.2	0.841	25.83	0.045	4.03	1.116	28.38	36.50	53.86	0.96	1.294	1.295	0.765	1.765
250	32.82	50.9	123.18	-2.2	18.11	0.389	23.53	0.046	2.94	1.161	41.67	41.69	83.70	1.55	1.474	1.252	0.722	1.738
251	29.78	48.53	124.11	-2.06	17.24	0.353	22.55	0.046	2.14	1.054	47.87	42.80	83.37	1.63	1.514	1.211	0.681	1.711
252	35.85	42.5	123.76	1.4	18.95	0.355	22.90	0.045	2.55	1.268	44.02	45.75	76.61	1.19	1.623	1.169	0.642	1.684
253	38.27	42	122.47	3.05	19.97	0.389	23.67	0.045	2.00	1.354	39.15	48.58	70.84	1.10	1.725	1.129	0.604	1.657
254	37.44	30.7	117.89	3.96	22.21	0.439	24.60	0.045	2.33	1.325	45.79	49.20	64.73	0.82	1.749	1.089	0.568	1.630
255	40.34	36.33	117.08	3.41	22.31	0.428	24.82	0.045	1.67	1.427	37.01	51.68	61.99	0.90	1.838	1.050	0.533	1.603
256	39.91	30.55	119.88	3.5	22.96	0.448	24.90	0.045	2.14	1.412	45.91	53.47	62.91	0.77	1.904	1.012	0.500	1.576
257	39.8	33.14	116.94	4.6	23.91	0.485	25.33	0.045	2.63	1.408	39.40	51.49	60.86	0.83	1.834	0.974	0.468	1.549
258	32.36	22.09	94.83	1.71	24.11	0.518	24.09	0.045	4.06	1.145	38.67	41.49	51.63	0.68	1.477	0.938	0.438	1.522
259	30.86	22.76	109.7	-0.46	22.5	0.383	24.78	0.045	3.65	1.092	56.55	43.81	66.36	0.74	1.553	0.902	0.409	1.495
260	34.12	41.19	115	4.79	20.76	0.447	23.69	0.045	2.10	1.207	34.90	42.94	67.27	1.21	1.523	0.867	0.381	1.468
261	24.64	23.98	110.14	2.73	22.11	0.576	24.55	0.045	4.89	0.872	58.81	37.40	70.02	0.97	1.325	0.833	0.355	1.442
262	32	29.69	113.09	0.19	21.76	0.515	24.44	0.045	3.24	1.132	51.22	45.30	67.60	0.93	1.607	0.799	0.331	1.416
263	35.6	40.79	115.61	2.48	21.2	0.512	23.82	0.046	2.10	1.260	36.75	45.26	67.88	1.15	1.608	0.767	0.307	1.389
264	37.12	33.83	114.45	3.29	22.3	0.516	24.24	0.045	2.04	1.313	40.22	49.53	61.63	0.91	1.762	0.735	0.285	1.363
265	35.94	26.76	113.15	2.16	22.31	0.454	24.24	0.045	2.09	1.272	48.29	50.93	60.05	0.74	1.813	0.705	0.264	1.337
266	34.55	29.89	111.09	2.49	22.71	0.426	23.96	0.045	2.25	1.222	44.16	48.78	59.82	0.87	1.737	0.675	0.244	1.312
267	32.88	18.5	93.62	6.01	24.03	0.471	24.07	0.045	2.39	1.163	36.22	43.34	44.27	0.56	1.541	0.646	0.225	1.286
268	35.66	12.28	98.27	7.48	26.01	0.543	26.47	0.045	2.61	1.262	42.85	46.75	44.04	0.34	1.664	0.618	0.207	1.261
269	30.79	30.45	99.76	-2.15	21.92	0.404	24.80	0.045	2.74	1.089	40.68	39.54	62.37	0.99	1.403	0.590	0.191	1.236
270	21.41	7.82	73.63	2.85	21.89	0.478	22.74	0.046	3.54	0.758	41.54	33.91	36.86	0.37	1.202	0.564	0.175	1.211
271	11.75	17.77	50.54	-6.05	16.82	0.768	21.60	0.047	3.21	0.416	27.06	15.27	41.32	1.51	0.537	0.539	0.161	1.186
272	23.22	45.48	101.18	-0.4	14.74	0.806	20.85	0.048	2.27	0.822	32.87	29.12	72.45	1.96	1.027	0.514	0.147	1.162
273	22.27	45.53	93.68	-2.81	15.01	0.740	20.03	0.048	2.28	0.788	28.70	26.45	70.04	2.04	0.933	0.490	0.134	1.137
274	16.14	33.76	77.2	-6.15	11.7	0.527	17.14	0.049	4.70	0.571	33.46	20.05	63.30	2.09	0.703	0.467	0.122	1.114
275	12.07	28.24	76.22	-7.39	10.83	0.422	15.82	0.049	5.32	0.427	43.30	17.60	66.01	2.34	0.616	0.445	0.111	1.090
276																0.423	0.101	1.067
277																0.403	0.091	1.043
278																0.383	0.082	1.021
279																0.364	0.074	0.998
280																0.345	0.066	0.976

Table A5: Daily eddy covariance, energy balance component, and transpiration model results at BLK100 in 2002.

DOY	LE	H	Rn	G	Ta	e	Ts	θ	wind speed	λE_{uncorr}	res	LE_{corr}	H_{corr}	β	λE_{corr}	T_{Kc}	T_{GB}	EC Fourier
	Wm^{-2}	Wm^{-2}	Wm^{-2}	Wm^{-2}	°C	kPa	°C	m^3m^{-3}	$m\ s^{-1}$	$mm\ day^{-1}$	Wm^{-2}	Wm^{-2}	Wm^{-2}		$mm\ day^{-1}$	$mm\ day^{-1}$	$mm\ day^{-1}$	$mm\ day^{-1}$
281																0.328	0.059	0.954
282																0.311	0.052	0.932
283																0.294	0.046	0.911
284																0.279	0.041	0.890
285																0.264	0.036	0.870
286																0.250	0.031	0.849
287																0.236	0.027	0.829
288																0.223	0.023	0.810
289																0.211	0.019	0.791
290																0.199	0.016	0.772
291																0.187	0.013	0.753
292																0.177	0.011	0.735
293																0.166	0.009	0.717
294																0.157	0.007	0.699
295																0.147	0.005	0.682
296																0.139	0.004	0.665
297																0.130	0.003	0.648
298																0.122	0.003	0.632
299																0.115	0.002	0.616
300																0.108	0.002	0.601
301																0.101	0.001	0.586
302																0.095	0.001	0.571
303																0.089	0.000	0.556
304																0.083	0.000	0.542
305																0.078	0.000	0.528
306																0.073	0.000	0.515
307																0.068	0.000	0.501
308																0.063	0.000	0.488
309																0.059	0.000	0.476
310																0.055	0.000	0.464
311																0.051	0.000	0.452
312																0.048	0.000	0.440
313																0.045	0.000	0.428
314																0.042	0.000	0.417
315																0.039	0.000	0.406
316																0.036	0.000	0.396
317																0.034	0.000	0.385
318																0.031	0.000	0.375
319																0.029	0.000	0.366
320																0.027	0.000	0.356
321																0.025	0.000	0.347
322																0.023	0.000	0.338
323																0.022	0.000	0.329
324																0.020	0.000	0.320
325																0.019	0.000	0.312
326																0.017	0.000	0.304
327																0.016	0.000	0.296

Table A5: Daily eddy covariance, energy balance component, and transpiration model results at BLK100 in 2002.

DOY	LE	H	Rn	G	Ta	e	Ts	θ	wind speed	λE_{uncorr}	res	LE_{corr}	H_{corr}	β	λE_{corr}	T_{Kc}	T_{GB}	EC Fourier
	Wm^{-2}	Wm^{-2}	Wm^{-2}	Wm^{-2}	°C	kPa	°C	m^3m^{-3}	$m\ s^{-1}$	mm day^{-1}	Wm^{-2}	Wm^{-2}	Wm^{-2}		mm day^{-1}	mm day^{-1}	mm day^{-1}	mm day^{-1}
328																0.015	0.000	0.288
329																0.014	0.000	0.280
330																0.013	0.000	0.273
331																0.012	0.000	0.266
332																0.011	0.000	0.259
333																0.010	0.000	0.252
334																0.009	0.000	0.245
335																0.009	0.000	0.238
336																0.008	0.000	0.232
337																0.007	0.000	0.226
338																0.007	0.000	0.219
339																0.006	0.000	0.213
340																0.006	0.000	0.208
341																0.005	0.000	0.202
342																0.005	0.000	0.196
343																0.005	0.000	0.190
344																0.004	0.000	0.185
345																0.004	0.000	0.180
346																0.004	0.000	0.174
347																0.003	0.000	0.169
348																0.003	0.000	0.164
349																0.003	0.000	0.159
350																0.003	0.000	0.154
351																0.003	0.000	0.149
352																0.002	0.000	0.144
353																0.002	0.000	0.139
354																0.002	0.000	0.135
355																0.002	0.000	0.130
356																0.002	0.000	0.125
357																0.002	0.000	0.121
358																0.002	0.000	0.116
359																0.001	0.000	0.112
360																0.001	0.000	0.107
361																0.001	0.000	0.103
362																0.001	0.000	0.098
363																0.001	0.000	0.094
364																0.001	0.000	0.090
365																0.001	0.000	0.086

Table A6: Daily eddy covariance, energy balance component, and transpiration model results at FSL138 in 2002.

DOY	LE	H	Rn	G	Ta	e	Ts	θ	wind speed	λE_{uncorr}	res	LE_{corr}	H_{corr}	β	λE_{corr}	T_{Kc}	T_{GB}	EC Fourier
	Wm^{-2}	Wm^{-2}	Wm^{-2}	Wm^{-2}	°C	kPa	°C	m^3m^{-3}	$m\ s^{-1}$	mm day^{-1}	Wm^{-2}	Wm^{-2}	Wm^{-2}		mm day^{-1}	mm day^{-1}	mm day^{-1}	mm day^{-1}
1																0.000	0.000	0.163
2																0.000	0.000	0.158
3																0.000	0.000	0.153
4																0.000	0.000	0.148
5																0.000	0.000	0.143
6																0.000	0.000	0.139
7																0.000	0.000	0.134
8																0.000	0.000	0.130
9																0.000	0.000	0.126
10																0.000	0.000	0.122
11																0.000	0.000	0.118
12																0.000	0.000	0.114
13																0.000	0.000	0.111
14																0.000	0.000	0.108
15																0.000	0.000	0.105
16																0.000	0.000	0.102
17																0.000	0.000	0.100
18																0.000	0.000	0.097
19																0.000	0.000	0.096
20																0.001	0.000	0.094
21																0.001	0.000	0.093
22																0.001	0.000	0.092
23																0.001	0.000	0.091
24																0.001	0.000	0.091
25																0.001	0.000	0.091
26																0.001	0.000	0.092
27																0.001	0.000	0.093
28																0.001	0.000	0.094
29																0.001	0.000	0.096
30																0.001	0.000	0.098
31																0.002	0.000	0.101
32																0.002	0.000	0.104
33																0.002	0.000	0.108
34																0.002	0.000	0.112
35																0.002	0.000	0.117
36																0.003	0.000	0.123
37																0.003	0.000	0.129
38																0.003	0.000	0.135
39																0.003	0.000	0.142
40																0.004	0.000	0.150
41																0.004	0.000	0.158
42																0.004	0.000	0.167
43																0.005	0.000	0.177
44																0.005	0.000	0.187
45																0.006	0.000	0.198
46																0.006	0.000	0.210
47																0.007	0.000	0.222

Table A6: Daily eddy covariance, energy balance component, and transpiration model results at FSL138 in 2002.

DOY	LE	H	Rn	G	Ta	e	Ts	θ	wind speed	λE_{uncorr}	res	LE_{corr}	H_{corr}	β	λE_{corr}	T_{Kc}	T_{GB}	EC Fourier
	Wm^{-2}	Wm^{-2}	Wm^{-2}	Wm^{-2}	°C	kPa	°C	m^3m^{-3}	$m\ s^{-1}$	mm day^{-1}	Wm^{-2}	Wm^{-2}	Wm^{-2}		mm day^{-1}	mm day^{-1}	mm day^{-1}	mm day^{-1}
48																0.008	0.000	0.235
49																0.008	0.000	0.249
50																0.009	0.000	0.263
51																0.010	0.000	0.278
52																0.011	0.000	0.294
53																0.012	0.000	0.311
54																0.013	0.000	0.329
55																0.014	0.000	0.347
56																0.016	0.000	0.366
57																0.017	0.000	0.386
58																0.018	0.000	0.406
59																0.020	0.000	0.428
60																0.022	0.000	0.450
61																0.023	0.000	0.473
62																0.025	0.001	0.497
63																0.028	0.002	0.522
64																0.030	0.002	0.547
65																0.032	0.003	0.573
66																0.035	0.004	0.601
67																0.038	0.005	0.629
68																0.041	0.006	0.657
69																0.044	0.008	0.687
70																0.047	0.009	0.717
71																0.051	0.011	0.749
72																0.055	0.013	0.781
73																0.059	0.015	0.814
74																0.064	0.018	0.847
75																0.068	0.020	0.882
76																0.074	0.023	0.917
77																0.079	0.027	0.953
78																0.085	0.030	0.990
79																0.091	0.034	1.027
80																0.097	0.039	1.065
81																0.104	0.043	1.104
82																0.111	0.049	1.144
83																0.119	0.054	1.185
84																0.127	0.060	1.226
85																0.136	0.067	1.268
86																0.145	0.074	1.310
87																0.154	0.082	1.353
88																0.165	0.091	1.397
89																0.175	0.100	1.442
90																0.187	0.110	1.487
91																0.198	0.120	1.532
92																0.211	0.132	1.579
93																0.224	0.144	1.625
94																0.238	0.157	1.673

Table A6: Daily eddy covariance, energy balance component, and transpiration model results at FSL138 in 2002.

DOY	LE	H	Rn	G	Ta	e	Ts	θ	wind speed	λE_{uncorr}	res	LE_{corr}	H_{corr}	β	λE_{corr}	T_{Kc}	T_{GB}	EC Fourier
	Wm^{-2}	Wm^{-2}	Wm^{-2}	Wm^{-2}	°C	kPa	°C	m^3m^{-3}	$m\ s^{-1}$	mm day^{-1}	Wm^{-2}	Wm^{-2}	Wm^{-2}		mm day^{-1}	mm day^{-1}	mm day^{-1}	mm day^{-1}
95																0.252	0.171	1.720
96																0.267	0.186	1.769
97																0.283	0.202	1.817
98																0.300	0.219	1.867
99																0.317	0.237	1.916
100																0.335	0.257	1.966
101																0.354	0.277	2.016
102																0.374	0.299	2.067
103																0.395	0.322	2.118
104																0.416	0.347	2.169
105																0.439	0.373	2.221
106																0.462	0.400	2.273
107																0.486	0.429	2.325
108																0.511	0.460	2.377
109																0.538	0.492	2.429
110																0.565	0.526	2.482
111																0.593	0.561	2.534
112																0.622	0.598	2.587
113																0.652	0.637	2.639
114																0.683	0.678	2.692
115																0.716	0.720	2.744
116																0.749	0.765	2.797
117																0.783	0.811	2.849
118																0.819	0.859	2.902
119																0.855	0.910	2.954
120																0.893	0.962	3.006
121																0.931	1.016	3.057
122																0.971	1.073	3.109
123	76.93	77.98	178.9	10.04	19.92	0.490		0.078	2.06	2.722		83.86		1.01	2.905	1.012	1.131	3.160
124	61.9	45.51	154.07	4.1	16.93	0.540		0.080	2.35	2.190		86.43		0.74	2.994	1.054	1.191	3.211
125	63.44	41.95	157.64	5.35	18.62	0.560		0.079	1.58	2.245		91.67		0.66	3.176	1.096	1.254	3.261
126	74.47	38.66	122.01	4.64	17.81	0.590		0.078	2.55	2.635		77.26		0.52	2.677	1.140	1.318	3.312
127	73.83	33.34	113.36	4	16.74	0.370		0.078	4.31	2.612		75.34		0.45	2.610	1.185	1.385	3.361
128	55.49	50.45	159.02	3.72	13.48	0.240		0.077	2.47	1.963		81.34		0.91	2.818	1.231	1.453	3.411
129	75.01	44.17	165.52	4	15.41	0.390		0.077	2.15	2.654		101.66		0.59	3.522	1.278	1.524	3.459
130	69.79	47.98	165.87	3.08	13.89	0.310		0.077	3.79	2.469		96.47		0.69	3.342	1.326	1.596	3.508
131	51.19	55.04	172.76	3.61	14.22	0.390		0.076	3.67	1.811		81.51		1.08	2.824	1.374	1.670	3.556
132	65.88	36.27	147.84	3.41	15.6	0.320		0.076	1.97	2.331		93.15		0.55	3.227	1.424	1.747	3.603
133	86.48	37.44	165.19	5.73	18.68	0.440		0.074	1.99	3.060		111.28		0.43	3.855	1.474	1.825	3.649
134	67.63	28.98	158.66	5.97	20.11	0.460		0.074	2.69	2.393		106.89		0.43	3.703	1.526	1.905	3.695
135	85.37	26.2	164.17	6.8	20.98	0.540		0.073	2.81	3.020		120.41		0.31	4.172	1.578	1.986	3.741
136	79.29	32.95	168.93	7.05	21.45	0.590		0.072	2.13	2.805		114.36		0.42	3.962	1.631	2.070	3.786
137	93.68	31.4	175.8	5.77	21.3	0.570		0.072	2.52	3.314		127.35		0.34	4.412	1.685	2.154	3.830
138	99.17	37.51	183.31	5.16	20.62	0.540		0.071	3.00	3.509		129.26		0.38	4.478	1.739	2.241	3.873
139	87.19	51.29	184.15	3.05	18.67	0.440		0.071	4.51	3.085		114.02		0.59	3.950	1.794	2.329	3.915
140	67.74	66.12	155.39	0.39	12.05	0.380		0.072	4.90	2.397		78.44		0.98	2.717	1.850	2.418	3.957
141	55.47	59.01	167.47	2.72	10.9	0.290		0.071	2.11	1.963		79.83		1.06	2.766	1.906	2.508	3.998

Table A6: Daily eddy covariance, energy balance component, and transpiration model results at FSL138 in 2002.

DOY	LE	H	Rn	G	Ta	e	Ts	θ	wind speed	λE_{uncorr}	res	LE_{corr}	H_{corr}	β	λE_{corr}	T_{Kc}	T_{GB}	EC Fourier
	Wm^{-2}	Wm^{-2}	Wm^{-2}	Wm^{-2}	°C	kPa	°C	m^3m^{-3}	$m\ s^{-1}$	$mm\ day^{-1}$	Wm^{-2}	Wm^{-2}	Wm^{-2}		$mm\ day^{-1}$	$mm\ day^{-1}$	$mm\ day^{-1}$	$mm\ day^{-1}$
142	61.65	61.57	171.63	3.23	11.71	0.330		0.071	1.51	2.181		84.25		1.00	2.919	1.963	2.600	4.038
143	63.45	48.05	171.65	5.24	16.13	0.400		0.070	3.41	2.245		94.70		0.76	3.281	2.020	2.692	4.077
144	75.33	46.71	172.45	5.53	16.85	0.380		0.070	1.48	2.665		103.03		0.62	3.569	2.077	2.786	4.115
145	86.5	35.67	175.55	5.25	19.29	0.470		0.066	2.28	3.060		120.58		0.41	4.177	2.135	2.880	4.152
146	83.14	40.46	175.61	6.71	20.45	0.600		0.066	1.83	2.942		113.61		0.49	3.936	2.193	2.975	4.189
147	87.57	36.58	175.54	6.16	21.24	0.610		0.065	2.06	3.098		119.47		0.42	4.139	2.252	3.071	4.224
148	90.07	35.24	176.45	6.15	20.85	0.560		0.065	1.74	3.187		122.41		0.39	4.241	2.310	3.167	4.259
149	100.83	27	181.33	6.47	21.97	0.520		0.065	1.91	3.567		137.93		0.27	4.778	2.368	3.263	4.292
150	107.65	25.65	185.97	7	24.29	0.540		0.066	1.88	3.809		144.53		0.24	5.007	2.427	3.359	4.324
151	87.26	10.23	149.56	6.2	24.45	0.720		0.066	2.49	3.087		128.32		0.12	4.445	2.485	3.456	4.356
152	78.32	9.67	133.39	4.69	22.3	0.730		0.067	2.47	2.771		114.56		0.12	3.969	2.544	3.552	4.386
153	88.02	27.21	164.8	6.06	21.08	0.510		0.066	1.81	3.114		121.26		0.31	4.201	2.602	3.647	4.415
154	85.34	18.64	164.35	6.57	22.89	0.520		0.066	3.12	3.019		129.50		0.22	4.486	2.660	3.743	4.443
155	100.93	21.01	175.62	7.33	24.76	0.500		0.065	2.18	3.571		139.29		0.21	4.826	2.717	3.837	4.470
156	99.82	19.55	183.54	9.22	27.34	0.770		0.064	1.72	3.532		145.77		0.20	5.050	2.774	3.931	4.495
157	126.51	8.47	185.67	7.92	26.36	0.690		0.064	2.11	4.476		166.60		0.07	5.772	2.830	4.023	4.520
158	119.67	15.72	184.16	6.78	24.71	0.520		0.064	2.09	4.234		156.78		0.13	5.432	2.886	4.115	4.543
159	129.75	9.03	178.91	5.5	24.06	0.370		0.064	4.13	4.591		162.13		0.07	5.617	2.941	4.205	4.565
160	65.33	47.37	181.38	3.27	15.29	0.250		0.065	5.79	2.311		103.25		0.73	3.577	2.996	4.293	4.586
161	77.85	39.25	175.85	5.15	17.93	0.380		0.065	2.92	2.754		113.48		0.50	3.932	3.049	4.380	4.606
162	92.94	37.97	188.59	6.19	19.23	0.480		0.064	2.01	3.288		129.50		0.41	4.486	3.101	4.465	4.625
163	98.85	34.29	193.48	6.03	21.61	0.530		0.064	2.03	3.497		139.17		0.35	4.821	3.153	4.548	4.642
164	105.54	30.47	195.94	6.23	22.64	0.560		0.064	2.58	3.734		147.21		0.29	5.100	3.203	4.629	4.658
165		1.32	10.29	4.87	21.84	0.570		0.064	68430					0.06		3.253	4.707	4.672
166			189	8.05	25.68	0.540		0.063	141420					0.06		3.301	4.783	4.686
167			190.36	7.68	25.98	0.470		0.062	141420					0.06		3.347	4.856	4.698
168			190.91	7.94	25.92	0.560		0.062	141420					0.06		3.392	4.926	4.709
169			190.37	8.62	27.37	0.750		0.062	141420					0.06		3.436	4.993	4.718
170			190.34	8.48	26.43	0.810		0.062	141420					0.06		3.478	5.057	4.727
171			171.46	5.98	24.88	0.860		0.063	141420					0.06		3.519	5.117	4.734
172			117.98	3.98	21.8	0.870		0.063	141420					0.06		3.558	5.175	4.739
173			196.54	5.84	20.59	0.780		0.064	141420					0.06		3.595	5.228	4.744
174			200.38	6.07	23.81	0.650		0.063	141420					0.06		3.630	5.278	4.747
175			199.48	6.72	24.29	0.630		0.063	141420					0.06		3.663	5.324	4.748
176			197.46	7.52	25.19	0.650		0.063	141420					0.06		3.694	5.366	4.749
177		17.46	191.1	6.72	25.01	0.680		0.062	64819			149.16		0.24	5.168	3.724	5.405	4.748
178	111.35	24.27	195.97	7.72	25.15	0.730		0.062	1.55	3.940		154.56		0.22	5.355	3.751	5.439	4.746
179	106.94	13.54	182.01	7.21	25.73	0.740		0.062	2.14	3.784		155.16		0.13	5.375	3.776	5.468	4.742
180	114.62	21.99	195.45	8.04	26.09	0.780		0.062	1.92	4.055		157.24		0.19	5.447	3.799	5.494	4.738
181	116.28	14.9	198.77	7.54	27.4	0.730		0.062	3.08	4.114		169.51		0.13	5.872	3.820	5.516	4.731
182	112.28	9.42	189.02	7.19	27.08	0.720		0.062	3.08	3.973		167.76		0.08	5.812	3.839	5.533	4.724
183	113.81	27.61	199.82	6.67	24.64	0.690		0.062	2.77	4.027		155.44		0.24	5.385	3.855	5.545	4.716
184	103.37	29.66	198.29	6.9	24.48	0.710		0.062	1.33	3.657		148.72		0.29	5.152	3.869	5.553	4.706
185	104.25	25.16	194.44	6.86	25.62	0.750		0.062	2.20	3.688		151.11		0.24	5.235	3.880	5.557	4.695
186	106.94	24.91	200.56	6.81	25.58	0.750		0.062	2.79	3.784		157.15		0.23	5.444	3.890	5.556	4.682
187	107.42	22.07	195.48	6.72	26.07	0.760		0.062	2.76	3.801		156.59		0.21	5.425	3.896	5.551	4.669
188	115.24	19.32	198.89	7.21	26.72	0.710		0.061	2.65	4.077		164.16		0.17	5.687	3.901	5.541	4.654

Table A6: Daily eddy covariance, energy balance component, and transpiration model results at FSL138 in 2002.

DOY	LE	H	Rn	G	Ta	e	Ts	θ	wind speed	λE_{uncorr}	res	LE_{corr}	H_{corr}	β	λE_{corr}	T_{Kc}	T_{GB}	EC Fourier
	Wm^{-2}	Wm^{-2}	Wm^{-2}	Wm^{-2}	°C	kPa	°C	m^3m^{-3}	$m\ s^{-1}$	$mm\ day^{-1}$	Wm^{-2}	Wm^{-2}	Wm^{-2}		$mm\ day^{-1}$	$mm\ day^{-1}$	$mm\ day^{-1}$	$mm\ day^{-1}$
189	105.44	20.3	202.25	7.51	25.26	0.650		0.061	1.35	3.731		163.30		0.19	5.657	3.903	5.527	4.638
190	105.97	13.81	180.77	8.16	28.25	0.710		0.061	1.34	3.749		152.71		0.13	5.290	3.903	5.509	4.621
191	116.65	11.27	165.77	8.76	29.71	0.750		0.061	1.30	4.127		143.18		0.10	4.960	3.900	5.486	4.602
192	78.4	13.86	127.69	6.88	27.76	1.040		0.061	1.74	2.774		102.66		0.18	3.557	3.895	5.459	4.583
193	90.3	17.78	151.03	7.71	28.67	1.210		0.061	2.04	3.195		119.74		0.20	4.148	3.887	5.428	4.562
194	89.32	13.03	138.64	6.87	28.43	1.090		0.061	2.29	3.160		114.99		0.15	3.984	3.877	5.392	4.540
195	91.42	14.66	138.9	6.79	28.32	1.030		0.061	1.94	3.235		113.85		0.16	3.944	3.865	5.353	4.517
196	111.49	15.54	165.16	6.76	27.1	0.830		0.061	2.63	3.945		139.02		0.14	4.816	3.850	5.309	4.493
197	89.81	20.29	145.59	6.64	26.52	0.790		0.061	1.72	3.178		113.34		0.23	3.927	3.833	5.261	4.468
198	74.09	13.62	114.57	5.08	25.43	0.950		0.061	1.74	2.621		92.49		0.18	3.204	3.814	5.210	4.442
199	68.2	27.94	133.31	3.79	22.69	1.030		0.062	2.36	2.413		91.88		0.41	3.183	3.792	5.155	4.415
200	78.92	43.73	167.14	6.27	23.37	0.960		0.062	1.10	2.792		103.51		0.55	3.586	3.768	5.097	4.386
201	81.92	29.56	155.54	5.74	24.18	0.770		0.062	1.99	2.898		110.08		0.36	3.814	3.742	5.035	4.357
202	92.8	31.18	156.6	5.23	24.4	0.600		0.062	2.85	3.283		113.30		0.34	3.925	3.714	4.970	4.327
203	81.86	5.21	117.73	3.42	23.52	0.470		0.062	2.88	2.896		107.47		0.06	3.723	3.684	4.901	4.296
204	82.17	31.22	149.6	5.25	24.22	0.690		0.062	1.99	2.907		104.61		0.38	3.624	3.652	4.830	4.264
205	75.27	16.79	142.23	6.95	26.98	0.990		0.061	2.21	2.663		110.61		0.22	3.832	3.617	4.756	4.231
206	85.02	21.6	149.28	7.77	27.56	1.020		0.061	1.89	3.008		112.84		0.25	3.909	3.581	4.679	4.197
207	95.59	19.95	151.05	7.1	27.75	0.620		0.061	1.53	3.382		119.09		0.21	4.126	3.543	4.599	4.163
208	92.15	16.71	144.41	5.94	25.1	0.630		0.062	1.97	3.260		117.21		0.18	4.061	3.503	4.518	4.127
209	88.53	23.48	153.16	6.48	26.03	0.650		0.061	1.25	3.132		115.93		0.27	4.016	3.462	4.434	4.091
210	96.09	26.32	156.94	6.7	26.9	0.610		0.061	1.14	3.400		117.94		0.27	4.086	3.418	4.348	4.054
211	94.7	16.34	151.02	6.35	27.34	0.690		0.061	2.16	3.351		123.38		0.17	4.274	3.374	4.260	4.016
212	78.32	9.4	124.49	6.33	27.67	0.830		0.061	1.93	2.771		105.50		0.12	3.655	3.327	4.170	3.978
213	62.55	0.76	88.14	4.66	26.45	0.920		0.062	1.91	2.213		82.48		0.01	2.857	3.279	4.079	3.939
214	80.96	21.84	146.43	6.21	26.72	0.850		0.061	2.60	2.864		110.43		0.27	3.826	3.230	3.987	3.899
215	82.43	27.81	144.45	5	25.02	0.730		0.062	3.10	2.916		104.27		0.34	3.612	3.180	3.893	3.858
216	85.58	27.11	147.18	4.61	22.51	0.550		0.062	2.23	3.028		108.27		0.32	3.751	3.128	3.799	3.817
217	68.58	37.14	147.2	4.66	21.15	0.600		0.062	1.81	2.426		92.46		0.54	3.203	3.075	3.704	3.776
218	74.44	38.48	144.23	4.4	21.68	0.700		0.062	2.40	2.634		92.18		0.52	3.193	3.022	3.608	3.734
219	74	29.28	137.3	4.54	21.35	0.640		0.062	2.13	2.618		95.12		0.40	3.295	2.967	3.511	3.691
220	75.19	27.7	139.38	5.66	22.29	0.610		0.062	1.57	2.660		97.72		0.37	3.385	2.911	3.414	3.648
221	78.13	26.5	142.57	5.28	22.58	0.670		0.062	1.22	2.764		102.52		0.34	3.552	2.855	3.317	3.604
222	77.26	25.3	143.06	5.44	22.77	0.700		0.062	1.15	2.734		103.67		0.33	3.592	2.798	3.221	3.560
223	73.23	24	137.36	5.58	24.65	0.700		0.062	1.31	2.591		99.25		0.33	3.438	2.740	3.124	3.516
224	74.38	18.24	134.38	6.44	27.29	0.700		0.062	1.18	2.632		102.74		0.25	3.559	2.682	3.027	3.471
225	82.6	10.95	132.98	6.95	28.54	0.670		0.061	1.41	2.922		111.28		0.13	3.855	2.623	2.931	3.426
226	75.74	2.81	117.75	6.63	28.57	0.710		0.061	1.78	2.680		107.14		0.04	3.712	2.564	2.836	3.380
227	68.74	5.67	104.04	5.66	27.39	0.750		0.061	1.69	2.432		90.88		0.08	3.149	2.504	2.741	3.334
228	75.92	15.06	133.57	6.09	27.49	0.720		0.061	1.51	2.686		106.38		0.20	3.685	2.445	2.647	3.288
229	87.43	7.52	129.5	6	27.52	0.560		0.061	1.78	3.093		113.72		0.09	3.940	2.385	2.555	3.242
230	83.29	18.11	138	5.81	25.97	0.580		0.061	1.69	2.947		108.58		0.22	3.762	2.325	2.463	3.196
231	84.81	20.92	135.07	4.92	24.59	0.460		0.062	2.11	3.001		104.40		0.25	3.617	2.266	2.372	3.149
232	80.89	22.12	136.62	3.91	22.57	0.390		0.062	2.41	2.862		104.21		0.27	3.610	2.206	2.283	3.102
233	63.69	33.96	135.42	3.09	19.42	0.440		0.063	1.58	2.253		86.31		0.53	2.990	2.147	2.195	3.056
234	62.37	35.4	137.71	3.74	20.37	0.500		0.062	1.87	2.207		85.46		0.57	2.961	2.087	2.109	3.009
235	67.94	33.07	139.09	4.83	22.08	0.510		0.062	1.57	2.404		90.30		0.49	3.128	2.029	2.024	2.962

Table A6: Daily eddy covariance, energy balance component, and transpiration model results at FSL138 in 2002.

DOY	LE	H	Rn	G	Ta	e	Ts	θ	wind speed	λE_{uncorr}	res	LE_{corr}	H_{corr}	β	λE_{corr}	T_{Kc}	T_{GB}	EC Fourier
	Wm^{-2}	Wm^{-2}	Wm^{-2}	Wm^{-2}	°C	kPa	°C	m^3m^{-3}	$m\ s^{-1}$	$mm\ day^{-1}$	Wm^{-2}	Wm^{-2}	Wm^{-2}		$mm\ day^{-1}$	$mm\ day^{-1}$	$mm\ day^{-1}$	$mm\ day^{-1}$
236	63.88	32.29	138.26	4.3	21.38	0.520		0.062	1.77	2.260		88.98		0.51	3.083	1.970	1.941	2.915
237	65.51	32.87	138.99	4.3	21.55	0.520		0.063	1.48	2.318		89.69		0.50	3.107	1.912	1.859	2.868
238	63.35	7.13	127.04	5.48	25.89	0.420		0.062	3.31	2.241		109.26		0.11	3.785	1.854	1.779	2.821
239	54.75	24.46	122.49	5.97	24.12	0.530		0.062	1.76	1.937		80.54		0.45	2.790	1.797	1.701	2.774
240	56.79	26.16	120.58	4.38	22.89	0.600		0.062	2.06	2.009		79.55		0.46	2.756	1.741	1.625	2.727
241	60.78	27.62	129.73	4.48	22.22	0.640		0.062	2.08	2.150		86.12		0.45	2.983	1.685	1.551	2.681
242	57.73	29.96	133.95	3.99	21.36	0.610		0.063	2.36	2.043		85.56		0.52	2.964	1.630	1.479	2.634
243	59.4	33.78	134.12	3.92	20.17	0.550		0.063	1.23	2.102		83.00		0.57	2.875	1.576	1.409	2.588
244	59.7	32.42	133.94	4.49	21.94	0.620		0.063	1.17	2.112		83.89		0.54	2.906	1.522	1.341	2.541
245	64.79	27.46	134.76	5.37	24.22	0.610		0.063	1.26	2.292		90.87		0.42	3.148	1.470	1.275	2.495
246	67.29	10.43	125.08	5.59	24.66	0.650		0.062	2.16	2.381		103.45		0.16	3.584	1.418	1.211	2.450
247	60.21	5.5	92.88	3.26	23.25	0.820		0.063	2.33	2.130		82.12		0.09	2.845	1.367	1.149	2.404
248	51.12	4.39	81.32	1.59	21.39	0.860		0.064	2.66	1.809		73.42		0.09	2.544	1.317	1.089	2.359
249	42.34	14.11	80.15	1.46	19.08	0.820		0.064	2.29	1.498		59.02		0.33	2.045	1.268	1.031	2.314
250	42.52	49.79	-6419	1.22	15.7	0.460		0.065	1.55	1.504				1.17		1.220	0.976	2.269
251	43.25	33.1	-6999	3.06	17.38	0.410		0.064	1.79	1.530				0.77		1.173	0.922	2.225
252	43.79	40.9	-6999	2.46	16.12	0.440		0.064	1.13	1.549				0.93		1.128	0.870	2.181
253	47.33	39.21	-6999	3.33	17.9	0.480		0.064	1.16	1.675				0.83		1.083	0.821	2.137
254	52.96	27.54	-6999	4.15	20.82	0.500		0.064	1.41	1.874				0.52		1.039	0.773	2.094
255			-6999	15.56				0.060								0.997	0.727	2.051
256																0.955	0.684	2.009
257																0.915	0.642	1.967
258																0.875	0.602	1.926
259																0.837	0.564	1.885
260																0.800	0.527	1.844
261																0.764	0.493	1.804
262			-6999	9.28				0.061								0.730	0.460	1.765
263			-2315	11.12				0.056								0.696	0.428	1.726
264			211.29	14.36				0.060								0.663	0.399	1.688
265			221.37	14.68				0.060								0.632	0.371	1.650
266			219.67	14.46				0.057								0.601	0.344	1.612
267			237.24	14.68				0.060								0.572	0.319	1.576
268			286.97	16.07				0.060								0.544	0.295	1.540
269			227.59	13.11				0.060								0.517	0.273	1.504
270			251.16	12.26				0.061								0.491	0.252	1.469
271			293.4	3.49				0.039								0.465	0.232	1.435
272			143.42	6.36				0.063								0.441	0.213	1.401
273			135.03	5.72				0.061								0.418	0.196	1.368
274			314.75	0.77				0.052								0.396	0.180	1.336
275			85.32	-0.46				0.066								0.374	0.164	1.304
276			-195.04	7.54				0.064								0.354	0.150	1.273
277			183.65	9.34				0.063								0.335	0.137	1.242
278			130.48	7.1				0.061								0.316	0.125	1.212
279			161.31	313.5				0.060								0.298	0.113	1.183
280			119.11	8.32				0.063								0.281	0.102	1.154
281			72.73	1.99				0.065								0.265	0.092	1.126
282																0.249	0.083	1.099

Table A6: Daily eddy covariance, energy balance component, and transpiration model results at FSL138 in 2002.

DOY	LE	H	Rn	G	Ta	e	Ts	θ	wind speed	λE_{uncorr}	res	LE_{corr}	H_{corr}	β	λE_{corr}	T_{Kc}	T_{GB}	EC Fourier
	Wm^{-2}	Wm^{-2}	Wm^{-2}	Wm^{-2}	°C	kPa	°C	m^3m^{-3}	$m\ s^{-1}$	$mm\ day^{-1}$	Wm^{-2}	Wm^{-2}	Wm^{-2}		$mm\ day^{-1}$	$mm\ day^{-1}$	$mm\ day^{-1}$	$mm\ day^{-1}$
283																0.235	0.075	1.072
284																0.221	0.067	1.046
285																0.207	0.060	1.020
286																0.195	0.053	0.995
287																0.183	0.047	0.971
288																0.171	0.041	0.947
289																0.161	0.036	0.924
290																0.150	0.032	0.902
291																0.141	0.028	0.880
292																0.132	0.024	0.858
293																0.123	0.020	0.838
294																0.115	0.017	0.818
295																0.107	0.014	0.798
296																0.100	0.012	0.779
297																0.093	0.010	0.760
298																0.087	0.008	0.742
299																0.081	0.006	0.725
300																0.075	0.004	0.708
301																0.070	0.003	0.691
302																0.065	0.002	0.675
303																0.061	0.001	0.660
304																0.056	0.000	0.645
305																0.052	0.000	0.630
306																0.048	0.000	0.616
307																0.045	0.000	0.602
308																0.042	0.000	0.589
309																0.038	0.000	0.576
310																0.036	0.000	0.564
311																0.033	0.000	0.552
312																0.030	0.000	0.540
313																0.028	0.000	0.529
314																0.026	0.000	0.518
315																0.024	0.000	0.507
316																0.022	0.000	0.497
317																0.020	0.000	0.486
318																0.019	0.000	0.477
319																0.017	0.000	0.467
320																0.016	0.000	0.458
321																0.015	0.000	0.449
322																0.013	0.000	0.440
323																0.012	0.000	0.432
324																0.011	0.000	0.423
325																0.010	0.000	0.415
326																0.010	0.000	0.407
327																0.009	0.000	0.400
328																0.008	0.000	0.392
329																0.007	0.000	0.385

Table A6: Daily eddy covariance, energy balance component, and transpiration model results at FSL138 in 2002.

DOY	LE	H	Rn	G	Ta	e	Ts	θ	wind speed	λE_{uncorr}	res	LE_{corr}	H_{corr}	β	λE_{corr}	T_{Kc}	T_{GB}	EC Fourier
	Wm^{-2}	Wm^{-2}	Wm^{-2}	Wm^{-2}	°C	kPa	°C	m^3m^{-3}	$m\ s^{-1}$	$mm\ day^{-1}$	Wm^{-2}	Wm^{-2}	Wm^{-2}		$mm\ day^{-1}$	$mm\ day^{-1}$	$mm\ day^{-1}$	$mm\ day^{-1}$
330																0.007	0.000	0.377
331																0.006	0.000	0.370
332																0.006	0.000	0.363
333																0.005	0.000	0.357
334																0.005	0.000	0.350
335																0.004	0.000	0.343
336																0.004	0.000	0.337
337																0.004	0.000	0.330
338																0.003	0.000	0.324
339																0.003	0.000	0.317
340																0.003	0.000	0.311
341																0.003	0.000	0.305
342																0.002	0.000	0.299
343																0.002	0.000	0.293
344																0.002	0.000	0.287
345																0.002	0.000	0.281
346																0.002	0.000	0.275
347																0.002	0.000	0.269
348																0.001	0.000	0.263
349																0.001	0.000	0.257
350																0.001	0.000	0.251
351																0.001	0.000	0.245
352																0.001	0.000	0.240
353																0.001	0.000	0.234
354																0.001	0.000	0.228
355																0.001	0.000	0.222
356																0.001	0.000	0.217
357																0.001	0.000	0.211
358																0.001	0.000	0.205
359																0.001	0.000	0.200
360																0.001	0.000	0.194
361																0.000	0.000	0.189
362																0.000	0.000	0.184
363																0.000	0.000	0.178
364																0.000	0.000	0.173
365																0.000	0.000	0.168

Table A7: Daily eddy covariance, energy balance component, and transpiration model results at PLC018 in 2002.

DOY	LE	H	Rn	G	Ta	e	Ts	θ	wind speed	λE_{uncorr}	res	LE_{corr}	H_{corr}	β	λE_{corr}	T_{Kc}	T_{GB}	EC Fourier
	Wm^{-2}	Wm^{-2}	Wm^{-2}	Wm^{-2}	°C	kPa	°C	m^3m^{-3}	$m\ s^{-1}$	$mm\ day^{-1}$	Wm^{-2}	Wm^{-2}	Wm^{-2}		$mm\ day^{-1}$	$mm\ day^{-1}$	$mm\ day^{-1}$	$mm\ day^{-1}$
1																0.000	0.000	0.049
2																0.000	0.000	0.048
3																0.000	0.000	0.047
4																0.000	0.000	0.045
5																0.000	0.000	0.044
6																0.000	0.000	0.043
7																0.000	0.000	0.042
8																0.000	0.000	0.041
9																0.000	0.000	0.040
10																0.000	0.000	0.040
11																0.001	0.000	0.039
12																0.001	0.000	0.038
13																0.001	0.000	0.037
14																0.001	0.000	0.036
15																0.001	0.000	0.036
16																0.001	0.000	0.035
17																0.001	0.000	0.035
18																0.001	0.000	0.034
19																0.001	0.000	0.034
20																0.001	0.000	0.033
21																0.001	0.000	0.033
22																0.001	0.000	0.032
23																0.001	0.000	0.032
24																0.001	0.000	0.032
25																0.002	0.000	0.032
26																0.002	0.000	0.031
27																0.002	0.000	0.031
28																0.002	0.000	0.031
29																0.002	0.000	0.031
30																0.002	0.000	0.031
31																0.003	0.000	0.032
32																0.003	0.000	0.032
33																0.003	0.000	0.032
34																0.003	0.000	0.032
35																0.003	0.000	0.033
36																0.004	0.000	0.033
37																0.004	0.000	0.033
38																0.004	0.000	0.034
39																0.005	0.000	0.035
40																0.005	0.000	0.035
41																0.005	0.000	0.036
42																0.006	0.000	0.037
43																0.006	0.000	0.037
44																0.007	0.000	0.038
45																0.007	0.000	0.039
46																0.008	0.000	0.040
47																0.008	0.000	0.041

Table A7: Daily eddy covariance, energy balance component, and transpiration model results at PLC018 in 2002.

DOY	LE	H	Rn	G	Ta	e	Ts	θ	wind speed	λE_{uncorr}	res	LE_{corr}	H_{corr}	β	λE_{corr}	T_{Kc}	T_{GB}	EC Fourier
	Wm^{-2}	Wm^{-2}	Wm^{-2}	Wm^{-2}	°C	kPa	°C	m^3m^{-3}	$m\ s^{-1}$	$mm\ day^{-1}$	Wm^{-2}	Wm^{-2}	Wm^{-2}		$mm\ day^{-1}$	$mm\ day^{-1}$	$mm\ day^{-1}$	$mm\ day^{-1}$
48																0.009	0.000	0.042
49																0.010	0.000	0.043
50																0.010	0.000	0.045
51																0.011	0.000	0.046
52																0.012	0.000	0.047
53																0.013	0.000	0.049
54																0.013	0.000	0.050
55																0.014	0.000	0.052
56																0.015	0.000	0.053
57																0.016	0.000	0.055
58																0.018	0.000	0.057
59																0.019	0.000	0.058
60																0.020	0.000	0.060
61																0.021	0.000	0.062
62																0.023	0.000	0.064
63																0.024	0.001	0.066
64																0.026	0.001	0.068
65																0.027	0.001	0.070
66																0.029	0.001	0.072
67																0.031	0.001	0.074
68																0.032	0.001	0.077
69																0.034	0.002	0.079
70																0.036	0.002	0.081
71																0.039	0.002	0.083
72																0.041	0.002	0.086
73																0.043	0.003	0.088
74																0.046	0.003	0.091
75																0.048	0.003	0.093
76																0.051	0.004	0.096
77																0.054	0.004	0.099
78																0.057	0.005	0.101
79																0.060	0.005	0.104
80																0.063	0.006	0.107
81																0.067	0.007	0.110
82																0.070	0.007	0.112
83																0.074	0.008	0.115
84																0.078	0.009	0.118
85																0.082	0.010	0.121
86																0.086	0.011	0.124
87																0.090	0.012	0.127
88																0.095	0.013	0.130
89																0.099	0.014	0.133
90																0.104	0.015	0.136
91																0.109	0.017	0.139
92																0.114	0.018	0.142
93																0.120	0.020	0.145
94																0.125	0.022	0.149

Table A7: Daily eddy covariance, energy balance component, and transpiration model results at PLC018 in 2002.

DOY	LE	H	Rn	G	Ta	e	Ts	θ	wind speed	λE_{uncorr}	res	LE_{corr}	H_{corr}	β	λE_{corr}	T_{Kc}	T_{GB}	EC Fourier
	Wm^{-2}	Wm^{-2}	Wm^{-2}	Wm^{-2}	°C	kPa	°C	m^3m^{-3}	$m\ s^{-1}$	$mm\ day^{-1}$	Wm^{-2}	Wm^{-2}	Wm^{-2}		$mm\ day^{-1}$	$mm\ day^{-1}$	$mm\ day^{-1}$	$mm\ day^{-1}$
95																0.131	0.024	0.152
96																0.137	0.025	0.155
97																0.143	0.028	0.158
98																0.149	0.030	0.161
99																0.156	0.032	0.165
100																0.162	0.035	0.168
101																0.169	0.037	0.171
102																0.176	0.040	0.174
103																0.183	0.043	0.177
104																0.191	0.046	0.181
105																0.199	0.049	0.184
106																0.206	0.053	0.187
107																0.214	0.057	0.190
108																0.223	0.061	0.194
109																0.231	0.065	0.197
110																0.240	0.069	0.200
111																0.249	0.073	0.203
112																0.258	0.078	0.206
113																0.267	0.083	0.210
114																0.276	0.088	0.213
115																0.286	0.093	0.216
116																0.296	0.099	0.219
117																0.306	0.105	0.222
118																0.316	0.111	0.225
119																0.326	0.117	0.228
120																0.337	0.124	0.231
121																0.348	0.130	0.234
122	2.87	123.49	108.5	13.09	20.4	0.370		0.069	1.35	0.102		2.17		43.01	0.077	0.358	0.137	0.237
123	4.43	104.32	151.93	6.34	16.96	0.450		0.075	1.61	0.157		5.93		23.55	0.210	0.369	0.145	0.240
124	3.88	90.48	142.52	6.1	17.78	0.470		0.075	2.02	0.137		5.61		23.32	0.198	0.381	0.152	0.243
125	3.95	87.75	141.04	7.44	19.35	0.500		0.074	1.60	0.140		5.75		22.23	0.204	0.392	0.160	0.246
126	4.94	93.47	144.49	6.52	18.73	0.470		0.074	2.46	0.175		6.93		18.91	0.245	0.403	0.168	0.249
127	5.18	87.8	140.69	5.55	18.38	0.290		0.074	3.70	0.183		7.53		16.95	0.266	0.415	0.176	0.252
128	5.15	94.96	136.79	3.19	14.62	0.170		0.076	2.71	0.182		6.87		18.44	0.243	0.426	0.185	0.255
129	4.41	97.1	147.89	3.99	16.32	0.310		0.076	1.96	0.156		6.25		22.02	0.221	0.438	0.193	0.257
130	3.92	100.12	145.69	2.99	14.8	0.280		0.076	3.48	0.139		5.38		25.54	0.190	0.450	0.202	0.260
131	5.1	101.44	151	1.52	14.71	0.380		0.077	3.38	0.180		7.16		19.88	0.253	0.462	0.212	0.263
132	5.37	80.67	126	2.91	17.21	0.260		0.077	2.38	0.190		7.68		15.02	0.272	0.474	0.221	0.265
133	4.76	88.67	142.39	7.02	19.78	0.340		0.074	1.98	0.168		6.90		18.63	0.244	0.486	0.231	0.268
134	5.9	78.86	136.17	7.46	21.43	0.380		0.073	2.51	0.209		8.96		13.37	0.317	0.498	0.241	0.271
135	5.59	87.46	142.16	8.01	21.44	0.450		0.072	1.87	0.198		8.06		15.65	0.285	0.510	0.251	0.273
136	5.69	84.29	143.79	8.08	22.87	0.470		0.072	1.89	0.201		8.58		14.81	0.304	0.523	0.261	0.276
137	6.05	94.75	146.23	8.22	22.85	0.470		0.072	2.19	0.214		8.28		15.67	0.293	0.535	0.271	0.278
138	6.55	102.48	156.53	7.31	22.64	0.430		0.072	2.91	0.232		8.96		15.64	0.317	0.547	0.282	0.280
139	5.85	120.31	160.65	5.81	21	0.380		0.073	5.01	0.207		7.18		20.55	0.254	0.559	0.293	0.283
140	4.14	125.11	142.16	1.46	13.43	0.330		0.076	4.68	0.146		4.51		30.21	0.159	0.572	0.304	0.285
141	3.11	114.02	155.86	-1.11	11.18	0.250		0.078	1.82	0.110		4.17		36.62	0.147	0.584	0.315	0.287

Table A7: Daily eddy covariance, energy balance component, and transpiration model results at PLC018 in 2002.

DOY	LE	H	Rn	G	Ta	e	Ts	θ	wind speed	λE_{uncorr}	res	LE_{corr}	H_{corr}	β	λE_{corr}	T_{Kc}	T_{GB}	EC Fourier
	Wm^{-2}	Wm^{-2}	Wm^{-2}	Wm^{-2}	°C	kPa	°C	m^3m^{-3}	$m\ s^{-1}$	$mm\ day^{-1}$	Wm^{-2}	Wm^{-2}	Wm^{-2}		$mm\ day^{-1}$	$mm\ day^{-1}$	$mm\ day^{-1}$	$mm\ day^{-1}$
142	2.86	90.51	148.44	1.23	13.17	0.280		0.077	1.39	0.101		4.51		31.69	0.160	0.596	0.326	0.290
143	3.63	92.11	149.54	4.02	16.65	0.360		0.075	2.54	0.128		5.52		25.38	0.195	0.608	0.337	0.292
144	4.9	95.12	148.71	5.1	18.58	0.290		0.074	1.81	0.173		7.04		19.42	0.249	0.620	0.349	0.294
145	4.62	98.48	149.24	6.86	20.67	0.370		0.073	2.47	0.163		6.38		21.31	0.226	0.633	0.360	0.296
146	3.53	96.17	150.36	7.83	21.17	0.510		0.072	1.58	0.125		5.05		27.24	0.179	0.644	0.372	0.298
147	5.29	94.08	140.46	6.7	21.44	0.530		0.072	2.26	0.187		7.12		17.79	0.252	0.656	0.383	0.300
148	6.2	94.8	147.95	7.34	22.54	0.450		0.072	2.11	0.219		8.63		15.29	0.305	0.668	0.395	0.302
149	6.8	87.14	148.4	8.73	24.83	0.370		0.070	2.40	0.241		10.11		12.82	0.358	0.680	0.407	0.303
150	6.08	94.36	152.83	10.02	26.38	0.350		0.069	2.21	0.215		8.64		15.51	0.306	0.691	0.419	0.305
151	5.21	79.5	125.06	8.44	25.9	0.560		0.070	2.39	0.184		7.17		15.26	0.254	0.703	0.430	0.307
152	6.02	63.14	100.83	5.06	23.07	0.650		0.072	2.33	0.213		8.34		10.48	0.295	0.714	0.442	0.308
153	5.89	81.78	137.53	5.39	21.92	0.470		0.072	1.74	0.208		8.88		13.88	0.314	0.725	0.454	0.310
154	6.04	96.13	151.08	6.82	22.96	0.460		0.071	2.01	0.214		8.53		15.92	0.302	0.736	0.465	0.312
155	5.76	88.5	149.91	7.02	24.49	0.410		0.071	1.63	0.204		8.73		15.36	0.309	0.746	0.477	0.313
156	7.07	88.4	153.5	10.37	27.91	0.600		0.068	1.34	0.250		10.60		12.51	0.375	0.757	0.488	0.314
157	7.49	89.08	151.83	10.22	27.98	0.520		0.068	2.26	0.265		10.98		11.89	0.389	0.767	0.499	0.316
158	8.5	90.81	149.13	8.74	26.4	0.400		0.068	2.08	0.301		12.02		10.69	0.425	0.777	0.510	0.317
159	9.16	95.45	146.83	6.66	24.87	0.280		0.070	3.85	0.324		12.27		10.42	0.434	0.787	0.521	0.318
160				0.79				0.073								0.796	0.532	0.319
161																0.805	0.542	0.321
162	5.01	93.13			-2103	-2127			3012	0.177				18.58		0.814	0.552	0.322
163	5.31	101.76	238.58	14.06	25.97	0.420		0.064	3.05	0.188		11.13		19.16	0.394	0.822	0.562	0.323
164	6.98	89.77	160.21	8.11	25.74	0.470		0.069	1.22	0.247		10.97		12.87	0.388	0.831	0.572	0.324
165	6.59	89.28	152.96	8.76	26.6	0.350		0.068	1.42	0.233		9.91		13.55	0.351	0.839	0.581	0.324
166	6.95	83.8	152.55	8.7	27.39	0.360		0.068	1.20	0.246		11.02		12.06	0.390	0.846	0.591	0.325
167	7.58	79.18	150.75	8.76	29.41	0.410		0.068	2.32	0.268		12.41		10.45	0.439	0.853	0.599	0.326
168	6.15	89.21	152.46	8.64	28.65	0.670		0.068	3.33	0.218		9.28		14.52	0.328	0.860	0.608	0.327
169	25.3	97.99	155.89	9.53	25.87	0.790		0.067	1.69	0.895		30.03		3.87	1.063	0.867	0.616	0.327
170	22.14	95.42	163.42	8.78	26.35	0.770		0.067	3.27	0.783		29.12		4.31	1.030	0.873	0.623	0.328
171	6.72	70.97	181.62	3.52	21.02	0.740		0.071	2.01	0.238		15.41		10.57	0.545	0.878	0.630	0.328
172	6.9	96.47	106.07	1.31	24.59	0.580		0.072	1.43	0.244		6.99		13.99	0.247	0.884	0.637	0.329
173	6.61	104.47	164.98	5.02	25.77	0.490		0.070	2.63	0.234		9.52		15.80	0.337	0.889	0.644	0.329
174	6.03	100.33	171.49	7.46	26.96	0.520		0.068	2.26	0.213		9.30		16.64	0.329	0.893	0.649	0.329
175	6.05	93.14	168.08	7.92	28.01	0.490		0.068	2.23	0.214		9.77		15.39	0.346	0.897	0.655	0.330
176	5.98	100.24	165.24	8.71	28.02	0.500		0.067	2.95	0.212		8.81		16.77	0.312	0.901	0.660	0.330
177	4.33	93.31	163.49	8.5	27.8	0.530		0.067	2.01	0.153		6.87		21.57	0.243	0.904	0.664	0.330
178	6.48	83.6	158.81	9.26	27.94	0.570		0.066	2.49	0.229		10.76		12.91	0.381	0.907	0.668	0.330
179	5.41	93.82	147.33	8.2	29.52	0.630		0.067	2.77	0.191		7.59		17.34	0.268	0.909	0.672	0.330
180	6.4	101.39	161.61	9.13	29.9	0.500		0.066	3.59	0.226		9.05		15.84	0.320	0.911	0.675	0.330
181	6.29	90.65	167.15	9.18	29.35	0.530		0.066	3.31	0.223		10.25		14.41	0.363	0.912	0.677	0.330
182	6.19	136.52	153.09	8.4	30.95	0.400		0.066	3.80	0.219		6.28		22.04	0.222	0.913	0.679	0.330
183			146.21	8.2				0.066								0.914	0.680	0.330
184																0.914	0.681	0.330
185																0.914	0.681	0.329
186																0.913	0.681	0.329
187																0.912	0.680	0.329
188																0.910	0.679	0.328

Table A7: Daily eddy covariance, energy balance component, and transpiration model results at PLC018 in 2002.

DOY	LE	H	Rn	G	Ta	e	Ts	θ	wind speed	λE_{uncorr}	res	LE_{corr}	H_{corr}	β	λE_{corr}	T_{Kc}	T_{GB}	EC Fourier
	Wm^{-2}	Wm^{-2}	Wm^{-2}	Wm^{-2}	°C	kPa	°C	m^3m^{-3}	$m\ s^{-1}$	mm day^{-1}	Wm^{-2}	Wm^{-2}	Wm^{-2}		mm day^{-1}	mm day^{-1}	mm day^{-1}	mm day^{-1}
189																0.908	0.677	0.328
190	5.71	123.19	227.55	18.05	36.77	0.450		0.057	1.33	0.202		9.28		21.56	0.328	0.905	0.674	0.327
191	6.97	81.61	162.53	9.96	32.25	0.470		0.064	1.62	0.247		12.01		11.71	0.425	0.902	0.672	0.327
192	16.72	71.95	120.15	7.16	29.59	1.000		0.067	1.90	0.592		21.31		4.30	0.754	0.899	0.668	0.326
193	16.24	94.3	169.27	5.11	30	1.100		0.068	2.13	0.575		24.12		5.81	0.853	0.895	0.664	0.325
194	7.66	89.48	145.12	7.55	30.42	0.920		0.066	2.17	0.271		10.85		11.68	0.384	0.891	0.660	0.325
195	7.02	81.11	141.46	6.55	29.86	0.900		0.067	2.03	0.248		10.75		11.55	0.380	0.886	0.655	0.324
196	5.95	108.41	169.61	6.66	28.62	0.710		0.067	2.26	0.211		8.48		18.22	0.300	0.881	0.649	0.323
197	5.46	83.85	145.69	6.16	28.13	0.650		0.067	1.65	0.193		8.53		15.36	0.302	0.875	0.643	0.322
198	6.03	87.47	135.47	4.59	26.85	0.820		0.069	2.41	0.213		8.44		14.50	0.299	0.869	0.637	0.321
199	11.84	93.01	151.73	2.01	23.85	0.930		0.070	2.32	0.419		16.91		7.85	0.598	0.863	0.630	0.320
200	4.67	96.53	167.69	4.35	25.74	0.790		0.069	1.48	0.165		7.54		20.69	0.267	0.856	0.623	0.320
201	5.18	87.52	151.69	5.78	27.61	0.610		0.068	2.53	0.183		8.15		16.88	0.288	0.849	0.615	0.318
202	5.66	89.61	153.92	4.4	27.05	0.450		0.069	3.38	0.200		8.88		15.83	0.314	0.841	0.607	0.317
203	4.25	71.73	126.95	1.88	25.77	0.330		0.071	3.49	0.150		7.00		16.87	0.248	0.833	0.598	0.316
204	3.81	89.12	151.27	3.14	26.14	0.540		0.070	2.41	0.135		6.07		23.38	0.215	0.825	0.590	0.315
205	4	71.61	134.05	5.45	28.03	0.860		0.069	2.17	0.142		6.80		17.91	0.241	0.817	0.580	0.314
206	5.7	83.57	148.06	6.89	28.91	0.870		0.068	1.53	0.202		9.01		14.67	0.319	0.808	0.571	0.313
207	4.67	83.33	154.57	5.6	27.96	0.510		0.068	1.70	0.165		7.91		17.85	0.280	0.799	0.561	0.312
208	5.47	79.07	147.3	5.23	27.65	0.460		0.068	2.41	0.194		9.19		14.47	0.325	0.789	0.551	0.310
209	4.04	78.66	153.57	5.49	27.97	0.460		0.068	1.63	0.143		7.23		19.47	0.256	0.779	0.541	0.309
210	5.3	76.49	153.79	6.36	29.54	0.440		0.067	1.62	0.188		9.55		14.44	0.338	0.769	0.530	0.308
211	5.11	88.35	152.11	5.84	29.18	0.530		0.068	2.05	0.181		8.00		17.27	0.283	0.759	0.520	0.307
212	4.53	67.38	130.3	4.96	28.87	0.650		0.068	1.89	0.160		7.90		14.86	0.279	0.749	0.509	0.305
213	3.93	50.47	92.84	2.88	27.55	0.760		0.070	1.98	0.139		6.50		12.84	0.230	0.738	0.497	0.304
214	4.71	87.75	155.26	3.91	27.69	0.730		0.069	2.47	0.167		7.71		18.61	0.273	0.727	0.486	0.302
215	3.87	95.65	159.23	3.05	25.78	0.630		0.070	3.04	0.137		6.07		24.74	0.215	0.716	0.475	0.301
216	5.79	92.68	159.56	2.15	23.39	0.460		0.071	1.90	0.205		9.26		16.00	0.327	0.704	0.463	0.299
217	1.95	89.57	157.65	1.63	22.64	0.480		0.071	1.88	0.069		3.32		45.93	0.118	0.693	0.451	0.298
218	3.79	89.36	155.36	1.52	23.18	0.490		0.072	2.71	0.134		6.26		23.56	0.221	0.681	0.440	0.296
219	3.34	80.4	146.99	2.17	23.37	0.420		0.071	2.13	0.118		5.78		24.11	0.204	0.669	0.428	0.295
220	2.98	74.45	149.08	2.76	24.6	0.330		0.071	1.77	0.105		5.63		24.98	0.199	0.657	0.416	0.293
221	3.8	71.3	146.75	3.55	26.13	0.320		0.071	1.71	0.134		7.25		18.75	0.256	0.645	0.404	0.292
222	3.46	75.95	146.41	3.8	26.36	0.350		0.070	1.43	0.122		6.21		21.97	0.220	0.633	0.392	0.290
223	3.98	69.95	141.38	4.13	27.34	0.400		0.070	1.57	0.141		7.39		17.57	0.261	0.620	0.381	0.289
224	4.54	65.46	139.49	5.08	28.85	0.480		0.069	1.40	0.161		8.72		14.43	0.308	0.608	0.369	0.287
225	4.28	69.11	139.69	5.28	29.3	0.480		0.069	1.05	0.151		7.84		16.14	0.277	0.596	0.357	0.285
226	5.71	69.77	139.18	5.07	29.58	0.540		0.069	1.25	0.202		10.15		12.23	0.359	0.583	0.346	0.284
227	4.41	59.21	116.06	4.05	28.19	0.610		0.070	1.74	0.156		7.76		13.43	0.275	0.571	0.334	0.282
228	5.16	65.06	138.9	3.86	28.81	0.550		0.069	1.24	0.183		9.92		12.61	0.351	0.558	0.323	0.280
229	5.43	66.56	136.28	4.28	28.66	0.430		0.069	1.61	0.192		9.96		12.25	0.352	0.545	0.311	0.279
230	5.69	74.4	143.76	3.73	27.89	0.400		0.070	1.50	0.201		9.95		13.07	0.352	0.533	0.300	0.277
231	6.22	70.47	139.8	2.19	25.89	0.340		0.070	2.15	0.220		11.16		11.33	0.395	0.520	0.289	0.275
232	3.13	75.54	146.42	1.06	24.21	0.270		0.072	2.59	0.111		5.78		24.12	0.205	0.508	0.278	0.274
233	2.97	69.82	144.94	-0.41	22.94	0.350		0.073	2.65	0.105		5.93		23.47	0.210	0.495	0.268	0.272
234	3.21	82.98	148.81	-0.02	21.92	0.390		0.073	1.98	0.114		5.54		25.86	0.196	0.483	0.257	0.270
235	3.08	80.73	149.36	0.89	22.86	0.400		0.072	1.18	0.109		5.46		26.20	0.193	0.470	0.247	0.268

Table A7: Daily eddy covariance, energy balance component, and transpiration model results at PLC018 in 2002.

DOY	LE	H	Rn	G	Ta	e	Ts	θ	wind speed	λE_{uncorr}	res	LE_{corr}	H_{corr}	β	λE_{corr}	T_{Kc}	T_{GB}	EC Fourier
	Wm^{-2}	Wm^{-2}	Wm^{-2}	Wm^{-2}	°C	kPa	°C	m^3m^{-3}	$m\ s^{-1}$	$mm\ day^{-1}$	Wm^{-2}	Wm^{-2}	Wm^{-2}		$mm\ day^{-1}$	$mm\ day^{-1}$	$mm\ day^{-1}$	$mm\ day^{-1}$
236	3.21	75.89	149.03	0.6	23.13	0.420		0.073	2.18	0.114		6.02		23.67	0.213	0.458	0.237	0.267
237	3.64	72.8	146.92	1.25	23.73	0.390		0.073	1.72	0.129		6.94		20.01	0.245	0.446	0.227	0.265
238	3.62	66.13	147.09	1.54	25.62	0.350		0.072	2.54	0.128		7.55		18.26	0.267	0.434	0.217	0.263
239	2.06	63.22	133.02	1.65	24.5	0.390		0.072	1.50	0.073		4.15		30.69	0.147	0.421	0.208	0.261
240	2.4	70.38	131.19	0.63	23.63	0.500		0.073	2.25	0.085		4.31		29.30	0.152	0.410	0.198	0.260
241	3.73	68.5	137.69	0.49	23.57	0.530		0.073	2.55	0.132		7.09		18.36	0.251	0.398	0.189	0.258
242	3.71	77.21	145.17	0.87	23.66	0.480		0.073	2.79	0.131		6.62		20.84	0.234	0.386	0.180	0.256
243	3.27	78.06	142.51	0.5	22.19	0.370		0.073	1.39	0.116		5.71		23.85	0.202	0.375	0.172	0.254
244	2.71	66.34	140.81	1.02	24.11	0.470		0.073	1.42	0.096		5.49		24.52	0.194	0.363	0.164	0.252
245	3.56	66.44	143.17	2.44	25.57	0.480		0.072	1.37	0.126		7.16		18.66	0.253	0.352	0.156	0.251
246	3.11	63.21	140.91	2.48	26.35	0.560		0.072	2.26	0.110		6.49		20.31	0.230	0.341	0.148	0.249
247	3.38	27.04	65.64	-0.6	23.88	0.740		0.074	1.87	0.120		7.36		8.00	0.260	0.330	0.140	0.247
248	2.86	14.23	46.69	-3.73	21.98	0.820		0.076	2.59	0.101		8.44		4.98	0.299	0.319	0.133	0.245
249	4.04	30.43	69.22	-1.83	21.15	0.740		0.076	2.03	0.143		8.33		7.54	0.295	0.309	0.126	0.244
250	2.86	80.01	142.06	-3.48	17.56	0.380		0.077	2.03	0.101		5.02		27.99	0.178	0.298	0.119	0.242
251	2.54	68.06	137.58	-2.56	18.04	0.330		0.077	1.32	0.090		5.04		26.84	0.178	0.288	0.113	0.240
252	1.97	69.91	138.08	-2.48	17.86	0.330		0.077	1.20	0.070		3.85		35.57	0.136	0.278	0.106	0.238
253	2.36	66.61	137.94	-1.31	19.69	0.350		0.076	1.24	0.083		4.76		28.21	0.169	0.268	0.100	0.236
254	3.31	63.16	137.42	-0.17	21.82	0.370		0.076	1.48	0.117		6.85		19.08	0.242	0.259	0.095	0.235
255	2.8	62.97	134.62	0	21.79	0.360		0.075	1.20	0.099		5.73		22.51	0.203	0.249	0.089	0.233
256	2.64	60.38	133.79	-0.07	21.94	0.400		0.075	1.15	0.093		5.61		22.84	0.198	0.240	0.084	0.231
257	4.01	57.47	129.92	0.16	23.66	0.420		0.075	2.75	0.142		8.46		14.35	0.299	0.231	0.079	0.229
258	2.14	63.36	125.41	0.92	23.04	0.470		0.075	2.76	0.076		4.07		29.55	0.144	0.222	0.074	0.228
259	3.27	60.07	129.98	-0.85	21.14	0.340		0.075	1.82	0.116		6.75		18.40	0.239	0.214	0.069	0.226
260	2.73	56.05	122.64	-1.9	20.56	0.410		0.076	1.79	0.097		5.78		20.56	0.205	0.206	0.065	0.224
261	2.82	50.93	128.61	0.02	21.6	0.580		0.075	4.00	0.100		6.75		18.05	0.239	0.197	0.061	0.222
262	1.99	54.78	127.65	-0.42	21.46	0.500		0.076	1.63	0.070		4.49		27.57	0.159	0.190	0.056	0.220
263	2.49	58.31	127.73	-0.85	21.08	0.480		0.076	1.54	0.088		5.27		23.47	0.186	0.182	0.053	0.219
264	2.37	56.5	126	-0.25	22	0.470		0.075	1.33	0.084		5.08		23.80	0.180	0.174	0.049	0.217
265	2.69	55.78	123.79	-0.29	22.37	0.430		0.075	1.22	0.095		5.71		20.73	0.202	0.167	0.046	0.215
266	3.15	51.62	123.1	-0.59	22.45	0.380		0.075	1.56	0.111		7.11		16.36	0.252	0.160	0.042	0.213
267	3.38	45.23	109.83	-0.86	22.68	0.410		0.076	1.58	0.120		7.70		13.38	0.272	0.153	0.039	0.212
268	3.36	43.28	109.05	0.86	24.4	0.500		0.075	2.26	0.119		7.79		12.87	0.276	0.147	0.036	0.210
269	1.91	56.29	118.25	-1.06	21.4	0.350		0.076	1.97	0.068		3.92		29.47	0.139	0.140	0.034	0.208
270	2.64	31.05	75.91	-3.2	20.23	0.470		0.077	2.12	0.093		6.20		11.75	0.219	0.134	0.031	0.206
271	17.04	7.5	34.09	-5.9	14.92	0.860		0.079	1.89	0.603		27.77		0.44	0.982	0.128	0.029	0.205
272	22.94	46.45	135.78	-6.89	14.93	0.760		0.081	1.89	0.812		47.17		2.03	1.669	0.122	0.026	0.203
273	5.8	57.43	114.99	-4.46	15.08	0.640		0.080	1.62	0.205		10.96		9.90	0.388	0.117	0.024	0.201
274	7.51	39.02	79.4	-8.6	10.72	0.470		0.083	3.61	0.266		14.20		5.20	0.503	0.111	0.022	0.200
275	3.55	54.91	106.51	-8.37	9.89	0.400		0.083	4.70	0.126		6.98		15.46	0.247	0.106	0.020	0.198
276	2.23	48.32	115.5	-6.1	13.57	0.300		0.083	2.28	0.079		5.36		21.63	0.190	0.101	0.019	0.196
277	0.83	38.27	79.66	-1.88	15.47	0.450		0.080	1.08	0.029		1.73		46.23	0.061	0.096	0.017	0.194
278	1.87	48.86	113.15	-3.77	15.18	0.540		0.081	1.16	0.066		4.31		26.19	0.152	0.091	0.016	0.193
279	1.84	44.37	112.26	-2.13	17.38	0.530		0.080	1.38	0.065		4.55		24.13	0.161	0.087	0.014	0.191
280	2.59	41.74	110.04	-1.64	18.47	0.500		0.080	1.70	0.092		6.52		16.14	0.231	0.083	0.013	0.189
281	2.32	38.39	105.56	-2.54	17.33	0.310		0.080	1.20	0.082		6.16		16.53	0.218	0.078	0.012	0.188
282																0.074	0.011	0.186

Table A7: Daily eddy covariance, energy balance component, and transpiration model results at PLC018 in 2002.

DOY	LE	H	Rn	G	Ta	e	Ts	θ	wind speed	λE_{uncorr}	res	LE_{corr}	H_{corr}	β	λE_{corr}	T_{Kc}	T_{GB}	EC Fourier
	Wm^{-2}	Wm^{-2}	Wm^{-2}	Wm^{-2}	°C	kPa	°C	m^3m^{-3}	$m\ s^{-1}$	mm day^{-1}	Wm^{-2}	Wm^{-2}	Wm^{-2}		mm day^{-1}	mm day^{-1}	mm day^{-1}	mm day^{-1}
283																0.071	0.009	0.184
284																0.067	0.008	0.182
285																0.063	0.008	0.181
286																0.060	0.007	0.179
287																0.057	0.006	0.177
288																0.054	0.005	0.176
289																0.051	0.005	0.174
290																0.048	0.004	0.172
291																0.045	0.004	0.171
292																0.043	0.003	0.169
293																0.040	0.003	0.167
294																0.038	0.002	0.166
295																0.036	0.002	0.164
296																0.034	0.002	0.162
297																0.032	0.001	0.160
298																0.030	0.001	0.159
299																0.028	0.001	0.157
300																0.026	0.001	0.155
301																0.025	0.001	0.154
302																0.023	0.000	0.152
303																0.022	0.000	0.150
304																0.021	0.000	0.149
305																0.019	0.000	0.147
306																0.018	0.000	0.145
307																0.017	0.000	0.143
308																0.016	0.000	0.142
309																0.015	0.000	0.140
310																0.014	0.000	0.138
311																0.013	0.000	0.137
312																0.012	0.000	0.135
313																0.011	0.000	0.133
314																0.011	0.000	0.131
315																0.010	0.000	0.130
316																0.009	0.000	0.128
317																0.009	0.000	0.126
318																0.008	0.000	0.125
319																0.007	0.000	0.123
320																0.007	0.000	0.121
321																0.006	0.000	0.119
322																0.006	0.000	0.118
323																0.006	0.000	0.116
324																0.005	0.000	0.114
325																0.005	0.000	0.113
326																0.004	0.000	0.111
327																0.004	0.000	0.109
328																0.004	0.000	0.107
329																0.004	0.000	0.106

Table A7: Daily eddy covariance, energy balance component, and transpiration model results at PLC018 in 2002.

DOY	LE	H	Rn	G	Ta	e	Ts	θ	wind speed	λE_{uncorr}	res	LE_{corr}	H_{corr}	β	λE_{corr}	T_{Kc}	T_{GB}	EC Fourier
	Wm^{-2}	Wm^{-2}	Wm^{-2}	Wm^{-2}	°C	kPa	°C	m^3m^{-3}	$m\ s^{-1}$	$mm\ day^{-1}$	Wm^{-2}	Wm^{-2}	Wm^{-2}		$mm\ day^{-1}$	$mm\ day^{-1}$	$mm\ day^{-1}$	$mm\ day^{-1}$
330																0.003	0.000	0.104
331																0.003	0.000	0.102
332																0.003	0.000	0.100
333																0.003	0.000	0.099
334																0.002	0.000	0.097
335																0.002	0.000	0.095
336																0.002	0.000	0.094
337																0.002	0.000	0.092
338																0.002	0.000	0.090
339																0.002	0.000	0.089
340																0.002	0.000	0.087
341																0.001	0.000	0.085
342																0.001	0.000	0.084
343																0.001	0.000	0.082
344																0.001	0.000	0.080
345																0.001	0.000	0.079
346																0.001	0.000	0.077
347																0.001	0.000	0.076
348																0.001	0.000	0.074
349																0.001	0.000	0.072
350																0.001	0.000	0.071
351																0.001	0.000	0.069
352																0.001	0.000	0.068
353																0.001	0.000	0.066
354																0.001	0.000	0.065
355																0.001	0.000	0.063
356																0.001	0.000	0.062
357																0.000	0.000	0.061
358																0.000	0.000	0.059
359																0.000	0.000	0.058
360																0.000	0.000	0.056
361																0.000	0.000	0.055
362																0.000	0.000	0.054
363																0.000	0.000	0.052
364																0.000	0.000	0.051
365																0.000	0.000	0.050

Table A8: Daily eddy covariance, energy balance component, and transpiration model results at PLC074 in 2002.

DOY	LE	H	Rn	G	Ta	e	Ts	θ	wind speed	λE_{uncorr}	res	LE_{corr}	H_{corr}	β	λE_{corr}	T_{Kc}	T_{GB}	EC Fourier
	Wm^{-2}	Wm^{-2}	Wm^{-2}	Wm^{-2}	°C	kPa	°C	m^3m^{-3}	$m\ s^{-1}$	mm day^{-1}	Wm^{-2}	Wm^{-2}	Wm^{-2}		mm day^{-1}	mm day^{-1}	mm day^{-1}	mm day^{-1}
1																0.000	0.000	0.136
2																0.000	0.000	0.137
3																0.000	0.000	0.138
4																0.000	0.000	0.140
5																0.000	0.000	0.141
6																0.000	0.000	0.143
7																0.000	0.000	0.144
8																0.000	0.000	0.146
9																0.000	0.000	0.148
10																0.000	0.000	0.150
11																0.000	0.000	0.152
12																0.000	0.000	0.154
13																0.001	0.000	0.157
14																0.001	0.000	0.159
15																0.001	0.000	0.162
16																0.001	0.000	0.164
17																0.001	0.000	0.167
18																0.001	0.000	0.170
19																0.001	0.000	0.173
20																0.001	0.000	0.176
21																0.001	0.000	0.179
22																0.001	0.000	0.183
23																0.001	0.000	0.186
24																0.001	0.000	0.190
25																0.001	0.000	0.193
26																0.002	0.000	0.197
27																0.002	0.000	0.201
28																0.002	0.000	0.205
29																0.002	0.000	0.209
30																0.002	0.000	0.213
31																0.002	0.000	0.218
32																0.002	0.000	0.222
33																0.003	0.000	0.227
34																0.003	0.000	0.231
35																0.003	0.000	0.236
36																0.003	0.000	0.241
37																0.004	0.000	0.246
38																0.004	0.000	0.251
39																0.004	0.000	0.256
40																0.005	0.000	0.261
41																0.005	0.000	0.267
42																0.005	0.000	0.272
43																0.006	0.000	0.278
44																0.006	0.000	0.283
45																0.007	0.000	0.289
46																0.007	0.000	0.295

Table A8: Daily eddy covariance, energy balance component, and transpiration model results at PLC074 in 2002.

DOY	LE	H	Rn	G	Ta	e	Ts	θ	wind speed	λE_{uncorr}	res	LE_{corr}	H_{corr}	β	λE_{corr}	T_{Kc}	T_{GB}	EC Fourier
	Wm^{-2}	Wm^{-2}	Wm^{-2}	Wm^{-2}	°C	kPa	°C	m^3m^{-3}	$m\ s^{-1}$	mm day^{-1}	Wm^{-2}	Wm^{-2}	Wm^{-2}		mm day^{-1}	mm day^{-1}	mm day^{-1}	mm day^{-1}
47																0.008	0.000	0.301
48																0.008	0.000	0.307
49																0.009	0.000	0.313
50																0.010	0.000	0.319
51																0.011	0.000	0.326
52																0.011	0.000	0.332
53																0.012	0.000	0.338
54																0.013	0.000	0.345
55																0.014	0.000	0.352
56																0.015	0.000	0.358
57																0.016	0.000	0.365
58																0.017	0.000	0.372
59																0.018	0.000	0.379
60																0.020	0.000	0.386
61																0.021	0.000	0.393
62																0.023	0.000	0.400
63																0.024	0.000	0.408
64																0.026	0.000	0.415
65																0.027	0.000	0.422
66																0.029	0.001	0.430
67																0.031	0.001	0.437
68																0.033	0.001	0.445
69																0.035	0.001	0.453
70																0.038	0.001	0.460
71																0.040	0.001	0.468
72																0.043	0.002	0.476
73																0.045	0.002	0.484
74																0.048	0.002	0.492
75																0.051	0.003	0.500
76																0.054	0.003	0.508
77																0.057	0.004	0.516
78																0.061	0.004	0.524
79																0.064	0.005	0.533
80																0.068	0.006	0.541
81																0.072	0.006	0.549
82																0.076	0.007	0.557
83																0.081	0.008	0.566
84																0.085	0.009	0.574
85																0.090	0.010	0.583
86																0.095	0.012	0.591
87																0.100	0.013	0.600
88																0.106	0.014	0.608
89																0.111	0.016	0.617
90																0.117	0.017	0.625
91																0.123	0.019	0.634
92																0.130	0.021	0.642

Table A8: Daily eddy covariance, energy balance component, and transpiration model results at PLC074 in 2002.

DOY	LE	H	Rn	G	Ta	e	Ts	θ	wind speed	λE_{uncorr}	res	LE_{corr}	H_{corr}	β	λE_{corr}	T_{Kc}	T_{GB}	EC Fourier
	Wm^{-2}	Wm^{-2}	Wm^{-2}	Wm^{-2}	°C	kPa	°C	m^3m^{-3}	$m\ s^{-1}$	mm day^{-1}	Wm^{-2}	Wm^{-2}	Wm^{-2}		mm day^{-1}	mm day^{-1}	mm day^{-1}	mm day^{-1}
93																0.136	0.023	0.651
94																0.143	0.025	0.659
95																0.150	0.028	0.668
96																0.158	0.030	0.676
97																0.166	0.033	0.685
98																0.174	0.036	0.694
99																0.182	0.039	0.702
100																0.190	0.043	0.711
101																0.199	0.046	0.719
102																0.209	0.050	0.728
103																0.218	0.054	0.736
104																0.228	0.058	0.745
105																0.238	0.063	0.753
106																0.248	0.067	0.762
107																0.259	0.072	0.770
108																0.270	0.078	0.778
109																0.282	0.083	0.787
110																0.293	0.089	0.795
111																0.305	0.095	0.803
112																0.318	0.102	0.811
113																0.330	0.109	0.820
114																0.343	0.116	0.828
115																0.357	0.123	0.836
116																0.370	0.131	0.844
117																0.384	0.139	0.852
118																0.398	0.148	0.859
119																0.413	0.157	0.867
120																0.428	0.166	0.875
121																0.443	0.176	0.883
122																0.458	0.186	0.890
123																0.474	0.196	0.898
124																0.490	0.207	0.905
125																0.506	0.218	0.912
126																0.523	0.230	0.920
127																0.539	0.242	0.927
128																0.556	0.254	0.934
129																0.574	0.266	0.941
130																0.591	0.280	0.948
131																0.609	0.293	0.955
132																0.626	0.307	0.961
133																0.644	0.321	0.968
134																0.662	0.335	0.974
135																0.681	0.350	0.981
136																0.699	0.365	0.987
137																0.718	0.381	0.993
138																0.736	0.396	0.999

Table A8: Daily eddy covariance, energy balance component, and transpiration model results at PLC074 in 2002.

DOY	LE	H	Rn	G	Ta	e	Ts	θ	wind speed	λE_{uncorr}	res	LE_{corr}	H_{corr}	β	λE_{corr}	T_{Kc}	T_{GB}	EC Fourier
	Wm^{-2}	Wm^{-2}	Wm^{-2}	Wm^{-2}	°C	kPa	°C	m^3m^{-3}	$m\ s^{-1}$	mm day^{-1}	Wm^{-2}	Wm^{-2}	Wm^{-2}		mm day^{-1}	mm day^{-1}	mm day^{-1}	mm day^{-1}
139																0.755	0.412	1.005
140																0.773	0.429	1.010
141																0.792	0.445	1.016
142																0.811	0.462	1.022
143																0.830	0.479	1.027
144																0.848	0.496	1.032
145	22.83	108.28	159.17	7.95	20.36	0.457	24.41	0.067	2.15	0.808	20.11	25.90	125.32	4.74	0.918	0.867	0.514	1.037
146	23.51	109.2	161.79	10.29	21.33	0.576	25.24	0.066	1.80	0.832	18.80	26.84	124.67	4.65	0.953	0.886	0.531	1.042
147	24.93	111.16	-1930	9.27	21.65	0.612	25.48	0.066	2.27	0.882	-2076		-1648	4.46		0.904	0.549	1.047
148	27.68	100.76	157.72	10.24	22.99	0.541	25.97	0.066	2.11	0.979	19.04	31.39	116.09	3.64	1.114	0.923	0.567	1.052
149	27.1	98.23	-1936	11.23	24.48	0.467	26.35	0.066	2.24	0.959	-2072		-1651	3.62		0.941	0.584	1.056
150	28.95	98.69	153.56	11.94	26.04	0.477	27.56	0.065	2.07	1.024	13.98	32.80	108.82	3.41	1.169	0.959	0.602	1.060
151	23.84	85.91	128.98	9.62	26.11	0.647	27.51	0.065	2.45	0.843	9.60	27.22	92.14	3.60	0.969	0.977	0.620	1.065
152	24.26	51.3	99.52	2.92	23.02	0.742	25.49	0.067	2.16	0.858	21.04	27.82	68.78	2.11	0.988	0.994	0.638	1.069
153	30.42	93.62	158.87	9.77	21.79	0.565	25.68	0.067	1.87	1.076	25.06	35.78	113.32	3.08	1.268	1.012	0.656	1.073
154	28.63	99.58	160.2	7.85	22.55	0.561	26.57	0.066	1.67	1.013	24.14	33.62	118.73	3.48	1.192	1.029	0.674	1.076
155	31.58	92.92	165.55	10.71	23.92	0.538	26.70	0.066	1.44	1.117	30.34	36.98	117.85	2.94	1.316	1.046	0.692	1.080
156	35.85	94.15	162.91	13.13	27.12	0.745	28.50	0.064	1.46	1.268	19.79	40.11	109.67	2.63	1.431	1.063	0.709	1.083
157	36.94	85.44	149.12	12.1	27.34	0.677	29.14	0.064	2.14	1.307	14.64	40.42	96.60	2.31	1.442	1.079	0.727	1.087
158	34.01	89.53	141.29	9.71	25.93	0.526	28.84	0.065	2085	1.203	8.05	35.58	96.00	2.63	1.269	1.095	0.744	1.090
159	41.01	84.68	-12414	6.05	24.21	0.403	28.02	0.065	2086	1.451	-12546		-8852	2.07		1.110	0.761	1.093
160	22.33	120.66	168.75	-0.05	16.16	0.282	25.35	0.068	3.38	0.790	25.80	24.93	143.87	5.40	0.878	1.126	0.778	1.096
161	21.5	108.09	163.4	5.56	18.23	0.406	24.95	0.068	1.69	0.761	28.24	25.28	132.55	5.03	0.893	1.140	0.795	1.098
162	26.72	115.97	172.42	9.65	21.3	0.476	26.38	0.066	2.07	0.945	20.08	30.50	132.27	4.34	1.080	1.155	0.811	1.101
163	26.77	107.26	159.19	11.43	24.22	0.473	27.64	0.065	2.27	0.947	13.73	28.61	119.16	4.01	1.018	1.169	0.827	1.103
164	26.01	110.94	140.54	10.76	25.23	0.501	28.56	0.064	2.57	0.920	-7.17	25.09	104.69	4.27	0.893	1.182	0.843	1.105
165	30.55	98.32	142.48	11.62	25.97	0.566	29.15	0.064	1.62	1.081	1.98	30.34	100.51	3.22	1.080	1.195	0.858	1.107
166	33.62	99.32	118.92	10.82	26.23	0.538	29.45	0.064	1.64	1.190	-24.84	29.26	78.84	2.95	1.042	1.207	0.873	1.109
167	36.44	83.35	67.98	11.27	27.01	0.465	29.53	0.064	1.66	1.289	-63.08	19.50	37.20	2.29	0.694	1.219	0.887	1.111
168	31.13	89.25	-1.09	11.68	27.47	0.527	30.06	0.064	1.67	1.101	-133.15		-15.27	2.87	0.086	1.230	0.901	1.112
169	31.35	87.72	-0.84	11.94	28.44	0.728	30.75	0.063	2.37	1.109	-131.85		-18.07	2.80	0.186	1.241	0.914	1.113
170	30.35	103.62	15.27	11.01	26.93	0.830	30.89	0.063	2.04	1.074	-129.71		-6.91	3.41	0.394	1.251	0.927	1.114
171	26.76	118.47	-16650	10.38	26.14	0.807	30.47	0.064	2.79	0.947	-16805		-14841	4.43		1.260	0.939	1.115
172	21.54	71.55	-6191	-0.47	22.41	0.877	27.98	0.066	1.67	0.762	-6283		-5073	3.32		1.269	0.951	1.116
173	29.16	106.66	85.87	11.82	23.93	0.666	28.44	0.065	1.64	1.032	-61.76		58.33	3.66		1.277	0.962	1.117
174	27.29	121.07	-73.03	9.95	25.35	0.591	29.65	0.064	2.31	0.966	-231.36		-70.40	4.44		1.285	0.972	1.117
175	27.46	109.4	-2243	11.2	26.51	0.582	30.20	0.064	2.16	0.972	-2391		-1721	3.98		1.291	0.982	1.117
176	29.56	100.66	-2399	12.48	27.39	-2083	30.89	0.063	2.17	1.046	-2541		-1990	3.40		1.298	0.991	1.117
177	24.47	105.12	-4455	9.46	27.15	0.601	30.79	0.063	2.31	0.866	-4595		-3523	4.30		1.303	0.999	1.117
178	30.2	99.86	-333	11.96	27.71	0.660	31.23	0.063	1.99	1.069	-475		-283	3.31		1.308	1.006	1.117
179	27.13	96.56	-4350	9.63	27.12	0.696	30.83	0.064	2.12	0.960	-4484		-3897	3.56		1.312	1.013	1.116
180	27.08	100.41	172.02	12.58	28.44	0.712	31.52	0.063	2.43	0.958	31.96	33.53	125.91	3.71	1.196	1.315	1.019	1.116
181	28.1	106.37	174.29	12.66	29.96	0.664	32.52	0.062	2.91	0.994	27.17	32.48	129.16	3.79	1.161	1.318	1.024	1.115
182	26.04	96.12	163.88	10.85	29.46	0.648	32.23	0.063	2.73	0.921	30.87	31.20	121.83	3.69	1.115	1.319	1.029	1.114
183	23.57	115.94	175.12	9.17	27.48	0.596	31.92	0.063	2.47	0.834	26.44	27.28	138.67	4.92	0.974	1.321	1.032	1.113
184	26.42	106.54	173.56	9.35	26.96	0.609	31.48	0.064	1.64	0.935	31.25	30.15	134.07	4.03	1.076	1.321	1.035	1.112

Table A8: Daily eddy covariance, energy balance component, and transpiration model results at PLC074 in 2002.

DOY	LE	H	Rn	G	Ta	e	Ts	θ	wind speed	λE_{uncorr}	res	LE_{corr}	H_{corr}	β	λE_{corr}	T_{Kc}	T_{GB}	EC Fourier
	Wm^{-2}	Wm^{-2}	Wm^{-2}	Wm^{-2}	°C	kPa	°C	m^3m^{-3}	$m\ s^{-1}$	mm day^{-1}	Wm^{-2}	Wm^{-2}	Wm^{-2}		mm day^{-1}	mm day^{-1}	mm day^{-1}	mm day^{-1}
185	27.05	102.09	169.23	10.79	28.25	0.694	31.78	0.063	2.42	0.957	29.30	33.57	124.88	3.77	1.197	1.321	1.037	1.110
186	26.92	112.1	176.98	10.47	28	0.704	31.95	0.063	2.65	0.952	27.49	32.21	134.29	4.16	1.150	1.319	1.039	1.108
187	26.26	107.02	169.77	9.16	27.87	0.721	31.75	0.063	4169	0.929	27.34	30.57	130.04	4.08	1.091	1.318	1.039	1.106
188	31.91	104.36	176.99	10.86	28.16	0.710	32.07	0.063	2.15	1.129	29.85	37.00	129.13	3.27	1.321	1.315	1.038	1.104
189	32.07	99.46	175.78	9.74	28.62	0.578	32.21	0.063	2085	1.135	34.51	39.42	126.61	3.10	1.408	1.312	1.037	1.102
190	31.45	93.52	173.93	12.52	30.69	0.646	32.82	0.062	1.61	1.113	36.45	37.90	123.52	2.97	1.356	1.307	1.035	1.100
191	37.02	83.08	177.09	13.62	31.99	0.643	33.59	0.062	1.68	1.310	43.38	44.53	118.95	2.24	1.598	1.303	1.032	1.097
192	31.52	72.91	137.28	5.45	29.12	1.090	33.05	0.063	2.07	1.115	27.40	34.07	97.76	2.31	1.216	1.297	1.029	1.095
193	29.35	101.18	174.13	14.69	29.94	1.161	32.87	0.062	2.02	1.038	28.91	35.73	123.71	3.45	1.278	1.291	1.024	1.092
194	24.27	83.69	151.23	11.01	30.11	1.027	33.66	0.062	2.07	0.859	32.26	28.77	111.46	3.45	1.030	1.284	1.019	1.089
195	24.48	86.96	153.43	10.32	29.64	0.997	33.02	0.062	2.08	0.866	31.66	31.24	111.87	3.55	1.117	1.276	1.013	1.086
196	32.99	110.63	183.87	9.46	27.73	0.827	32.83	0.063	2.07	1.167	30.79	39.11	135.30	3.35	1.398	1.268	1.006	1.082
197	21.77	80.88	149.86	9.12	27.35	0.773	32.21	0.063	1.58	0.770	38.08	27.85	112.89	3.72	0.993	1.259	0.998	1.079
198	20.65	79.16	137.47	5.98	26.65	0.898	31.51	0.064	2.20	0.731	31.69	25.73	105.77	3.83	0.917	1.250	0.990	1.075
199	20.41	98.57	147.14	2.99	23.68	1.004	29.91	0.065	2.19	0.722	25.16	25.42	118.73	4.83	0.904	1.239	0.981	1.071
200	22.57	115.32	180.95	10.7	25.48	0.863	30.71	0.064	1.65	0.799	32.36	26.71	143.53	5.11	0.951	1.228	0.972	1.067
201	21.97	94.28	163.73	10.35	27.51	0.698	31.69	0.063	2.32	0.777	37.14	26.28	127.11	4.29	0.938	1.217	0.961	1.063
202	24.46	97.53	162.4	6.95	26.75	0.560	31.33	0.064	2.80	0.865	33.46	28.32	127.13	3.99	1.010	1.205	0.950	1.059
203	17.73	74.09	135.38	3.73	25.19	0.433	29.61	0.065	2.86	0.627	39.82	22.31	109.34	4.18	0.795	1.192	0.939	1.054
204	19.17	100.62	161.71	9.09	25.36	0.635	29.78	0.064	2.26	0.678	32.83	25.16	127.46	5.25	0.896	1.179	0.927	1.050
205	17.2	78.36	136.6	9.29	27.65	0.953	30.96	0.064	2.09	0.609	31.75	22.86	104.46	4.56	0.816	1.165	0.914	1.045
206	25.15	84.73	156.32	10.61	28.59	0.974	31.83	0.063	1.71	0.890	35.83	31.57	114.14	3.37	1.128	1.151	0.901	1.040
207	26.28	90.11	167.82	9.17	27.64	0.647	31.62	0.063	1.80	0.930	42.25	32.67	125.98	3.43	1.167	1.137	0.887	1.035
208	23.46	84.63	158.51	7.72	27.17	0.580	31.28	0.063	2.23	0.830	42.71	29.68	121.12	3.61	1.060	1.121	0.872	1.030
209	25.13	82.39	165.8	9.18	27.78	0.612	31.40	0.063	1.70	0.889	49.09	32.96	123.66	3.28	1.177	1.106	0.858	1.025
210	21.95	82.03	167.82	10.51	29.5	0.580	32.04	0.063	1.73	0.777	53.33	28.84	128.48	3.74	1.031	1.090	0.843	1.019
211	22.29	87.68	163.13	9.62	28.59	0.669	32.05	0.063	2.04	0.789	43.53	29.75	123.75	3.93	1.064	1.073	0.827	1.014
212	22.91	75.3	141.53	8.43	28.65	0.769	31.72	0.063	1.95	0.811	34.90	28.37	104.73	3.29	1.014	1.057	0.811	1.008
213	18.48	63.8	116.14	4.43	27.13	0.886	30.79	0.064	1.86	0.654	29.43	23.93	87.79	3.45	0.854	1.040	0.795	1.002
214	21.2	96.89	165.7	9.91	27.37	0.840	31.22	0.063	2.28	0.750	37.71	27.78	128.01	4.57	0.991	1.022	0.778	0.996
215	16.51	112.25	164.64	5.06	25.41	0.705	30.64	0.064	2.71	0.584	30.81	19.82	139.76	6.80	0.707	1.004	0.762	0.990
216	20.2	104.84	168.68	4.95	23.55	0.552	29.91	0.064	1.93	0.715	38.69	23.26	140.47	5.19	0.829	0.986	0.745	0.984
217	17.97	106.97	166.86	4.75	22.35	0.562	29.17	0.065	1.96	0.636	37.17	21.60	140.51	5.95	0.768	0.968	0.727	0.977
218	16.48	98.69	161.34	5.43	23.29	0.570	29.16	0.065	2.31	0.583	40.73	21.18	134.73	5.99	0.752	0.950	0.710	0.971
219	17.04	90.51	156.27	4.45	22.79	0.501	28.66	0.065	1.95	0.603	44.28	22.73	129.09	5.31	0.807	0.931	0.692	0.964
220	18.13	92.74	161.91	5.62	24.16	0.448	28.93	0.065	1.86	0.641	45.43	22.99	133.30	5.12	0.818	0.912	0.675	0.958
221	27.47	80.1	159.28	6.69	25.23	0.468	29.12	0.065	1.63	0.972	45.01	32.70	119.89	2.92	1.166	0.893	0.657	0.951
222	25.67	84.31	159.44	6.45	25.76	0.477	29.21	0.064	1.58	0.908	43.01	32.71	120.28	3.28	1.168	0.874	0.639	0.944
223	21.26	81.71	154.22	7.91	26.77	0.535	29.50	0.064	1.65	0.752	43.34	27.66	118.65	3.84	0.989	0.855	0.622	0.937
224	26.64	70.18	151.24	9.36	28.6	0.621	30.32	0.064	1.56	0.943	45.06	34.20	107.68	2.63	1.224	0.836	0.604	0.930
225	29.82	77.31	154.83	8.39	28.4	0.709	30.64	0.063	1.28	1.055	39.32	34.88	111.56	2.59	1.249	0.816	0.586	0.923
226	27.42	68.46	150.61	10.36	29.15	0.704	30.73	0.063	1.50	0.970	44.36	35.83	104.42	2.50	1.282	0.797	0.568	0.915
227	25.32	63.45	129.03	4.61	27.88	0.761	30.73	0.064	1.82	0.896	35.65	31.09	93.32	2.51	1.112	0.778	0.551	0.908
228	20.53	73.35	150.03	8.41	28.12	0.696	30.11	0.064	1.41	0.726	47.75	27.00	114.63	3.57	0.967	0.758	0.533	0.901
229	24.9	70.91	149.73	7.26	27.71	0.588	30.29	0.064	1.68	0.881	46.66	30.71	111.77	2.85	1.099	0.739	0.516	0.893
230	23.29	80.89	152.88	7.08	27.67	0.531	30.31	0.064	1.68	0.824	41.62	29.11	116.69	3.47	1.040	0.720	0.499	0.885

Table A8: Daily eddy covariance, energy balance component, and transpiration model results at PLC074 in 2002.

DOY	LE	H	Rn	G	Ta	e	Ts	θ	wind speed	λE_{uncorr}	res	LE_{corr}	H_{corr}	β	λE_{corr}	T_{Kc}	T_{GB}	EC Fourier
	Wm^{-2}	Wm^{-2}	Wm^{-2}	Wm^{-2}	°C	kPa	°C	m^3m^{-3}	$m\ s^{-1}$	mm day^{-1}	Wm^{-2}	Wm^{-2}	Wm^{-2}		mm day^{-1}	mm day^{-1}	mm day^{-1}	mm day^{-1}
231	18.6	76.28	146.86	5.06	25.46	0.464	29.29	0.065	1.90	0.658	46.92	23.62	118.18	4.10	0.842	0.701	0.481	0.878
232	21.59	73.13	155.41	2.27	24.23	0.383	28.90	0.065	2085	0.764	58.41	28.11	125.04	3.39	1.001	0.682	0.465	0.870
233	14.09	82.77	152.83	3.04	22.57	0.441	27.54	0.066	2.09	0.499	52.93	19.52	130.27	5.87	0.692	0.663	0.448	0.862
234	13.03	99.19	157.09	2.76	21.43	0.487	27.16	0.066	1.94	0.461	42.12	16.94	137.39	7.61	0.602	0.644	0.432	0.854
235	14.38	93.23	158.95	4.18	22.48	0.496	27.51	0.066	1.35	0.509	47.16	19.88	134.89	6.49	0.707	0.625	0.415	0.846
236	16.75	89.36	157.66	4.43	22.85	0.504	27.16	0.066	2.01	0.593	47.13	21.89	131.34	5.34	0.779	0.607	0.400	0.838
237	15.58	80.07	154.78	4.96	23.84	0.481	27.40	0.066	1.82	0.551	54.17	21.15	128.67	5.14	0.753	0.589	0.384	0.830
238	20.85	72.24	153.94	4.89	25.33	0.504	27.68	0.065	1.83	0.738	55.96	26.95	122.10	3.46	0.959	0.570	0.369	0.822
239	15.73	77.5	143.36	4.18	23.79	0.522	27.28	0.066	1.42	0.557	45.96	21.94	117.25	4.93	0.779	0.553	0.354	0.814
240	16.14	79.53	137.58	3.6	23.3	0.607	26.92	0.066	1.97	0.571	38.32	20.49	113.49	4.93	0.728	0.535	0.339	0.805
241	13.85	78.37	145.92	5.19	23.44	0.615	26.91	0.066	2.25	0.490	48.51	18.67	122.06	5.66	0.664	0.518	0.325	0.797
242	14.61	90.79	150.33	3.95	23.35	0.570	27.02	0.066	2.29	0.517	40.98	17.48	128.90	6.21	0.622	0.501	0.311	0.788
243	13.84	95.1	152.01	1.63	21.62	0.471	26.36	0.066	1.54	0.490	41.43	18.12	132.26	6.87	0.645	0.484	0.297	0.780
244	20.17	73.78	149.63	5.06	23.59	0.594	26.32	0.066	1.34	0.714	50.62	26.06	118.51	3.66	0.929	0.467	0.284	0.772
245	15.79	76.47	152.97	6.04	24.91	0.601	27.10	0.066	1.39	0.559	54.68	23.20	123.74	4.84	0.828	0.451	0.271	0.763
246	17.95	55.94	127.9	4.61	25.49	0.669	26.84	0.066	1.88	0.635	49.40	25.42	97.86	3.12	0.906	0.435	0.258	0.755
247	15.8	44.84	89.65	-0.91	23.65	0.826	26.00	0.067	1.82	0.559	29.91	18.58	71.97	2.84	0.660	0.419	0.246	0.746
248	6.12	13.66	51.31	-2.67	21.45	0.890	23.02	0.069	2.08	0.217	34.20	12.76	41.22	2.23	0.453	0.404	0.234	0.737
249	11.04	31.9	75.58	-2.29	21.03	0.797	23.60	0.069	2.12	0.391	34.93	14.48	63.38	2.89	0.513	0.389	0.223	0.729
250	13.08	90.52	147.28	-0.51	17.89	0.446	22.63	0.069	2.11	0.463	44.19	16.80	130.99	6.92	0.594	0.374	0.212	0.720
251	14.01	86.01	148.16	-1.51	16.89	0.444	22.21	0.069	1.33	0.496	49.64	19.36	130.30	6.14	0.685	0.360	0.201	0.711
252	13.75	85.19	147.13	0.66	17.66	0.421	21.99	0.069	1.32	0.486	47.53	18.85	127.62	6.20	0.668	0.346	0.191	0.703
253	13.18	81.93	147.46	1.81	19.36	0.440	22.67	0.069	1.35	0.466	50.54	18.86	126.79	6.22	0.670	0.332	0.181	0.694
254	15.14	69.27	144.37	4.31	21.61	0.500	23.40	0.068	1.54	0.536	55.64	20.57	119.49	4.57	0.732	0.319	0.171	0.685
255	12.48	81.59	145.06	1.06	21.18	0.486	23.56	0.068	1.46	0.442	49.92	17.11	126.89	6.54	0.610	0.306	0.162	0.677
256	15.74	73.11	144.11	2.45	20.93	0.520	23.33	0.068	1.27	0.557	52.82	21.18	120.48	4.64	0.754	0.293	0.153	0.668
257	11.44	74.74	140.22	4.47	22.72	0.532	23.77	0.068	2.07	0.405	49.57	15.84	119.91	6.53	0.564	0.281	0.144	0.659
258	10.83	72.77	129.18	2.22	22.7	0.556	24.08	0.068	2.48	0.383	43.37	13.79	113.18	6.72	0.491	0.269	0.136	0.650
259	15.33	69.98	136.43	-1.9	20.66	0.441	23.29	0.069	1.66	0.542	53.02	19.75	118.59	4.56	0.700	0.258	0.128	0.642
260	10.95	68.6	128.36	3.16	19.96	0.498	22.03	0.069	1.61	0.387	45.64	13.70	111.49	6.26	0.486	0.246	0.121	0.633
261	12.34	67.07	132.37	1.16	21.24	0.629	23.51	0.068	2.46	0.437	51.79	15.92	115.29	5.43	0.564	0.235	0.114	0.624
262	14.1	65.57	134.62	1.21	21.1	0.578	22.87	0.068	2085	0.499	53.74	19.60	113.81	4.65	0.695	0.225	0.107	0.616
263	12.01	73.07	136.26	1.09	20.4	0.563	22.48	0.069	1.47	0.425	50.09	17.31	117.86	6.08	0.615	0.215	0.100	0.607
264	10.98	71.36	135.57	1.74	21.5	0.572	22.66	0.068	1.47	0.388	51.48	15.88	117.95	6.50	0.566	0.205	0.094	0.598
265	12.05	68.19	133.21	1.21	21.91	0.515	22.84	0.068	1.42	0.426	51.76	17.20	114.80	5.66	0.613	0.195	0.088	0.590
266	12.78	61.19	130.53	1.89	22.17	0.468	22.55	0.069	1.70	0.452	54.68	19.16	109.48	4.79	0.683	0.186	0.082	0.581
267	12.09	50.87	109.04	1.26	22.03	0.560	22.13	0.069	1.34	0.428	44.81	16.57	91.21	4.21	0.590	0.177	0.077	0.573
268	10.9	48.13	117.45	4.15	24.4	0.591	23.57	0.068	1.85	0.386	54.26	16.92	96.38	4.41	0.603	0.169	0.072	0.564
269	12.15	65.04	124.17	-2.03	20.73	0.459	22.46	0.069	1.72	0.430	49.00	16.37	109.83	5.35	0.580	0.160	0.067	0.556
270	9.14	38.19	86.05	-1.91	19.76	0.535	20.71	0.070	2.04	0.323	40.63	12.78	75.17	4.18	0.453	0.152	0.063	0.547
271	81.16	13.92	39.23	-8.61	14.5	0.892	19.54	0.072	1.59	2.872		82.79	-34.95	0.17	2.900	0.145	0.058	0.539
272	40.37	57.83	134.49	-4.09	14.96	0.782	17.57	0.074	1.73	1.428	40.38	50.46	88.11	1.43	1.775	0.137	0.054	0.530
273	13.4	66.3	117.5	-3.58	14.88	0.676	17.92	0.073	1.60	0.474	41.39	19.94	101.15	4.95	0.702	0.130	0.050	0.522
274	17.77	51.38	89.27	-8.72	10.94	0.505	15.88	0.074	2.86	0.629	28.85	11.63	86.37	2.89	0.408	0.124	0.047	0.514
275	8.93	66.39	105.18	-6.81	9.91	0.424	15.42	0.075	4.03	0.316	36.66	10.66	101.33	7.44	0.373	0.117	0.043	0.505
276	11.09	53.52	116.84	-1.79	13.8	0.351	15.60	0.074	2.15	0.392	54.02	16.12	102.50	4.83	0.567	0.111	0.040	0.497

Table A8: Daily eddy covariance, energy balance component, and transpiration model results at PLC074 in 2002.

DOY	LE	H	Rn	G	Ta	e	Ts	θ	wind speed	λE_{uncorr}	res	LE_{corr}	H_{corr}	β	λE_{corr}	T_{Kc}	T_{GB}	EC Fourier
	Wm^{-2}	Wm^{-2}	Wm^{-2}	Wm^{-2}	°C	kPa	°C	m^3m^{-3}	$m\ s^{-1}$	mm day^{-1}	Wm^{-2}	Wm^{-2}	Wm^{-2}		mm day^{-1}	mm day^{-1}	mm day^{-1}	mm day^{-1}
277	7.17	49.03	88.37	-0.19	15.18	0.499	17.80	0.072	1.22	0.254	32.36	10.18	78.38	6.84	0.359	0.105	0.037	0.489
278	9.77	63.22	118.6	-2.45	14.5	0.592	16.67	0.073	1.21	0.346	48.05	14.52	106.53	6.47	0.513	0.099	0.034	0.481
279	11.45	63.26	118.64	-0.87	16.81	0.613	17.25	0.072	1.35	0.405	44.80	15.76	103.75	5.53	0.558	0.094	0.032	0.473
280	12.19	50.95	114.42	0.95	18.43	0.580	17.72	0.072	25001	0.431	50.34	16.89	96.58	4.18	0.599	0.089	0.029	0.465
281																0.084	0.027	0.457
282																0.079	0.025	0.449
283																0.074	0.023	0.441
284																0.070	0.021	0.434
285																0.066	0.019	0.426
286																0.062	0.017	0.418
287																0.058	0.016	0.411
288																0.055	0.014	0.403
289																0.052	0.013	0.396
290																0.048	0.012	0.389
291																0.045	0.011	0.381
292																0.043	0.010	0.374
293																0.040	0.009	0.367
294																0.037	0.008	0.360
295																0.035	0.007	0.353
296																0.033	0.006	0.347
297																0.031	0.006	0.340
298																0.029	0.005	0.333
299																0.027	0.005	0.327
300																0.025	0.004	0.320
301																0.023	0.004	0.314
302																0.022	0.003	0.308
303																0.020	0.003	0.302
304																0.019	0.002	0.296
305																0.018	0.002	0.290
306																0.016	0.002	0.284
307																0.015	0.002	0.278
308																0.014	0.001	0.272
309																0.013	0.001	0.267
310																0.012	0.001	0.261
311																0.011	0.001	0.256
312																0.010	0.001	0.251
313																0.010	0.001	0.246
314																0.009	0.001	0.241
315																0.008	0.000	0.236
316																0.008	0.000	0.231
317																0.007	0.000	0.226
318																0.007	0.000	0.222
319																0.006	0.000	0.217
320																0.006	0.000	0.213
321																0.005	0.000	0.208
322																0.005	0.000	0.204

Table A8: Daily eddy covariance, energy balance component, and transpiration model results at PLC074 in 2002.

DOY	LE	H	Rn	G	Ta	e	Ts	θ	wind speed	λE_{uncorr}	res	LE_{corr}	H_{corr}	β	λE_{corr}	T_{Kc}	T_{GB}	EC Fourier
	Wm^{-2}	Wm^{-2}	Wm^{-2}	Wm^{-2}	°C	kPa	°C	m^3m^{-3}	$m\ s^{-1}$	mm day^{-1}	Wm^{-2}	Wm^{-2}	Wm^{-2}		mm day^{-1}	mm day^{-1}	mm day^{-1}	mm day^{-1}
323																0.004	0.000	0.200
324																0.004	0.000	0.196
325																0.004	0.000	0.193
326																0.004	0.000	0.189
327																0.003	0.000	0.185
328																0.003	0.000	0.182
329																0.003	0.000	0.178
330																0.003	0.000	0.175
331																0.002	0.000	0.172
332																0.002	0.000	0.169
333																0.002	0.000	0.166
334																0.002	0.000	0.163
335																0.002	0.000	0.161
336																0.002	0.000	0.158
337																0.001	0.000	0.156
338																0.001	0.000	0.153
339																0.001	0.000	0.151
340																0.001	0.000	0.149
341																0.001	0.000	0.147
342																0.001	0.000	0.145
343																0.001	0.000	0.144
344																0.001	0.000	0.142
345																0.001	0.000	0.140
346																0.001	0.000	0.139
347																0.001	0.000	0.138
348																0.001	0.000	0.137
349																0.001	0.000	0.136
350																0.001	0.000	0.135
351																0.000	0.000	0.134
352																0.000	0.000	0.133
353																0.000	0.000	0.133
354																0.000	0.000	0.132
355																0.000	0.000	0.132
356																0.000	0.000	0.132
357																0.000	0.000	0.132
358																0.000	0.000	0.132
359																0.000	0.000	0.132
360																0.000	0.000	0.132
361																0.000	0.000	0.132
362																0.000	0.000	0.133
363																0.000	0.000	0.134
364																0.000	0.000	0.134
365																0.000	0.000	0.135

Table A9: Daily eddy covariance, energy balance component, and transpiration model results at PLC185 in 2002.

DOY	LE	H	Rn	G	Ta	e	Ts	θ	wind speed	λE_{uncorr}	res	LE_{corr}	H_{corr}	β	λE_{corr}	T_{Kc}	T_{GB}	EC Fourier
	Wm^{-2}	Wm^{-2}	Wm^{-2}	Wm^{-2}	°C	kPa	°C	m^3m^{-3}	$m\ s^{-1}$	$mm\ day^{-1}$	Wm^{-2}	Wm^{-2}	Wm^{-2}		$mm\ day^{-1}$	$mm\ day^{-1}$	$mm\ day^{-1}$	$mm\ day^{-1}$
1																0.000	0.000	0.069
2																0.000	0.000	0.068
3																0.000	0.000	0.068
4																0.000	0.000	0.067
5																0.000	0.000	0.066
6																0.000	0.000	0.066
7																0.000	0.000	0.065
8																0.000	0.000	0.065
9																0.000	0.000	0.064
10																0.000	0.000	0.064
11																0.000	0.000	0.063
12																0.000	0.000	0.063
13																0.000	0.000	0.063
14																0.000	0.000	0.063
15																0.000	0.000	0.062
16																0.000	0.000	0.062
17																0.000	0.000	0.063
18																0.000	0.000	0.063
19																0.000	0.000	0.063
20																0.000	0.000	0.063
21																0.000	0.000	0.063
22																0.000	0.000	0.064
23																0.000	0.000	0.064
24																0.000	0.000	0.065
25																0.000	0.000	0.066
26																0.000	0.000	0.066
27																0.000	0.000	0.067
28																0.001	0.000	0.068
29																0.001	0.000	0.069
30																0.001	0.000	0.070
31																0.001	0.000	0.072
32																0.001	0.000	0.073
33																0.001	0.000	0.074
34																0.001	0.000	0.076
35																0.001	0.000	0.078
36																0.001	0.000	0.079
37																0.001	0.000	0.081
38																0.001	0.000	0.083
39																0.001	0.000	0.085
40																0.002	0.000	0.088
41																0.002	0.000	0.090
42																0.002	0.000	0.092
43																0.002	0.000	0.095
44																0.002	0.000	0.097
45																0.002	0.000	0.100
46																0.003	0.000	0.103
47																0.003	0.000	0.106

Table A9: Daily eddy covariance, energy balance component, and transpiration model results at PLC185 in 2002.

DOY	LE	H	Rn	G	Ta	e	Ts	θ	wind speed	λE_{uncorr}	res	LE_{corr}	H_{corr}	β	λE_{corr}	T_{Kc}	T_{GB}	EC Fourier
	Wm^{-2}	Wm^{-2}	Wm^{-2}	Wm^{-2}	°C	kPa	°C	m^3m^{-3}	$m\ s^{-1}$	$mm\ day^{-1}$	Wm^{-2}	Wm^{-2}	Wm^{-2}		$mm\ day^{-1}$	$mm\ day^{-1}$	$mm\ day^{-1}$	$mm\ day^{-1}$
48																0.003	0.000	0.109
49																0.003	0.000	0.112
50																0.004	0.000	0.116
51																0.004	0.000	0.119
52																0.004	0.000	0.123
53																0.004	0.000	0.127
54																0.005	0.000	0.131
55																0.005	0.000	0.134
56																0.006	0.000	0.139
57																0.006	0.000	0.143
58																0.007	0.000	0.147
59																0.007	0.000	0.152
60																0.008	0.000	0.156
61																0.008	0.000	0.161
62																0.009	0.000	0.166
63																0.010	0.000	0.170
64																0.010	0.000	0.176
65																0.011	0.000	0.181
66																0.012	0.000	0.186
67																0.013	0.000	0.191
68																0.014	0.000	0.197
69																0.015	0.000	0.202
70																0.016	0.000	0.208
71																0.017	0.000	0.214
72																0.018	0.000	0.220
73																0.020	0.000	0.226
74																0.021	0.001	0.232
75																0.022	0.001	0.238
76																0.024	0.001	0.244
77																0.026	0.001	0.251
78																0.027	0.002	0.257
79																0.029	0.002	0.264
80																0.031	0.002	0.270
81																0.033	0.003	0.277
82																0.035	0.003	0.284
83																0.037	0.004	0.291
84																0.040	0.004	0.298
85																0.042	0.005	0.305
86																0.045	0.005	0.312
87																0.047	0.006	0.319
88																0.050	0.007	0.326
89																0.053	0.008	0.333
90																0.056	0.009	0.341
91																0.060	0.010	0.348
92																0.063	0.011	0.356
93																0.067	0.012	0.363
94																0.070	0.013	0.371

Table A9: Daily eddy covariance, energy balance component, and transpiration model results at PLC185 in 2002.

DOY	LE	H	Rn	G	Ta	e	Ts	θ	wind speed	λE_{uncorr}	res	LE_{corr}	H_{corr}	β	λE_{corr}	T_{Kc}	T_{GB}	EC Fourier
	Wm^{-2}	Wm^{-2}	Wm^{-2}	Wm^{-2}	°C	kPa	°C	m^3m^{-3}	$m\ s^{-1}$	mm day^{-1}	Wm^{-2}	Wm^{-2}	Wm^{-2}		mm day^{-1}	mm day^{-1}	mm day^{-1}	mm day^{-1}
95																0.074	0.014	0.378
96																0.078	0.016	0.386
97																0.082	0.017	0.393
98																0.087	0.019	0.401
99																0.091	0.021	0.408
100																0.096	0.023	0.416
101																0.101	0.025	0.424
102																0.106	0.027	0.431
103																0.111	0.029	0.439
104																0.117	0.032	0.447
105																0.122	0.034	0.454
106																0.128	0.037	0.462
107																0.134	0.040	0.470
108																0.141	0.043	0.477
109																0.147	0.047	0.485
110																0.154	0.050	0.492
111																0.161	0.054	0.500
112																0.168	0.057	0.507
113																0.175	0.061	0.515
114																0.182	0.066	0.522
115																0.190	0.070	0.529
116																0.198	0.075	0.537
117																0.206	0.080	0.544
118																0.214	0.085	0.551
119																0.223	0.090	0.558
120																0.231	0.096	0.565
121																0.240	0.102	0.572
122																0.249	0.108	0.579
123																0.258	0.114	0.586
124																0.268	0.120	0.592
125																0.277	0.127	0.599
126																0.287	0.134	0.605
127																0.297	0.141	0.612
128																0.307	0.149	0.618
129																0.317	0.156	0.624
130																0.327	0.164	0.630
131																0.338	0.172	0.636
132																0.348	0.181	0.642
133																0.359	0.189	0.648
134																0.370	0.198	0.653
135																0.381	0.207	0.659
136																0.392	0.217	0.664
137																0.403	0.226	0.669
138																0.414	0.236	0.674
139																0.425	0.246	0.679
140																0.436	0.256	0.684
141																0.448	0.266	0.689

Table A9: Daily eddy covariance, energy balance component, and transpiration model results at PLC185 in 2002.

DOY	LE	H	Rn	G	Ta	e	Ts	θ	wind speed	λE_{uncorr}	res	LE_{corr}	H_{corr}	β	λE_{corr}	T_{Kc}	T_{GB}	EC Fourier
	Wm^{-2}	Wm^{-2}	Wm^{-2}	Wm^{-2}	°C	kPa	°C	m^3m^{-3}	$m\ s^{-1}$	$mm\ day^{-1}$	Wm^{-2}	Wm^{-2}	Wm^{-2}		$mm\ day^{-1}$	$mm\ day^{-1}$	$mm\ day^{-1}$	$mm\ day^{-1}$
142																0.459	0.276	0.693
143																0.470	0.287	0.697
144	12.61	88.25	55.21	-1033	18.67	0.336	25.27	0.071	2.20	0.446	987.36		986.29	7.00	3.617	0.481	0.298	0.702
145	11.64	84.68	146.34	8.48	20.71	0.419	26.36	0.071	2.56	0.412	41.53	17.32	120.54	7.27	0.614	0.493	0.309	0.706
146	12.91	86.54	146.49	9.24	21.35	0.548	27.40	0.071	2.04	0.457	37.81	19.08	118.18	6.70	0.676	0.504	0.319	0.709
147	12.75	98.15	158.28	9.3	21.37	0.586	27.73	0.070	2.60	0.451	38.08	18.41	130.57	7.70	0.653	0.515	0.331	0.713
148	12.16	77.22	147.1	10.2	22.79	0.513	28.47	0.070	2.41	0.430	47.51	19.34	117.55	6.35	0.686	0.526	0.342	0.717
149	13.86	75.28	149.12	12.1	24.61	0.434	29.62	0.069	2.41	0.490	47.87	21.03	115.98	5.43	0.748	0.537	0.353	0.720
150	13.2	81.69	152.29	12.36	26.63	0.423	30.93	0.068	2.53	0.467	45.04	20.30	119.64	6.19	0.724	0.548	0.364	0.723
151	12.14	76.03	142.92	10.73	26.55	0.603	31.17	0.068	3.15	0.430	44.01	19.33	112.85	6.26	0.689	0.559	0.375	0.726
152	17.4	43.42	93.23	1.38	23.27	0.700	28.37	0.071	2.67	0.616	31.03	25.53	66.31	2.50	0.906	0.570	0.387	0.729
153	13.02	79.09	152.42	9.7	22.47	0.522	28.88	0.070	2.41	0.461	50.61	18.32	124.40	6.07	0.649	0.580	0.398	0.732
154	10.75	79.65	152.81	7.24	23.17	0.502	29.63	0.069	2.36	0.380	55.17	17.35	128.22	7.41	0.615	0.590	0.409	0.734
155	13.61	76.74	152.13	10.55	24.4	0.471	30.01	0.069	1.81	0.482	51.23	21.01	120.57	5.64	0.746	0.601	0.421	0.736
156	13.03	77.4	159.4	13.61	28.1	0.626	32.33	0.067	1.82	0.461	55.35	21.18	124.60	5.94	0.755	0.611	0.432	0.738
157	18.72	76.87	155.76	12.54	28.14	0.586	33.43	0.067	2.45	0.662	47.64	28.17	115.05	4.11	1.004	0.620	0.443	0.740
158	14.21	79.99	151.09	9.8	26.88	0.448	33.00	0.067	2.30	0.503	47.08	22.69	118.59	5.63	0.808	0.630	0.454	0.742
159	14.71	72.77	145.23	5.4	25.26	0.336	32.00	0.068	2.83	0.520	52.36	23.49	116.34	4.95	0.835	0.639	0.465	0.744
160	11.47	105.14	158.14	-3.85	16.22	0.266	27.27	0.072	4.02	0.406	45.38	13.21	148.78	9.17	0.465	0.649	0.476	0.745
161	9.86	83.04	151.74	3.85	18.84	0.373	26.91	0.071	2.24	0.349	54.99	13.37	134.52	8.42	0.472	0.657	0.486	0.746
162	11.53	87.94	159.27	8.48	21.99	0.435	29.10	0.070	2.52	0.408	51.32	16.90	133.88	7.63	0.599	0.666	0.497	0.747
163	14	81.18	160.04	9.76	24.2	0.439	30.26	0.069	2.63	0.495	55.09	21.29	128.99	5.80	0.756	0.674	0.507	0.748
164	12.96	88.52	162.88	9.71	25.66	0.453	31.34	0.067	3.13	0.459	51.69	18.85	134.32	6.83	0.671	0.682	0.517	0.749
165	12.95	78.11	154.79	11.56	26.55	0.510	32.49	0.067	1.70	0.458	52.17	20.69	122.54	6.03	0.736	0.690	0.527	0.750
166	13.82	74.94	155.58	9.96	26.81	0.484	32.93	0.066	2.25	0.489	56.85	22.10	123.52	5.42	0.787	0.697	0.537	0.750
167	13.33	69.08	151.84	10.62	27.54	0.415	33.12	0.066	1.85	0.472	58.81	22.48	118.74	5.18	0.802	0.704	0.546	0.750
168	13.56	72.77	154.19	10.63	28.11	0.463	33.75	0.066	2.09	0.480	57.23	22.85	120.70	5.37	0.815	0.711	0.555	0.750
169	11.67	70.32	161.51	9.23	28.94	0.664	33.87	0.066	3.35	0.413	70.28	19.88	132.39	6.03	0.709	0.717	0.564	0.750
170	13.02	89.47	164.33	11.04	27.69	0.779	34.37	0.066	2.81	0.461	50.81	19.53	133.76	6.87	0.695	0.723	0.572	0.749
171	14.15	92.74	157.73	6.27	26.52	0.740	33.50	0.066	3.31	0.501	44.57	20.70	130.76	6.55	0.736	0.729	0.580	0.749
172	14.54	46.63	93.35	-3.43	23.01	0.801	29.86	0.069	2.14	0.514	35.61	19.63	77.15	3.21	0.695	0.734	0.588	0.748
173	13.48	87.75	162.4	10.74	24.41	0.635	30.95	0.068	2.17	0.477	50.43	19.56	132.10	6.51	0.695	0.739	0.595	0.747
174	13.23	91.79	168.15	8.21	26.23	0.544	32.44	0.067	2.91	0.468	54.92	20.01	139.93	6.94	0.713	0.743	0.602	0.746
175	13.27	90.2	165.43	8.89	26.57	0.536	32.95	0.066	2.56	0.470	53.07	21.35	135.19	6.80	0.760	0.747	0.609	0.745
176	12.68	80.76	162.4	9.96	27.75	0.546	33.60	0.066	2.63	0.449	59.00	20.45	131.99	6.37	0.729	0.751	0.615	0.743
177	10.91	60.04	122.93	4.82	27.65	0.561	32.50	0.067	2.57	0.386	47.15	16.77	101.34	5.50	0.598	0.754	0.621	0.742
178	12.86	84.09	161.09	11.26	28.06	0.592	33.95	0.066	2.31	0.455	52.89	19.88	129.96	6.54	0.708	0.756	0.626	0.740
179	12.55	74.62	149.88	8.07	27.37	0.624	33.78	0.067	2.61	0.444	54.64	20.17	121.63	5.95	0.719	0.759	0.631	0.738
180	13.07	81.05	159.57	10.71	28.79	0.668	34.64	0.066	2.71	0.462	54.73	20.49	128.37	6.20	0.731	0.760	0.635	0.736
181	14.48	81.92	165.6	10.27	30.2	0.628	35.31	0.066	3.50	0.512	58.93	22.79	132.54	5.66	0.814	0.762	0.639	0.734
182	13.32	76.35	152.23	8.76	30.04	0.590	35.07	0.066	3.35	0.471	53.80	20.83	122.63	5.73	0.744	0.763	0.642	0.731
183	12.48	89.99	163.81	6.78	27.88	0.529	34.46	0.066	3.13	0.442	54.56	18.17	138.85	7.21	0.648	0.763	0.645	0.729
184	13.18	84.63	160.2	8.73	27.18	0.543	34.48	0.066	2.00	0.466	53.65	20.24	131.23	6.42	0.722	0.763	0.648	0.726
185	12.31	82.72	161.98	7.69	28.27	0.653	34.45	0.066	3.00	0.436	59.27	18.43	135.87	6.72	0.657	0.762	0.649	0.723
186	12.01	89.53	166.64	7.62	28.29	0.652	34.39	0.066	3.39	0.425	57.48	18.27	140.75	7.46	0.651	0.761	0.651	0.720
187	12.47	92.25	170.28	8.35	28.54	0.671	34.57	0.066	3.23	0.441	57.21	18.50	143.44	7.40	0.660	0.760	0.652	0.717
188	13.13	89.99	167.84	8.63	28.7	0.646	34.97	0.066	2.66	0.465	56.09	20.28	138.93	6.85	0.724	0.758	0.652	0.713

Table A9: Daily eddy covariance, energy balance component, and transpiration model results at PLC185 in 2002.

DOY	LE	H	Rn	G	Ta	e	Ts	θ	wind speed	λE_{uncorr}	res	LE_{corr}	H_{corr}	β	λE_{corr}	T_{Kc}	T_{GB}	EC Fourier
	Wm^{-2}	Wm^{-2}	Wm^{-2}	Wm^{-2}	°C	kPa	°C	m^3m^{-3}	$m\ s^{-1}$	$mm\ day^{-1}$	Wm^{-2}	Wm^{-2}	Wm^{-2}		$mm\ day^{-1}$	$mm\ day^{-1}$	$mm\ day^{-1}$	$mm\ day^{-1}$
189	12.44	81.35	164.04	8.89	28.83	0.513	35.13	0.066	2.19	0.440	61.37	21.93	133.22	6.54	0.783	0.756	0.652	0.710
190	12.74	68.7	160.57	11.27	31.34	0.514	36.29	0.065	2.06	0.451	67.85	20.46	128.84	5.39	0.732	0.753	0.651	0.706
191	13.81	73.71	162.23	12.89	32.52	0.568	37.36	0.064	2.09	0.489	61.82	23.11	126.23	5.34	0.828	0.750	0.650	0.703
192	21.48	45.06	102.84	-0.89	29.72	1.052	35.16	0.066	2.66	0.760	37.19	25.39	78.34	2.10	0.905	0.746	0.648	0.699
193	12.95	86.88	162.7	12.29	30.04	1.140	35.30	0.065	2.37	0.458	50.58	19.27	131.14	6.71	0.688	0.742	0.646	0.695
194	14.13	69.68	140.45	7.28	30.55	0.972	35.99	0.065	2.63	0.500	49.36	19.97	113.21	4.93	0.715	0.737	0.643	0.691
195	10.82	66.78	137.33	7.3	29.97	0.943	35.31	0.065	2.42	0.383	52.43	18.27	111.76	6.17	0.653	0.733	0.640	0.686
196	12.92	91.59	168.91	7.77	28.52	0.771	35.53	0.065	2.42	0.457	56.63	20.58	140.56	7.09	0.735	0.727	0.636	0.682
197	13.12	68.45	137.68	5.23	27.44	0.722	34.73	0.066	1.97	0.464	50.89	19.71	112.74	5.22	0.703	0.721	0.632	0.677
198	10.32	63.74	121.92	1.54	26.74	0.837	33.36	0.067	2.68	0.365	46.31	16.45	103.93	6.17	0.586	0.715	0.628	0.673
199	13.27	77.48	140.74	1.18	24.41	0.966	31.57	0.068	2.51	0.470	48.83	20.20	119.37	5.84	0.718	0.709	0.623	0.668
200	12.24	86.49	163.18	8.8	26.1	0.830	33.16	0.066	2.08	0.433	55.65	18.24	136.14	7.07	0.649	0.702	0.617	0.663
201	11.51	75.9	151.82	6.45	27.53	0.661	33.98	0.066	2.52	0.407	57.96	17.69	127.68	6.60	0.631	0.695	0.611	0.658
202	12.32	79.33	154.43	4.12	26.99	0.505	33.34	0.067	3.30	0.436	58.65	18.80	131.51	6.44	0.670	0.687	0.605	0.653
203	9.96	55.03	123.31	0.98	26.15	0.392	31.27	0.068	3.43	0.352	57.33	17.61	104.72	5.52	0.626	0.679	0.598	0.648
204	10.34	74.55	147.38	6.19	26.58	0.589	31.41	0.068	2.87	0.366	56.30	15.81	125.38	7.21	0.563	0.671	0.591	0.643
205	9.45	68.41	135.96	6.78	28.3	0.906	33.08	0.067	2.57	0.334	51.32	16.27	112.92	7.24	0.580	0.663	0.583	0.637
206	11.21	65.93	137.78	7.71	29.05	0.909	33.96	0.066	2.08	0.397	52.93	17.44	112.63	5.88	0.623	0.654	0.575	0.632
207	10.98	72.72	155.05	7.23	28.15	0.578	34.08	0.066	2.35	0.388	64.12	17.32	130.50	6.62	0.618	0.645	0.567	0.627
208	10.14	69.05	147.54	5.06	27.4	0.538	33.54	0.067	2.57	0.359	63.30	17.87	124.61	6.81	0.637	0.635	0.559	0.621
209	9.29	62.5	152.61	7.39	28	0.536	33.77	0.066	2.02	0.329	73.43	19.75	125.47	6.73	0.704	0.626	0.550	0.615
210	9.8	69.06	157.84	8.5	29.35	0.503	34.68	0.066	2.15	0.347	70.48	17.03	132.31	7.05	0.609	0.616	0.541	0.610
211	10.91	71.79	152.44	5.81	29	0.600	34.34	0.066	2.57	0.386	63.94	19.47	127.17	6.58	0.696	0.606	0.531	0.604
212	9.47	59.52	132.31	5.5	28.95	0.704	33.69	0.066	2.26	0.335	57.82	16.93	109.88	6.28	0.604	0.596	0.521	0.598
213	7.74	54.37	111.81	2.02	27.67	0.818	32.88	0.067	2.27	0.274	47.69	13.41	96.39	7.03	0.478	0.585	0.512	0.592
214	10.71	66.63	141.71	5.33	27.67	0.790	32.81	0.067	2.72	0.379	59.04	18.24	118.13	6.22	0.650	0.575	0.501	0.586
215	10.64	85.47	156.44	1.4	25.75	0.636	31.83	0.068	3.29	0.376	58.93	16.21	138.83	8.03	0.577	0.564	0.491	0.580
216	10.18	81.73	160.57	2.4	23.77	0.523	31.11	0.068	2.30	0.360	66.26	15.71	142.46	8.03	0.558	0.553	0.481	0.574
217	8.58	82.18	158.31	1.92	22.94	0.526	30.41	0.068	2.46	0.304	65.63	11.22	145.18	9.58	0.398	0.542	0.470	0.568
218	9.61	79.02	154.15	2.33	23.19	0.551	30.07	0.069	2.80	0.340	63.18	14.27	137.54	8.22	0.506	0.531	0.459	0.562
219	8.69	69.57	145.25	2.85	23.41	0.465	30.05	0.069	2.26	0.307	64.15	13.99	128.41	8.01	0.497	0.519	0.449	0.555
220	8.92	71.17	151.86	4.61	25.03	0.388	30.80	0.068	2.38	0.316	67.16	13.93	133.32	7.98	0.495	0.508	0.438	0.549
221	8.25	60.78	145.99	4.47	25.61	0.393	30.95	0.068	2.00	0.292	72.50	12.65	128.88	7.37	0.450	0.497	0.427	0.543
222	8.49	59.93	142.6	5.66	26.62	0.399	31.21	0.068	1.91	0.300	68.53	16.61	120.33	7.06	0.592	0.485	0.416	0.537
223	8.27	62.97	142.34	6.02	27.38	0.475	31.80	0.067	1.97	0.293	65.08	14.80	121.52	7.62	0.528	0.474	0.405	0.530
224	8.6	58.81	141.19	7.47	28.97	0.531	32.63	0.067	1.85	0.304	66.31	16.24	117.48	6.84	0.581	0.462	0.393	0.524
225	8.87	56.38	142.24	7.88	29.6	0.541	33.48	0.066	1.52	0.314	69.11	16.53	117.83	6.35	0.592	0.451	0.382	0.518
226	8.72	52.41	136.65	8.09	29.92	0.604	33.61	0.066	1.77	0.309	67.43	17.34	111.22	6.01	0.620	0.439	0.371	0.511
227	7.51	48.27	115.77	2.37	28.63	0.665	33.32	0.067	1.99	0.266	57.62	13.85	99.55	6.43	0.495	0.428	0.360	0.505
228	8.61	58.27	139.22	6.02	28.29	0.623	32.55	0.067	1.51	0.305	66.31	16.06	117.14	6.76	0.574	0.416	0.349	0.499
229	9.53	61.63	141.35	5.18	28.42	0.514	32.76	0.067	1.90	0.337	65.02	18.53	117.65	6.47	0.662	0.405	0.338	0.492
230	9.2	62.01	144.68	4.31	27.8	0.473	32.58	0.067	1.91	0.326	69.15	15.92	124.44	6.74	0.569	0.394	0.327	0.486
231	9.17	63.14	139.54	2.79	25.91	0.416	31.38	0.068	2.13	0.324	64.45	15.28	121.47	6.89	0.544	0.383	0.317	0.480
232	8.96	60.95	144.78	0.74	25.59	-2083	31.26	0.068	2086	0.317	74.12	12.54	131.50	6.80	0.446	0.371	0.306	0.473
233	7.69	59.9	144.53	-0.31	22.93	0.411	29.25	0.069	2.64	0.272	77.24	9.58	135.25	7.79	0.340	0.360	0.295	0.467
234	8.02	76.32	148.6	-0.11	21.91	0.449	28.53	0.069	2.29	0.284	64.37	10.79	137.92	9.52	0.383	0.349	0.285	0.461
235	7.45	70.49	147.28	2.57	22.77	0.457	28.96	0.069	1.49	0.264	66.76	11.20	133.51	9.46	0.398	0.339	0.275	0.455

Table A9: Daily eddy covariance, energy balance component, and transpiration model results at PLC185 in 2002.

DOY	LE	H	Rn	G	Ta	e	Ts	θ	wind speed	λE_{uncorr}	res	LE_{corr}	H_{corr}	β	λE_{corr}	T_{Kc}	T_{GB}	EC Fourier
	Wm^{-2}	Wm^{-2}	Wm^{-2}	Wm^{-2}	°C	kPa	°C	m^3m^{-3}	$m\ s^{-1}$	$mm\ day^{-1}$	Wm^{-2}	Wm^{-2}	Wm^{-2}		$mm\ day^{-1}$	$mm\ day^{-1}$	$mm\ day^{-1}$	$mm\ day^{-1}$
236	8.27	66.32	148.64	2.04	23.32	0.471	28.77	0.069	2.51	0.293	72.00	14.46	132.14	8.02	0.513	0.328	0.265	0.448
237	8.26	60.08	144.76	3.08	24.47	0.449	29.02	0.069	2.25	0.292	73.33	12.57	129.11	7.27	0.447	0.317	0.255	0.442
238	7.91	60.41	145.26	3.55	26.24	0.418	29.51	0.068	2.50	0.280	73.40	11.49	130.23	7.64	0.408	0.307	0.245	0.436
239	6.62	58.78	133.34	2.95	25.15	0.440	29.49	0.068	2.09	0.234	64.99	9.49	120.90	8.88	0.337	0.297	0.235	0.430
240	7.2	60.1	132.67	1.46	24.4	0.550	29.07	0.069	2.56	0.255	63.90	11.31	119.89	8.35	0.402	0.286	0.226	0.424
241	8.3	62.06	137.87	2.19	23.31	0.590	28.41	0.069	2.53	0.294	65.33	13.29	122.40	7.48	0.472	0.276	0.217	0.417
242	7.98	66.3	142.4	1.06	23.43	0.540	28.38	0.069	2.70	0.282	67.05	11.71	129.62	8.30	0.416	0.267	0.208	0.411
243	7.16	65.98	141.63	0.29	22.34	0.420	27.82	0.069	1.75	0.253	68.20	11.22	130.12	9.22	0.399	0.257	0.199	0.405
244	6.56	59.47	137.65	3.49	23.6	0.527	27.87	0.069	1.49	0.232	68.14	8.75	125.41	9.07	0.311	0.248	0.190	0.399
245	8.18	57.33	139.86	4.26	25.55	0.549	28.80	0.069	1.56	0.289	70.09	13.83	121.77	7.00	0.493	0.238	0.182	0.393
246	6.06	43.75	121.65	2.95	25.51	0.614	28.60	0.069	2085	0.214	68.90	12.85	105.86	7.22	0.458	0.229	0.174	0.388
247	10.37	27.23	74.06	-3.8	23.58	0.793	26.99	0.070	1.95	0.367	40.26	15.24	62.62	2.63	0.541	0.221	0.166	0.382
248	4.61	19.84	64.86	-3.01	22	0.871	24.68	0.072	2.80	0.163	43.42	10.97	56.90	4.31	0.389	0.212	0.158	0.376
249	5.07	24.5	69.97	-4.4	21.61	0.787	24.74	0.072	2.91	0.179	44.80	9.73	64.64	4.83	0.344	0.204	0.151	0.370
250	7.1	71.51	139.41	-2.97	18.12	0.416	23.36	0.072	2.59	0.251	63.76	9.99	132.38	10.07	0.353	0.195	0.144	0.365
251	6.04	61.71	137.43	-2.23	18.58	0.369	23.25	0.072	2.01	0.214	71.90	7.62	132.03	10.22	0.269	0.187	0.137	0.359
252	6.76	63.43	136.49	-0.33	18.39	0.368	22.90	0.072	1.62	0.239	66.62	9.26	127.56	9.38	0.328	0.179	0.130	0.353
253	6.33	62.31	136.95	0.88	19.72	0.393	23.67	0.072	1.65	0.224	67.44	9.64	126.43	9.85	0.342	0.172	0.123	0.348
254	7.22	51.19	132.99	2.78	21.9	0.430	24.48	0.071	1.85	0.255	71.79	13.04	117.16	7.09	0.463	0.165	0.117	0.343
255	7.38	58.66	134.83	0.8	21.97	0.426	24.89	0.071	1.84	0.261	67.98	13.31	120.71	7.95	0.473	0.157	0.111	0.337
256	7.24	56.07	132.8	1.5	21.6	0.449	24.73	0.071	1.48	0.256	67.99	13.27	118.03	7.74	0.471	0.150	0.105	0.332
257	6.99	56.24	133.34	3.83	23.33	0.495	25.32	0.070	2.42	0.247	66.28	11.94	117.58	8.04	0.424	0.144	0.099	0.327
258	6.44	47.85	117.23	-0.03	23.51	0.535	25.20	0.071	3.10	0.228	62.97	11.13	106.13	7.44	0.395	0.137	0.094	0.322
259	6.49	56.21	127.88	-2.83	21.71	0.386	24.52	0.071	2.38	0.230	68.01	8.61	122.09	8.66	0.305	0.131	0.089	0.316
260	5.74	51.3	122.16	1.59	20.11	0.460	23.21	0.072	1.86	0.203	63.53	8.01	112.55	8.94	0.284	0.125	0.084	0.311
261	5.42	49.19	127.72	-0.52	21.65	0.607	24.17	0.071	3.14	0.192	73.63	6.59	121.66	9.07	0.233	0.119	0.079	0.307
262	5.45	48.16	126.18	-0.5	21.7	0.533	24.06	0.071	2085	0.193	73.07	7.27	119.41	8.83	0.258	0.113	0.074	0.302
263	6.47	50.29	126.42	1.13	21.1	0.531	23.43	0.072	1.71	0.229	68.52	10.93	114.35	7.77	0.388	0.108	0.070	0.297
264	6.33	51.73	125.34	1.51	22.39	0.524	24.14	0.071	1.75	0.224	65.77	12.36	111.47	8.18	0.439	0.102	0.066	0.292
265	6.03	48.47	122.65	0.37	22.75	0.474	24.34	0.071	1.68	0.213	67.78	12.01	110.27	8.03	0.427	0.097	0.062	0.288
266	6.81	43.91	121.9	0.64	22.45	0.436	23.83	0.071	1.90	0.241	70.53	13.04	108.22	6.45	0.463	0.092	0.058	0.283
267	6.51	35.02	102.01	1.64	22.71	0.483	24.04	0.071	1.48	0.230	58.83	11.91	88.45	5.38	0.423	0.088	0.054	0.278
268	5.86	36.61	107.44	1.72	23.91	0.553	25.12	0.071	1.95	0.207	63.26	10.73	94.99	6.25	0.382	0.083	0.051	0.274
269	6.73	48.31	114.86	-2.57	21.87	0.405	23.91	0.072	2.17	0.238	62.38	11.49	105.94	7.18	0.406	0.079	0.048	0.270
270	5.14	27.09	78.99	-3.08	19.32	0.514	21.98	0.073	2.37	0.182	49.84	8.79	73.28	5.27	0.311	0.075	0.045	0.265
271	29.88	11.59	44.11	-12.81	15.17	0.853	19.62	0.075	2.14	1.057	15.45	34.22	22.70	0.39	1.200	0.071	0.042	0.261
272	7.59	46.67	120.24	-2.08	15.51	0.774	18.22	0.076	2.35	0.269	68.06	15.27	107.04	6.15	0.537	0.067	0.039	0.257
273	4.57	46.71	100.78	-4.96	15.5	0.679	18.91	0.075	2.07	0.162	54.46	7.65	98.10	10.21	0.269	0.063	0.036	0.253
274	13.15	41.5	86.97	-11.27	10.95	0.499	16.12	0.078	3.55	0.465	43.59	12.34	85.90	3.16	0.432	0.060	0.034	0.249
275	6.44	74.64	119.16	-9.93	10.13	0.422	14.66	0.078	4.81	0.228	48.01	7.08	122.01	11.60	0.248	0.056	0.031	0.245
276	3.47	36.27	111.76	-2.23	14.14	0.334	14.93	0.078	2.98	0.123	74.24	4.33	109.66	10.45	0.152	0.053	0.029	0.241
277	4.58	47.15	94.89	0.53	15.86	0.450	18.58	0.075	1.63	0.162	42.62	5.70	88.66	10.29	0.201	0.050	0.027	0.238
278	4.14	47.66	109.77	-3.39	15.14	0.549	16.93	0.076	1.45	0.146	61.36	6.25	106.90	11.52	0.221	0.047	0.025	0.234
279	3.63	41.81	110.5	-1.29	17.68	0.559	17.81	0.076	1.94	0.128	66.36	4.52	107.28	11.52	0.160	0.044	0.023	0.230
280	4.27	31.09	108.57	0.25	19.27	0.542	18.48	0.075	2.22	0.151	72.97	6.78	101.54	7.29	0.240	0.042	0.022	0.227
281																0.039	0.020	0.223
282																0.037	0.018	0.220

Table A9: Daily eddy covariance, energy balance component, and transpiration model results at PLC185 in 2002.

DOY	LE	H	Rn	G	Ta	e	Ts	θ	wind speed	λE_{uncorr}	res	LE_{corr}	H_{corr}	β	λE_{corr}	T_{Kc}	T_{GB}	EC Fourier
	Wm^{-2}	Wm^{-2}	Wm^{-2}	Wm^{-2}	°C	kPa	°C	m^3m^{-3}	$m\ s^{-1}$	$mm\ day^{-1}$	Wm^{-2}	Wm^{-2}	Wm^{-2}		$mm\ day^{-1}$	$mm\ day^{-1}$	$mm\ day^{-1}$	$mm\ day^{-1}$
283																0.035	0.017	0.216
284																0.032	0.016	0.213
285																0.030	0.014	0.210
286																0.028	0.013	0.207
287																0.027	0.012	0.204
288																0.025	0.011	0.201
289																0.023	0.010	0.198
290																0.022	0.009	0.195
291																0.020	0.009	0.192
292																0.019	0.008	0.189
293																0.018	0.007	0.187
294																0.016	0.006	0.184
295																0.015	0.006	0.181
296																0.014	0.005	0.179
297																0.013	0.005	0.176
298																0.012	0.004	0.174
299																0.011	0.004	0.172
300																0.011	0.004	0.169
301																0.010	0.003	0.167
302																0.009	0.003	0.165
303																0.008	0.003	0.163
304																0.008	0.002	0.160
305																0.007	0.002	0.158
306																0.007	0.002	0.156
307																0.006	0.002	0.154
308																0.006	0.001	0.152
309																0.005	0.001	0.150
310																0.005	0.001	0.148
311																0.005	0.001	0.146
312																0.004	0.001	0.144
313																0.004	0.001	0.143
314																0.004	0.001	0.141
315																0.003	0.001	0.139
316																0.003	0.000	0.137
317																0.003	0.000	0.135
318																0.003	0.000	0.134
319																0.002	0.000	0.132
320																0.002	0.000	0.130
321																0.002	0.000	0.129
322																0.002	0.000	0.127
323																0.002	0.000	0.125
324																0.002	0.000	0.124
325																0.001	0.000	0.122
326																0.001	0.000	0.121
327																0.001	0.000	0.119
328																0.001	0.000	0.117
329																0.001	0.000	0.116

Table A9: Daily eddy covariance, energy balance component, and transpiration model results at PLC185 in 2002.

DOY	LE	H	Rn	G	Ta	e	Ts	θ	wind speed	λE_{uncorr}	res	LE_{corr}	H_{corr}	β	λE_{corr}	T_{Kc}	T_{GB}	EC Fourier
	Wm^{-2}	Wm^{-2}	Wm^{-2}	Wm^{-2}	°C	kPa	°C	m^3m^{-3}	$m\ s^{-1}$	$mm\ day^{-1}$	Wm^{-2}	Wm^{-2}	Wm^{-2}		$mm\ day^{-1}$	$mm\ day^{-1}$	$mm\ day^{-1}$	$mm\ day^{-1}$
330																0.001	0.000	0.114
331																0.001	0.000	0.113
332																0.001	0.000	0.111
333																0.001	0.000	0.110
334																0.001	0.000	0.108
335																0.001	0.000	0.107
336																0.001	0.000	0.105
337																0.000	0.000	0.104
338																0.000	0.000	0.103
339																0.000	0.000	0.101
340																0.000	0.000	0.100
341																0.000	0.000	0.098
342																0.000	0.000	0.097
343																0.000	0.000	0.096
344																0.000	0.000	0.094
345																0.000	0.000	0.093
346																0.000	0.000	0.092
347																0.000	0.000	0.090
348																0.000	0.000	0.089
349																0.000	0.000	0.088
350																0.000	0.000	0.086
351																0.000	0.000	0.085
352																0.000	0.000	0.084
353																0.000	0.000	0.083
354																0.000	0.000	0.081
355																0.000	0.000	0.080
356																0.000	0.000	0.079
357																0.000	0.000	0.078
358																0.000	0.000	0.077
359																0.000	0.000	0.076
360																0.000	0.000	0.075
361																0.000	0.000	0.074
362																0.000	0.000	0.073
363																0.000	0.000	0.072
364																0.000	0.000	0.071
365																0.000	0.000	0.070

Table B1. Particle size data and classification according to U.S.Dept. Agric. textural triangle. Abbreviations: L, loam; CL, clay loam; SiCL, silty clay loam; SiL, silt loam; C, clay; SL, sandy loam; LS, loamy sand; S, sand..

Site and tube	Depth	Sand	Silt	Clay	Texture
	(cm)		%		
BLK1001	0-10	34	45	21	L
	25-35	49	36	15	L
	65-75	20	44	36	SiCL/CL
	105-115	28	40	32	L
	125-135	25	44	31	CL
	145-155	29	42	29	CL
	165-175	23	49	28	CL
	185-195	32	41	27	L/CL
	202-215	28	43	29	CL
BLK1002	25-35	13	23	64	C
	45-55	13	21	66	C
	65-75	11	27	62	C
	85-95	17	32	51	C
	125-135	14	29	57	C
	145-155	9	25	66	C
	185-195	28	59	13	SiL
	225-235	30	40	30	CL
BLK0091	45-55	36	42	22	L
	85-95	52	34	14	L/SL
	105-115	60	31	9	SL
	145-155	59	36	5	SL
	245-255	87	10	3	S
	305-315	74	24	2	LS
BLK0092	15-25	58	40	2	SL
	45-55	60	28	12	SL
	85-95	78	14	8	LS/SL
	105-115	60	34	6	SL
	165-175	25	65	7	SiL
	225-235	83	15	2	LS
	285-295	88	9	3	LS
PLC0451	0-8	85	11	4	LS
	15-25	83	14	3	LS
	45-55	82	14	4	LS
	85-95	90	7	3	S
	165-175	91	6	3	S
	225-235	95	1	4	S
	275	94	1	5	S
	365-385	92	4	4	S
FSL1384	5-15	20	67	13	SiL
	45-55	22	59	19	SiL

Site and tube	Depth	Sand	Silt	Clay	Texture
	(cm)		%		
	85-95	25	51	24	SiL
	105-115	30	49	21	L
	125-135	30	48	22	L
	145-155	24	52	24	SiL
	165-175	25	58	17	SiL
	205-215	14	60	26	SiCL
	225-235	29	48	23	L
	265-275	82	13	5	LS
PLC018	0-8	88	9	3	LS
	15-25	84	8	8	LS
	45-55	80	14	6	LS
	105-115	91	5	4	S
	185-195	92	0	8	S
	305-315	54	40	6	SL
	385-395	85	12	3	LS
-	485-495	84	12	4	LS
PLC185	25-35	44	42	14	L
	65-75	42	52	6	SiL
	85-95	14	67	19	SiL
	125-135	28	58	14	SiL
	165-175	93	5	3	S
	205-215	23	65	13	SiL
	265-275	64	29	7	SL
	305-315	64	31	5	SL
	385-395	99	0	1	S
PLC074	0-1	80	18	3	LS
	1-8	80	19	2	LS
	8-18	84	15	1	LS
	18-28	82	16	2	LS
	28-51	66	29	5	SL
	51-58	74	23	3	LS
	58-86	83	15	2	LS
	86-104	90	9	1	S
	104-170	99	1	1	S
	170-229	96	2	2	S

Table B2: Soil water retention curve van Genuchten (1980) model parameters

Site/Sample	Ks	α	n	θs	θr
	m/s				
BLK100	2.37E-06	8.362471	1.168302	0.63	0.05
FSL138	7.90-07	18.43449	1.219446	0.668894	0.05
PLC074	4.63E-07	15.19534	1.359438	0.386782	0
PLC185	1.12E-05	13.08711	1.509642	0.413916	0